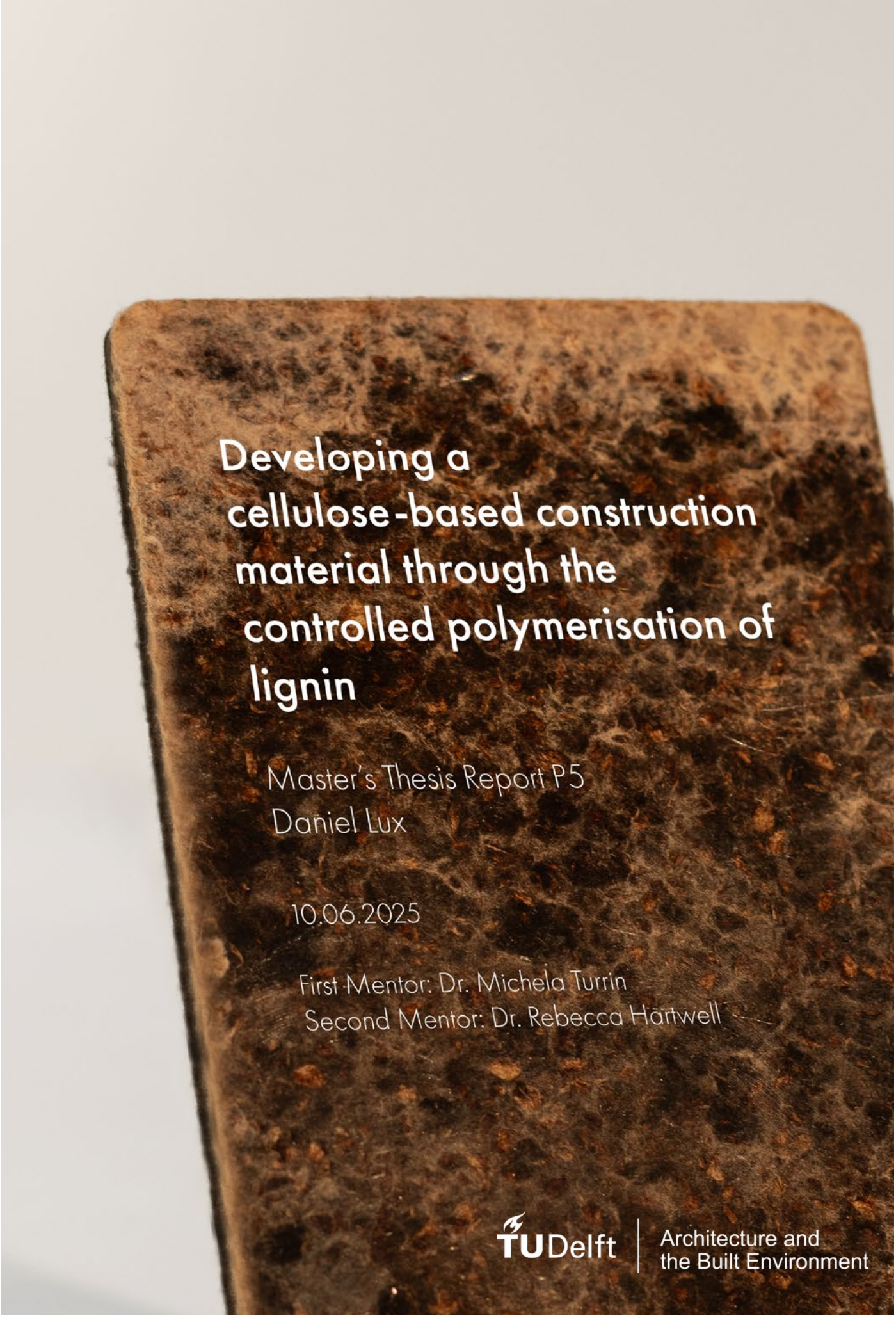

Developing a cellulose-based construction material through the controlled polymerisation of lignin

Master's Thesis Report P5

Daniel Lux

10.06.2025

First Mentor: Dr. Michela Turrin
Second Mentor: Dr. Rebecca Hartwell

TU Delft | Architecture and the Built Environment

Master's Thesis Project Report P5

TU Delft Faculty of Architecture & the Built Environment

MSc of Building Technology at Department of Architectural Engineering and Technologies (AE+T)

Author: **Daniel Lux**

"Developing a cellulose-based construction material through the controlled polymerisation of lignin"

First Mentor:

Dr. Michela Turrin, Section Leader of Secition Digital Technoliges (AE+T)

Second Mentor:

Dr. Rebecca Hartwell, Post-doctoral researcher at ReStruct Groep (AE+T)

Graduation Year of 2025

Abstract

In this master's thesis, the pressing need for novel, bio-based and fully circular construction materials is examined. Building on existing TU Delft research, the work focuses on cellulose and lignin as the principal constituents of a new wood-like composite, using waste streams as the source. The experimental setup, inspired by a range of studies on lignin-reinforced materials, employs a hot-pressing procedure. The literature review highlights a clear gap: the combined use of cellulose and lignin, each derived from by-products, to form an innovative material matrix, with the goal to make use of lignins adhesive qualities.

The methodology includes an innovative computational method designed to provide controlled variability of structural properties, that can be directly integrated into a component design. Many material variations, like moisture content, lignin types, C/L-ratio, pre-treatment and recyclability have been explored. Principal findings from this study include identifying optimal cellulose-to-lignin (C/L) ratios for distinct mechanical performances—3:2 for flexural strength and 2:3 for compressive strength. Additionally, Soda lignin shows the best mechanical performance and the plates can be successfully reprocessed. Computational simulations using Rhino 8, Karamba3D and Wallacei proved effective in predicting and optimising mechanical properties, significantly streamlining material development. Multidimensional scaling was used to map high-dimensional material data into a two-dimensional space, clustering formulations by performance and revealing trade-offs (e.g., stiffness vs. toughness) to guide blend selection.

Microscopic analyses further supported the viability of lignin as a natural adhesive, while highlighting areas needing improvement, such as brittleness and susceptibility to warping and blistering. A link was established between mechanical testing data and component modelling, which opens up possibilities to optimise both design and material composition for sustainable and resource efficient structures.

Overall, this research successfully demonstrates the potential of fully circular waste-based cellulose-lignin composites and paves the way for scalable, high-performance, sustainable building materials.

Key words – Bio-based, Cellulose, Lignin, Construction Material, Computational Method

Acknowledgements

While working on my research topic I encountered many instances where I wouldn't have been able to continue with my own resources or knowledge. Therefore, I hereby want to thank all the following for their assistance and guidance throughout my graduation project:

- Michela Turrin, for the support and advice throughout the project and enabling the collaboration with the researchers at Aerospace Engineering.
- Rebecca Hartwell, for continuously supporting me and spending a huge effort on assisting me with my experiments and introducing me to so many facilities and people throughout the Campus.
- Mark Ablonczy, for the enormous help with the planning and execution of all my experiments at Aerospace Engineering.
- Kunal Masania, for enabling me to conduct my experiments at the Aerospace facilities, especially lending me the mould for my samples.
- Barbara Lubelli, for allowing me to conduct my sample prep at the Heritage & Technologies Lab.
- Aditya Babu and Willem Bottger from NPSP, for generously investing their time in my project, for facilitating the production of large-format plates, and for granting me access to their facilities.
- Fred Veer, for arranging and assisting with the flexural tests at the Mechanical Behaviour Lab in Mechanical Engineering.
- Aleksandra Kondakova, for her expert training on the DSC instrument and her invaluable assistance in interpreting the results.
- Paul de Ruiter and the Lama lab team for their support
- Alessio Vigorito, Diederik Veenendaal and Rik Rozendaal for their advice and interest.

I also want to thank ISOCELL for providing me with their insulation material for my research purposes.

Without the enormous help by the inspiring network of researchers and mentorship that I have received none of the results of my project would have been possible to achieve.

Thank you!

Table of Contents

1 Introduction 1

2 Literature Review 13

3 Experiments 47

4 Material Analysis 77

5 Design and Application 115

6 Conclusion and Recommendations 139

7 Reflection 143

8 References 147

9 Appendix 155

Chapter 1 Introduction

1.1 Context - Cellulose and Lignin in the Construction Industry 1

1.2 Existing Literature from TU Delft – brief history and conclusions of the preceding research 1

1.3 Defining the Research Gap and the related Problem Statements 4

1.4 Research Question 4

1.5 Research Scope 4

1.6 Objectives 5

1.7 Methodology 6

1.7.1 Literature Review 6

1.7.2 Material Development & Experiments 6

1.7.3 Computational Method 8

1.7.4 Design Development 9

1.8 Research Workflow 10

1. Introduction

1.1 Context - Cellulose and Lignin in the Construction Industry

The construction industry is the biggest contributor to global CO_2 emissions. Heavy reliance on energy-intensive materials like steel, concrete, and bricks is a driving factor for that footprint (UNEP, 2024). The urgent need for more sustainable practices has fuelled the search for bio-based, renewable materials to reduce environmental impact. This research proposes using cellulose and lignin - two of the most abundant natural polymers on the planet - to develop a fully bio-based construction material with properties comparable to wood, without relying on traditional forestry practices.

Circularity in the construction industry has mainly two imperatives: the need to minimize greenhouse gas emissions and to address the increasing scarcity of natural resources. Circular materials that utilize renewable waste streams hold the potential to tackle both of these challenges effectively. Rather than investing additional energy in creating new raw materials, this research focuses on utilizing cellulose and lignin, abundant by-products of industrial processes, as the foundation for a new construction material.

Apart from lignocellulosic materials as a whole, cellulose as a raw material is already recognized for its mechanical properties, within the construction industry. Lignin as a raw material is on the other hand not yet represented in the industry and ways for its valorisation are mostly discussed in scientific literature only.

Cellulose is known for its tensile strength, while lignin acts as a natural binder with adhesive properties. Their availability as waste from industries such as paper production positions them as promising candidates for creating high-performance, sustainable building materials. For instance, Kraft lignin and alkali lignin, by-products of the paper pulping process, offer significant potential for use through polymerization and as binding agents. The use of these materials also aligns with the EU's commitment to a circular economy (European Commission (2020)), reducing reliance on primary resources and promoting material reuse. Another important ambition to pursue is not only the use of reused materials but also to create a new material mixture that is fully circular, low-emitting and one that can be reused over and over again.

By developing a construction material based on cellulose and lignin, this research aims to reduce the carbon footprint of traditional building practices while enhancing the material's performance through novel production techniques and introduction of computational methods. The proposed approach could establish a framework for designing bio-based materials tailored for specific applications in the construction industry, such as structural members, floor joists, and other load-bearing elements. Additionally, utilizing cellulose and lignin as raw materials has the potential to reduce unused or incinerated waste from industrial processes, such as paper production, contributing to a circular economy and mitigating the environmental impact of these by-products.

1.2 Existing Literature from TU Delft – brief history and conclusions of the preceding research

Within the research topic Wood Without Trees (NWO-SIA, 2025) both master students from the Building Technology track and researchers from the AE+T Department at the faculty of architecture at TU Delft have been developing different material mixtures for the application of both a cold and a hot extrusion process (Fig. 1).

In 2018 Thomas Liebrand, a master student wrote the first thesis on “3d printed fibre reinforced lignin: exploring the options to use wood in an additive manufacturing process” (Liebrand, 2018). Both polymers are mixed in an acetone-water solution and cold extruded in a 3d-printer setup. The solid materials were sourced from the kraft-pulping process. While the study confirmed the resulting material’s potential as an innovative wood-based option for architectural applications, due to the toxicity and flammability of acetone further material development would need to focus on finding alternative binding agents.

In 2022 Cristopher Bierach and Alexsander Coelho wrote their master thesis on the same topic of cellulose and lignin in additive manufacturing. In 2023 they published their work in the combined journal article “Wood-based 3D printing” (Bierach et al., 2023). With the prior experience from Liebrand the study faced two major challenges:

- Developing a material recipe with the right consistency (viscosity, adhesion) for 3D printing
- Achieving mechanical properties comparable to conventional building materials.

In their experiments they tested 12 different binders in combination with cellulose and lignin. Methylcellulose which is known as a food-safe gelatinizer performed best as a binder resulting in a homogeneous and extrudable paste. Samples of this mixture were produced and tested for their mechanical properties. This is where the research shows the potential for improvement, as the strength of the material is comparable to rigid polymer foams. The two prototypes produced – a window frame and a structural node – showed the feasibility of a future material being used in such a way to create customizable, eco-friendly building components.

In the most recent research from 2024, “Wood Without Trees: 3D printing cellulose and lignin” from Christopher Bierach, Alexsander Coelho and Thomas Liebrand (Figure 1, right), both cold and hot extrusion methods were examined for their potential in 3D printing lignin-cellulose-based materials. The cold extrusion involved creating a paste-like mixture, primarily using nanocellulose as a binder. Just like in Bierach et al., 2023 the Methylcellulose-based mixtures performed best, offering clay-like consistency that enabled stable multi-layer prints up to 200 mm in height. Similar challenges also remained the same as high shrinkage during the drying process. The hot extrusion process aimed to produce a thermoplastic blend using lignin with a natural deep eutectic solvent (NaDES) of urea and d-glucose. In an a promising, initial process to be further developed they aimed to produce a material under heat and pressure. The subsequent separation of NaDES from lignin and cellulose indicated the need for further compounding techniques or alternative binders for a consistent thermoplastic matrix

Wood-based 3D printing: potential and limitation to 3D print building elements with cellulose & lignin:

by Christopher Bierach · Alexsander Alberts Coelho · Michela Turrin · Serdar Asut · Ulrich Knaack

2023

2024

Wood Without Trees: 3D printing cellulose and lignin

by Alexsander Alberts Coelho · Christopher Bierach · Thomas Liebrand · Michela Turrin

Figure 1. Overview of preceding publications on the research topic *Wood without Trees.*

1.3 Defining the Research Gap and the related Problem Statements

Following the description of the preceding research from the TU Delft researchers, two major fields are identified to be addressed within this project. While the development of a mixture suited for a cold paste extrusion was focused on in both the 2023 and 2024 papers, a mixture that is used for manufacturing at high temperatures was explored with only unsuccessful result. The polymerisation of the lignin within this mixture was not mentioned.

Lignin however is starting to gain much more acknowledgement in the previous years for its natural adhesive properties when processed in the right conditions. This characteristic implies that a mixture that harnesses the improved mechanical strengths can be devoid of any additional binder or adhesive – making the mixture simpler in its composition. When looking at adhesives used in traditional wood-based boards like MDF, plywood or laminated beams we often encounter formaldehyde containing resins (UF) or melamine resins (MF) or PMDI glue, all of which are of concern in terms of sustainability and recyclability of these wood products (Dunky, 2003). Especially those boards that make use of the UF resins are known to show formaldehyde evaporation and are ecologically only conditionally recommended (Mitteldichte Faserplatten | Material-Archiv, n.d.)

Circling back to lignin, it's inherent "strength" to be a natural adhesive due to its superior bonding properties (Yang et al., 2023) is not yet effectively used in construction materials, but shows big potential. Papers like Qin et al., 2023 demonstrate the structural capabilities when Lignin and Cellulose are cross-linked, and the lignin acts as a polyphenolic binder resulting in excellent flexural stability (Qin et al., 2023). Giving up on an additional binder opens the possibility of endlessly loosening and repolymerizing the lignin, enabling circular material use.

Another field of concern that was found in the existing research from TU Delft students is the process of the development of a new mixture, particularly the way of applying a mixture deemed to be suitable enough for application to a geometric case study. The traditional trial-and-error approaches of figuring out mixture concentrations, testing mechanical properties requires rigorous sampling and repetition. Lastly, when the material has gone through multiple improvement or experimental steps, and the timeframe of a research project comes to an end the application to a geometry is not able to receive enough attention. In the case of the two master theses, the outcomes included geometrically feasible designs and acceptable material behaviour. However, due to the lack of in-depth analysis of these case studies, the results remained limited to conceptual models rather than being validated as functional structural solutions.

One of the key challenges in developing the cellulose-lignin mixtures lies in the managing of complex interactions between material properties, additives and production methods. By leveraging computational tools, it becomes possible to systematically explore a wide range of material compositions and their corresponding performance metrics. Such a tool can enable controlled variability, where first and foremost the mechanical material properties are optimized by adjusting parameters in a predictable way. Especially, the early integration of computational methods can also facilitate real-time feedback loops, allowing for the refinement of both the material mix and the production process during early development stages. This is followed by the exploration of design applications which can also benefit from this level of control over the three categories, composition, production and geometry.

By incorporating computational frameworks into the material development workflow, the process can become more efficient, flexible and scalable, ultimately addressing the need for more holistic and sustainable workflows in the entirety of the chain of a material, from development to end-of-life.

1.4 Research Question

The focus of this research is to build upon the advancements made in the "Wood without Trees" research topic. Specifically, the aim is to develop a new material mixture suitable for a hot-pressing procedure that could ultimately be adapted for a hot extrusion process. While the insights and findings from previous theses within this topic are acknowledged and leveraged, they are treated as equally valuable as any other external publication reviewed during the literature study. This ensures that the current research remains distinct, original, and independently developed, integrating the existing body of knowledge without being constrained by it.

With the implementation of a computational method to have a controlled variability within the experiments the results from these experiments should be directly contributing to the design of a functional structural member.

Summarizing this context the following main research question arose:

How can an optimised mixture and a suitable hot-press production method be developed that uses by-product-lignin and -cellulose, to utilize lignin's natural binding properties through controlled polymerization?

Further Sub-research questions address the underlying fields of interest to be explored or problems to be investigated:

- How can the early integration of computational software help with a more efficient and flexible material design?
- What is the state of art in utilizing polymerization of lignin in construction materials, as a natural adhesive in wood-like materials?
- What are the limits of relying on solely cellulose and lignin as the main mixture's ingredients
- What additives are needed to improve the material quality in both appearance and mechanical performance?
- How can the batch-based production and limited sample size of hot press processes be addressed?
- How can the hot-pressing procedure be used to develop a hot extrusion process?
- How can controlled variability in the material composition be achieved using a computational design tool?
- What are the design implications that are specific to the production process and material composition?

1.5 Research Scope

This master thesis report is describing the research process of six months. With this timeframe the scope of the research must be defined reasonably. Besides answering the main research question and addressing the related topics of the sub-research questions, this research aims to define the material's potentials and limitations, adding upon the findings from the previous work. Furthermore, apart from the materials functionality, also the prototypes functionality should be demonstrated as the conclusion of this paper – and so, setting itself apart from

the preceding master's theses from 2022 on material and design level that were not able to validate the outcomes of their mock-ups.

Especially, during the material development phase the aimed at workflow needs to address the risks of unsuccessful experiments and provide back-up scenarios. Of highest priority in the process is the demonstration of the lignin polymerisation process that can be utilized with means of heat and pressure.

1.6 Objectives and limitations

This thesis follows the methodology of the Architectural Engineering and Technologies Department "Research through Design". This approach aims to effectively combine research objectives & design objectives to create a coherent research result that demonstrates significance of the research on ethical, socio-cultural and/or scientific levels but also produces innovative outcomes (Stappers & Giaccardi, 2017).

Considering this research approach, the main research objective can be summarized to the development of a cellulose- and lignin-based wood-like material, along with a production technique, that achieves mechanical properties suitable for use in the construction industry. Additionally, the design objective integrated into the research focuses on developing a method to design a sustainable structural member as replacement of traditional building components, using a computationally optimized mixture formulation, production process and parametrized shaping. The use of such a software tool aims to allow a controlled variability when designing the material mixture and respond to specific design needs.

For both of these aspects within the research a set of guidelines for the decision-making process has to be determined. The following list describes these objectives that should be actively pursued in the following steps:

The selection of suitable materials for the development of a mixture should be bio-based and non-toxic or generally not harmful.

Each material should stem from an existing resource stream and is ideally a widely underutilized waste product in order to maintain circularity.

The experiment design and production methods should employ simple techniques that ensure the reproducibility of each step - avoiding use of dependence on highly specialized equipment, or hard to obtain materials.

The computational solution needs to be robust, adaptable, and capable of integrating real-time input. This means, not reliant on proprietary software.

1.7 Methodology

1.7.1 Literature review

This report reviews several core topics in sequence. First, it establishes the chemical fundamentals of cellulose and lignin. It then examines recent methods for lignin polymerization, explores additive-manufacturing approaches for cellulose-based materials, and considers analogous wood-like composites. Finally, it surveys computational tools for material-scale modelling and multi-factor experimental design. Sources include peer-reviewed articles, conference proceedings, and technical reports accessed primarily through Scopus and Google Scholar, with supplementary Google searches used—for instance, to locate material suppliers.

The literature that is reviewed is largely selected on the publication date, usually not older than 3 years as the valorisation of lignin in other ways than energy production is a very recent interest in the construction environment. Additionally, the sources selected, not including the computational methods, are also limited to the fields Material Science, Environmental Science, and construction.

The literature review will first focus on explaining the chemical and biological nature on lignocellulosic compounds.

Furthermore, looking at the availability of these materials will be part of the literature research. Lignin as a raw material is available from multiple chemical extraction treatments. These treatments will be described and compared, based on functionality of the lignin and availability.

The state of the art of the (re)polymerization of lignin within wood-based and non-wood based lignocellulosic materials will also be reviewed. Besides wood derived cellulose, cellulose is also often available in shape natural fibrous cellulose or non-wood fibres. The investigation of these material sources will be relevant as it could provide superior flexural strength and be part of the review process. The last reviewed part in this segment are possible cellulose matrices that can be used in the hot-pressing process. This segment will be concluded and discussed based on the information researched.

This is followed by the investigation of comparative computational approaches used for modelling, designing and manufacturing construction materials. Underlying frameworks within these approaches will be summarized and compared. So will be the utilized software for material modelling and predicting, to give exemplary cases that can inform the computational method of this research.

1.7.2 Material Development & Experiments

Resulting from the reviewed literature, production methods that are in line with the project objectives are selected and combined to a new process. Each step will be based on a specific piece of literature that provides evidence of its functionality. Figure 22 shows how multiple sources are pieced together to come up with a new solution of a production methods that is specific to this design task.

Before the materials are tested for their mechanical properties the materials will be assessed on different criteria before and after the production. The literature review will also focus on the used methods of analysing the performance and behaviour of the created materials, in order to make a informed decision about what procedures should be selected for this research.

The design of the mechanical testing is following standards from European norms and international standards. This includes the shape of test specimens for wood based or

composite materials and conventionally tested strength properties for these material types (tensile strength, bending resistance etc.). Another factor to determine the material properties that should be tested are the input values of the chosen modelling software. All of the facilities used for the prototyping, production, testing and general work are listed in Table 1.

The development of a new construction material from previously not combined raw materials, can be described as a bottom-up approach. This means that the use-cases of the material are to be decided by the resulting material properties. Generally, the material design will see multiple iterations and a trial-and-error process in order to prototype a material and then this material can be used to continue with the member design stage (Figure 2). This process can therefore be tedious and slow and most of all, it could still not end in meaningful results that can be used to create a new component for construction purposes. In order to address this issue, integration of computational methods will be considered, so that the data of the trials used in an informative way to create material relationships and allow for modelling and anticipating those.

Table 1. Name of Laboratory or Facility used and the respective action performed there.

Name	Action
Heritage & Technologies Lab at the Faculty of Architecture and the Built Environment	Sample Preparation, Mixture making, weighing of materials. Material Design.
Composites Lab & Printing Lab – DASML at the Faculty of Aerospace Engineering	Hot-pressing and mechanical testing (compression and tension test including DIC).
Mechanical Behaviour Labs at the Faculty of Mechanical Engineering	Facility for mechanical testing, mainly four point bending test.
Lab of the ChemE/O&O group of the Faculty of Applied Sciences	Differential Scanning Calorimetry (DSC) of lignin types and samples.
NPSP, Delft	Hot-pressing of large scale samples

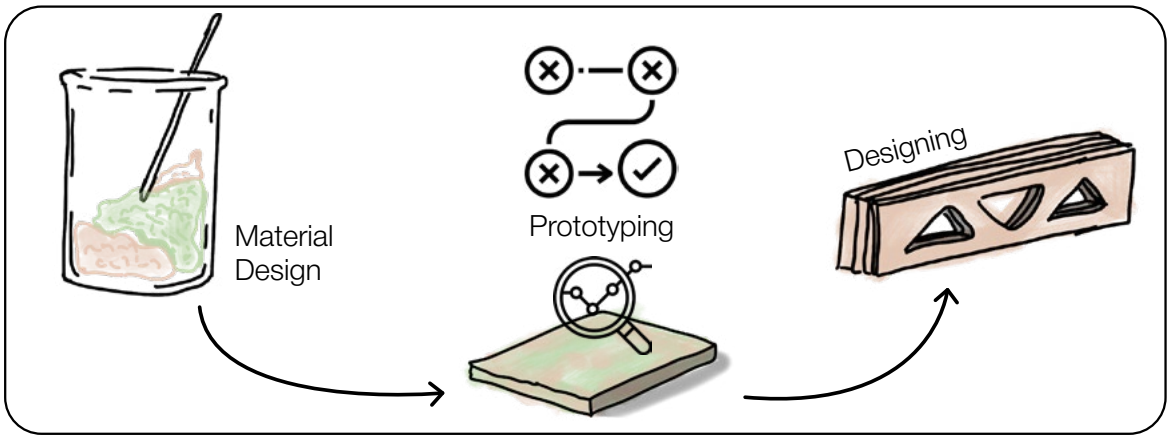

Figure 2. Schematic depiction of the potential trial and error, bottom up process of material design to component design.

1.7.3 Computational Method

Within the research through design approach at TU Delft, design exploration and material research are intertwined to create an iterative process of knowledge production and discovery. By developing and applying a design and optimisation tool during the material experimentation phase, immediate feedback loops are created that shape both the direction and depth of the research. This interaction addresses the short comings that are present in the trial-and -error based approach, it refines the design outcomes but also deepens the understanding of the material's properties and potential applications.

The computational method will make use of multiple software for analysing, simulating and designing that must be integrated into one another. In Figure 3 the potential integration of the computational tools that help the material process are shown.

While the research objectives define what values the material should adhere to, the design objectives govern the process of how the materials is developed. At the start the process the design of experiments creates the first list of parameters that can influence the performance of the final product. However, before these parameters can be taken into account in the optimization, the parameters are tested based on the resulting materials strengths. Once the data of the initial material tests can produce a reliable material profile, these values can be fed into both structural modelling- and material modelling software. Within these two tools, another set of parameters are determined that can have an influence on the performance.

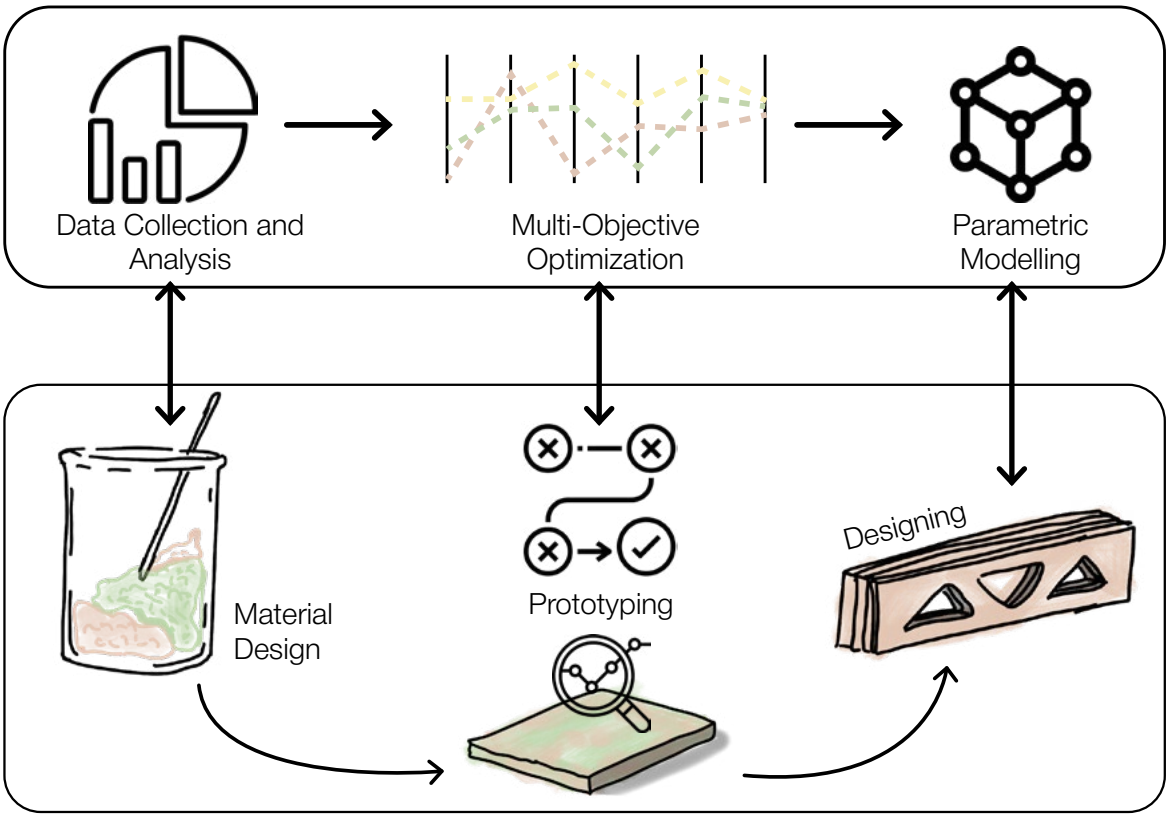

Figure 3. Schematic depiction of the computational workflow that can be deployed in combination with the material development process.

Meanwhile, the design of a structural member gives the basic dimensioning, environmental constraints and strength requirements to derive a preliminary structural shape. At this stage, the computational methods must interact. With the help of tools like multi-factorial optimization, an optimal combination of all parameters can be found – and if necessary, the tool makes adjustments to the parameters in the respective step. The way the parameters are adjusted is based on the requirements that are given by the structural member design. For example, if a beam is to be designed that has to carry a certain load, the tool tries to adjust multiple parameters to satisfy the load requirements, and possible sizing constraints. Finally, the prototypes as the output of the optimization step are analysed and tested to validate or calibrate the tool.

In the research phase of this report computational methods of material design and program solutions are investigated to build up a suitable computational repertoire.

1.7.4 Design Development

The design assignment of this project can be broken down into these two distinct focus fields:

1. Focus on the polymerization of Lignin within a cellulose mixture. Harnessing lignin's natural adhesive qualities through hot-pressing

2. Influence of computational and analytical software on the material development and design process, through optimization, simulating and predicting of material behaviour

Through the combination of these two fields the project aims to perform material tests that can ultimately be applied to the design of a structural member like a floor joist.

The material tests are a way to explore and get a feel of the material properties and apply the methods found in the literature review phase. From this process it is to be expected that the review of more literature is required to continuously inform this process based on the current experiment results. This phase will not yet explore design variations but rather produce samples based on the geometric requirement of structural performance tests. Meanwhile the computational method must be developed. During the literature review phase, the framework of this method is already predefined and the main goals are described. As the material development comes along, the design of this computational method will also be adjusted to accommodate the behaviour of the material.

Once the material and fabrication method have had their initial testing and a material profile based on mixture ratios and mechanical properties can be created the computational tool is used to perform the first optimizations. The geometry input of a designed structural member and its environment will create certain constraints on the material mixture and structural design. The computational tool formulates the ratios of all mixture contents, the assembly pattern of the individually hot-pressed components and a structural analysis of the input geometry.

Based on this virtual model of the design structural member. The accuracy of the model is tested by producing the prototype pieces and validating the structural behaviour through strength tests.

The outcome of this design will then be the demonstration of a simulated member design and the validation of the new hot press production method and material mix through physical models.

1.8 Research Workflow

Following the described problem statements and research question, this research will divide into the steps below:

1. Theoretical Research Framework
2. Literature Review on Material Design and Computational Methods
3. Material Experimentation and Tool Development
4. Mechanical Testing and Creating of Material Profile
5. Data Integration into Computational Tool
6. Material Simulation
7. Validation of Simulation within Prototype Design

The Framework of the project workflow can be separated into three main segments, as seen in Figure 3. The project begins with a research phase. For the start of the research phase, the problem statement, research question, and objectives of the entire project are determined. A holistic literature review is conducted to be able to outline the relevance and context of the research topic. More detailed research is focused on the investigation of suitable lignin and cellulose sources, as well as novel polymerization techniques of lignin.

Meanwhile, additional research is done on the design goal, a computational framework that aids the testing and material optimization process, this encompasses software solutions for the individual computationally aided steps and suitable programming languages.

This first stage is the preparation of the material development and testing phase. Three processes are developed parallel. Firstly, following research phase a selection of materials decided on that are used for production on samples. Following that the mechanical properties of the produced samples must be investigated. Secondly, the computational tool will be developed. Thirdly, the production of the samples and the mechanical testing has to be prepared, documented in laboratory reports and finally produced.

All the three parts will take place roughly in the same time frame. Finishing this segment the production process, if successful, will be improved and the final material composition is defined. During phase multiple material compositions/ trials and alternatives are tested and the findings well documented.

This constitutes the factual results of the thesis research. As it is expected that the reliability of the data produced is quite low, due to limited time, the following step will be based on assumptions and preliminary models in order to provide a proof of concept for the application of the computational method.

The findings of the second segment will be fed into the computational tool in the third segment. The material composition will be optimized based on an exemplary construction element with certain structural requirements. With the material and structural simulations, certain characteristics are selected in two or three alternatives. To validate the functionality of the computational tool these prototypes are tested on the desired mechanical properties in a final step.

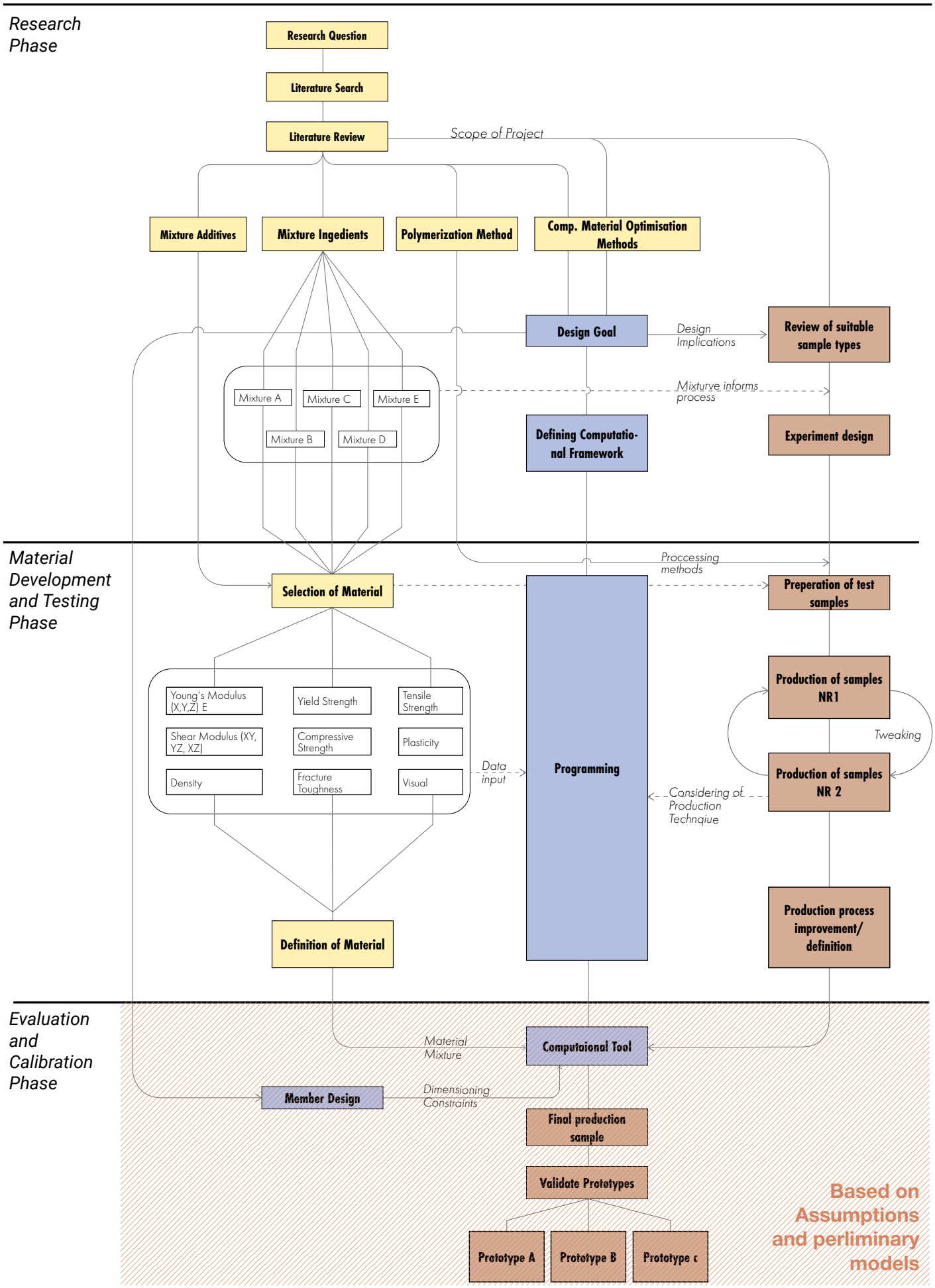

Figure 4. Project workflow showing three main work segments and the topic strands running parallel

Chapter 2
Literature Review

2.1 Research Direction 13

2.2 Basics of Woods Structure 13

2.3 Cellulose 14

2.4 Hemicellulose 15

2.5 Lignin 15

2.5.1 Kraft Pulping 17

2.5.2 Soda Pulping 17

2.6 Polymerization of Lignin and Production Methods 18

2.7 Cellulose Sources for the Composite Fibre Selection 27

2.8 Material Testing 41

2.9 Research Discussion - Material Design and Production Methods 37

2.10 Computational Methods 42

2.11 Discussion of Computational Approach 50

2. Literature Review

2.1 Research Direction

Within the research topic Wood without Trees the employed strategies to create a material mixture can be described as making a polymeric composite that has the typical composition of fibre, filler and matrix. This contrasts with the proposed strategy described in the research gap and research question. The literature review will be directed to only the investigation of literature on the latter. These two directions are here shown in Figure 5 and summarized for clarity in the following descriptions

Direction A: Matrix-Reinforced Cellulose–Lignin Composites

An external binder is used to create a matrix to bind the cellulose and lignin. Cellulose and lignin can affect the failure behaviour like ductility due to their fibrous structure. A binder like bioplastics or resins give good bending resistance, tensile strength etc. (Cold and Hot extrusion)

Direction B: Direct Lignin–Cellulose Polymerization Systems

The Lignin can be melted/ softened/ solved and reset within a cellulose structure. With the aim to recreate lignin's natural "strength" to be a natural adhesive and possibly chemically cross-link lignin to cellulose fibres. (Hot-Treatment)

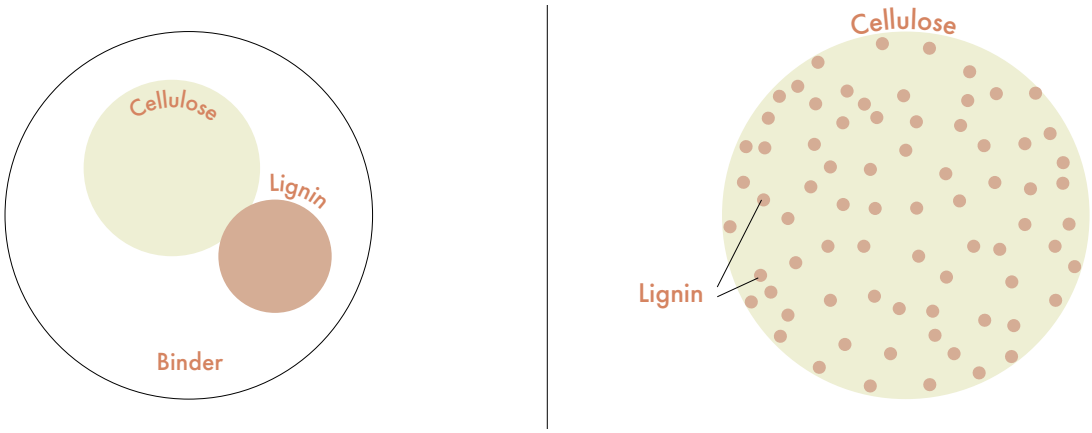

Figure 5. (left) abstract diagram of direction a). (right) abstract diagram of direction b)

2.2 Basics of Woods Structure

Before addressing each material ingredient individually this summary explains the origins of the polymers in their natural state, as a building block of the cell structure of wood. These basics will allow to better understand the terminology that is used in the description of the experiments and

The hierarchy with which a piece of wood is assembled from its smallest to largest component starts at the nanoscale of a cell wall and ends in the macrostructure of a wood stem. On the molecular level, a cell wall is made up of cellulose microfibrils, hemicelluloses and lignin. There are also different types of cells in wood, the basic cell types are tracheids, vessel members, fibres, and parenchyma. Most common cell types in hardwoods are fibres, whereas tracheids are the prevalent type in softwoods (Rowell, 2005).

Due to the alignment of the wood cells along one direction wood has a pronounced structural anisotropy, meaning that the structural properties vastly differ according to the direction in which the wood is used. (Chen et al., 2020). Figure 5 depicts how the anisotropy looks like on a cell- and molecular scale.

The following subsections will describe each of the material's structural significance, chemical description and interactions. The distribution of these chemical components in wood's cell walls is depended on the species but roughly cellulose 30–35 wt%, hemicellulose 15–35 wt%, and lignin 20–35 wt% (Qianli, 2022), further details will be disregarded in these sections, as the aim of the research is to utilize already isolated polymers.

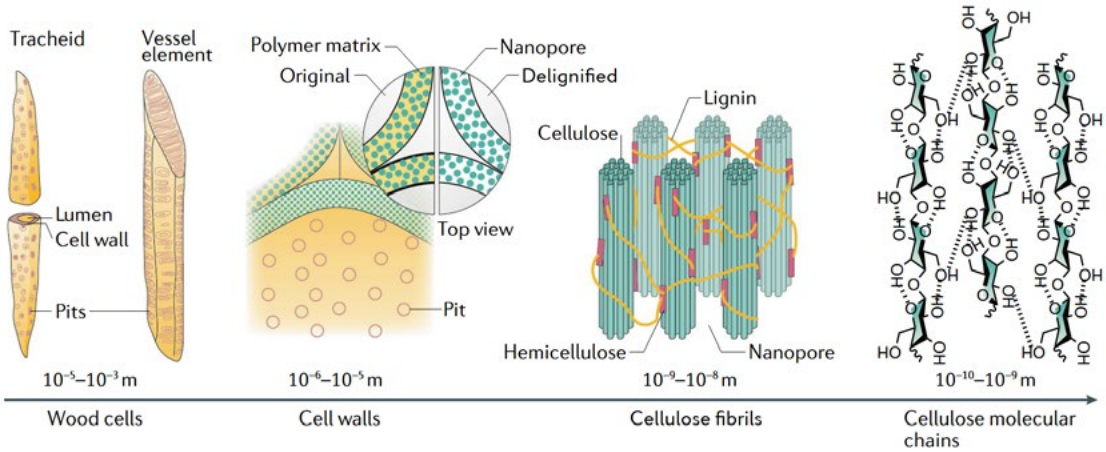

Figure 6. Anisotropy of wood structure (Chen et al., 2020)

2.3 Cellulose

Cellulose is the most abundant organic polymer on the planet. The polymer's basic building block is the cellobiose, which is a two-sugar unit repeated thousands of times. The polymer chains have the tendency to form hydrogen bonds between and within molecules. This increases the packing density of the cellulose. As the density becomes higher the cellulose forms crystalline regions. Typically, the amount of crystalline regions of cellulose extracted from wood is 65%. The crystallinity of cellulose is very important as it makes the cellulose accessible or inaccessible to water. In a crystalline state cellulose is inaccessible to water. When non-crystalline the cellulose is accessible to water, however, part of these regions are covered by lignin and hemicellulose (Rowell, 2005, p. 38). Cellulose is typically considered highly hydrophobic.

As the cellulose is the main structural polymer of wood cells the mechanical properties of a wood material is based on the properties of the cellulose elements on different scales. The mentioned purely crystalline native cellulose has a modulus of elasticity of 140 GPa and 150 GPa which lies in the midrange when compared to typical engineered synthetic polymer. A tensile strength of 3–6 GPa of highly crystalline cellulose nanofibrils (CNFs) can also be measured (Jakob et al., 2022). Native cellulose is often also described as cellulose I. Cellulose II, III and IV are all derivatives of cellulose I extracted through a specific chemical procedure. Other known types of cellulose from treatment processes are Cross and Bevan-, Kürschner- (both containing parts hemicellulose) and Kraft cellulose (Rowell, 2005).

As an example of cellulose's sole strength, Dong et al., 2022 demonstrates in a process called "wood healing" how just cellulose structures alone - by removing all non-cellulosic contents from a piece of balsa wood and densification - can result in much stronger materials.

2.4 Hemicellulose

The remaining parts of polysaccharides, besides cellulose, in wood are grouped as hemicelluloses. As seen in the Figure 6 hemicellulose also forms cross-links with the cellulose fibrils trough hydrogen bonds. Hemicellulose polymers are distinctively shorter in length than cellulose chains. They are made up of mainly six different type of sugar molecules, with each two optical isomer variants. These shorter polymer chains are closely associated with cellulose and are contributors to the structural performance of a tree's wood. For example trees that are under a lot of compression stress show a large amount of D-galactose content (as well as higher lignin content) (Rowell, 2005). Hemicellulose is soluble in alkali and can easily be hydrolysed (cleavage of chemical bonds) in acids, while cellulose is not even soluble in strong alkali. Studies like Hosseinaei et al., 2012 indicate that the removal of hemicellulose can decrease the water absorption and an increase the tensile properties of wood-based composites.

2.5 Lignin

The third kind of complex organic polymers, and the second most abundant organic polymers on the planet (Ez-Zahraoui et al., 2023). Considered as an encrusting substance and embedding agent it chemically cross-links with the cellulose microfibrils and hemicellulose, therefore providing stiffness to wood cells. A plant's lignin is a highly irregular molecule, made up of phenolic precursors. While in context of wood, lignin is distinguished between hardwood and softwood lignin. However, each tree species has its very own variation of a lignin molecule structure. (Rowell, 2005). The cross-linking capabilities of a type of lignin is heavily influenced by the functional groups (aliphatic hydroxyl, phenolic hydroxyl and methoxyl groups). These also vary heavily based on the species of tree the lignin is derived from (Chio et al., 2019). Lignin is broadly classified into natural and technical lignin. In nature the natural lignin does not exist on its own, but always in a lignocellulosic biomaterial. Thus, the term technical or modified lignin is used to describe when lignin that is extracted from biomass or recovered from an industrial process (Bilal et al., 2024). The application and quality of each technical lignin are determined by its production method.

The main types of lignin from different production methods are kraft lignin, soda lignin, organosolv lignin, pyrolytic lignin and hydrolysis lignin. The following table summarizes key aspects of the lignin types.

Table 2. Comparison of different lignin extraction precesses

Type	Description
Kraft	- Accounts for 80% of industrial lignin production; primarily used for heat and energy generation - Produced via kraft pulping, using sodium hydroxide and sodium sulphide at 155–175 °C to break ether bonds, creating a black liquor by-product. - High molecular variation limits industrial applications, but its purity shows promise for high-value products like carbon fibres, resins, and thermoplastic polymers. - Highly hydrophobic, strong odour and limited reactivity

Type	Description
Soda	- Derived from non-woody biomass like agricultural waste and is sulphur-free, closer to natural lignin than kraft lignin. Quality dependent on feedstock type. - Produced through soda pulping with sodium hydroxide under high pressure and temperatures of 140–170 °C, hydrolysing ether bonds. Outcome is alkaline lignin
Organosolv	- Sulphur-free and high-purity lignin extracted using organic solvents like methanol, ethanol, or acetone, insoluble in water - Produced under high temperature and pressure, ideal lignin for biomaterial production - Low molecular weight limits adhesive applications, but its purity makes it ideal for biorefineries, biofuels, biosurfactants, and paints.
Pyrolytic	- Byproduct of fast pyrolysis often used for heat generation. - Produced via polymerization during pyrolysis, generating a viscous bio-oil that can be purified for high-value chemicals.
Hydrolosis	- Contains 50–75% lignin along with impurities like cellulose and carbohydrates; sulphur-free and structurally like native lignin. - Produced during enzymatic or acidic hydrolysis of biomass, need for modification and purification.

Both the kraft- and alkali- (from the soda process) lignin are highly abundant, yet underutilized biopolymers from the pulping industry (Laurichesse & Avérous, 2014). In Figure 7 and Figure 8 the different extraction processes and the global scheme of the uses of lignin are displayed.

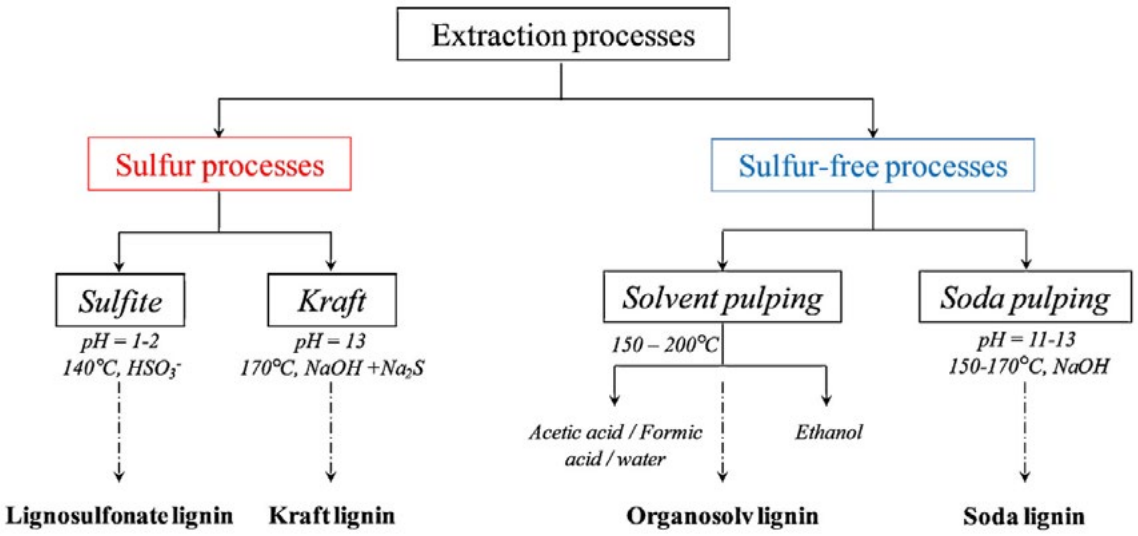

Figure 7. Lignin Extraction Process, from Laurichesse & Avérous, 2014

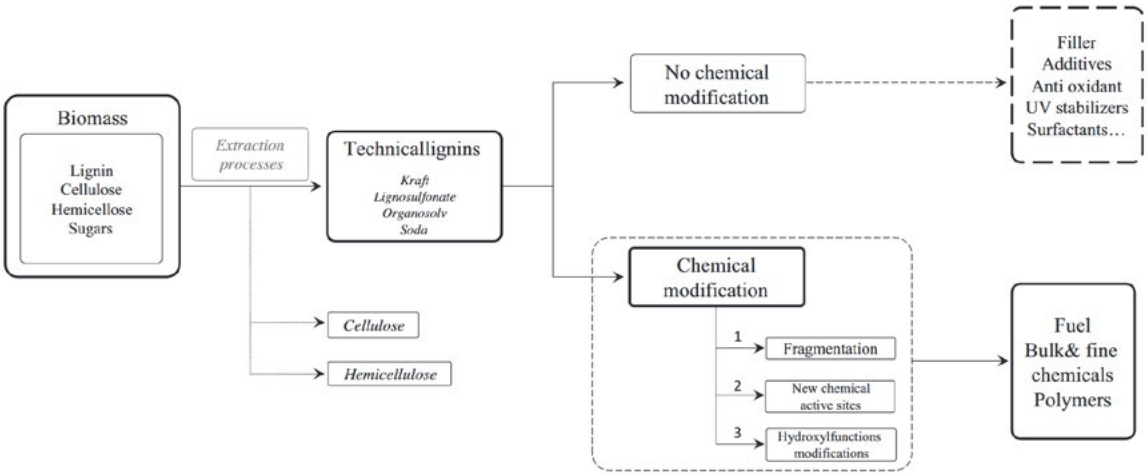

Figure 8. Global Lignin Use Scheme(bottom), from Laurichesse & Avérous, 2014

2.5.1 Kraft Pulping

The kraft pulping process is the dominant technology used for pulping in the paper industry, with approximately 130 million tonnes annual pulp production. Wood chips are treated at 170°C for approximately 2 hours in an aqueous solution containing sodium hydroxide and sodium sulfide. During this treatment, lignin is depolymerized into smaller, water- and alkali-soluble fragments due to the action of the hydroxide and hydrosulfide ions. Lignin is then recovered from the resulting black liquor through precipitation, achieved by reducing the pH with CO_2. The precipitated lignin is further isolated to obtain a high-purity lignin stream. The kraft process is widely used because of the ability to recycle the inorganic pulping agents (Na_2S and NaOH), ensuring cost efficiency and sustainability (Mathew et al., 2018).

2.5.2 Soda Pulping

The soda pulping, often soda-AQ (anthraquinone) pulping is another method of pulping plant-based materials. While this process has struggles in extracting lignin from hardwood materials it is mainly used for agricultural residues. The raw material is cocked in a caustic soda at temperatures of 150 to 160 degrees Celsius. This separates lignin from cellulosic materials (Singh et al., 2019). Caustic soda is a sodium hydroxide (NaOH) solution with water. Therefore, the soda pulping process produces sulphur free and alkali lignin, distinguishing it from the kraft pulping process. Nowadays, the soda pulping process, which makes around 5% of the total pulp production, is considered an outdated technique.

Spectroscopy analyses revealed that significant differences in the structural characteristics of alkaline lignins and kraft lignins can be observed. Alkali lignins exhibited a higher content of phenylglycerol structures (8–14%) compared to kraft lignins (<5%) (Zhao et al., 2019). This is a direct result of the extraction process. These phenolic end groups on the lignin molecules have a significant impact on the molecules reactivity (Kenny et al., 2023) and its cross-linking capabilities and are therefore to be considered in the choice of an appropriate lignin source in this research.

Effects of sulphur in lignin, particularly kraft lignin, are often an interference to the usability in various applications. Sulphur in lignin is considered as an impurity and is often undesirable when using lignin in further applications. It can also interfere with cross-linking reactions required

for lignin to act as a natural binder, compromising the mechanical properties of lignin-based composites (Daniel et al., 2019). Furthermore, the heat treatment of lignin's with a higher sulphur content also releases foul-smelling gasses and restrict the acceptability in products used in sensitive environments. During these heat treatments, the thermal and oxidative stability of lignin-based products is negatively impacted by the sulphur. Thus, Reduced sulphur content improves the lignin's reactivity, mechanical performance in composites, and suitability for bio-based applications (Evdokimov et al., 2018).

2.6 Polymerization of Lignin and Production Methods

The capabilities of lignin as a strong adhesive are demonstrated very well in a technique called wood welding (Leban, 2005). Here two pieces of wood are rubbed together at a high frequency and with high pressure. These conditions cause the lignin inside the two pieces to soften and start to flow. The "melted" materials of both contact surface mix together in this process. Once the wood cools down the molten material also sets. As a result, the interlayer between the wood is made of a dense composite forming a strong timber joint.

This technique showcases lignin's tendency to portray thermoplastic-like behaviour under heat and pressure, producing a dense interfacial composite that gives the joint with exceptional mechanical strength.

A condition to achieve polymerisation or cross linking of lignin within a cellulosic material base is this mentioned "melting" process. The point at which lignin softens is a characteristic that is referring to the glass transition temperature (T_g) of Lignin. Lignin is a highly amorphous molecule that has a glassy and hard structure at room temperature. Above the glass transition temperature lignin softens and is able to flow (Ganewatta et al., 2019).

"The glass transition temperature (T_g) of an amorphous material including lignin is used to determine the softening point and to speculate on the level of crosslinking when processing these materials at elevated temperatures." (International Organization for Standardization, 2024).

Generally, the glass transition temperature determines the point at which a material changes states between being ductile and being hard and brittle, this is unique to the amorphous portions of a material. The temperature point at which this shift occurs is unique to each material (Glass Transition Temperature, 2024).

For lignins the glass transition temperature is very dependent on the source – hardwood or softwood lignin – or if the lignin is in its natural shape, as part of woody material for example, or as an isolated material. In the field of wood densification the softening values of the lignocellulosic materials is of big importance, which is why most literature on the practical implications of the glass transition temperature is recorded there. In Morsing, 1998 multiple experimental measurements used to estimate the glass transition of wood polymers are collected. An observation is that the transition temperature shows relation to the moisture content of the material (Morsing, 1998).

The relationship between moisture and temperature is that higher moisture reduces the transition temperature and lower moisture increases the temperature (Figure 9). The literature suggests that the water molecules form secondary bonds with polar groups in the polymer molecules and increases the molecular distance. This reduces the secondary bonding strength between the polymer chains, which in turns allows more space for movement, reducing the needed energy to make the material deform (Kutnar & Sernek, 2007).

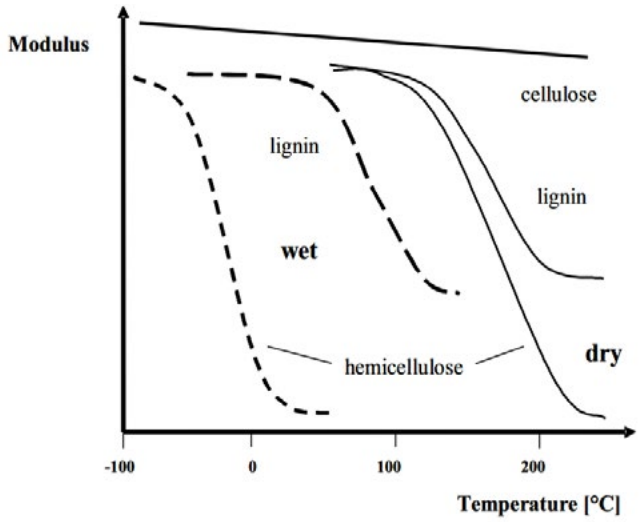

Figure 9. The glass-transition temperature of lignin as a function of moisture content, from Kuntar & Sernek, 2007

To better understand the cross-linking capability of lignin and the previously suggested effectiveness of the (re) polymerization that could depend on the cellulose structure in which the lignin is infused in, this part will explore different sources that demonstrate these principles.

Polymerization Methods

In the current field of research on lignin-based manufacturing of wood-like, bio-based materials that aim to replace conventional production methods there yet is little focus on the development of a construction material with real world application, an exception being research on glue-less particle boards. With the diagram of selected literature in Figure 10 this part aims to provide an overview and the description of multiple approaches that includes the heat treatment, of any kind, to enable the glue-like properties of lignin – and aims to provide the basis of research to produce a new production method as described in the methodology.

The first grouping of the academic sources can be done on whether the material is ultimately hot-pressed, meaning the use of high temperature and high pressure, or if it is used in an

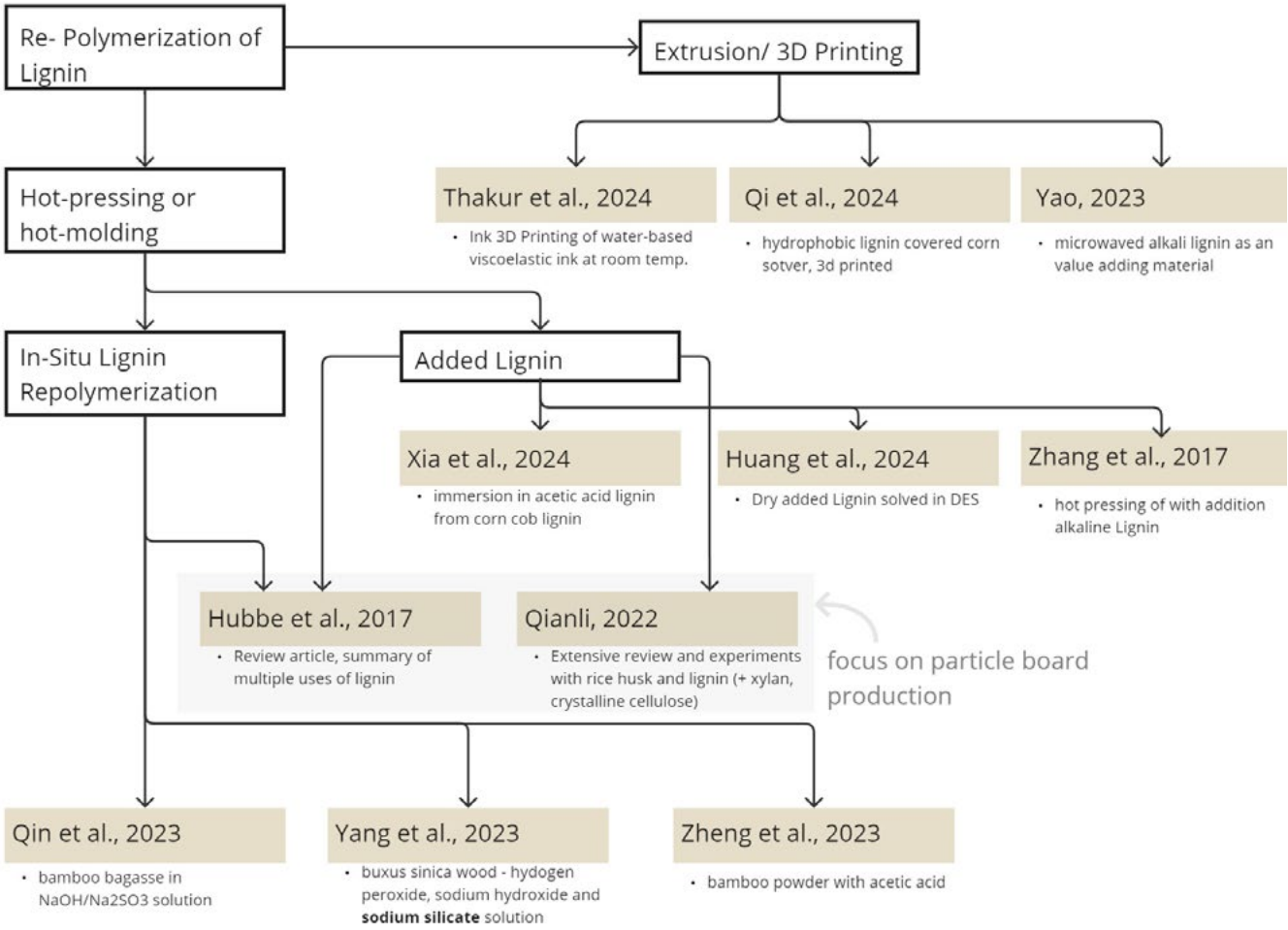

Figure 10. Selected literature on the polymerization of lignin in a cellulose-based material

extrusion process like 3D printing. In the latter case the three shown publications (Figure 10) demonstrate a variant of an extrusion process.

Extrusion based procedures

The most recent publication of 2024 from Thakur et al., which also mentions the research from TU Delft from 2023, describes their research of direct ink writing a room-temperature water-based ink. After a freezing step and heat treatment, the resulting material resembles natural wood on an aesthetic and structural level. This study focused formulating a mixture that is free of any type of binder or phase from secondary polymers. The mixture is made of 25 weight percent (wt%) hardwood lignin, it acts as the natural adhesive and binding agent. Furthermore, with equal amount of 37,5 wt% Cellulose nanocrystals (CNCs) and tempo-oxidized cellulose nanofibrils (TOCN) were used. While the CNCs provide rigidity and act as the reinforcement phase, the TOCNs interconnect within the structure by entangling and hydrogen bonding.

According to Parveen et al., 2017 the tempo-mediated oxidation is used for functionalising the nano crystalline cellulose with carboxylic groups. This results in a better aqueous dispersion of the cellulose.

To achieve a smooth extrusion and stability of the mixture, the rheological properties were optimized and end up mimicking the composition of natural wood.

Making the wood-like material is done in 4 steps in this study (Figure 11). Firstly, comes the ink preparation, mixing the ingredients in a planetary mixer by adding water, while ensuring the uniform dispersion of components and removing bubbles. The second step is the 3d-printing using the direct ink writing (DIW) technique. DIW is a type of extrusion-based printing technique that is typically done at room temperature. It provides multiple benefits namely its inexpensive use and low risk of clogging of extrusion nozzles (Thum, 2023). In this case the nozzle is a 25 gauge (0,455mm) needle for high resolution structures of ~200 µm. The researchers printed a variety of structures like a honeycomb pattern, miniature furniture all with an interlayer separation of less than 100 µm. In step three the models were freeze dried using dry ice to prevent any deformation or cracks and then the moisture was removed at negative 85 degrees Celsius in an evacuated environment, a process called Lyophilizing. This is followed by the fourth step in which the samples were heat treated at 180 degrees Celsius. This softens and re-solidifies the lignin to promote the fusion and reduction of voids (Figure

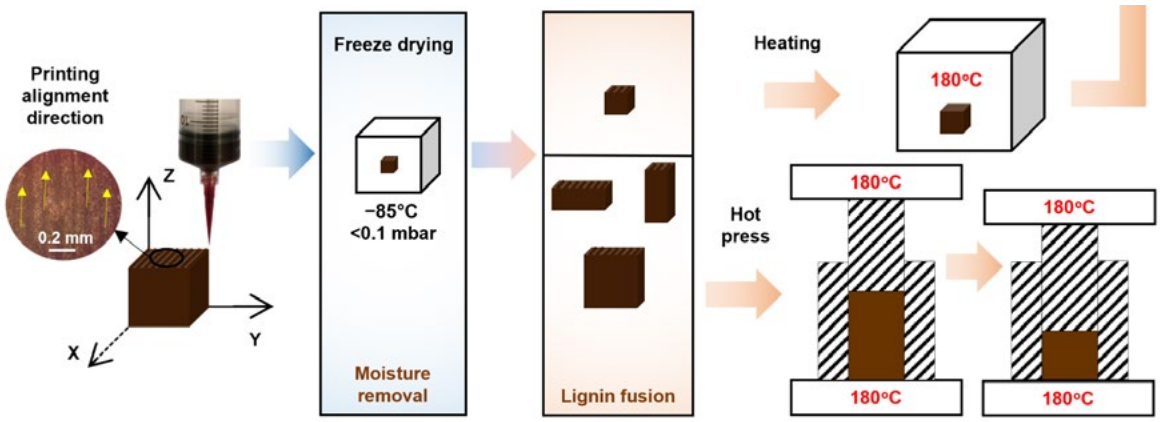

Figure 11. 3D Ink Printing and Hotpressing Process, from Thakur et al., 2024

8). Other samples were also hot pressed at 180 degrees Celsius to densify the material and provide additional strength. This saw a strength increase of up to 182% (~32 MPa) of the compressive strength and 1571% (~1,8GPa) of the flexural modulus from heat treated to hot pressed.

In this study thermogravimetric analysis (*Tg*A) was used to study the materials weight loss to evaluate the thermal stability, scanning electron microscopy (SEM) to observe the voids and interlayer bonding as a result of the heat treatment or hot pressing and other analysis were used to gain a comprehensive understanding of the materials behaviour.

Qi et al., also published in 2024, also uses an extrusion process. The mixture is however very different, and the preparation procedure of the material requires use of additional solvents. Most different here is the use of a plastic matrix and lignin from corn stover for in-situ regeneration, to improve the interfacial combination in a wood plastic composite (WPC). Wood-plastic composites are usually made from plant residues and waste plastics, making them eco-friendly, recyclable and low cost. However, WPCs have poor interfacial compatibility between plant fibres (polar) and plastics (nonpolar), affecting their mechanical strength and weather resistance. Thus, the lignin is used in this study as a natural compound to help with this challenge. The plastic used is high density polyethylene (HDPE).

The first step of this process is the in-situ regeneration of the lignin. This means the dissolution and regeneration of the lignin inside the corn stover. Deep eutectic solvents are used to extract the lignin and regenerate in an anti-solvent (water) which concentrates the lignin on the surface of the corn stover making regenerated corn stover (RCS).

Following this is the preparation of the HDPE and RCS composites. Using a high-speed mixer both are mixed making a homogenous mix. This is mix is extruded in a mini-twin-screw extruder at 175 degrees Celsius and then injection molded into a molding machine also at 175 degrees. The resulting samples demonstrate enhanced toughness, strength, and stabilities.

Hot-Pressing Procedure: Polymerization of added Lignin

The literature presented in the following was grouped based on lignin being added as an individual raw material to the mixture or material development process. All the sources use hot-pressing as the main manufacturing method.

The focus on alkali lignin as a sustainable adhesive for creating binder-free wood-lignin composites was already a focus in research much earlier. A study emphasizes the role of heat treatment and hot pressing, showing that lignin undergoes structural transformations, including cleavage and cross-linking, to achieve self-bonding (Zhang et al., 2017). The optimized composite, prepared at 160°C and 5 MPa, demonstrates strong internal bonding and is showcasing its potential as an eco-friendly alternative to synthetic adhesives. This study demonstrates the chemical transformation that lignin undergoes during the heat treatment process. Thorough analysis of this chemical process reveals the break-down of β-O-4′ linkages in lignin – ether bonds that form the main substructure in lignin molecules (Mukhtar et al., 2017)– which are relatively weak under heat. However, new linkages form the reorganization of the lignin fragments that are stronger and contribute to making a rigid structure. This process also increases the molecular weight of the lignin, as the fragments join into larger molecules.

In this study specifically works on creating a wood-lignin composite from poplar wood and industrial alkaline lignin. The poplar particles are mixed with lignin 20 wt% and shaped into

mats (5 mm thick) using a forming box. Then the hot pressing is conducted at temperatures between 130 to 180 degrees under 5 MPa for 20 minutes, enabling lignin to act as an adhesive. It is revealed that the lower temperatures favour β-O-4 linkages, while higher temperatures promote cross-linking with the more rigid bonds. A sweet spot was found at 160 degrees.

Xia et al., 2024 describes their research on a reconstructed piece of wood that displays high water stability. After being hot-pressed the lignin within the cellulose acts as a filler and adhesive which enhances the UV resistance and mechanical strength.

The materials used are bark from Broussonetia papyrifera (Paper mulberry) and lignin extracted from corncobs. Additionally, chemical agents are needed: Sodium hydroxide (NaOH), sodium sulfite (Na2SO3), sodium chlorite (NaClO2), acetic acid, and a TEMPO catalyst. The equipment used for the experiments are a hot press and a chemical impregnation system.

In four steps this research conducted the production of the wood sample that is used for testing.

Firstly, the bark had to be chemically pretreated to remove the hemicellulose and existing lignin. This is done in a NaOH and Na2SO3, and subsequent NaClO2 solution, and another step to do a tempo-mediated oxidation. It is mentioned that the presence of the hydroxyl groups of the hemicellulose within the wood reduces the hydrophilic behaviour of the wood, also facilitating the entering of bacteria leading to faster degradation.

The lignin from the corn cob also had to be extracted and dissolved in a mix of acetic acid and water.

With a set concentration of acetic acid and lignin of 1,3g/ml and 5g/ml, respectively the pieces were immersed for 12 hours. Afterwards the impregnated material is pressed at 5MPa and 180 degrees Celsius for 1,5 hours (Figure 12). This melts the lignin, allowing it to fill the gaps in the cellulose structure, form cross-links with the cellulose, and create a dense composite structure.

The key findings in this study that not only a superior strength behaviour could be achieved compared to the natural wood but also a significantly reduced water absorption rate and improved UV resistance were created. The study suggest that the material can be shaped into eco-friendly straws or other forms, outperforming plastic and paper in water resistance

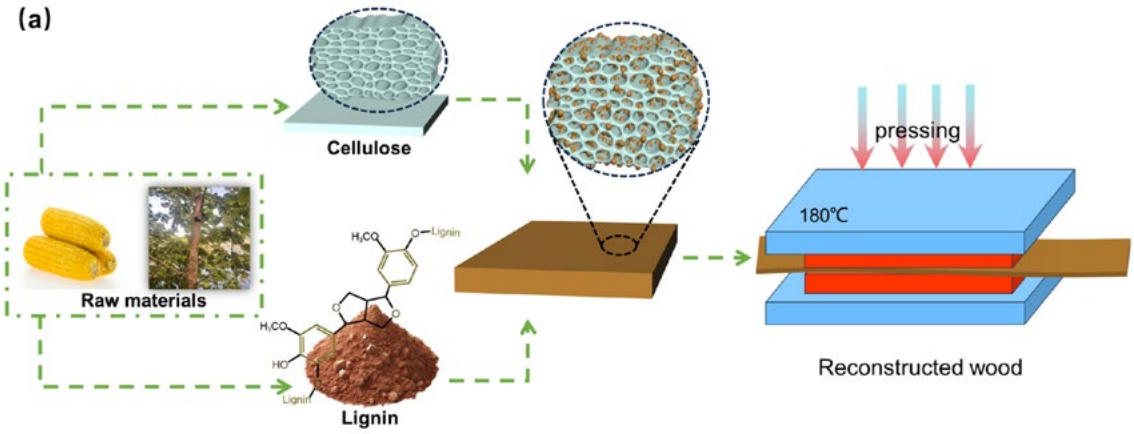

Figure 12. Material Preparation and Hot-Pressing Process. Xia et al., 2024

and strength. It also sees the potential as a green alternative in industries requiring lightweight, water-resistant materials.

Another example of a production process with added lignin is Huang et al., 2024. Here lignin is added to a to bagasse cellulose base materials to increase the wet strength of composite films. The lignin also acts as a reinforcement agent and improving the mechanical properties through self-polymerization and cross-linking during hot pressing.

The cellulose pulp from bagasse, with a low lignin content (~0,8%), is pulverized and mixed with the commercially available, but not further specified, lignin at various concentrations of 0 to 20 wt%. After that the mix is dissolved in an ionic liquid (made from 1-Methylimidazole and Chloropropene) for 1,5 hours at 90 degrees. The resulting solution is spread on a thin film, rinsed and dried. The resulting hydrogel films are hot pressed at 120 degrees and 5MPa for 2 hours.

As an outcome of these tests the created films the tensile strength was increased by up to 7 times, while 10 wt% lignin content yielded the best balance between strength and structural integrity. The films demonstrated other significant results not as relevant for a construction material.

Lastly, in the thesis from Qianli, 2022 a way to produce a substitution for standard wood boards from non-wood lignocellulosic is explored. It aims to develop high strength densified materials that are from a non-wood biomass, while adhering to an environmentally conscious procedure. The thesis provides an extensive review of lignocellulosic biomass including rice husk and bamboo. In the following material experiments each part explores the integration of HCW treatment and hot pressing to maximise the mechanical and physical properties of biomass-derived materials.

Following in Chapter 2 is the discussion of the preparation of a high strength board from rice husk pretreated in hot-compressed water without any external binders. During the hot-pressing, the lignin softens and flows, forming a matrix that binds cellulose and silica within the treated rice husk.

In the subsequent Chapter the fabrication of high-strength RH-based composite materials by blending HCW-treated RH with poly(vinyl alcohol) (PVA) and glycerol (GL) is explored. The incorporation of PVA and GL greatly enhanced the strength, toughness, and water resistance of the composite plates, with significant improvements in mechanical properties and reduced water absorption

After this the focus is on preparing another set of high-strength plates from bamboo residues treated by hydrothermal (HT) processing, investigating the effect of HT time on plate strength. The optimal treatment time of 77 minutes produced plates with maximum strength, where bamboo fibres reinforced the plates and hemicellulose, lignin, and soluble matter acted as binders, and no other additives were used.

The analysis of the produced materials reveals that there were specific strength improvements per material. In the rice husk plates (Chapter 2)(Figure 13), the created lignin matrix improved tensile strength by 2,8 times compared to the untreated material. In the bamboo-based plates (Chapter 4) the lignin matrix enhanced the tensile strength by 1,9 times.

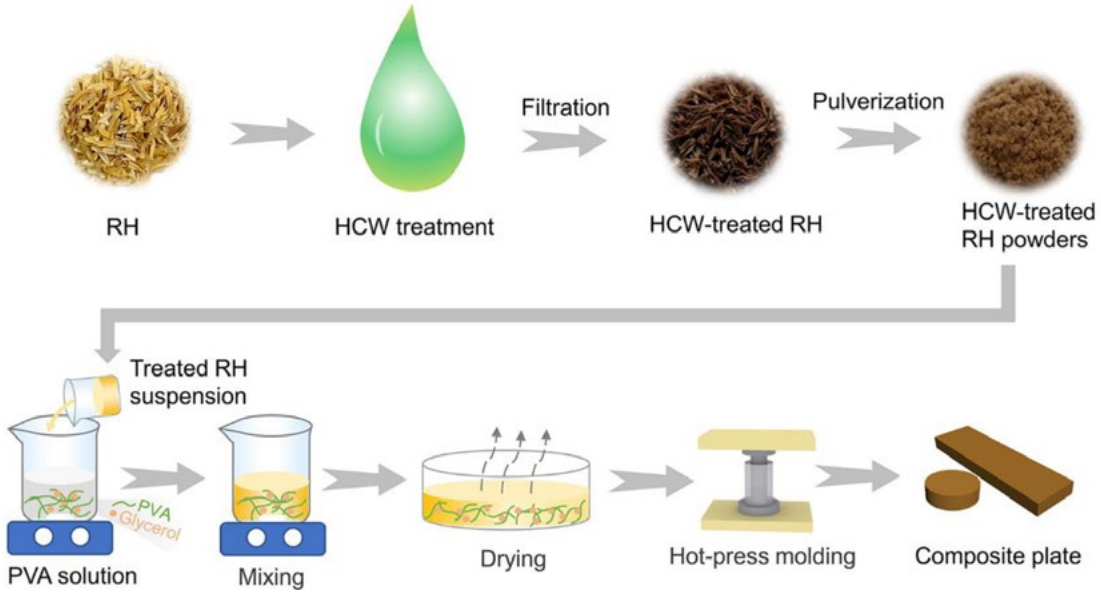

Figure 13. Rice Husk Composite Plate Propduction Process. From Qianli, 2022

Hot-Pressing Procedure: In-Situ Lignin Polymerization

Another example of hot-pressed, self-binding lignocellulosic boards is the study from Hubbe et al., 2017. The study examines the bonding mechanisms in multiple hypothesis, with the interest to find a way to produce particle boards without the commonly used chemical formaldehyde, that poses a lot of health hazards during use production and use.

Four critical links are defined for the development of bonding within the reconstituted wood products (by self-bonding or natural adhesives. These links are:

- Mechanical contact – the surfaces that need to adhere together should be in proximity (µm).
- Molecular contact – the plasticized materials like lignin must be able to flow between the reinforcing components.
- Chemical bonding – strong covalent bonds or a network of secondary forces between the adhesive and lignocellulosic components.
- Structural integrity – "arrangement of particles or fibres needs to have suitable uniformity, connectivity, and absence of large defects" (Hubbe et al., 2017, p. 4).

These four mechanisms are described in their underlying principles based on existing literature for a hot-pressed board.

The mechanical contact is achieved by applying pressure and heat so that particle deformation and softening create close surface contact, thus the higher board density correlates with a stronger material bond. Otherwise, the flow of matrix components like lignin and hemicellulose needs to bond the particles together. A high-density and uniform particle packing also improve the bonding.

For the molecular contact it is defined that the plasticised lignin or hemicellulose are required to wet the cellulose fibres at the molecular scale. Here the wettability depends on the surface

energy. The removal of waxy substances will improve the bonding. Also, the moisture content affects the glass transition temperature of lignin, it can be used to enable a better flow and contact.

The glass transition temperature is the critical point where pure polymeric materials become soft. For lignin this temperature has been reported between 200 and 220 degrees Celsius.

In order to provide the appropriate chemical bonding mainly covalent forces are needed otherwise secondary forces like hydrogen bonds or van der Waals forces should provide a robust connection. From the literature, covalent bonds are described to form at high temperatures especially at the board's surface layers. Lignin condensation and cross-linking under heat will also strengthen the bonds.

The structural integrity refers to uniformity of the material particles and absence of defects in the particle arrangements. It is found that the compression ratio and particle distribution influence structural integrity and steam pre-treatment as an example can improve the structural bonding by exposing the lignin at the fibre surfaces.

Furthermore , the additives and activation methods of these are described. Lignin is functional as a self-binder and is central to the binderless board bonding. During the hot-pressing, lignin undergoes condensation reactions which will enhance the structural integrity and water resistance. Additionally, the steam treatment already mentioned can be used to expose more of the lignin on the fibre surfaces of the lignocellulosic material. Additionally, the supplementation of the native lignin with an industrial or modified lignin is mentioned. It can further enhance the bonding in cases where the biomass has insufficient lignin.

Besides lignin, tannins, sugars and proteins can are listed for use as an additive. These can complement the lignin in creating a stronger material. Tannins, a polyphenolic compound, have high reactivity with lignin and cellulose forming both covalent and secondary bonds, under acidic conditions.

Sugars can serve as a cross-linking agent and help to integrate fibres within the matrix. The proteins are mentioned as they can form hydrogen bonds and covalent linkages with lignocellulosic components. Other additives mentioned are glyoxal or diamines, and oxidative agents and enzymatic treatments.

Lastly, through pre- and post-treatments the created material can be further optimized. Steam explosion for example can increase the exposure of the lignin and the bonding strength. Grinding of the raw materials can enhance the particle conformability and surface area, reducing defects.

After treatments could include the controlled curing conditions to prevent warping and enhancing the long-term stability.

The following three pieces of literature all have in common that they are utilizing in-situ lignin repolymerization (Figure 7) to produce a high strength sample plate through a hot-pressing procedure to activate lignin's adhesive properties.

In Qin et al., 2023 "All-natural and high-performance structural material based on lignin-reinforced cellulose" bamboo particles are used to create this plate like material. Through partial delignification and hot-pressing the lignin is used as a natural polyphenolic binder that strengthens the cellulose matrix without any synthetic adhesives.

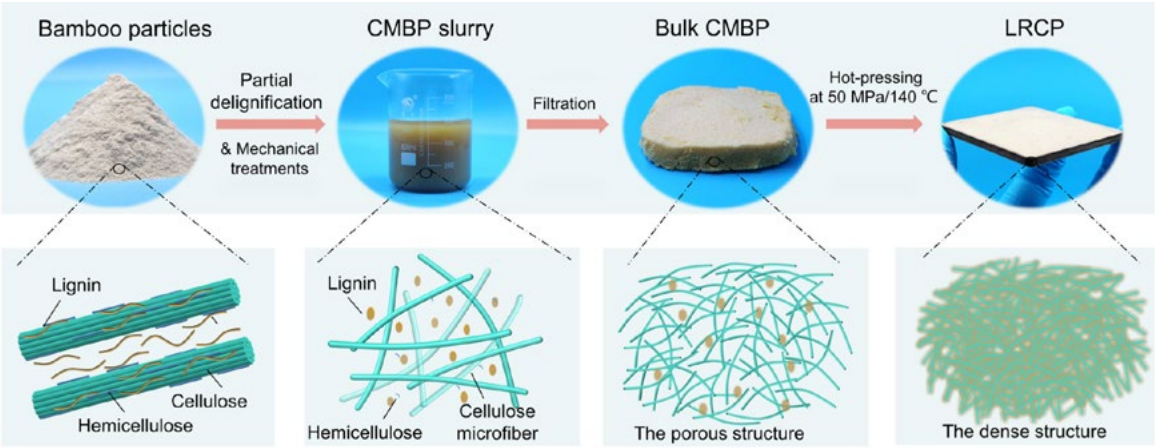

Figure 14. Schematic Illustration of the assembly process of LRCPs. From Qin et al. 2023

The bamboo particles are partially delignified using a sodium hydroxide and sodium sulphite solution. This removes part of the hemicellulose and lignin to expose the cellulose microfibres for better bonding.

The particle slurry from this step is filtrated to a pulp and pre-pressed in multiple stages.

During the final hot-pressing at 140 degrees Celsius and 50 MPa the residual lignin is driven into the cellulose matrix and forms a dense, high strength structure by acting as a binder between the exposed cellulose fibres (Figure 14).

The key results from this study demonstrate advanced mechanical properties and water and flame resistance. Both the compressive and flexural strength surpass the ones of natural bamboo with 178 MPa and 162 MPa, respectively. This strength is also consistent across different directions, unlike natural bamboo.

Zheng et al., 2023 explore the use of acetic acid pre-treatment and ball milling to enhance the adhesion properties of lignin and produce high-performance bio-composites from bamboo. These composites are then compacted through hot pressing, utilising the lignin of the bamboo material as a natural adhesive to bond the cellulose fibres.

First the Moso bamboo powder is treated in acetic acid (CH3COOH) with varying concentrations (0%– 12%) to remove the hemicellulose and enhance the exposure of the lignin around the cellulose bundles. Then Ball milling is used to disrupt the cellular structure which increases the material's density and enables better bonding during the hot-pressing. After a mixing, rinsing and drying process the resulting powder is used to produce plates in a hot press. At 180 degrees Celsius and 30 MPa for one hour the lignin precipitates and re-solidifies as a binder, creating a dense and robust composite. These samples are tested on their mechanical, water resistance, thermal and flame resistance behaviour (Figure 15).

The tensile strength of the material reaches 286 MPa which is 200% higher than the untreated composites. The bending strength reaches 56,5 MPa, with a bending modulus of 9.25 GPa. These improvements are attributed to lignin's adhesive role and the compact structure achieved during the hot-pressing. Also, the water resistance with 8,9% after 24 hours is attributed to lignin forming a hydrophobic carbonised layer during the thermal pressing process. While, the flame resistance through a layer of charring and the reduced porosity was improved, the thermal conductivity also increased due to the denser packing of fibres.

Figure 15. Schematic Preparation of Bamboo Biocomposite Plates. From Zheng et al., 2023

Very similarly to the previous papers, Yang et al., 2023 provide a method of the fabrication of high strength, fire retardant bio composites from small diameter wood using a combination of alkaline pre-treatment and sodium silicate impregnation, followed by hot-pressing. This process utilizes the skeletal effect of cellulose and lignin as a natural adhesive, that enhances the mechanical, hydrophobic and fire-retardant properties of this composite.

The pretreatment of the wood particles requires the use of several chemicals and the in-situ binding of wood fibre. The wood used in this study is from the plant Buxus sinica, a shrub or small tree. The wood is crushed and then sieved and dried to have a even powder. The powder is mixed with hydrogen peroxide, sodium hydroxide and a sodium silicate solution at higher temperatures and later rinsed. The hemicellulose is removed in this step and the sodium silicate improves the fire resistance as well as the structural bonding. This powder with a residual water content of 6% to 8% was hot pressed in moulds at 170 degrees Celsius and 75 MPa which again activates the lignin's' adhesive properties, while densifying the plate.

The measured tensile strength of this material is 106 MPa, which is documented as a significant improvement over the untreated wood composites. This increase is attributed to the removal of the hemicellulose which often disrupt the fibre bonding and the lignin being activated as an adhesive. The hot-pressing process, combined with pre-treatment, resulted in a highly compact structure with reduced voids, which ensures better stress distribution and improving the overall mechanical integrity. Finally, Yang et al. (2023) demonstrates the successful fabrication of fire-retardant and water-resistant bio composites through sodium silicate impregnation and alkaline pre-treatment, combined with hot pressing. The resulting composites exhibit exceptional hydrophobicity, with a water contact angle of 99.96°, and significantly improved thermal stability, making them suitable for moisture-rich or high-temperature environments. Additionally, the incorporation of sodium silicate enhances flame resistance by forming a protective char layer, which ensures the durability and safety for eco-friendly construction and furniture applications

2.7 Cellulose Sources for the Composite Fibre Selection

2.7 Cellulose Sources for the Composite Fibre Selection

In the previous Chapter, which focuses on how lignin is polymerized within a cellulose matrix, the process by which this matrix was created was largely secondary. Moreover, the type of cellulose matrix was primarily a reconstructed piece of wood or a wood-based powder/ particles. Building on that, the following section examines various cellulose sources and methods to convert them into a functional matrix. This investigation is guided by the principle of using straightforward experimental designs and production methods, a consideration that shaped the selection of cellulose sources. The selection of the sources is mapped out in Figure 16

As already mentioned, the literature that was described in the previous Chapter utilizes wood particles as the main feedstock for their material development (Qin et al., 2023; Yang et al., 2023; Zheng et al., 2023). Other possibilities are the cellulose products that are derived from an existing process or waste/ resource stream, are non-wood cellulosic materials or chemically refined cellulose.

Chemical Cellulose

The chemically refined cellulose which is often referred to as nanocellulose or cellulose nanofibers are a product of harsh chemical treatments, in order to separate the cellulose from the surrounding non-fibrous material (hemicellulose and lignin). This treatment results in the degradation of the cellulose fibres and loss in the mechanical strength compared to their native state. However, the use of cellulose in the nanoscale allows to make use of the mechanical strength more effectively, as less material defects are present at the nanoscale than the microscale particles with also higher purity (cellulose contents above 85%). Two types nanocellulose types are often referred to, the nanofibrils and the nanocrystals as CNFs and CNCs, respectively.

Campos et al., 2021 makes use of microcrystalline cellulose (NCC), another description of CNCs, to create a 3D printable paste, with additives like glycerine and starch. The NCC is

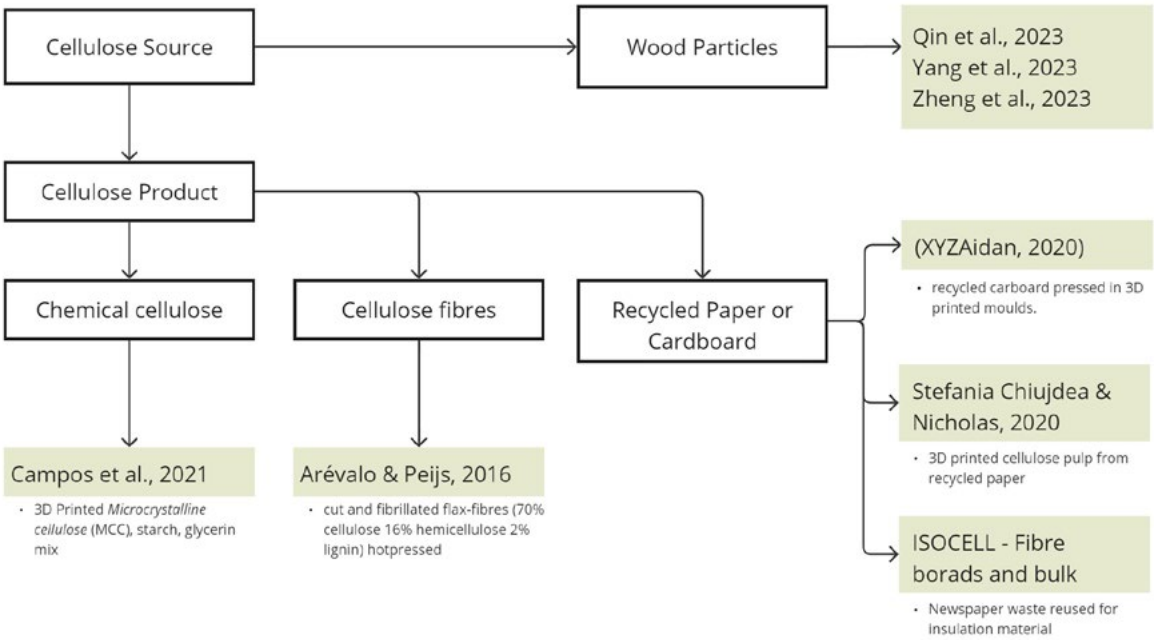

Figure 16. Mapping of the selected literature about cellulose sources

chosen over its high strength, crystallinity, and biodegradability. Specifically, challenges like shrinkage and delamination of layers during drying are addressed in this study.

An exemplary mixture from this study with a good balance of mechanical performance and minimal defects during drying is a composition of 60g NCC, 300g water + 40g starch, 50g glycerine and 50g coffee grounds.

The nanocrystalline cellulose acts as the main structural polymer in the mixture of ingredients, due to its rigidity and high tensile strength. Starch in this mixture acts as a natural binder that creates viscous paste, facilitating the extrusion process. Glycerine is used to enhance the flexibility of the paste also reducing the brittleness. The coffee grounds are an additional natural fibre that is added to reduce the water content in the mixture, improve the texture and minimise the shrinkage and delamination. Other fibres like sawdust and fruit peels were also tested.

The pastes were extruded in a cold extrusion process using a Lutum 4.0 3D printer with a nozzle size between 3 and 6mm depending on the fibre granularity. The printed samples were then dried at 35-55 degrees Celsius for 24 hours. The long drying process minimised the shrinkage and preserved the structural integrity.

The addition of natural fibres overall improved the stiffness and layer bonding of the samples. It also affected the workability in a positive way compared to a mixture with only NCC as a fibre. While all tested mixtures were compatible with the paste extrusion modelling but here the mixtures with natural fibres outperformed the pure NCC in terms of structural integrity and reduced drying-induced issues. The authors conclude that the drying state still remains the critical issue due to the shrinkage from water evaporation.

Cellulose Fibres

Non-wood cellulosic fibres demonstrate their potential for production of construction materials in several studies, particularly due to their outstanding mechanical properties. Specifically, they can provide high tensile strength to composites with continuous fibre reinforcement. Table 3 shows a selection of fibres that were used in the studies of Jakob et al., 2022. This

Type of fibre	Tensile strength (MPa)	Modulus of elasticity (GPa)
Cotton	285–800	5.5–12.6
Jute	395–775	27–55
Flax	345–1830	28–100
Hemp	310–1110	32–70
Ramie	400–940	44–128
Sisal	350–700	9–22
Curauá	545	64
Kenaf	195–665	60–66
E-glass	2000–3000	70

Table 3. Table with the tensile strength of a selection of natural fibres (Jakob et al., 2022)

makes natural cellulose fibres a relevant for consideration for further investigation. Arévalo & Peijs, 2016 explores the production of binder less and all-cellulose based fibreboards from microfibrillated flax fibres, without the use of synthetic binders or resins. In a hot pressing process the study highlights the self-binding capacity of cellulose, relying on hydrogen bonding within the hierarchical network of cells of the flax fibres of micro- and nanofibrillated cellulose.

The flax fibres, consisting of 70% cellulose, 16% hemicellulose and 2% lignin, were chosen for their low lignin content. This ensures better self-binding, while minimising the thermal degradation and odour during the production process. As the sole processing aid was water.

The production steps divide into three steps. First, the flax fibres were mechanically refined. In a Valley beater 100g of fibres were fibrillated in 15L of water. 6 hours of refinement optimised the microfibrillation, increasing the fibre surface area and enhancing hydrogen bonding. Following this, the fibre pulp was partially de-watered to a water content of 50%. Lastly, the pulp formed into a cake was dried and compressed in a hot press at 140 degrees Celsius with the pressure gradually increasing to 8 MPa in three stages over 1 hour. Perforated aluminium plates and glass fibre membranes facilitated even drying and minimised warping (Figure 17). The low hot-pressing temperature minimised the potential that lignin would plasticise in the process.

The panels produced with 10mm flax fibres refined for 6 hours achieved a flexural modulus of 17 GPa and a flexural strength of 120 MPa. These results outperform conventional natural fibre-reinforced plastics and panel boards like MDF (Tensile strength of 10,2 – 25,2 MPa and flexural modulus of 2,9 – 5 GPa)[1]. The refinement of reduced the porosity to 11% enhancing the fibre network's density and mechanical strength. A test of the moisture absorbency resulted in 37% absorbed water after 24 hours. The researchers conclude that the drying and hot-pressing process is batch-based, which limits scalability and the development of a continuous production method, such as twin-screw extrusion could reduce water usage and drying efficiency.

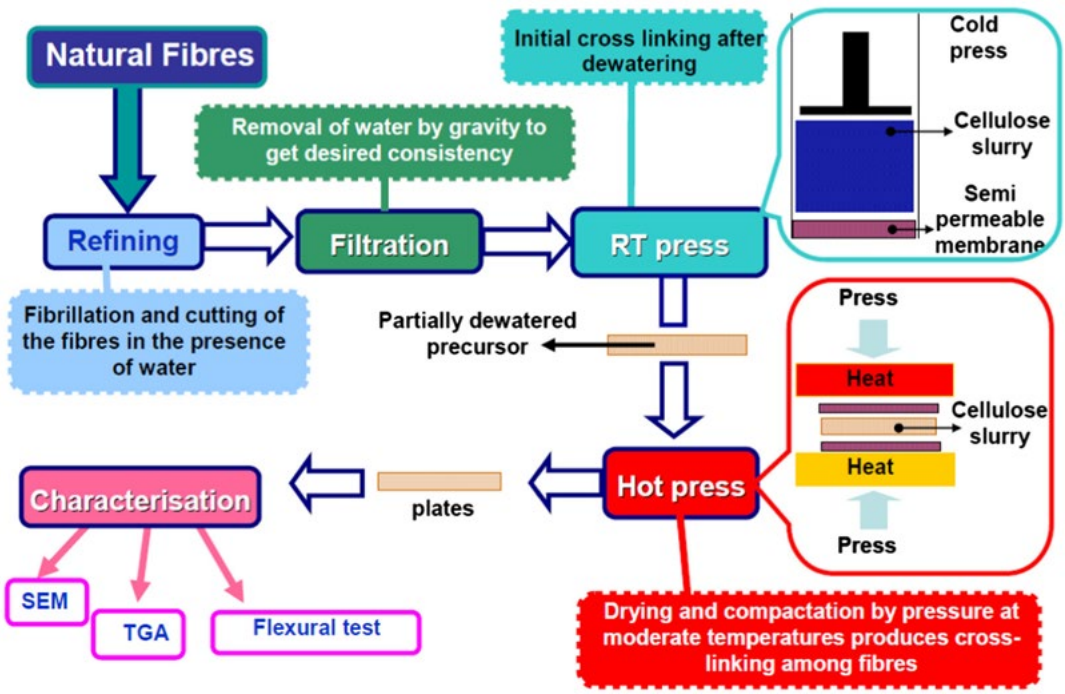

Figure 17. Schematic Experiment Procedure. From Arévalo & Peijs, 2016

1. Ansys® Granta EduPack 2024 R2 Version: 24.2.1, Medium density fibreboard parallel to board.

Recycled Paper and Carboard

With regards to the objective to achieve circularity in the production and disposal of a potential wood-like material, this segment will focus on cellulose structures emerging from existing waste streams in the construction industry, specifically paper, newspaper and cardboard waste.

Generally, cellulose pulp from the kraft process is used for production of high-quality paper. This paper shows the highest concentration of cellulose ranging from 85 – 99% and lignin from 0 – 15% (Kumar et al., 2009).

A much more common available source of cellulose pulp are the waste products from newspapers. Companies like ISOCELL from Germany have specialized on creating insulation materials, boards and plaster boards from cellulose that is sourced from clean and pure newspaper waste (Nachhaltige Wärmedämmung Aus Zellulosefaser | ISOCELL, 2025). The composition of this waste is not solely cellulose as described on the website of the ISOCELL. The composition of newspaper waste can range for cellulose from 40 – 70%, hemicellulose 10 – 40% and lignin 5 – 30%, with newspaper from chemical pulps showing the highest cellulose concentration (Kumar et al., 2009).

The first and academically published example demonstrating the use of paper waste is Stefania Chiujdea & Nicholas, 2020. The study explores 3D printing for producing biodegradable panels from the mentioned recycled paper. It focuses on the interaction between additive manufacturing techniques and material properties, addressing challenges like shrinkage delamination and drying time.

The ingredients used are recycled paper, the primary cellulose structure, glycerine, acting as a plasticiser, improving flexibility and brittleness, guar gum and xanthan gum, both organic binding agents adding elasticity and enabling the malleability during extrusion, cotton fibres as a reinforcement and wood flour to improve the mechanical strength and texture.

For the making of one batch of cellulose-based composite material 600ml of water, 6g xanthan gum + 4,5g guar gum, 45g recycled paper, 30g cotton fibre, 7,5ml glycerine and 22,5g of wood flour were mixed. In the fabrication process a 6-axis robotic arm with a 7 to 10mm nozzle extruded the mixture in the desired patter. The material was printed on a perforated metal mesh to facilitate airflow around the material for better drying conditions. Strategies like spatial printing trajectories and layer interlocking were developed to reduce delamination and allowed for complex geometries.

A compression test resulted in 741,3 N that were resisted before breaking, with 5mm of displacement. The porosity achieved via spatial printing trajectories, reduced drying times and prevented common issues like moulding and delamination. However, a shrinkage of 35% was observed.

The following source is a DIY guide “Recycle Cardboard Into Anything With 3D Printing” published on the website Instructables, targeting hobbyists and makers interested in recycling cardboard and paper into 3D objects using basic tools and 3D printing techniques (XYZAidan, 2020). The maker of this guide who also uploaded a video tutorial about this on YouTube describes here the step-by-step instructions with pictures and STL files for models, designed for accessibility and experimentations.

The guide demonstrates how to recycle cardboard and paper materials into solid 3D objects using 3D printed moulds, a blender and a vice. The process involves converting the paper/

cardboard into a pulp with the blender. Next is the adding of a water-soluble binder. Three variations are being presented in the guide, that the user can choose, which are PVA glue, rice paste and corn starch.

The mixed pulp is then poured into the previously 3D printed moulds and pressed with the vice until the water starts to flow out of the mould. The objects are dried for a day in the mould, so that the shrinkage of the material makes the releasing process easier, and then fully dried after the removal (Figure 18).

This process results it moulded objects that are rigid, lightweight, and share characteristics between paper and wood. The objects are strong and resistant to manual breakage but are not waterproof, as the start to break down when soaked.

Figure 18. "Recycle Cardboard Into Anything With 3D Printing!" from https://www.instructables.com/Recycle-Cardboard-Into-Anything-With-3D-Printing/

Lastly, in the investigation of suitable material sources, keeping in mind the easy obtainability of materials, cellulose feedstock in the form of insulation was investigated (Figure 19). Following an email correspondence material samples of the company ISOCELL, with headquarters in Germany, were sent for the experimentation part of this thesis project. The company provided cellulose fibreboards and cellulose bulk material for blowing into cavities, both used as an insulation material, that are solely made from collected newspaper waste. The only addition to this material is a fire retardant.

Figure 19. Isocell insulation material, from: https://www.isocell.com/en/product/zellulose

With a total GWP of -68.25 kg eq. CO_2 per kg[1] the material shows enormous potential for use in sustainable construction materials. Especially when used in large quantities.

1. from: https://www.bau-epd.at/fileadmin/user_upload/epds_Englisch/BAU-EPD-ISOCELL_2014-1-Ecoinvent_Zellulose_insitu-20140825-English.pdf (accessed 12.05.2025)

2.8 Material Testing

The process of the material testing is mainly determined by what mechanical properties are needed for the computational modelling software. Thus, the identification of these properties will have priority over other commonly tested characteristics like water absorption, fire resistance etc.

The module shown in Figure 20 shows the material properties required for Karamba 3D in Grasshopper.

The publicly available norms & regulations that give direction on testing and calculating these mechanical properties will be listed below. The material type is assumed to be wood-based, particle or fibre boards/ panels.

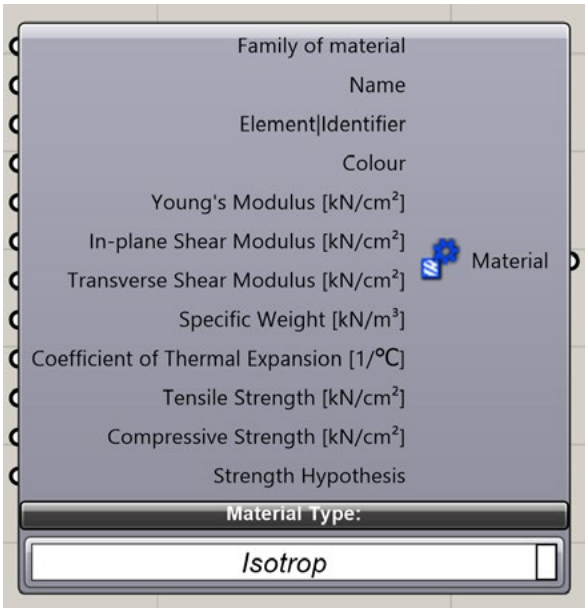

Figure 20. Screenshot from Karamba3D Module in Grasshopper. Material Properties Module for Isotropic Materials

- Young's Modulus (Modulus of Elasticity):

EN 310:1993 Wood-based panels – Determination of modulus of elasticity in bending and of bending strength.

- Shear Modulus:

EN 338:2003 Structural timber – Strength classes

EN 789:2004 Timber structures – Test methods – Determination of mechanical properties of wood based panels.

- Tensile Strength:

EN 319:1993 Particleboards and fibreboards - Determination of tensile

strength perpendicular to the plane of the board. And EN 789:2004

- Compressive Strength:

EN 338:2003 Structural timber – Strength classes

Additionally: ASTM D6641

EN 789:2004 Timber structures – Test methods – Determination of mechanical properties of wood based panels.

The Young's Modulus of wood-based panels is tested with a three-point bending test according to EN 310:1993, supported by EN 325:2012 and EN 326-1:1994. The test is measuring the modulus of elasticity in bending of panels with a nominal thickness of 3mm or greater. The method provides values for design and quality control purposes.

The minimum number of small test pieces cut from a single panel are described in Table 1 of EN 326-1:1994. Testing of the modulus of elasticity in bending and bending strength requires a sample number of 6. These specimens are cut according to a predetermined plan ensuring unbiased sampling from the panel (Figure 1). The size should be rectangular with a width of 50 ± 1mm and a length equal to 20 times the nominal thickness + 50mm, but not exceeding 1050 mm (EN 310:1993). Specimens are conditioned to a constant mass at 20 ± 2°C and 65 ± 5% relative humidity.

The apparatus for testing should include supports of 15mm diameter and a loading head of 30mm diameter, also ensuring parallel alignment. The distance between the supports should be 20 times the thickness of the panel, with a minimum of 100 mm and a maximum of 10000 mm.

The procedure of the test is conducted as follows.

First, the thickness at the intersection of diagonals on the specimen and the width at mid-length are measured using sliding calliper, as specified in EN 325:2012.

The specimen ins placed on the supports, ensuring its longitudinal axis is perpendicular to the supports and that the loading head is placed centrally over the specimen.

After the setup the loading is done. The load is applied at a constant cross-head movement to achieve the maximum load in 60 ± 30 seconds. Meanwhile the deflection is measured at the centre of the specimen with at least six pairs of incremental readings during the elastic range.

Finally, the maximum load is recorded with the corresponding deflection. The modulus of elasticity E_m (in N/mm2) is defined as:

$$E_m = \frac{l_I^3(F_2 - F_1)}{4\, bt^3\, (a_2 - a_1)}$$

where

$F_2 - F_1$ is the increment of the applied load between 40% and 10%,

$a_2 - a_1$ is the increment of specimen deflection corresponding to 40% and 10% applied load,

l_I is the span between the support pins and bt is the specimen width times thickness.

The shear modulus testing procedure for wood-based panel is based on EN 789:2004. The tests measure the in-plane and transverse rigidity based on the orientation of the test sample within the apparatus.

The specimens to be tested are of rectangular shape with a gauge length between 120 mm and 150 mm centred between the rails of the testing apparatus. This apparatus includes two rails that attach to the test piece and apply uniform pressure along the diagonal of the specimen. The load should be applied at a constant rate ensuring the maximum load to be applied within 300 ± 120 seconds. The deformation is measured as the average of the readings from both sides of the test piece. The shear modulus G_v (in N/mm2) from linear elasticity is obtained by:

$$G_v = \frac{0{,}5(F_2 - F_1)l_1}{(u_2 - u_1)lt}$$

where

$u_2 - u_1$ is the increment of deflection corresponding to 40% and 10% applied load,

l_1 is the gauge length and lt is the length of the test piece time the average thickness.

Additionally the shear modulus can be derived from the combination of the materials Poisson ratio and the elastic modulus *E* where:.

$$G = \frac{E}{2(1+\nu)}$$

The testing of wood based panel's tensile strength, perpendicular to the plane of the panel, is described in EN 789:2004 and EN 319:1993. Similarly to the previous tests, the sampling of specimens is specified in EN 326-1. According to EN 319 the dimensions should be square with a side length of 50 ± 1 mm. Cut out of a larger plate, the cut edges of the sample should be clean and precise with perpendicular corners. A tensile testing machine that is capable of applying force perpendicular to the test specimen's surface at a controlled rate is required. Self-aligning grips with ball and socket joints should be installed to prevent an uneven force distribution.

The test pieces need to be glued to a loading block using a suitable adhesive (like hot-melt or epoxy glue). With excess glue removed and a curing time of 24 to 72 hours, the specimen can be placed in the grips of the testing machine. The load will be applied at a constant rate so that the maximum load is reached within 60 ± 30 seconds.

The failure mode needs to be recorded so that it is ensured that the failure can be attributed to the panel and not at the glue line or loading blocks. If this happens the test is invalid and must be repeated.

The tensile strength f_t (in N/mm2) is defined as:

$$f_t = \frac{F_{max}}{A}$$

where

A is the cross section area of the specimen.

The compressive strength of the test samples is also measured according to EN 789:2004. The sampling guidelines from EN 326-1 are used to select an unbiased sample of the panel.

The dimensions of the specimen must be rectangular with a cross-sectional width of 50 mm ± 1 mm and a length proportional to the thickness of the panel. The dimensions must be compliant with Annex A of EN 789.

The compression testing machine should be capable of applying a uniform load along the longitudinal axis of the specimen with 1% accuracy of the applied load. The test peace must be prepared to have smooth ends, that are parallel to each other and perpendicular to the length of the specimen. Then the piece is positioned in the testing machine between two compression platens. The load will be applied at a constant rate so that the maximum load is reached within 300 ± 120 seconds. The Deformation is measured using gauges placed on the opposing faces of the specimen, with a gauge length of 75 to 125 mm. If the failure mode during testing is local buckling or splitting unrelated to compressive stress, the result should be discarded.

The compressive strength f_c (in N/mm2) using the formula:

$$f_c = \frac{F_{max}}{A}$$

2.9 Research Discussion – Material Design and Production Methods

In this discussion the results of the literature review on material types and properties, polymerisation, cellulose structures, production methods etc. will be interpreted in relation to the objectives that were set for this report. Furthermore, this segment aims to explore the implications on pursuing the research question and sub questions of the found information.

The research concludes that cellulose-lignin composites hold significant potential as sustainable alternatives to conventional construction materials. Through systematic exploration of material properties, additive selection, and production methods, this study identified that the process of hot-pressing and therefore the polymerization of lignin within cellulose is possible and therefore confirming the assumption from the research statements.

The process of performing this polymerisation varies from study to study in composition, source of materials, pretreatment and mixing of the materials. The most common process methods can be noticed in the hot-pressing temperatures. The temperature ranges of the experiments vary only between 140 and 180°C. The applied pressure in the studies, however, vary quite significantly again and range from 5 to 75 MPa, with different pressure times. The timing of the hot-pressing seems to also be connected to the sample thickness, with longer exposure the thicker the material is.

Strength Behaviour

Appendix Table 3 shows the collected mechanical properties that were reported in the literature. The highest flexural strength measured was by Yang et al. with 141,98 MPa, surpassing the all the other materials with more than 60 MPa distance. Their experiments were performed with Buxus sinica wood and in-situ lignin polymerisation. The recorded tensile strength of this material of 106 MPa was only closely surpassed by the material of Xia et al. with a tensile strength of 110 MPa, who utilised Bark of Broussonetia papyrifera and similarly relied on the in-situ lignin for the polymerization process.

The only literature that only relied external lignin sources which also reported on their material strength are Huang et al.. Both Liebarand and Bierach & Coelho documented strength behaviour, however, their research focused on a cold extruded paste and are therefore not comparable to the other literature in terms of their post-process behaviour. Huang et al. also only documented a tensile strength of 5 MPa. Also of note is that this research focused on the development of a thin film material, rather than a construction material. Drawing comparisons is therefore also not directly possible

These outcomes demonstrate that there is a noticeable research gap on the development of a hot-pressed material based on both cellulose and lignin as raw materials. It is noteworthy that the literature did not specify that the use of lignin and cellulose in the way proposed in this research project is not possible or not feasible in any way.

Additives

The information obtained from the state-of-the-art production types on the lignin polymerisation includes a range of mild to strong chemicals, of alkali and acidic nature. Considering the objectives set in the beginning of this research phase, serious considerations have to be made before including any of these chemicals in the production process.

For example, sodium hydroxide (Yang et al., 2023), which is a strong alkali, is used to remove lignin from lignocellulosic material. It requires the use of a professional laboratory environment and handling with a lot of care, due to its high corrosive action not only to the skin but also to equipment like metals. While it is a commonly used chemical in many industries like beauty

industry, its improper disposal can also cause environmental damages. All these factors are opposing the initially made objective to not rely on harmful substances. The use of NaOH has to be exceptionally justified in the case that the material development really requires it. Alternatively, a less hazardous replacement should be found.

Acetic acid on the other hand is a much more natural additive if compared to NaOH. It is the main component of vinegar, which contains 4% to 18 % acetic acid. It is also used widely used in several industry branches. Acetic acid is in the reviewed literature used to assists the breaking of lignin bonds to make the cellulose more accessible. The affects of these two chemicals can be described as similar as they both assist the better exposure of cellulose fibres. However, if one is replaceable with the other should be demonstrated in experiments .

Appendix Table 1 gives a summary of all relevant additives and chemicals used in the mixtures for certain property adjustments or to prepare the mixture in a specific way.

In summary not all materials are suitable for application in the experiments. The most likely use of some of these additives is to control the mixture properties, like the viscosity, water content and flow behaviour prior to hot-pressing. Methylcellulose, bentonite, alginate, guar gum, corn starch can all act as binders in the mixture, increasing the water content and improving the mixtures cohesion, while being non-harmful in application or handling.

Material Development

Mention the bottom-up approach and include the diagrams from P2

Analysing the material mixtures from all the papers reveals that the type of cellulose and the type of lignin is different in every approach. This is not unexpected due to the sheer abundance of cellulose sources. As described in the part about cellulose composition, each plant has a different cellulose structure, each wood type, hard wood or soft wood, shows different cell types, all effecting the properties of the material.

As cellulose does not appear on its own but in nature always in a lignocellulosic state, meaning in combination with lignin (but also hemicellulose) polymers, the type of lignin will also always be different. Each species of plant produces a different lignin macro molecule, with varying properties. The Cellulose-Lignin composition of all the literature sources is summarised in Appendix Table 2.

Taking Xia et al. as an example, this could imply that if the bark material is replaced with one from a different tree and the experiment would be conducted precisely the same, the structural behaviour can change, simply due to the varying chemical properties of the cellulose and lignin.

The consequence of this realisation is that besides the production method, both the sources of cellulose and lignin can directly impact the material behaviour. This must be considered when analysing the produced materials. In case of the cellulose the selection of the appropriate feedstock will be made upon the availability of the material, but also how feasible a scaled-up approach would be. Highly processed celluloses like CNCs or CNFs are obtainable in small quantities and sufficient for sampling material but not realistic to be used for building sized components. In that case the availability of the cellulose, such as the newspaper waste, is more appropriate because it accesses and existing material stream from waste products.

In case of the lignin the decision relies upon processing method that is used to isolate the complex organic polymer. In the literature Kraft and Soda(alkaline) lignin are already identified

as the major byproducts of the pulp industry. Kraft lignin makes up the highest amount of produced lignin as a byproduct in the industry with an annual production of 50 to 90 million tons – 98% of these are used for energy production. The production of soda lignin, also organosolv and hydrolysis lignin, is relatively small. This makes the selection process of the lignin source more difficult, as Kraft lignin shows overall less chemical reactivity, and its sulphur contents create health and environmental concerns in application and handling, especially in a process that applies heat to the material. Kraft lignin in the aspect of availability is the most ideal lignin source as it is highly abundant yet highly underutilized.

For the experiments in this research, it can not be guaranteed that the created sulphur vapours can be suctioned off or prevented during the operation of the hot press. So, another type of lignin could be used that is not as abundantly available but would be less problematic to work with.

When looking at the looking at the material mixing and subsequent polymerisation method that is used in the papers, two main concepts are used:

- Lignin-infused cellulose structure (polymerising lignin within an existing cellulose matrix).
- Mixing lignin into cellulose (creating the mixture first, then shaping and hot-pressing).

The first concept is very well demonstrated in Xia et al. where corncob lignin is used to infuse the cell structure of delignified bark. This technique is also mentioned as wetting the cellulose structure with the lignin solution. The second concept is represented in Thakur et al. as the only study to use lignin as a raw material. All the other studies that apply this concept perform the polymerisation with in-situ lignin, meaning the woods own lignin. Qin et al., Yang et al. and Zheng et al. demonstrate with method that very high performing materials can be created.

As a conclusion or proposal for the experimental phase for Figure 21 depicts the two methods of combining the mixture constituents lignin and cellulose.

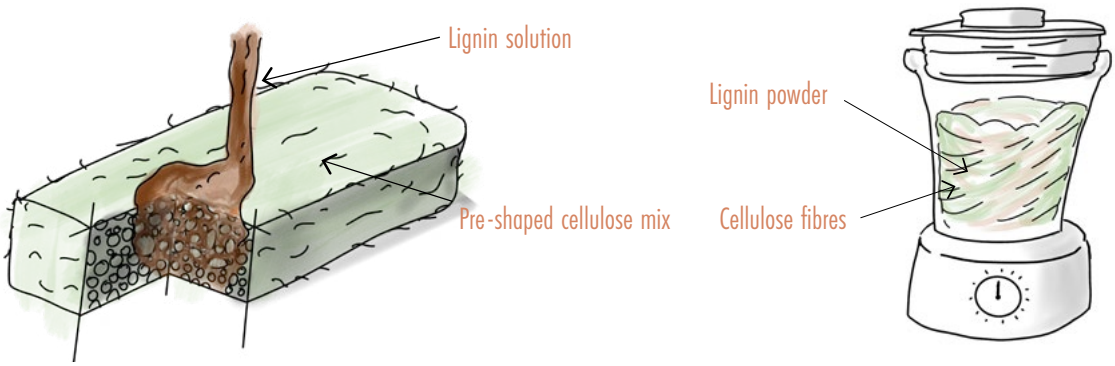

Figure 21. Possible methods of combining cellulose and lignin in the pre-pressed state.

Assumptions for Production Methods.

Following an initial talk with the personnel from the composites lab at the Faculty of Aerospace Engineering at TU Delft, it turns out that the hot-pressing process requires a very meticulous planning process and safety and risk assessments. Only the combination of moisture and trapped air in the material can cause sudden expansions when releasing the pressure, which can be dangerous to the operator and can cause damage to the machine. Additionally, any additive added to the mixture has to be evaluated by the personnel regarding possible unwanted reactions or release of dangerous fumes. Possible reactions to this safety precaution could mean to create a vacuum around the material that is being hot pressed, the material is fully dried with a certain amount of moisture left or the material is evacuated before being hot pressed to remove air bubbles. This constraint can be used to narrow down the production method to one specific path. However, it could be disadvantageous as the

Table 4. Possible material processing ways.

	Description	
Process 1	3D Printing and Hot Pressing The cellulose material mixture is extruded at cold temperature into the specified shape, dried and then infused with the lignin mix, dried again and hot-pressed	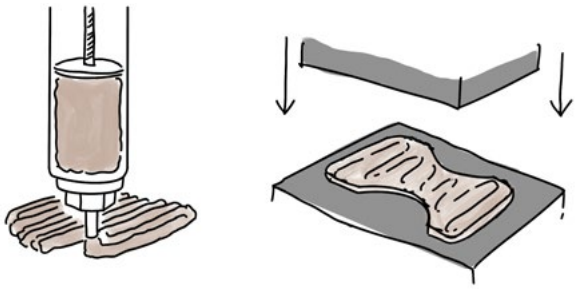
Process 2	Moulding and Hot Pressing Similarly, the cellulose material mixture is formed to the desired shape at cold temperature in a mould, dried and then infused with the lignin mix, dried again and hot-pressed	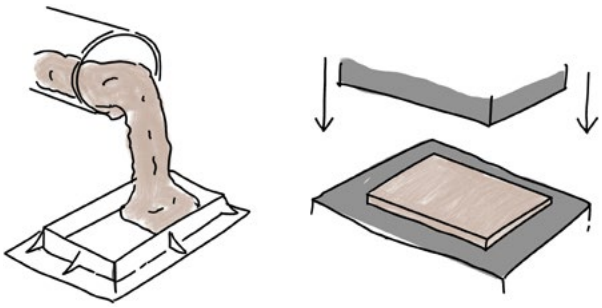
Process 3	Palletisation for Extrusion The material mixture is produced including cellulose and lignin and dried into pellets. Then the material is extruded at high temperatures in a single or twin-screw extruder barrel. The temperatures "melt" the lignin and sets again in the extruded material, solidifying the shape.	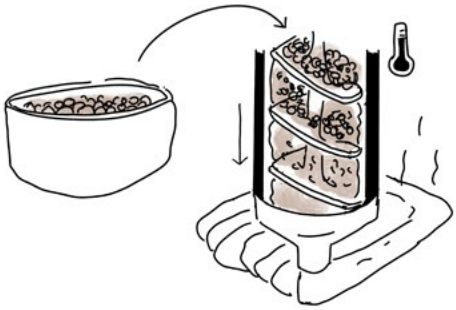

extrusion process, that should follow the development of a material mixture most likely won't have the same constraint.

The following list summarizes the possible production methods, that can be explored in the material testing process, following the research part.

Both, process 1 and 2 can also be explored using a cold mixing process where lignin is already worked into the material mix, then dried and hot pressed.

In Figure 22 an exemplary production process is displayed. This is an example for the use of wetting or impregnating the shaped cellulose material in a lignin solution. Each of the steps is based on a one or multiple of the scientific literatures. With this approach the reproducibility of the described methods can be tested, with the main benefit not to having to set up an entire approach from the base up.

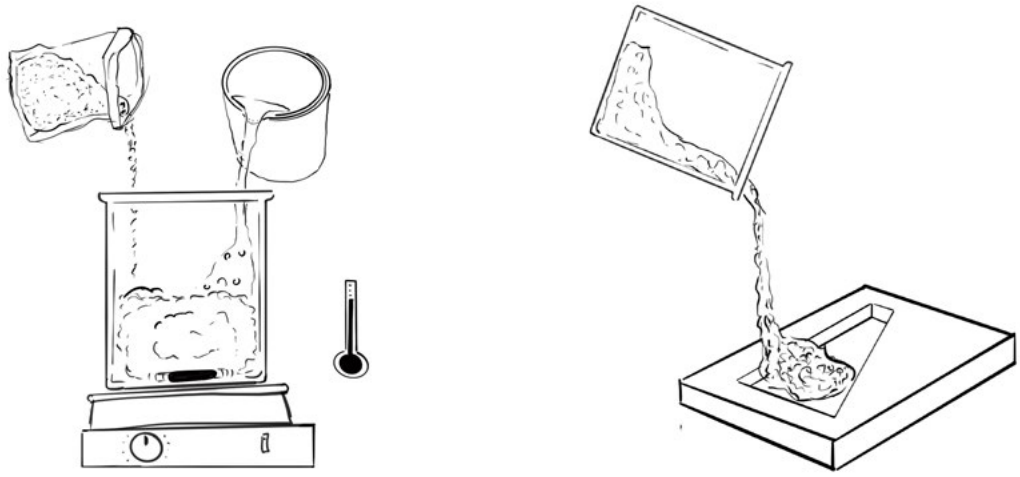

STEP 1:
Possible use of additional cross-linking polymer. (e.g. siloxane compounds) (Grade et al., 2024). Sturdy base mixture made of cellulose and other natural materials. Could use existing research.
- Investigate the pore sizes (Campos, 2021)

STEP 2:
Initial thickness 1.22 mm decreases to 0.1 mm after hot-pressing, and its density increases by 6.4 times (Xia et al., 2024)

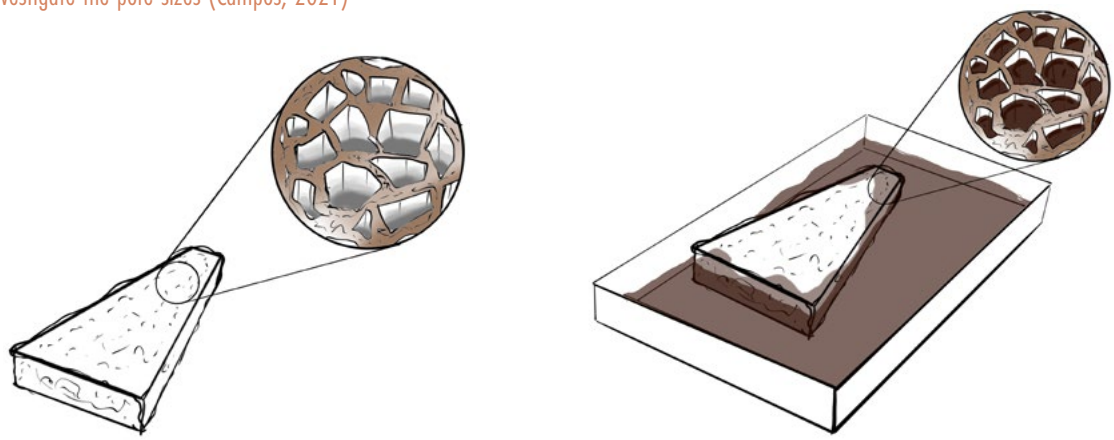

STEP 3:
Drying, Pore sizes 5-30 µm. (Xia et al., 2024)

STEP 4:
"Immersion of material sample in acetic acid lignin for 12 h." „The lignin spontaneously fills the cellulose framework gaps" (Xia et al., 2024)

Figure 22. Exemplary process of making a hot-pressed material from cellulose and lignin based on individual production steps from different sources.

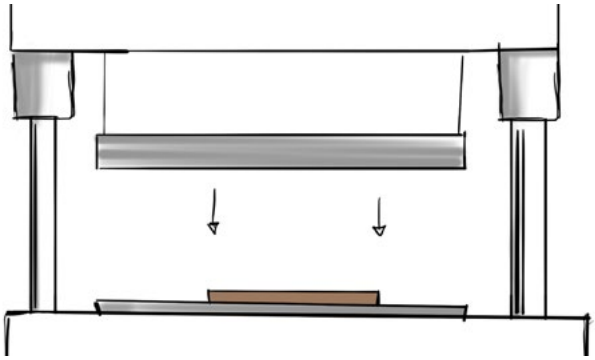

STEP 6
Hot-pressing:
„pre-pressed at 80 C, 1 MPa for 12 h and finally pressed at 140 C (120 C, 160 C), 50 MPa for 90 min (Qin et al., 2023)"
„The impregnated samples are hot-pressed at 5 MPa and 180 C for 1.5 h to obtain reconstructed wood" (Xia et al., 2024)

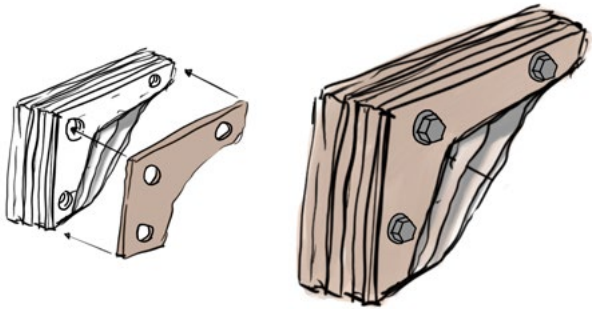

STEP 7
Assembly of structural component out of multiple hot-pressed layers. Connection between layers to be defined. Possible to use ILF - Individual Layer Fabrication

2.10 Computational Methods

To enable a more effective experimental phase and to be able to control the results of the experiments into an optimized direction for structural application, a suitable computational method is needed to achieve a workflow like described in the methodology.

After initial material tests and the understanding of the mixture relationships, these relationships have to be used in an optimisation process to be able to control achieve the controlled variability.

The following will review literature on topics like multi-objective optimization, machine learning integration and multi scale material modelling within the stage of material development. The aim is to provide enough material for a discussion of the self-derived computational framework in this research and to inform this process with methodologies on the late-stage optimisation process that are found in the literature. Figure 23 shows the selected literature that discuss the application computation optimisation frameworks in the construction industry, similar to this projects objective.

- (Lee et al., 2022) Proposed using AI-driven platforms for material discovery, integrating machine learning for predictive modelling of bio composites' mechanical properties.
- (Madurwar et al., 2015) Employed non-linear optimisation for developing sugar cane bagasse ash-based sustainable bricks using LINGO software. The model optimised compressive strength and embodied energy.
- (Laycock et al., 2024) Reviewed computational methods such as quantum-scale modelling, molecular dynamics, and macroscale simulations to predict and optimise biopolymer properties.

- (Feng, Hao, et al., 2024) Utilised molecular dynamics to understand nanoscale fibre interactions in natural composites, linking them to macroscopic properties.
- (Feng, Mekhilef, et al., 2024) Highlighted machine learning applications for wood materials, from defect detection to predicting mechanical properties. Techniques like neural networks and gradient boosting improved accuracy in material property predictions.
- (Kivikytö-Reponen et al., 2024) Showcased AI-driven multiscale modelling for transparent wood composites, leveraging surrogate models to optimise material properties.
- (DeRousseau et al., 2021) Developed a simulation-optimisation framework for concrete mix design to balance compressive strength, cost, embodied carbon, and durability. Utilised evolutionary algorithms like Borg to handle trade-offs among objectives.
- (Sandanayake et al., 2022) Used multi-objective genetic optimisation to integrate cost-effective mix designs for building materials using waste coffee cups.

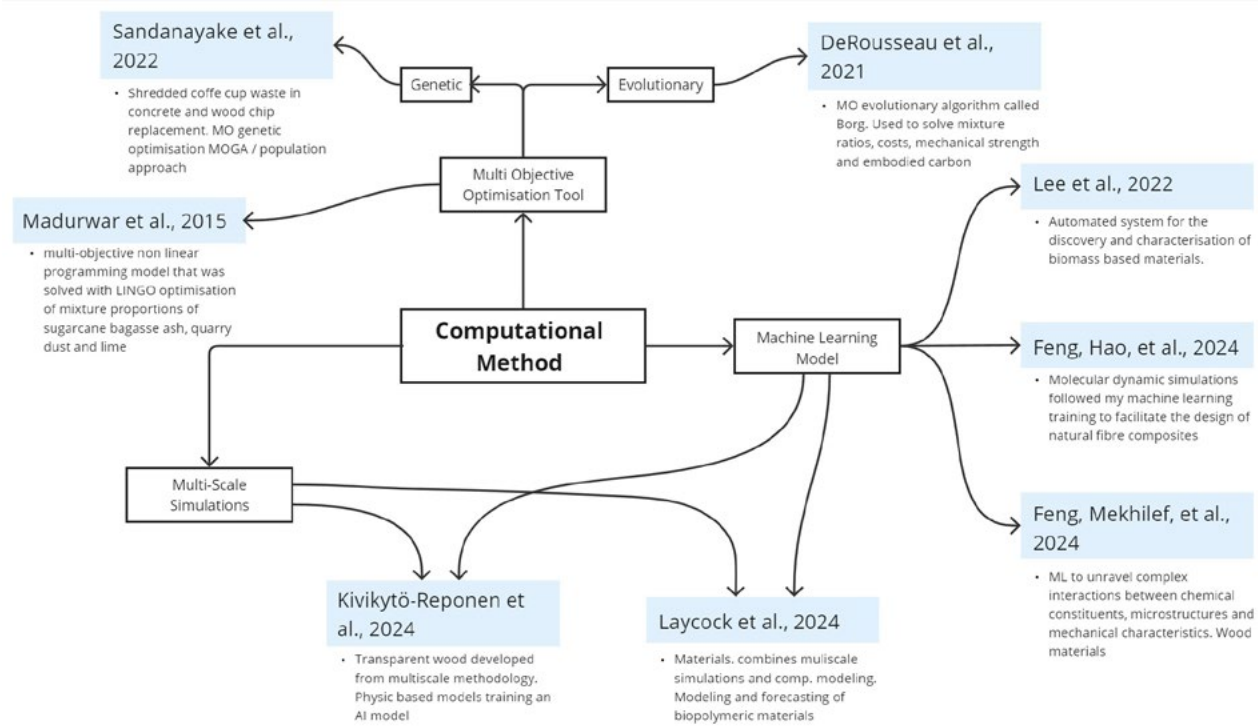

Figure 23. Diagram of selected literature on computational frameworks applied in construction material related optimisation problems

Of the applicable literature references the example of integrating machine learning for predictive modelling comes the closest to the aim of the computational approach of this research. Lee et al. (2022) describe a closed-loop biomaterials informatics platform combining automated fabrication with an AI-driven computational framework. Experimentally, biomass-based hydrogels are homogenized and loaded into a extrusion barrel mounted on a robotic arm. Printed specimens solidify via evaporation into standardized tensile, compression, and bending geometries, which are automatically detected, removed, and mechanically tested under constant load rates and vision-based monitoring

On the computational side, all input compositions, processing parameters, and resulting mechanical properties feed into a digital design environment (Figure 24). Initial analysis employs linear regression and singular value decomposition to uncover basic trends. For richer modelling, the authors suggest an attention-based transformer, FieldPerceiver, treating material components as neural tokens to capture multi-scale process–structure–function links.

To optimize exploration, they suggest to use Bayesian optimization with surrogate neural networks to suggest new formulations, helping reach target properties with fewer experiments. They also apply interpretation methods—like attention-map visualization and decision-tree analysis—to turn complex model outputs into clear design guidelines.

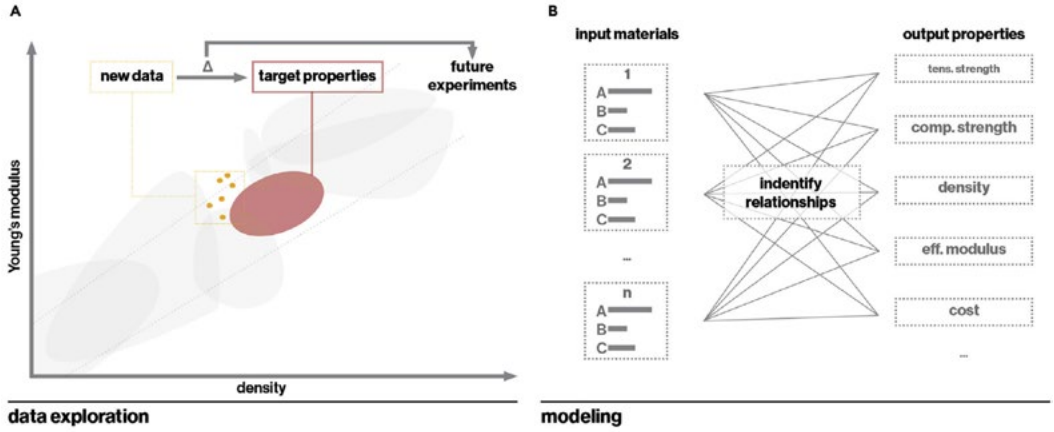

Figure 24. Modelling and selection of future experiments. (A) experimental data is added to growing dataset in order to examine the relationship between composite components and mechanical properties. The difference between the ideal target properties for the biocomposite and the current data can provide a vector to inform future experiments. (B) With sufficient data, models can be trained to identify relationships between input materials and output properties. From Lee et al. (2022)

2.11 Discussion of Computational Approach

The literature on the computational methods displays a variety of approaches that can be implemented in the workflow of this project. It noticeable, that mostly all of these approaches aim to provide simulation methods on the multi-scale level, meaning to simulate not only macro but also micro structural behaviour. This requires a lot of computational time. While this is useful, for projects were a very precise material behaviour is required, within this project the main aim is to create a computational approach that assists the development stage. The leveraging of tools like machine learning and multi-scale modelling has to be further evaluated for their compatibility with the projects objective and timeline.

With respect to the project workflow in Chapter 1.8 the computational approach can look similar to the workflow presented in Figure 4. In this sequence of steps the material experiments and testing are incorporated even though they do not inherently involve computational methods. As one of the first integral steps is the design of the experiments. Early on it determines the same variables that will reappear in the software and material models, like the mixture ratios of fibres and matrix, or possible additives etc. Another set of variables is introduced in the production of the samples, like hot-pressing temperature, time and so on.

The strength testing will produce the necessary information to put the variables in the process in context with a quantitative outcome. This data is the basis on which the material profile is

created. The material profile will describe a specific a mixture recipe and processing conditions and the resulting mechanical performance.

The variation in the profiles will be used to create material relationships. The relationships can be expressed in functions that are either an interpolation of the existing data points or a regression that assumes material relationships past the tested boundary conditions. Other possible relationships could be created or investigated using decision trees or neural networks.

Once those relationships are identified, they can be used in an optimisation process with different intentions of optimisation based on the application case. A likely application can be a structural component. With a digital model that can represent the structural performance based on the material relationships, the optimisation results can be also implemented and translated to an optimised structure.

Hereby the results of the design can still have an impact on the design of the experiment designs and processing conditions. This is what the computational method is striving for, flexibility in design and material exploration to determine possible applications — or rule out designs.

In Figure 25 the logical workflow and combination of testing data and computational integration is depicted. It shows how the early integration of such a computational approach is interwoven with the practical experimentation, as it has a major influence on what characteristics are kept track of, what variables are explored and how are they represented later in the virtual model. Lastly, the prototype design and validation can even refer back to the material relationship model to make adequate changes and make the results more accurate to the real validation data.

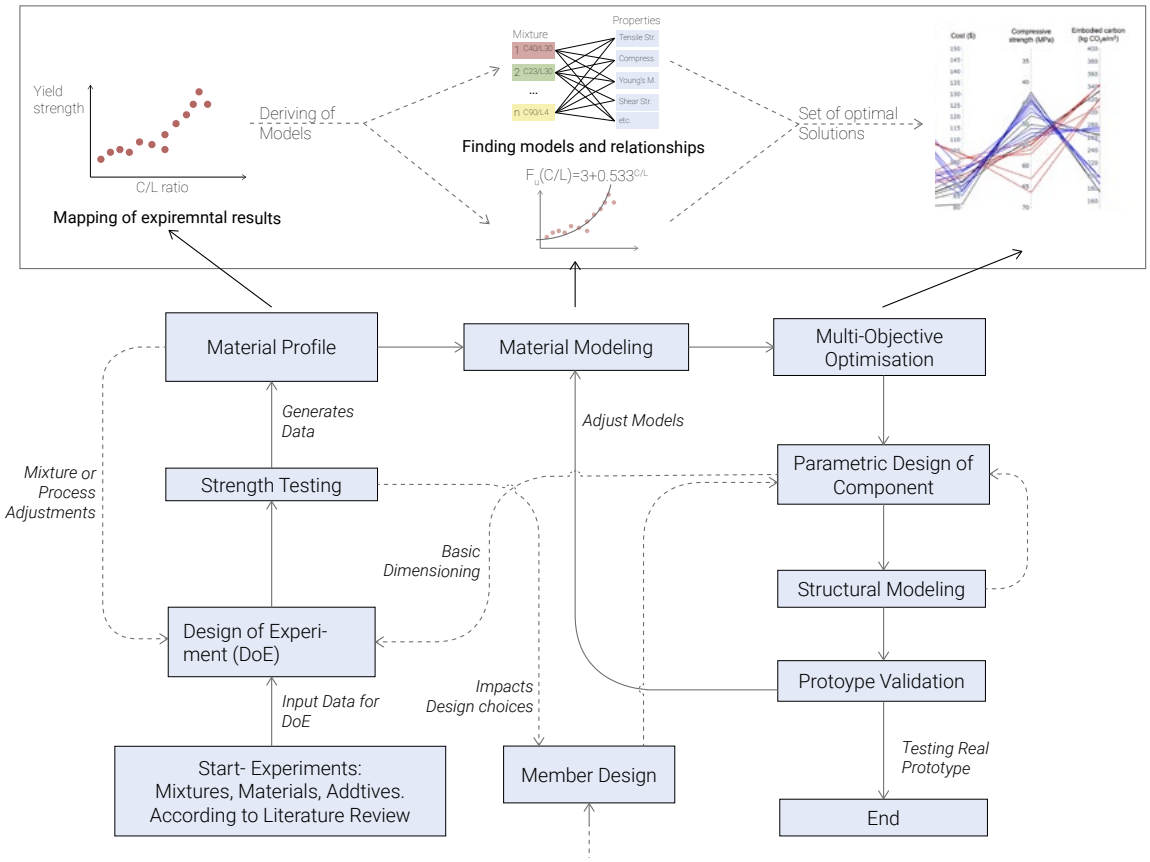

Figure 25. Workflow of potential computational tool that combines material testing and profiling with design and optimisation.

Chapter 3 Experiments

3.1 Mixture Constituents 47

3.2 Production Protocol 51

3.2.1 Step 1 - Mixing 52

3.2.2 Step 2 - Hot-Pressing 54

3.2.3 Step 3 - Post-Processing 56

3.3 Material Trials 59

3.3.1 Moisture Content Variations 60

3.3.2 Cellulose Lignin Variations 61

3.3.3 Lignin Type Variations 63

3.3.4 Cellulose Pretreatment 65

3.3.5 Recycling and Re-hot-pressing of Waste Material 67

3.3.6 Large Scale Hot-Pressing 69

3.4 Differential Scanning Calorimetry of Lignin Samples 71

3.5 Experiment Results 79

3. Experiments

The experimental phase begun after the P2 presentation. Generally, all the steps described in this Chapter went through several optimisation attempts to produce adequate mixtures, hot-pressing conditions and sample finishes to reach the final state of the procedure. In order to follow and recreate all the steps taken in the experimental phase, very rigorous documentation of all the steps was necessary. So, for the mixtures, hot-pressing and testing, protocols were used to write down steps, measurements, deviations and observations that seemed relevant to the process (see Appendix Table 4). The detailed description of all the experiments and how the methods evolved are documented in Chapter 3.3.

Two steps were necessary to fulfil in advance of the start of the experiments: the material procurement and the organisation of facilities to conduct the experiments at.

3.1 Mixture Constituents

Based on the conclusions from the literature review on possible material sources, the selection of the constituents of the material mixtures is focusing on availability, ease of procurement and design feasibility. Additionally, the objective of non toxic, waste-based materials should be kept in mind. The amount of variation is also kept in a reasonable scope. Despite the investigation of natural fibres sources like flax or hemp in the literature review (Chapter 2.7) those types of cellulose sources are not considered for a material trial. The long fibres would create more anisotropic behaviour, which is unfavourable for the virtual models, and the further development of the material to a filament for an extrusion process would be hindered by the long fibres.

Thus the materials are the following (also mentioned in 3.2.1):

- **ISOCELL®** newspaper cellulose insulation material. 3kg of bulk material from ISOCELL at Switzerland and Belgium. Two packages containing their added fire retardant and one sample without.
- **Kraft Paper** (cellulose 85 – 99% and lignin 0 – 15%). Material that was available from the previous work on the Wood without Trees research project.
- **Flax and Jute fibres**. Also available from the previous research.
- **Fibrillated pure cellulose**, type: Valida S231C contains that 8wt% cellulose and 92wt% water
- **Soda Lignin**. Most of the samples were made using the soda lignin that was available from the previous work on the Wood without Trees research project. Additionally, newly ordered soda lignin was used to assess the quality of the already available material.
- **Kraft Lignin**. This lignin type was also available from the previous research.
- **Organosolv Lignin**. Newly ordered lignin, that is used to determine differences in the lignin types as found in the literature review.

Figures 24 - Figure 27 show the three lignin types under the microscope at x250 magnification. The individual grain size ranges from 10 - 50 µm in diameter, with soda lignin demonstrating the largest grains. The difference in colour is similarly noticeable without magnification.

Figure 27 & Figure 29 show the fibres of the newspaper and kraft paper the consist of short fibres, that are ~50µm thick and 100s µm to 2 mm length. The newspaper shows how the fibres are coated in ink and possibly glue as well as other contaminations (little dots and speckles).

Figure 26. Image of Organosolv Lignin under Microscope with x250 magnification

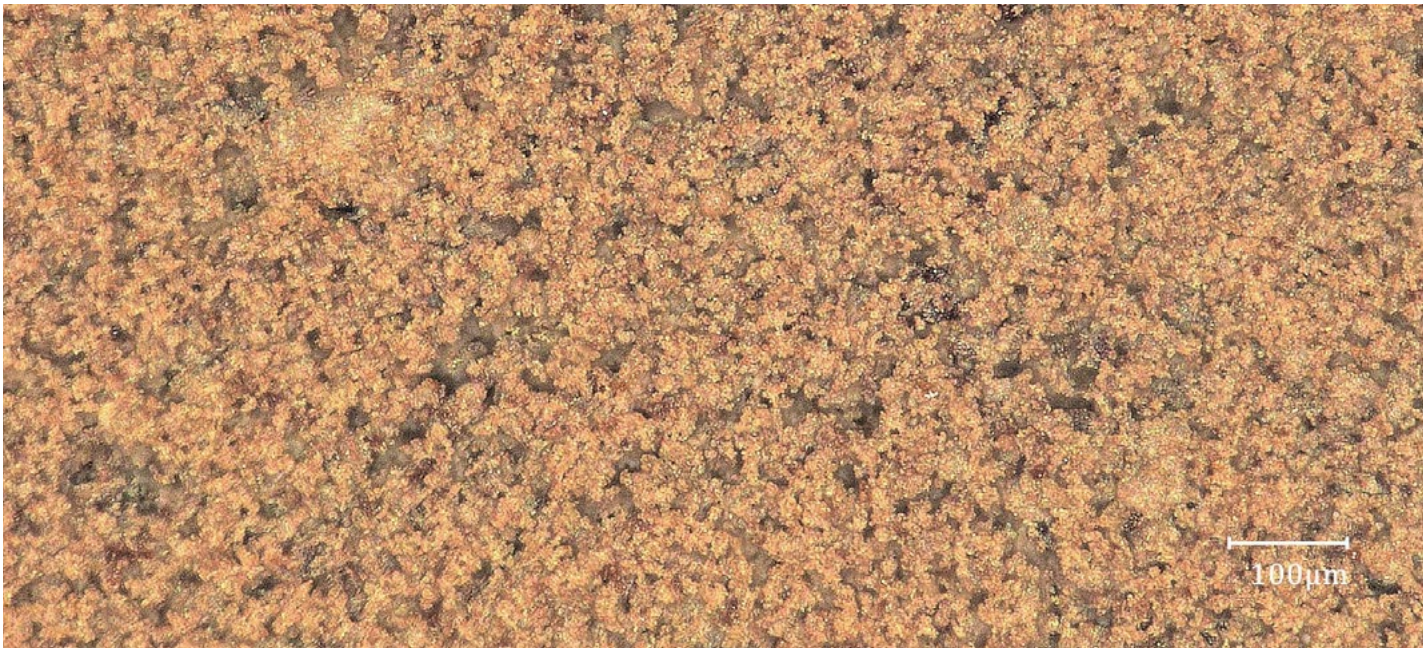

Figure 27. Image of Kraft Lignin under Microscope with x250 magnification

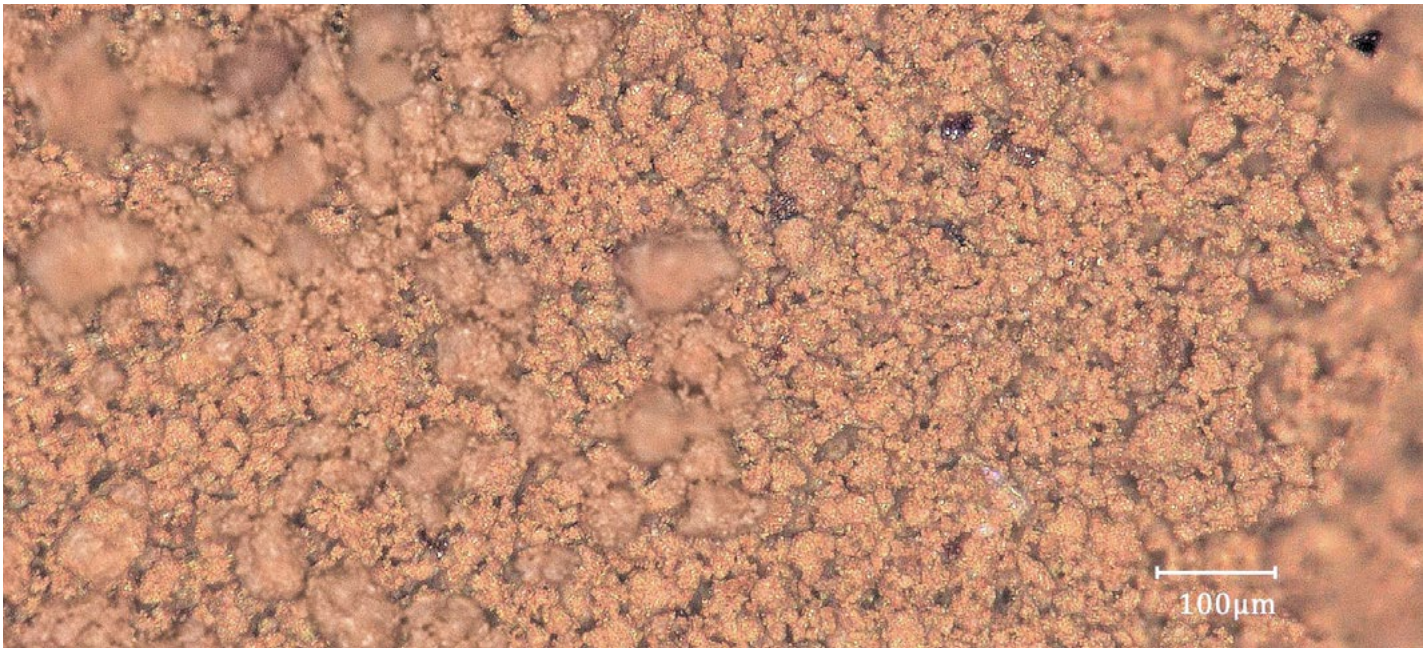

Figure 28. Image of Soda Lignin (Carl Roth) under Microscope with x250 magnification

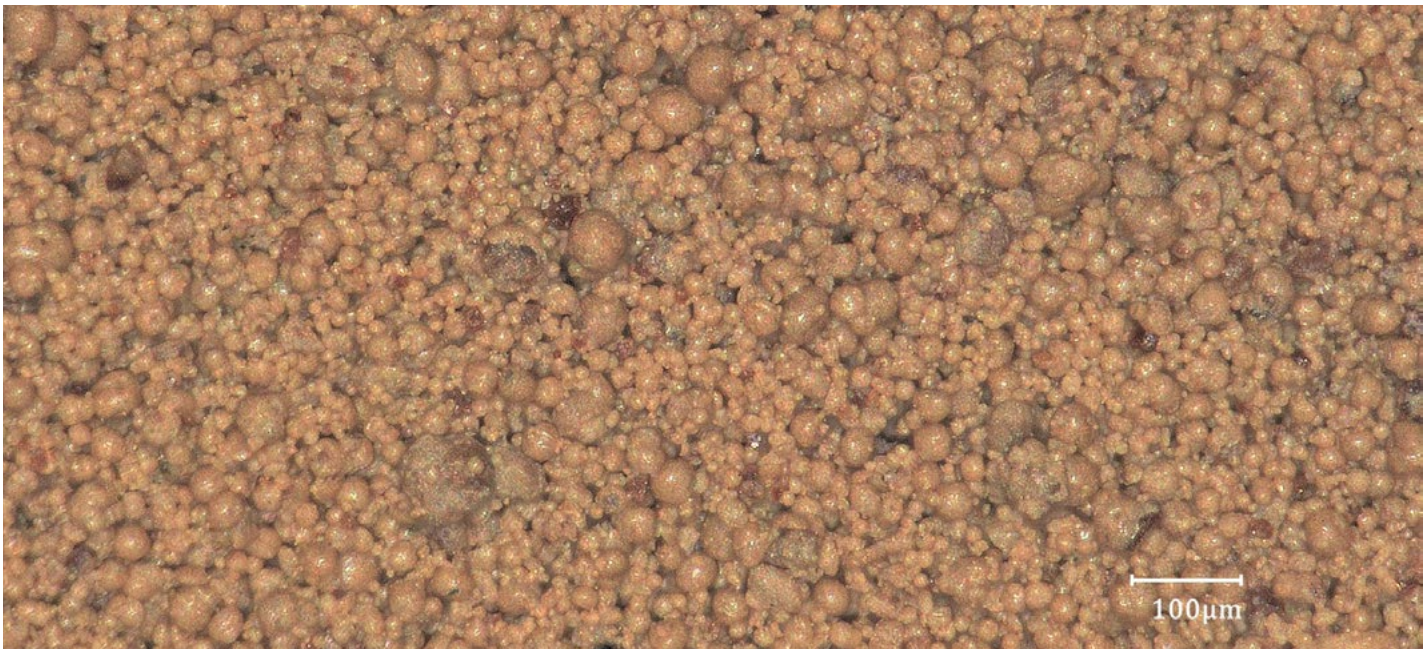

Figure 29. Image of shredded and untreated newspaper fibres with x150 magnification

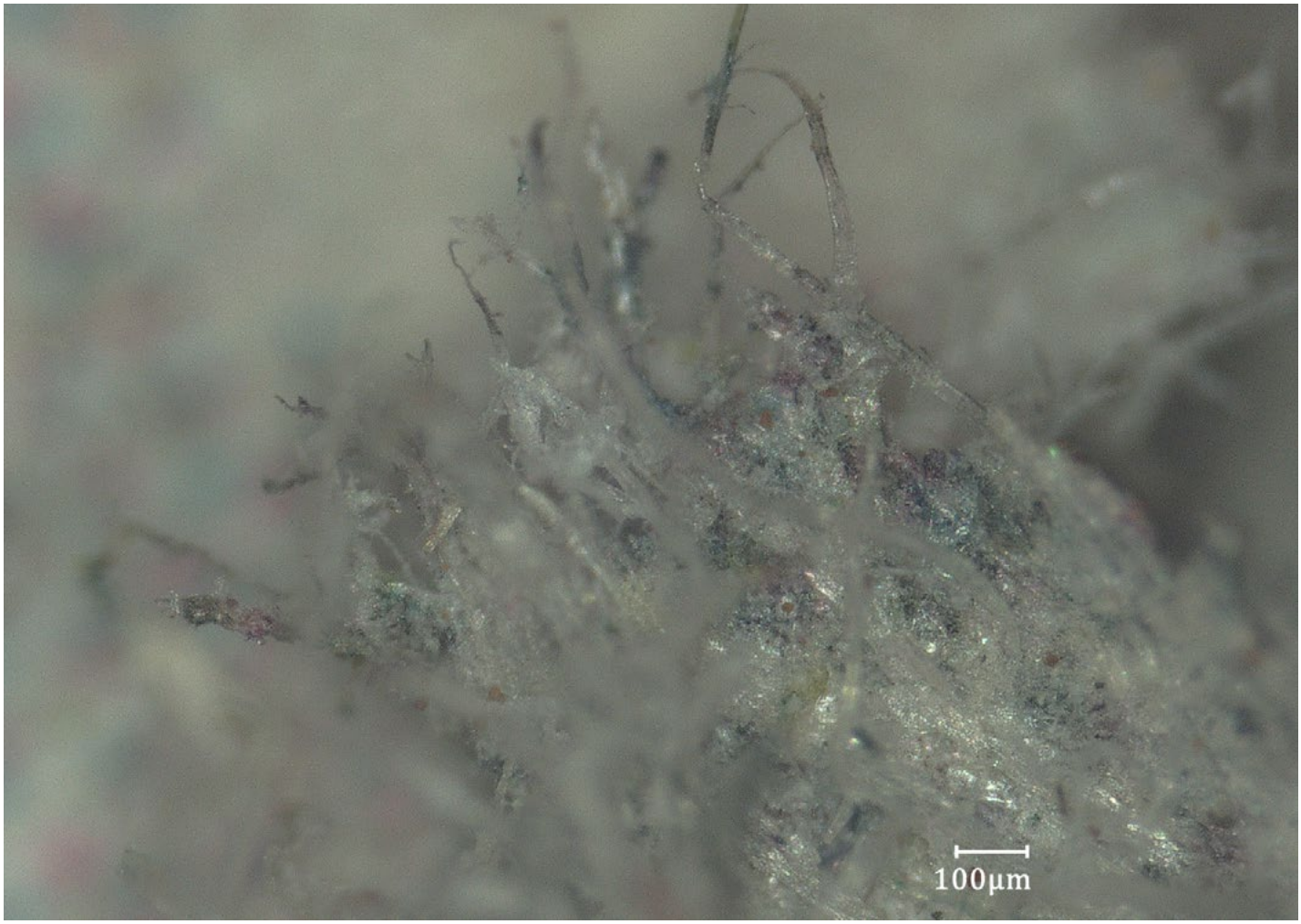

Figure 30. Image of shredded Kraft paper fibres with x150 magnification

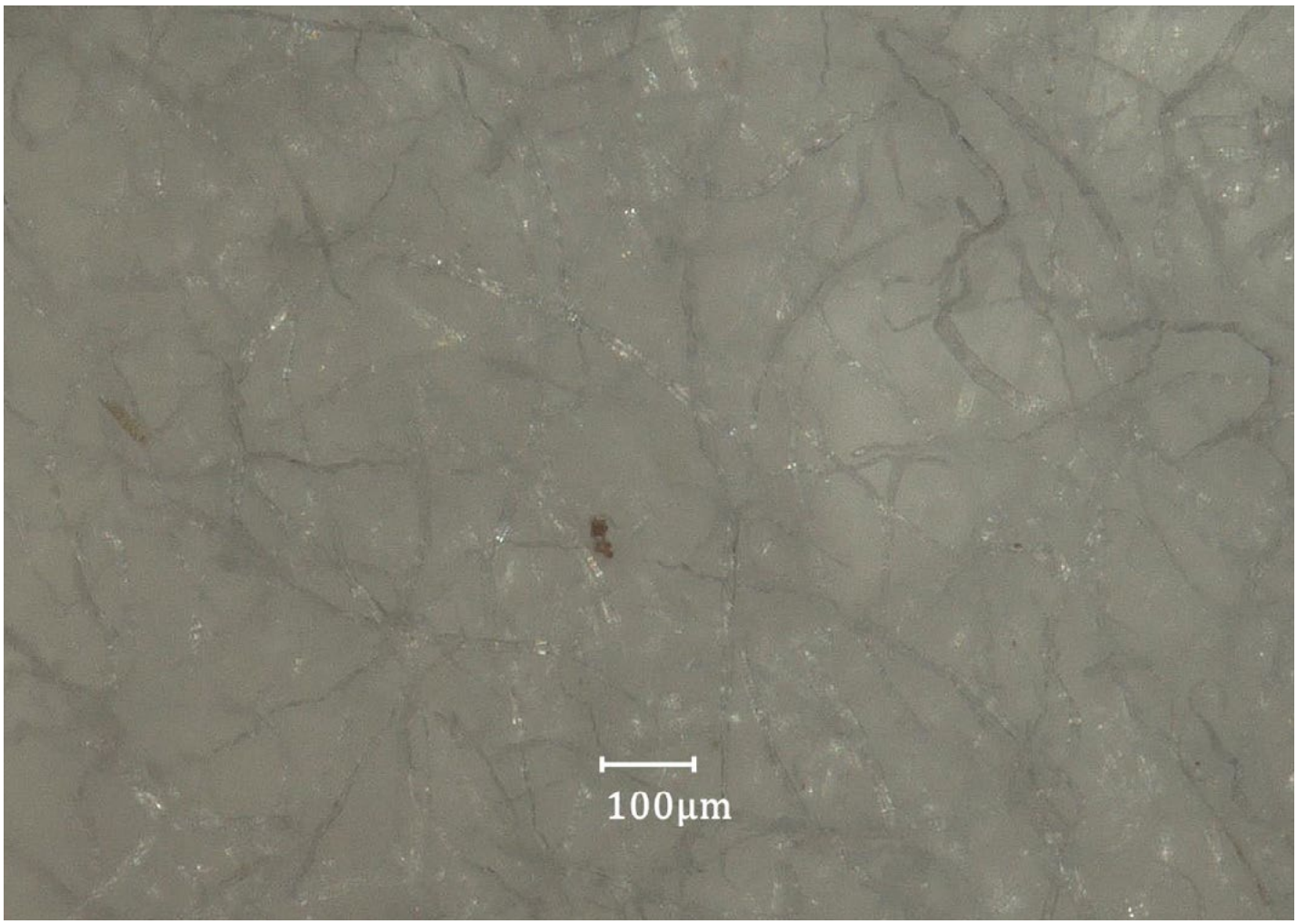

3.1 Production Protocols

3.2 Production Protocols

To recall, the design of the production steps came to be to answer the main research question and sub questions that are stated in Chapter 1.4. The focus for the experiments is therefore to produce a material mixture that can be applied in a hot-pressing process to create a material that demonstrates the polymerisation of lignin in a cellulose base.

For conducting all of the experiments and tests, the objectives described in Chapter 1.6 have to be kept in mind. In short, remembering the non-toxicity of all materials and additives used, utilizing renewable and largely waste (by-)products and ensuring reproducibility of all experiment steps.

The entire process from producing a mixture to testing the produced panels is therefore structured as follows:

1. Mixing and pretreatment of the materials in order to process them in the hot-pressing step.
2. Hot-pressing the material mixture
3. Preparing the materials for further processing, like mechanical tests or the design prototype.

All of the steps had to be evaluated for safety and the risks involved. The main risks during the different steps, although very minimal, mainly arise from exposure and possible inhalation of the lignin and cellulose dust. Both materials have no toxic affect on the skin but can cause physical irritation when ingested or inhaled. Besides that the handling of heavy machinery like the hot-press or mechanical testing machines require training for safe operation.

The following sub-Chapters will describe each of the steps in greater detail to lay out the applied techniques. Here the risks and safety measures will also be individually addressed. With the protocols defined for the experiments the material trials in section 3.3 are all based on these fundamental steps.

The preparation of the samples required a dust extractor hood, because both lignin and cellulose produce a lot of fine dust, which is not toxic but can be unpleasant to inhale. Thus, the material mixing was conducted at the Heritage & Technologies Lab at BK at TU Delft.

The hot-pressing was conducted at DASML at the faculty of Aerospace Engineering and an aluminium mould was kindly provided by Kunal Masania. The hot-pressing and material testing were carefully assisted and supervised by PhD candidate Mark Ablonsky.

The subsequent mechanical testing was both done at the faculty of Mechanical Engineering and Aerospace Engineering. The sample preparation (i.e. cutting, spray-painting...) was done in the model building hall of BK.

3.2.1 Step 1 - Mixing

The following documentation describes the steps taken and equipment needed for effortless reproduction of the final material. The description does not mention specific material ratios, as these are very dependent on the outcome that is aimed for. Information on the material ratios are documented in Chapter 4.

Materials:

- ISOCELL newspaper cellulose insulation
- Fibrillated pure cellulose, Kraft Paper
- Lignin (Kraft, Soda, Organosolv)
- Distilled water
- Optional: Plasticizer (e.g., Methylcellulose)

Preparation:

1. Weigh cellulose: Place cellulose into a clean metal bowl.
2. Weigh lignin: Use glass beaker to measure lignin.
3. Weigh gross weight of spray bottle and zero the scale.

Equipment:

- Precision balance (±0.01 g)
- Kitchen Blender or Food processor
- Spray Bottle for distilled water
- Metal bowls for mixing
- Metal mortar for bowl
- Glass beaker 800ml
- Scraper or Spatula
- Drying oven
- Zip-lock bags
- Vacuum pump/ cleaner.

Figure 31. Drawing of mixture preparation setup, showing what equipment is required. Mixing is inside a dust extractor hood at H&T Lab

Mixing:

4. After placing the cellulose in the mixing bowl spray a few sprays of the distilled water onto the fibres. Stir cellulose (Figure 32).

5. Pour the lignin on to the fibres and carefully incorporate the lignin under the cellulose.

6. Spray more water onto the mixture and keep stirring slowly. Keep track of the added water by weighing the now negative weight on the scale.

7. Repeat until the desired amount water is added to the mixture.

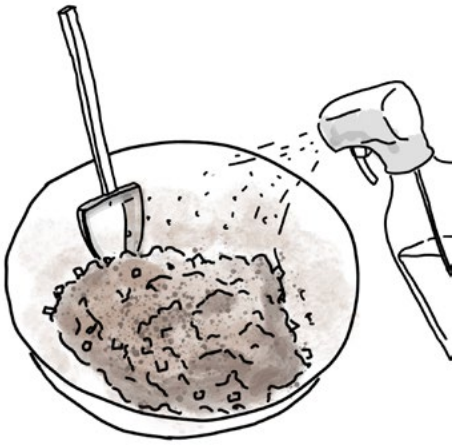

Figure 32. Adding water with spray bottle for better distribution of moisture

Blending:

1. After thoroughly stirring the mixture by hand so that the lignin mostly sticks to the wetted cellulose, transfer mix into the food processor.

2. Close the blender vessel with lid and cover openings in the lid to prevent dust from escaping.

3. Blend with high rpm for 30 seconds.

4. Manually stir mixture and loosen up clumps that form on the blades.

5. Blend with high rpm for another 30 seconds. Depending on the cellulose type repeat this until the mixture has a homogeneous texture and no visible chunks or large flakes.

Figure 33. Adding water with spray bottle for better distribution of moisture

Packaging:

1. Weigh and label zip-lock bag and zero the tare weight before filling with mixture.

2. Transfer mixture into bag and document weight to track losses during the mixing process.

3. Evacuate bag with a vacuum.

4. Optionally: Package multiple mixture bags in another sealable bag and evacuate to ensure that moisture is not lost by evaporation.

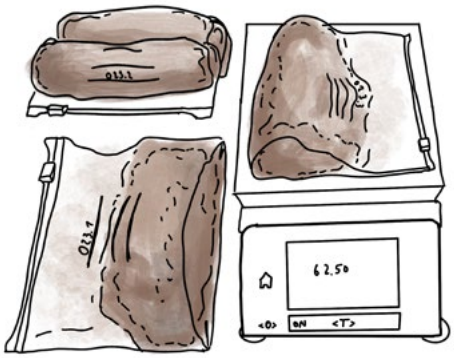

Figure 34. Adding water with spray bottle for better distribution of moisture

3.2.2 Step 2 – Hot Pressing

As mentioned above the hot-press that was used for these experiments is situated at the DASML at the faculty of aerospace engineering of TU Deflt.

Two different machines were used, a Joos LAP 100 and Joos LAP 200. They mainly differ in press surface area, with 500mm x 500mm (LAP 100) and 600mm x 600mm (LAP200) and the maximum operating force is 1000kN and 500kN respectively. The operation of the hot-press requires initial training by a technician. Based on the calibration of the machine the heating and cooling speed should remain less or equal to 6°C and 2°C respectively, otherwise the lag between the programmed time and the machine time increases too much.

Additionally, a trial press, using a thermal couple inside the mould (Appendix Figure 6), concluded that the mould core temperature has a delay of around 4 minutes in reference to the plate temperature (the temperature is ~20K). This requires additional holding time.

Preparation:

1. Use Kapton Tape and close off possible openings in the mould to prevent spilling
2. Lay a sheet of releasefilm on the bottom plate of the mould, optionally use tape to tighten and de-wrinkle the film on the underside.
3. Cut two sheets releasefilm to size of the hot-press plates, so that they lay over the seems between plates and frame.

Equipment:

- Aluminium/ Steel mould (specimen: 150mm by 90mm)
- Unperforated releasefilm, FEP, Max. Temp. 240 °C
- M8 Screwdriver
- “Coffee Mixer”; Spiked tool to loosen and even out fibres in mould
- Heat Resistant Kapton Tape
- 3D printed funnel in size of the mould opening
- Cellulose/Lignin Mixture
- Rubber hammer

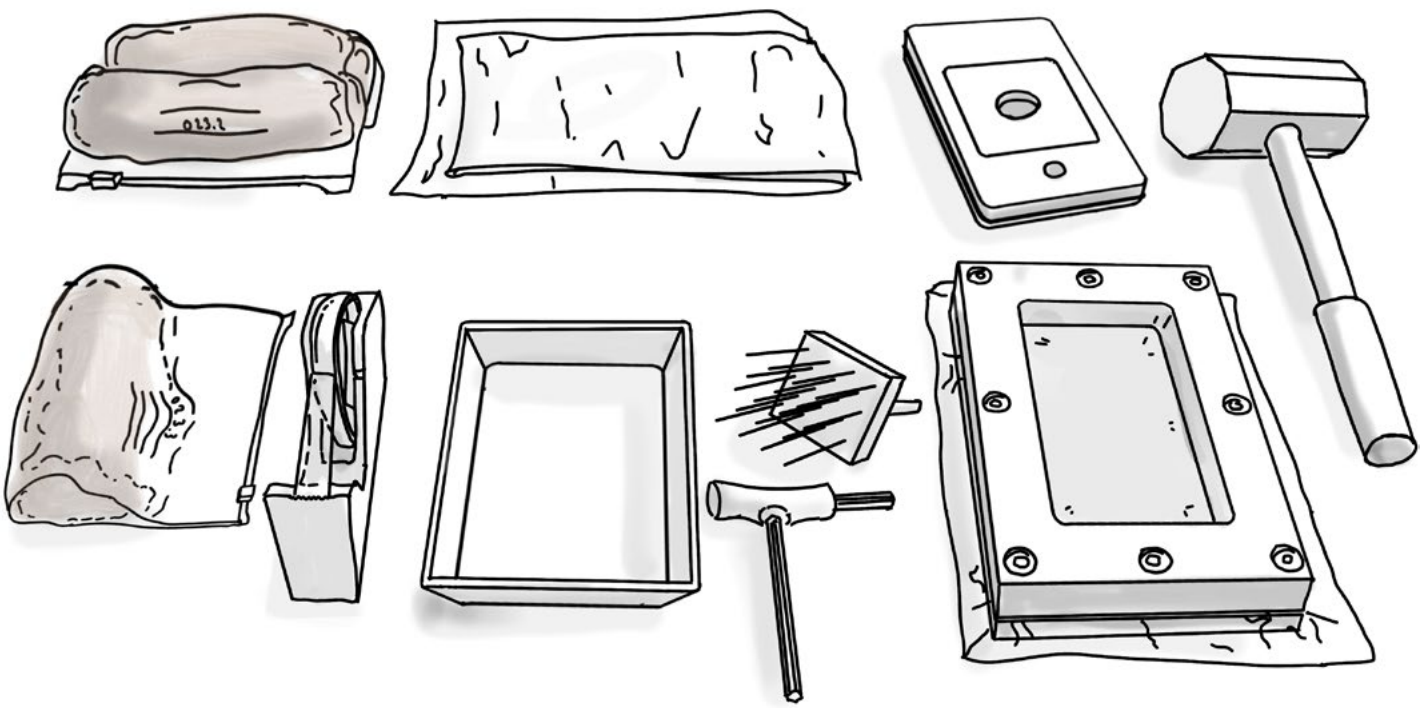

Figure 35. Drawing of hot-pressing preparation, showing what equipment is required

Loading the mould:

1. Use the 3d printed funnel to transfer the mixture into the mould
2. Use the mixing tool to loosen clumps of fibres and to evenly distribute the mixture in the mould, while not puncturing the releasefilm
3. Use a stamp or the top plate to press the mixture into the mould and compact it, so that the lid sits inside the opening
4. Place another sheet of releasefilm over the mixture and under the top mould-plate.
5. Place mould between the two releasefilm sheets, centred on the hot-press plates.

Figure 36. How to place the funnel on the mould and use the mixing tool.

Setting up the hot-press computer with the program:

1. Set the pressing area as 135 cm², based on the top mould-plate.
2. Open the program and open a logging file.
3. Close the press and pre-compress at 250kN
4. Run the program.

Figure 37. Mould inside the hot-press

Removing Sample:

1. After the program finishes release the mould and unscrew the bolts of the brim.
2. Use Rubber hammer to remove plate from mould and to remove top mould-plate from brim.
3. Optional: Place sample between to metal plates and add a heavy (ideally metal) weight to cool down sample more rapidly.
4. Place sample back into zip-lock bag to prevent uneven drying of residual moisture.

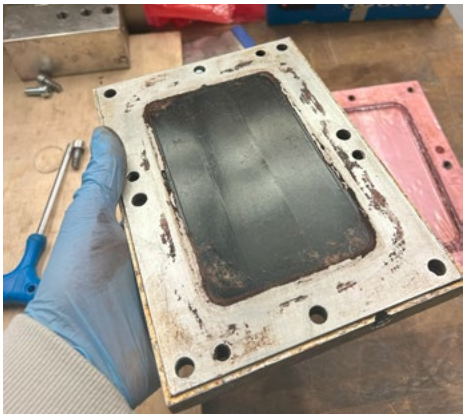

Figure 38. Pressed material into plate inside the mould brim.

The program specifics will be shown in Chapter 3.3 as they differ based on the mixture that is being hot-pressed.

3.2.3 Step 3 - Post-Processing

The last steps of the hot-pressing protocol describes how the plates are placed back into a zip-lock bag to prevent the moisture that remains in the material from drying off unevenly. This would have the undesirable effect of the plate warping. Thus, the plates are kept airtight until they are placed into a rack in which the plates have a more even airflow around the top and bottom surface. Figure 39shows the rack that can be used to stack multiple plates on-top of each other, 3d printed from PLA. After placing the plates in the racks and tying them together with rubber bands, the rack is either placed in a drying oven at 45°C with exhaust opening of 50%. Alternatively, the rack can be placed into a sealed container with moisture absorbing beads (e.g Calciumchloride) to remove residual water in the samples.

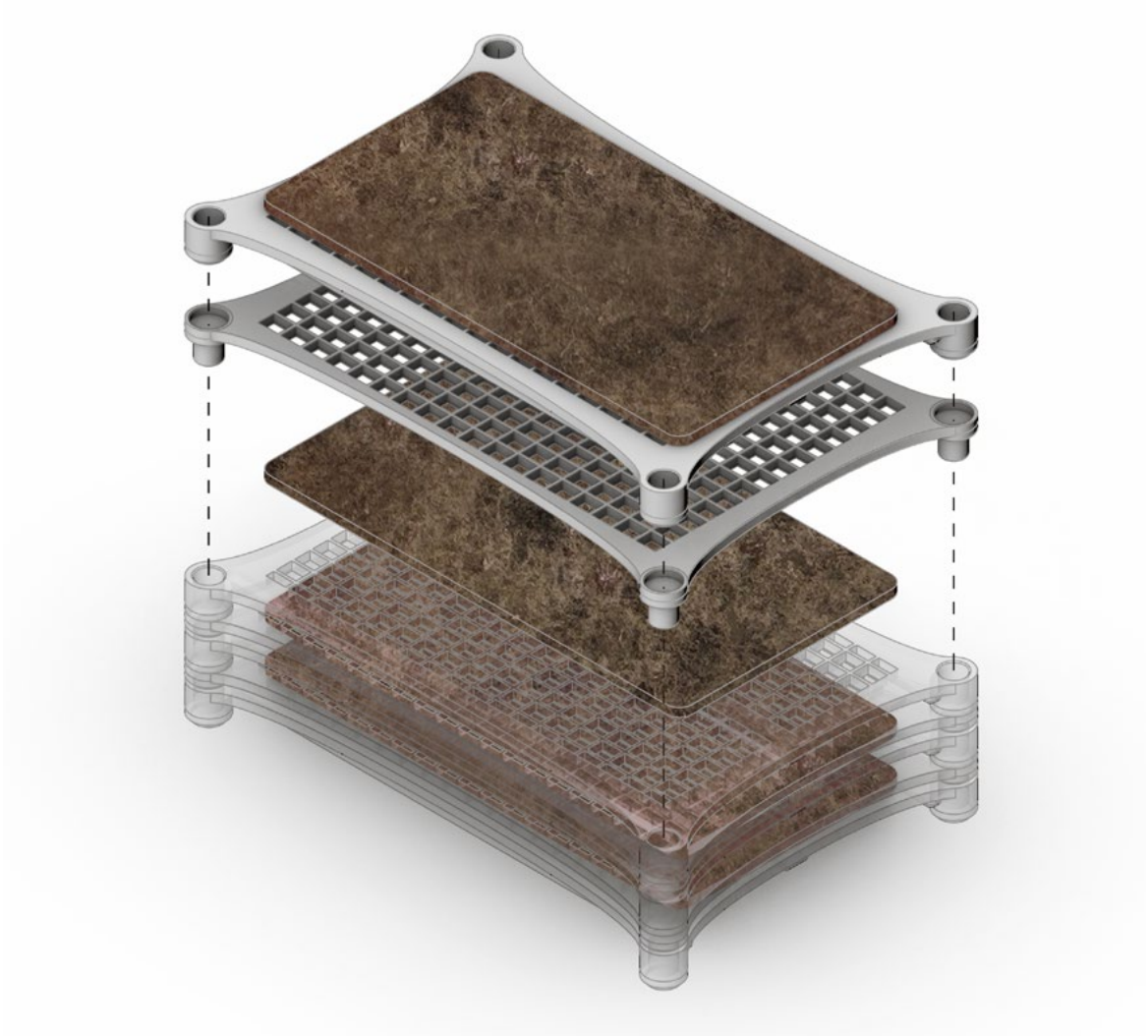

Figure 39. Rendering of drying rack for the hot-pressed samples

Once the plates have dried off most of the moisture, controllable by weighing and comparing with the dry-weight of the samples ingredients, the plates can be further processed. In preparation of the mechanical tests in Chapter 3.3 the plates have to be cut into the specimen shapes and sprayed for the digital image correlation (DIC) or receive finishing for the prototype assembly.

Figure 40. Photo cut specimens from plates.

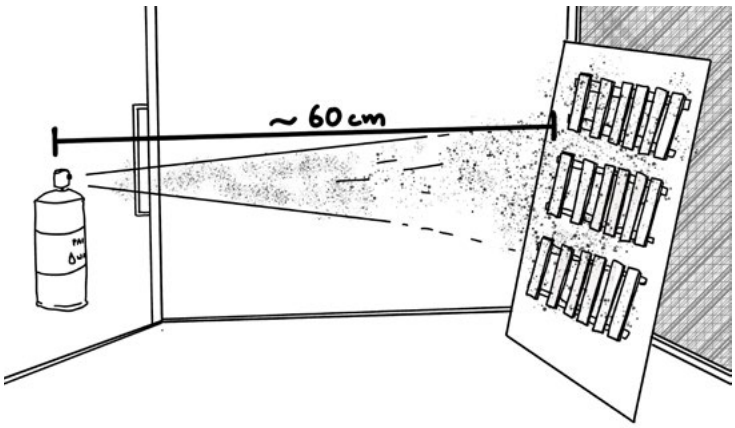

Figure 41. Schematic drawing of the spraying process for DIC.

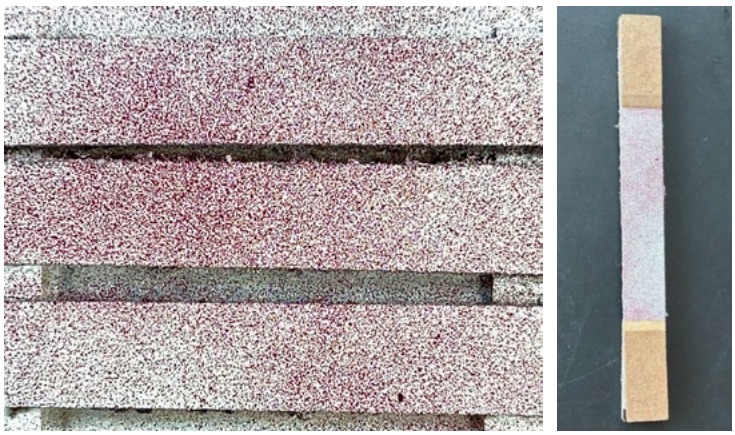

Figure 42. Close-up and total image of specimen with speckle pattern.

Cutting:

Due to the dimensions of the mould it is not always possible to follow the standards on specimen dimensions for the respective testing method that are presented in Chapter 2.8. Thus, all of the specimen retain the length of 150mm but are cut to different widths using a band saw.

Figure 40 shows the specimen of different mixture types cut into 15mm and 13mm wide strips for the tension and compression test. Each specimen is labelled with a unique number, additionally the last digit indicates what segment the sample is cut from. In “T. 28.2.1” the .1 means it is an edge piece. .2 and .3 are inner pieces. This way the analysis can later also take into account these variables.

Spray-painting:

For the DIC the samples also have to be spray painted. The illustration in Figure 41 shows the setup used to apply the speckles with a spray can onto the specimens that are pre-coated with a white mat spray. According to the specifications of the DIC system (Resolution, Lens, Area of interest) and the size of the specimen the speckles have to have a certain dimension. This is usually around 4px per speckle. The mist of a spraycan can create a fine enough pattern on the specimen. Alternatively there are speckle-kits with special tools to apply a pattern to a specimen. Figure 42 shows a close-up of the pattern and the final look.

3.3 Mixture Trials

3.3 Mixture Trials

The purpose of this section is now to explain the experiments that were made, based on the protocols described above. The mixing of the material samples went through some optimisation steps through trial-and-error to fine tune, control and ease the preparation of the samples, to be hot-pressed. This section will elaborate what these adoptions look like and explain the reasoning behind them.

To begin the experimental phase first only cellulose samples were produced and gradually the lignin was added to the mixes to see potential differences. The initial mixing process was based on the DIY-guide from (XYZAidan, 2020) that demonstrated a way to create a pulp that can be cold pressed in a 3d printed mould and dried to create a shape. In contrast to the guide, no glue or starch was used in making the slurry. This methods is using a lot of water to create a slurry in a blender with all the mixture ingredients. While this was favourable for the initial compacted cellulose plates, because the material would hold its shape pre-hot-pressing, once the lignin was added to the mixture, the pre-compacting resulted in a lot of lignin being washed out of the mould with the water, resulting in an inaccurate mixture composition. The mixing process was adjusted after a few trials to a “dry” process, meaning that much less water was used. In fact the amount of water added was precisely measured to be able to keep track of the moisture content in the mixture.

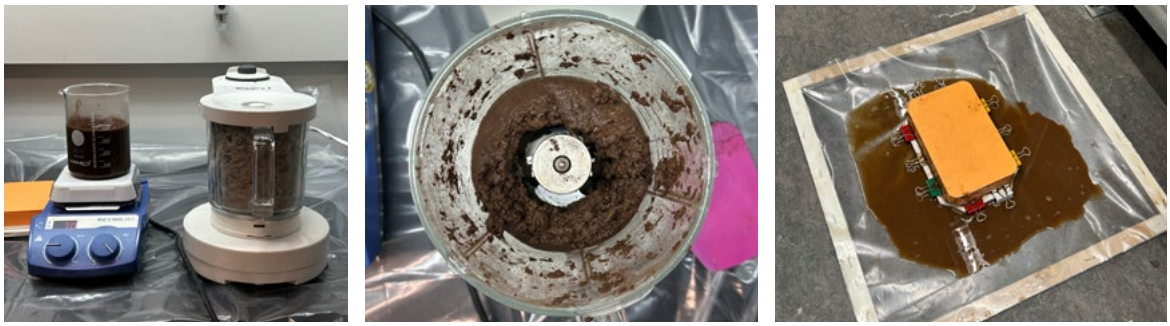

Figure 43. Mixing steps following the “wet”-process and the loss of lignin during the pre-compacting step.

The moisture content revealed itself to be one of the major factors in the entire preparation and pressing process, as it has impacts on how well the mixture constituents combine, under what conditions the material can be hot-pressed, how much the lignin flows during the hot-pressing and lastly what mechanical strength can be achieved. This introduces the first experimental trial, in Chapter 3.3.1, on the moisture content variation one important variable that should be included in the search for an answer to the research question, how controlled variability in the mixture can be achieved.

After getting a better understanding of mixture behaviour throughout the entire process, the next step was to vary the cellulose and lignin ratio (the only constituents making up the composite) and investigate the impact on, mainly, the material strength. Chapter 3.3.2 describes this process and the qualitative results prior to the mechanical tests.

Lastly, as a conclusion of the literature review the type of lignin used might also have an effect on the performance of the material. As a reminder, sulphur contents in kraft lignin have shown to impede the reactivity of lignin (Daniel et al., 2019), the extraction methods result in different availabilities of functional groups, thus affecting the cross-linking potential (Kenny et al., 2023) and the amount, type and availability of functional groups depends on the bio-material that the lignin is sourced from (Chio et al., 2019). These variations are inspected in Chapter 3.3.3 where the three lignin types (Figure 24,25,26) are tested in the mixture.

3.3.1 Moisture Content Variation

In this material trial six different mixture moisture levels were tested in the hot-press. The incremental 5wt% steps are from 0 wt% to 25 wt%. With a dry weight of 50g this is 0g to 12,5g of added water. The distilled water was added to the dry cellulose-lignin mix with a spray bottle to be able to control the amount and distribution well. The hot-pressing profile of this trial was determined from trial presses, both successful and unsuccessful. Appendix Figure 3 how the added moisture relates to the actual sample's moisture.

The aim of this trial was to find the influence and "sweet-spot" of the moisture content on the adhesive qualities or flow of lignin during hot-pressing and the overall impact on the material finish.

Results:

Visual comparison of the samples shows a gradual change in the surface finish of the samples from matt, light brown with isolated dark brown sheen spots to the full surface being dark brown and lustrous. Figure 45 shows the surface of the 10wt% sample under magnification, demonstrating the flow of lignin around the fibres with many surface defects.

Mixture Profile

C - 20g | 30g - L Soda

Hot-Pressing Profile

2 MPa | 85 °C

60 °C | 15 min

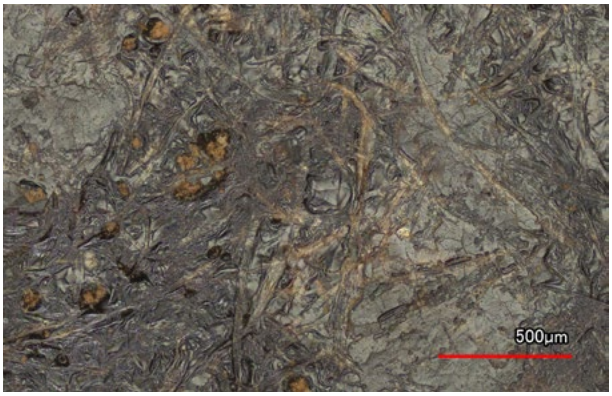

Figure 45. Surface of 10wt% sample at 10x magnification

Figure 44. Hot-pressed plates from the material trial of moisture content variation

The macroscopic change of the surface is noteworthy, with increasing moisture content the more blistering occurs on the samples surface (top and bottom).

In addition to the incremental changes in moisture and constant pressing conditions, three samples were pressed with different moisture levels and adjusted pressing profiles in order to validate the effect that moisture has on the flow behaviour, as previously shown in Figure 8,

Figure 46. From left to right, hot pressing examples of mixtures containing 5, 10 and 25 wt% of water

Hot-Pressing Profile*
19 Mpa
2.2 Mpa
140 °C
45°C
15 min

Hot-Pressing Profile
19 Mpa
2.2 MPa
90 °C
45°C
15 min

Hot-Pressing Profile
19 MPa
2.2 MPa
70 °C
45 °C
15 min

Mixture Profile
C - 30g
20g - L Soda

"The glass-transition temperature of lignin as a function of moisture content, from Kuntar & Sernek, 2007".

Results: Although the cellulose lignin mixture is different with a ratio of 3:2, as before 2:3, the surface appearance of the three samples shows that the flow of lignin is taking place. With the adaptation to the pressing process, the previously occurring blistering effect is not observable with these samples. All three samples show flow of lignin, while the 5% sample has the glossiest and dark surface finish. The 10% and 25% samples have less glossy finishes on the surfaces, both top and bottom. The felt stiffness does not seem to differ noticeably between the samples.

3.3.2 Cellulose Lignin Variation

This material trial consists of five different cellulose-lignin ratio (C/L ratio) mixtures that are hot-pressed at the same processing conditions. The aim of this trial is to observe the relationship of the mechanical strength to the changes in fibre and matrix content of the composite material. In theory the relationship of elastic modulus $E_{c,\ upper}$ to volume fraction v behaves as the volume-fraction-weighted average of the particle and matrix stiffness's:

$$E_{c\ Upper} = E_p v_p + E_m v_m$$

** two hot-press pressures are indicated. The first is a pre-compression step at room-temperature, the second is the pressure while hot.*

This section will report the qualitative results of the trial and the mechanical behaviour will be investigated in Chapter 4.1. If this theory applies to the material, a linear relationship between C/L ratio and elastic modulus should be observable in the results.

The moisture level is also kept at a constant 25 wt%, as a conclusion of the previous trial. One major advantage of pressing at lower temperatures is that the total process time is reduced (setting-up, filling the mould, heating and cooling, removing the sample). Mainly the cooling that has a maximum rate of 2 K/min impacts the length of the pressing time. Thus, as the lignin flow seemed to have been promoted the best with the highest moisture content, the pressing temperature was kept at 85 °C, this made the program length around 1 hour, with additional 15 minutes of preparing the test.

In addition, adjustments to the hot-pressing profile were made, as the blistering that is observed on the samples from the previous trials, was both aesthetically not desirable and could imply weakened mechanical properties. Changes of the procedure in form of a combination of pre-compressing, more careful filling of the mould and a proper cool-down phase to 40°C was applied. In total 5 sets of 3 were pressed in order to be used for mechanical testing.

Mixture Profile

20-40g ISO C.

20 - 40g Soda L.

25 wt%

Hot-Pressing Profile

19 Mpa
2.2 Mpa

40°C

85 °C

15 min

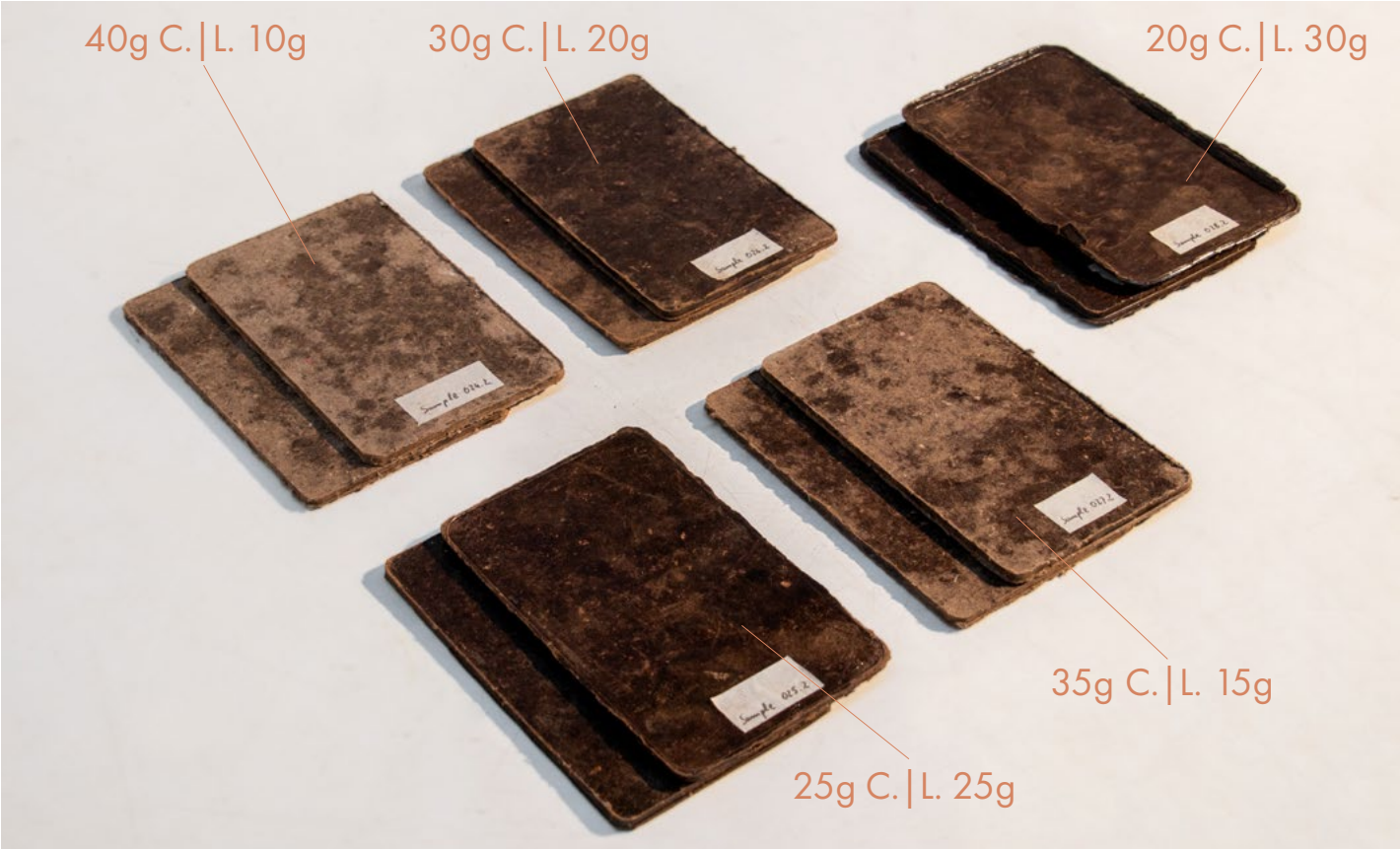

Figure 47. Hot-pressed plates from the material trial of cellulose lignin ratio variation

Results:

The hot-pressed samples demonstrate differences in finish, colour and patterning of the surfaces. Additionally, the samples of the same mixture type show very similar outcomes to each other in terms of their appearance, making them distinguishable from the other mixture types.

There are only minimal occurrences of blistering of the surfaces, both top and bottom. The thickness of the samples are even, varying around 3 ± 0,2mm with one outlier of +0,5mm.

3.3.3 Lignin Type Variation

This trial tests the three different lignin sources with the same material mixture and water content. The aim is to observe possible differences in outcomes and to produce samples that demonstrate a difference in mechanical performance, based on the theoretical background from the literature review (summarized in Section 3.3).

In preparation of this trial, Soda lignin and Organosolv lignin were newly ordered. Kraft lignin and another bag of Soda lignin were available from the previous research from Alexander Coelho and Christopher Bierach. The Soda lignin, ordered from Carl Roth GmbH + Co. KG, is specified to have a moisture content of ≤3,0 %, and a pH of 2,2-4,2. The powder creates more dust than the other samples, but also transfers easier between vessels with less static electrostatic adhesion. The micrograph of this lignin shows, how in contrast to the other two types, the powder is made up from spherical granules. The Organosolv lignin, ordered from chemicalpoint.eu, has a specified moisture content of ≤30 %. It arrived very crumbly with very hard clumps. In the first test with this lignin type, the clumps did not break up and pulverise during the blending. The hot-pressed sample also did not show proper flow of lignin. The clumps were visible dark spots in the plate. Therefore, the entire container of this lignin type was ground, using mortar and pestle and dried in a heating cabinet, until a similar fineness and shade of brown was achieved (Figure 48). The micrography in Chapter 3.1 show that the grain size of the ground powder is similar to the Kraft lignin.

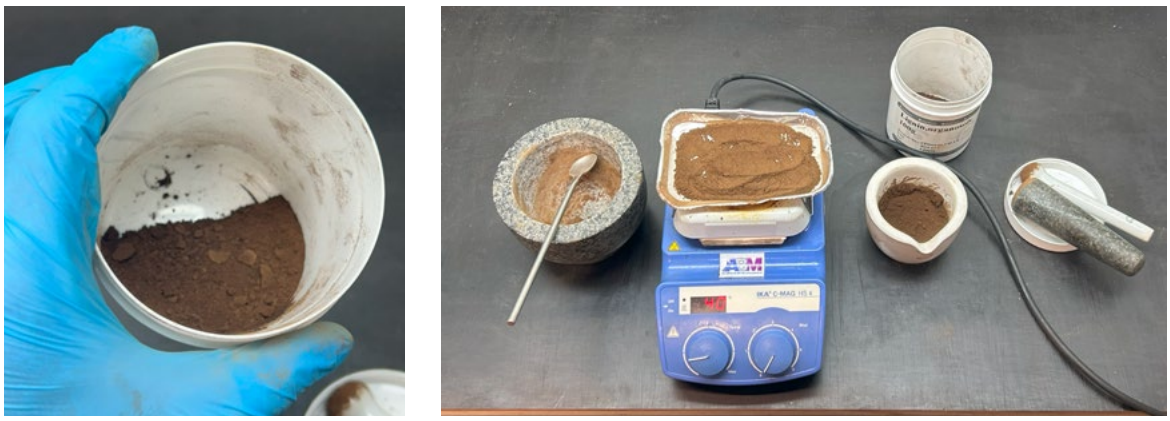

Figure 48. Left: crumbly and moist Organosolv lignin. Right: grinding and drying process to make the lignin finer.

The samples were mixed and pressed after the first mechanical tests were conducted, in accordance to the results of this, the mix was adjusted to a 1:1 ratio. The moisture levels was also set to 10 wt%. Based on this the pressing temperature was raised to 140°C, the pre-compression and holding time remained the same.

Results:

All of the samples show the flow of lignin during the pressing. The surface finish of the samples differs noticeably, with the Kraft lignin samples having the most uniform and even surface appearance. The Soda lignin samples (with the newly ordered lignin) has much deeper brown/ black and glossy surfaces than the Kraft lignin samples, but it also has patchy brims all around, where it appears that no lignin is present on the surface. The Organosolv lignin samples have the most unsuccessful outcome, the lignin distribution on the surface appears the worst.

Additionally, after the grinding process of the Organosolv lignin, these samples displayed a different behaviour during the hot-pressing process. While both the Kraft lignin and Soda lignin samples were dry and stiff during removal from the mould, the Organosolv lignin samples had wet patches around the corners, with liquid water pooling on the sample. The samples were additionally very flexible after removing them from the mould. After the drying process they reached similar stiffness as the other samples.

The following mechanical tests will properly investigate the material strength behaviour and show more quantitative data on the lignin type differences.

Mixture Profile

25g ISO C.

25g Lignin

10 wt%

Hot-Pressing Profile

19 Mpa
3.7 Mpa

35°C

140 °C

15 min

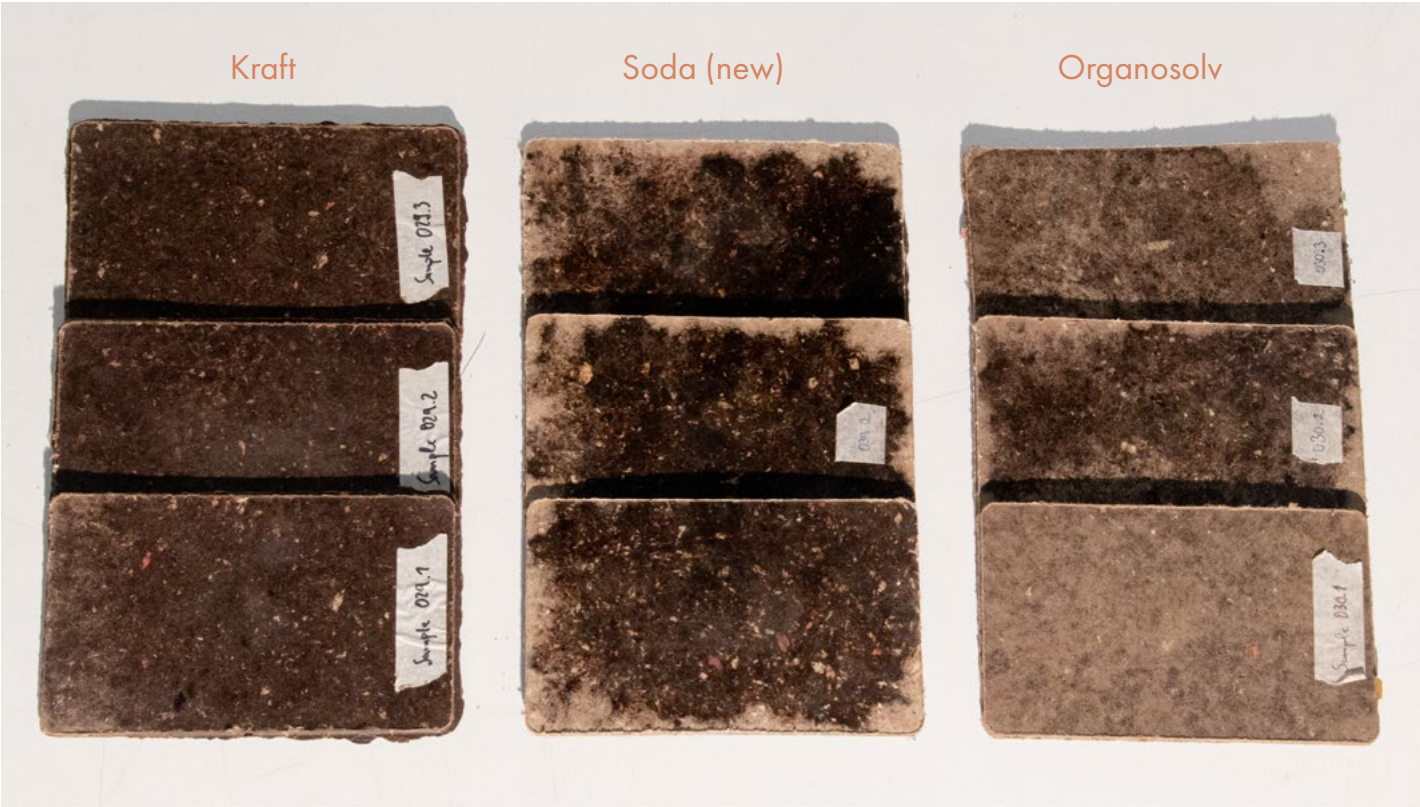

Figure 49. Photograph of the lignin variation trial, from left to right, Kraft lignin, Soda lignin (new), Organosolv lignin

3.3.4 Cellulose Pretreatment

Another trial that was conducted with a singular variation in the cellulose material. The literature review demonstrated many examples of hot-pressing processes of partly dignified wood, that had its hemicellulose removed and then repressed using the in-situ lignin. The resulting mechanical performance was at least partly contributed to the fact that the lignin was able to cross-link with a larger surface area on the cellulose fibres, fibre-surface that was previously occupied by the hemicellulose and native lignin. In this trial the cellulose, that is in form of newspaper shreds, are made up of around 40 – 70% cellulose, 10 – 40% hemicellulose and 5 – 30% lignin. When new lignin is added to the mixture, the chemical cross-link potential of that lignin with the cellulose fibres is reduced by the existing hemicellulose and lignin around the cellulose fibril bundles. The material bonding of the composite is then mainly achieved through mechanical interlocking of the fibres inside the matrix (Figure 51, Figure 79).

The literature on polymerization on lignin mentions that chemical pretreatment can be used to remove both those parts from the cellulose fibres through common methods like alkali treatment using sodium hydroxide to promote the chemical bonding between the materials constituents in the hot-pressing process (Figure 51).

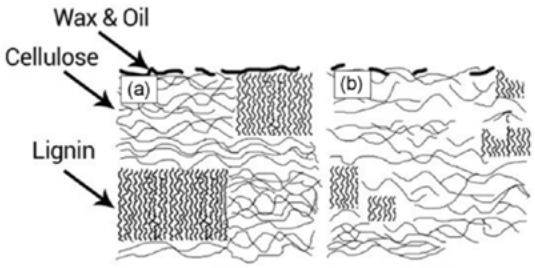

Figure 50. Schematic representation of a natural fibre showing (a) untreated and (b) alkaline treated From Amiandamhen et al., 2020

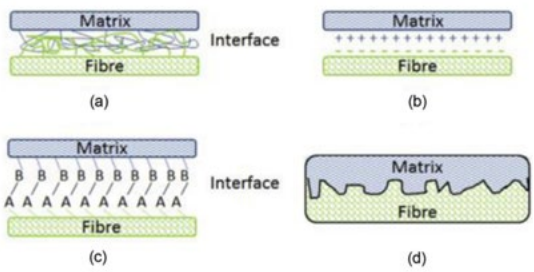

Figure 51. Fibre-matrix interfacial bonding mechanisms (a) molecular entanglement, (b) electrostatic adhesion, (c) chemical bonding, and (d) mechanical interlocking. From Amiandamhen et al., 2020

Sodium hydroxide is considered a strong alkali and was covered several times in the literature to pre-treat, and partly delignify wood material (Qin et al. (2023), Yang et al. (2023), Xia et al. (2024)). It can be obtained as a type of drain cleaner from drug stores. Personal protective equipment has to be used while working with a sodium hydroxide solution, and enough ventilation should be provided to the area that is worked in.

For this trial 140g of newspaper material have been blended in a blender with a rich amount of water. After staining the slurry through a straining cloth, the pulp was immersed in a 5% NaOH solution for 6 hours. The solution that was clear before was then coloured grey-green and opaque. The cellulose pulp was then strained in the cloth and washed for roughly 30 minutes, by repeatedly agitating the slurry inside the bag in a water bath. The run-off of the straining turned back to mostly a clear appearance. After thoroughly squeezing out most of the water, the pulp was ones more broken up in a blender into small pieces and then laid out on a large baking paper on a tray and dried at 45°C for 2 days.

The resulting dry cellulose particles weighed 75g, which meant 65g of material was washed out during the washing process. With these 75g. 3 samples of a 1:1 mixture were mixed to be hot-pressed, with a moisture level of 10wt%.

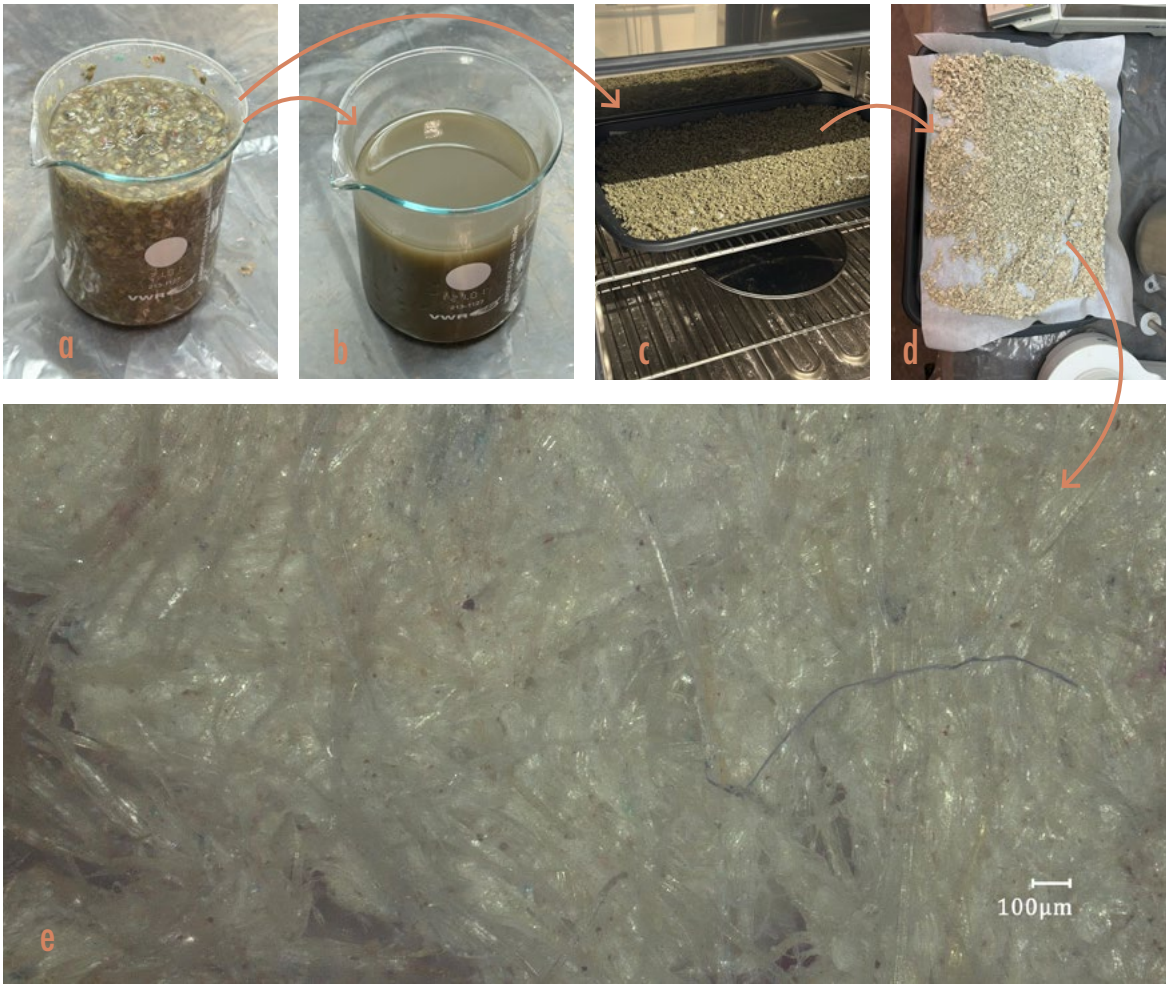

Figure 52. Order of processing steps: a) Soaking in NaOH solution b) Run-off c) after washing, blending d) dried sample e) Micrograph of shredded fibres at x100 magnification.

The micrograph in Figure 52 demonstrates how the previously dirty looking fibres (Figure 29) appear to be cleaner and rid of any leftover ink.

Using this pretreated sample of cellulose fibres the aim of this trial was to demonstrate in the subsequent mechanical testing, that the fibres that have been partly delignified demonstrate a stronger mechanical behaviour, and providing potential evidence for the effect of chemical cross-linking of the newly introduced lignin with the treated fibres.

Results:

The three produced plates have a very even, smooth and thoroughly black brown appearance on the bottom side of the plates (Figure 53). The top side of the samples is also glossy but has more of a patchy brown appearance. During the mixing process and filling of the mould it was noticeable, that the lignin was sticking less the fibres. The lignin might have fallen more to the bottom of the mould during filling the mould. Otherwise, the have a stiff and solid feeling to them.

Figure 53. Order of processing steps: a) Soaking in NaOH solution b) Run-off c) after washing, blending d) dried sample e) Micrograph of shredded fibres at x100 magnification.

3.3.5 Recycling and Re-hot-pressing of Waste Material

One of the key promises of using lignin as the composite's adhesive lies in its thermoplastic behaviour, which makes the material potentially reusable and reprocessable under similar hot-pressing conditions. To test this assumption, scrap samples and production cut-offs were reused to create a recycled cellulose-lignin plate. Most of the waste material originated from a 2:3 cellulose-to-lignin mixture.

To recreate the original processing conditions, the waste needed to be reduced to a similar powder-like form used in earlier trials (Figure 54). However, the toughness of the post-pressed material made it impossible to cut with household tools. As a first step, the scrap pieces were soaked in room-temperature water for one day to soften them without any additives or solvents. This treatment made it possible to cut and tear the pieces into smaller fragments suitable for blending.

The water used for soaking was also employed in the blending process. After 24 hours, the water had taken on a brown hue, suggesting that some lignin had begun to dissolve or disperse. In line with the aim to preserve and reuse as much material as possible, the water run-off from straining the pulp was collected and boiled down. Approximately 8g of solid residue remained and were incorporated back into the recycled mixture.

The strained pulp was then spread out, broken into small chunks, and dried in a drying cabinet. A total of 50 g of dried recycled material was prepared, and 10wt% water was added, as in the standard method outlined in Chapter 3.2.1.Due to an unexpected change

in lab equipment and materials, the hot-pressing was carried out at a lower temperature of 115°C, using an alternative release film with a maximum processing limit of 120°C. Cooling was only applied down to 60°C. To validate the effect of the new conditions, a reference sample made from fresh raw materials was also pressed under the same settings.

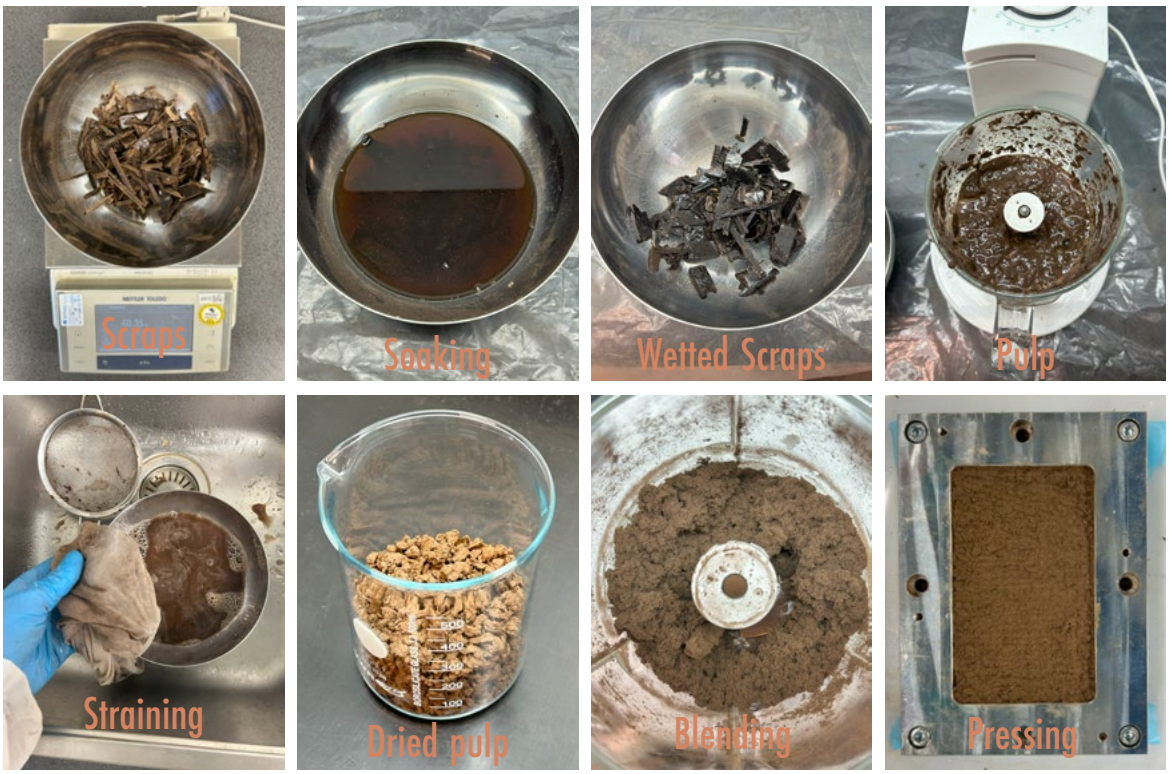

Figure 54. Processing steps for recycling and re-pressing the cellulose-lignin material

Results:

The hot-pressed recycled plate showed characteristic signs of lignin flow, similar to previous trials. Its appearance was a deep, consistently pigmented brown (Figure 56). Unlike earlier samples, however, the surface was matte rather than glossy—likely due to the use of a different release film and mould, as the reference sample also turned out matte under the same conditions. Microscopic observation revealed a highly uniform material structure. While some individual fibres were still visible, they appeared less distinct than in previous samples (Figure 55).

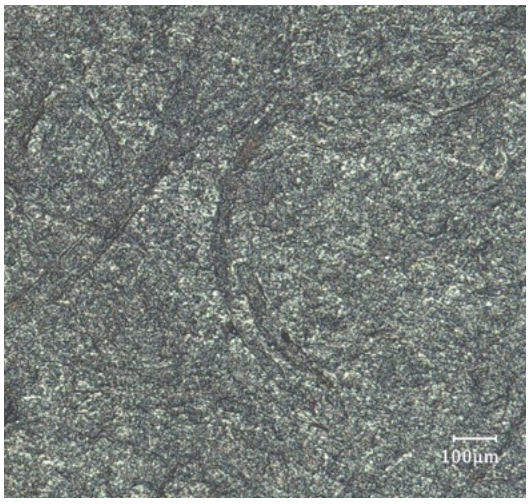

Figure 55. Microscopy of recycled sample x150

This trial marks a significant milestone in validating the circular potential of the cellulose-lignin composite. Demonstrating that production waste can be reprocessed into new plates using water and mechanical treatment—without additives—underscores the material's potential

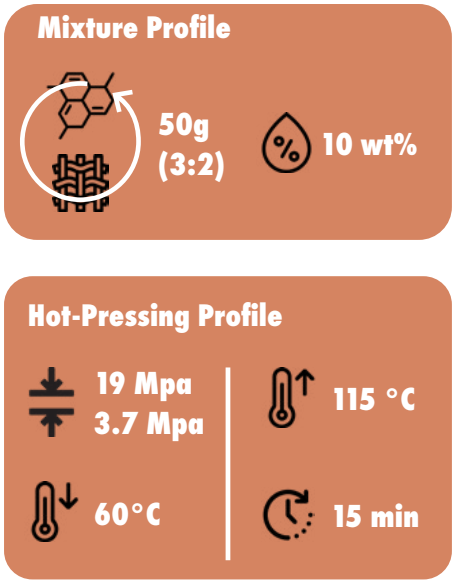

Figure 56. Normal and Recycled cellulose-lignin plate compared

for recyclability and end-of-life reusability. This is a major asset for future applications, especially in sustainable construction and product design, where material recovery and reuse are essential. However, the mechanical performance of the recycled plate still requires thorough testing. The reprocessing steps—particularly blending and shredding—likely shorten the fibre length, which may reduce mechanical strength. Further investigation is needed to assess whether this trade-off remains acceptable for intended applications.

3.3.6 Large Scale Hot-Pressing

In order to see if the same principles of the complete existing production process apply to larger sample sizes than the 15 by 9cm plates, an additional trial was conducted. The production of the resulting plates of A4 to A3 size happened both at the faculty of Aerospace Engineering and at NPSP[1], which focuses on development and production of innovative an environmentally friendly composite materials, mainly utilising thermoset resins.

The facilities of NPSP are optimised for the high quantity production of composite plates and are tailored primarily to the use of thermoset resins as the composite matrix. As such, their equipment and process chains are configured for materials like furan resin, which undergoes curing during hot-pressing. Once the resin hardened, such plates can be easily demoulded, and issues like blistering are typically not encountered.

For the cellulose-lignin trials, the mixture of newspaper shreds and lignin was pre-blended and mixed in the own H&T Lab. The mould used at NPSP measured 295mm by 245mm with a depth of 4mm. It was first brushed with castor oil and then lined with the FEP release film to ensure demouldability. The prepared dough was added gradually to the mould in layers, each of which was compacted using a solid block to minimise the volume and fit everything inside the mould. A total of 383g (+ 10wt% water) of material was used.

The hot-press was pre-heated to 140°C due to the long heating time required by the machine. Once the mould was secured, the press was closed and a pressure of 35 tonnes was applied—equivalent to approximately 4.75MPa (Figure 57). The initial pressing duration was 20 minutes. Upon release, a significant amount of vapour escaped rapidly, likely due to

1. https://www.npsp.nl/en

high internal pressure from water evaporation, which resulted in extensive blistering of the plate. To mitigate this, the same sample was pressed again under identical conditions for an additional 20 minutes. This second cycle slightly reduced the blistering. Afterwards, the plate was placed between two flat plates and weighted down to cool in a flat state.

Figure 57. Industrial Type Hot-press at NPSP, showing the mould fixed in the press (left) and pressure gauge (right)

At the faculty of Aerospace Engineering, a different mould was employed, measuring 370mm by 330mm. As per standard procedure, the mould was covered with release film and filled with the pre-mixed dough (490g of material mix + 10wt% water) in layers, each compacted to reduce the volume and make the mould top part fit (Appendix Figure 5). Given this substantial volume of the unpressed mix, this step was crucial for uniformity of the plate. The pressing protocol followed that of earlier Aerospace trials, with the exception of a slightly extended heating phase—20 minutes instead of 15—due to the larger thermal mass of the mould requiring more time to reach full processing temperature.

Results:

The large-scale trials highlighted both the challenges and potential of upscaling the cellulose-lignin material. At NPSP, the absence of a cooling cycle and rapid pressure release caused significant blistering, likely due to sudden water vapour expansion. A potential solution is "venting"—a pressing method involving periodic pressure release and lifting of the mould to allow vapour to escape. Warping after release from the mould is not an issue here.

Despite surface imperfections, the NPSP sample showed good internal cohesion, confirming lignin flow. The presence of more visible newspaper flakes likely stems from less thorough blending of the larger batch. In contrast, the samples pressed at Aerospace were uniform, blister-free, and closely resembled the smaller trials. Minor inconsistencies, such as uneven lignin flow at the edges, point to areas for refinement in mould loading (Figure 58).

Visually and by feel, all large samples appeared comparable in strength and stiffness to smaller plates, though mechanical testing is needed for confirmation. However, the warping of the

Figure 58. Large scale plates

panels seems to be of more significance at this size. Figuring out a sweet spot between the NPSP and Aerospace processing conditions, using as little amounts of water in the sample as possible, using high enough pressing temperatures to let water evaporate controlled or entirely getting rid of water in the mixtures can be explored in further experiments.

These results are a significant step towards validating the scalability of the cellulose-lignin composite plate production process. The successful transition from small-scale lab trials to A3-sized panels supports the feasibility of this approach for larger-scale manufacturing applications. However, further research is needed to determine the mechanical limits of upscaling—both in terms of maximum workable dimensions and how internal stress or heat distribution may affect the final performance.

Equally important is the potential to optimise the process chain further, incorporating controlled venting, improved mixing methods for bulk quantities, and refining the mould-loading strategy. All together, these insights not only highlight the robustness and flexibility of the developed material system, but also underline its promise as a scalable, bio-based alternative for structural or panellised applications.

3.4 Differential Scanning Calorimetry of Lignin Samples

Differential Scanning Calorimetry (DSC) is a thermo-analytical technique that records the heat flow into or out of a small specimen while it is subjected to a controlled temperature programme. Because amorphous or partially amorphous polymers absorb heat when their molecular segments gain mobility, a DSC trace shows the glass-transition temperature (T_g) as a characteristic step-change in the baseline. Unlike methods that monitor mass loss or

dimensional change, DSC measures the energetic characteristic of the molecular softening directly, providing a precise, reproducible way to locate T_g even when no visible softening occurs.

For lignin, T_g is the threshold that switches the macromolecule from a rigid, glassy state to a rubbery, flowable one. Its value governs whether lignin can migrate and wet the cellulose fibres and cross-link during the hot-pressing steps and possibly underpin binder-free composites. Literature and the present review show that T_g shifts with source (kraft, soda, organosolv), moisture content and chemical pretreatment; it can drop by tens of degrees when water acts as a plasticiser or rise when sulphur-bearing kraft lignin is poorly reactive. Accurately mapping those shifts is essential for three reasons:

1. To choose a lignin type whose T_g lies below the planned pressing temperature window of 140–180 °C, or to precisely choose a lignin type and its T_g for a specific application,

2. To calibrate the target moisture content that promotes flow without explosive vapour formation,

3. To assess how additives or partial delignification of the cellulose matrix alter the processing latitude.

DSC is uniquely suited because it needs only a few milligrams of each experimental batch, allowing rapid screening before committing to full-scale panel pressing. At the same time the small batches might not be representative of the entirety of the material. This requires to run multiple analysis to validate the results.

The planned procedure is straightforward. Prepare ~5 µg powders of each lignin variant and of representative lignin and cellulose-lignin mixes at controlled moisture levels, seal them in aluminium pans, and run DSC from 100 °C to 220 °C at 10 K min^{1}. Record the midpoint of the baseline shift as T_g, and perform a second heating to distinguish reversible glass transition from irreversible curing. The resulting T_g map will feed directly into the hot-press schedule for the composite trials.

Results:

The DSC data hint at a glass transition in both raw and hot-pressed lignin samples (Figure 59), but overlapping thermal events prevent firm conclusions about the hot-pressing process. Figure 59 shows the normalized heat-flow curve of a soda lignin specimen, with the derivative (in red) representing the rate of heat transfer per minute. The steady decline in heat flow up to ~150°C likely reflects residual moisture evaporation, though other phenomena may contribute. The artefact at ~210 °C, apparent in both the heat-flow and derivative traces, might correspond to T_g; however, the immediate recovery of the heat flow to baseline levels argues against that interpretation. Interestingly, every lignin sample in this batch shows that same little baseline shift just before the much bigger rise in heat flow that marks decomposition, similarly to the kind of broad T_g change seen in other technical lignins (Rojas et al., 2009). Other lignin analyses have yet to reveal definitive thermal transitions (see Appendix Figure 9).

o get a more definitive answer, it would help to vacuum-dry the samples (for example at 60°C for 24 h) to remove all water first and then run either DSC or repeated scans at different heating rates so that moisture loss, glass transition and decomposition each fall into distinct, separable events

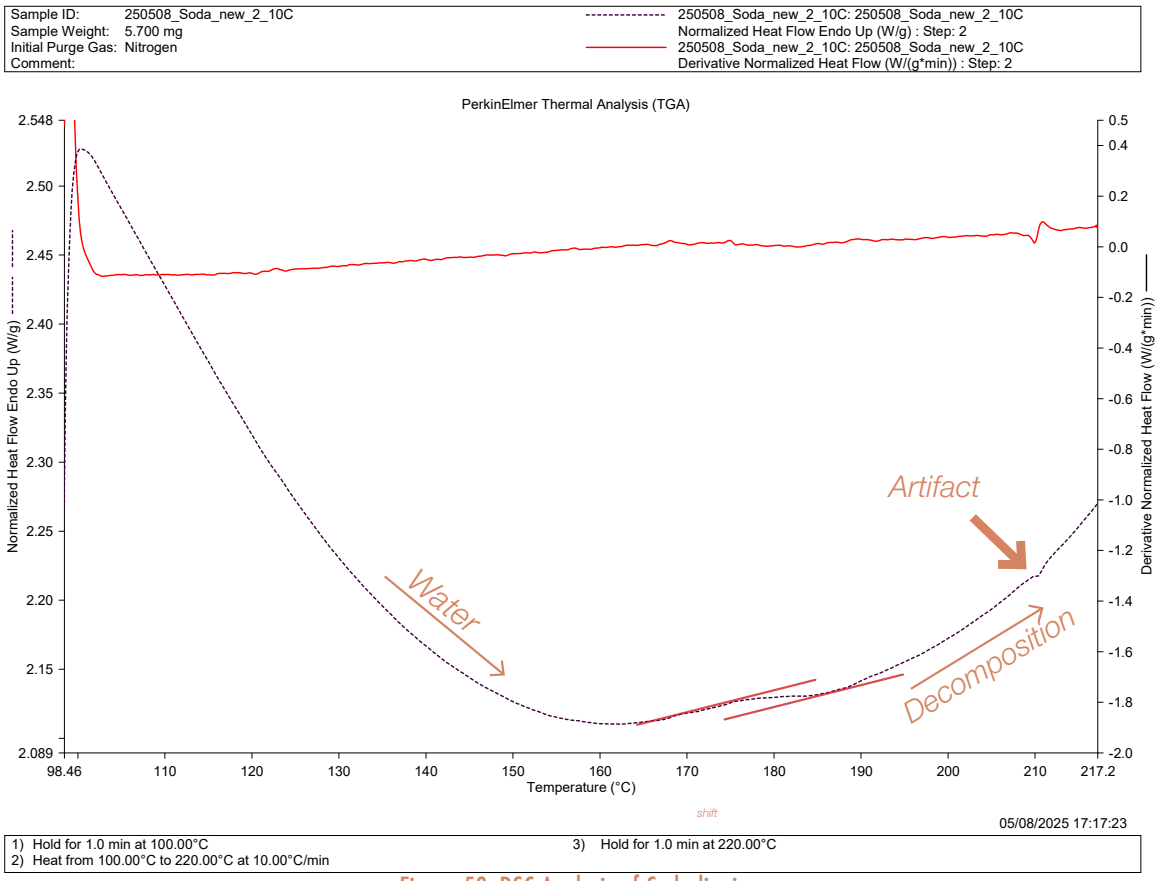

Figure 59. DSC Analysis of Soda lignin.

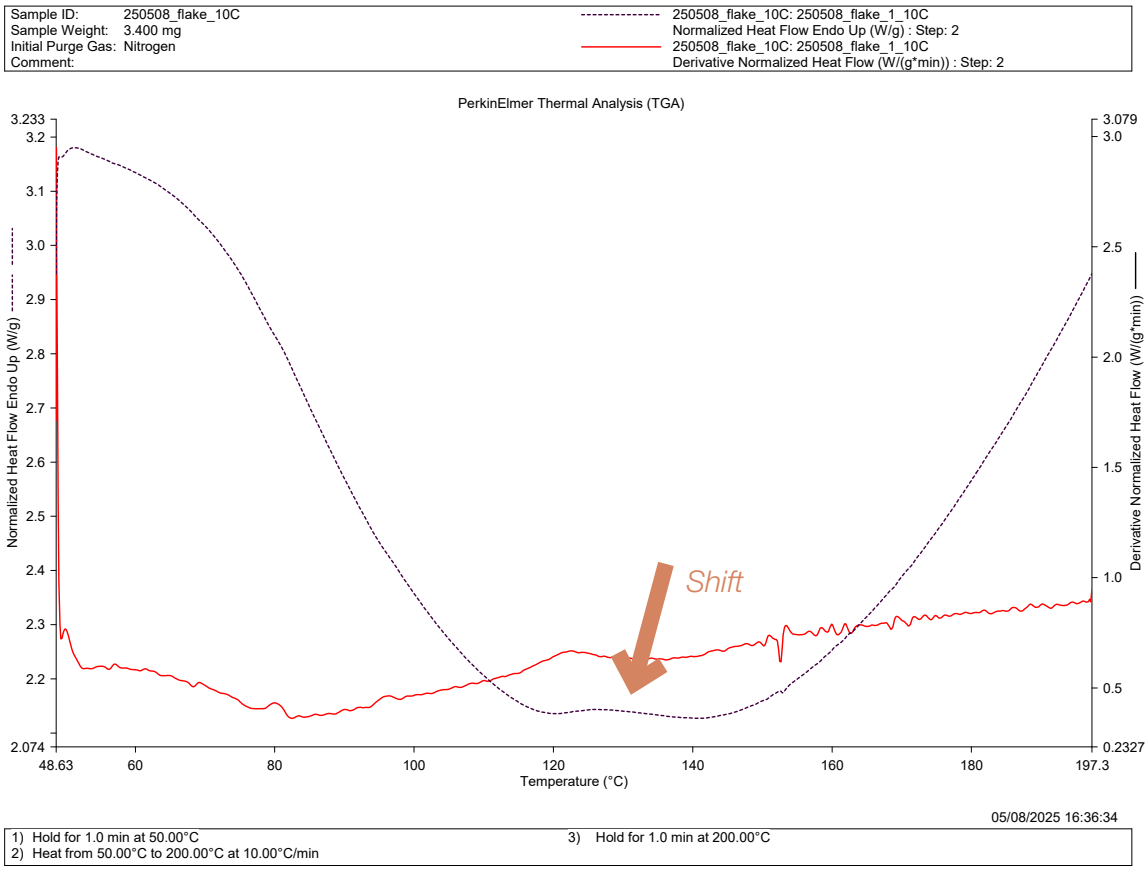

Figure 60. DSC Analysis of recycled sample flake.

3.5 Experiment Results

The conducted experiment trials have produced an array of results that are very valuable for the coming prototyping and mechanical testing. Before the gaining insight on the mechanical performance of the material samples the meaningful results of this Chapter will be summarized.

Throughout the entire experimental phase the visual inspection was key for assessing the quality of the samples produced through hot-pressing. The surface quality was greatly influenced by the moisture content of the samples and the related hot-pressing conditions. There is a great dependency of the pressing conditions from the moisture content. Setting the right moisture level in the mixture is crucial for the flow of lignin. While changing the moisture content, the capacity of the mould to hold liquids needs to be respected. If too much moisture is present it could cause the mould to overflow or rip the gaskets. This effect is increased if the pressing temperature is increased, as the temperature rises, more water will evaporate. This in turn increases the internal pressure, if the pressing pressure is then also increased, this can easily exceed the threshold of containment of the mould.

For pressing procedures that involve high moisture contents, high temperatures and pressures around 3 MPa, insufficient cool-down of the mould after the heating cycle is done, showed to lead to blistering issues on the samples surfaces. The tests showed that if the sample is cooled below 40°C when the pressure is released, the blistering will not occur. Most likely the trapped vapour that wants to expand due to the high temperatures, suddenly expands inside of the plate when the pressure drops rapidly.

Besides the visual inspection, the weight was a very telling measurement that can give indications on the processes taking place in the samples and during the processing. Throughout the material trials, the losses of all processing steps were kept track of. This was relevant as the packing and transporting of the unpressed mixtures from location to location didn't allow for a continuous production chain. Mainly early evaporation of the water inside the bagged samples needed to be prevented and monitored. In the end the losses stayed very constant throughout the entire process. The samples were then pressed to quite even thicknesses of ~**3.0 ± 0.2 mm** with a density of **~1230 kg/m³**.

In general the adjustments in moisture content, pressing temperature and cool-down significantly improved the surface finish and minimized the blistering. And optimal moisture content was identified at approximately 10 wt% at 140°C for balanced lignin flow, with a very even reflective surface, and a reasonable pressing time of 1.3 hrs per sample.

Successful, recycling and repressing of material scraps show promising potentials for fully circular reuse of the material.

The extensive records maintained in Excel, documenting numerous single-material experiments beyond those presented, allowed to be very methodical when planning father experiments.

When considering the initial pressing conditions proposed after the literature review, there is especially a disparity between the used pressing force. Most literature example were pressing their samples at pressures of 50MPa or more. The temperature ranges were also slightly higher at 160 to 180°C. Noteworthy, is that there was little to no mention of lignins glass transition temperature when discussing the hot-pressing steps.

Another aspect that was more clear during the mixture making were the material economics especially in regards to the lignin-to-cellulose ratio trial. Due to the momentary high cost of the lignin samples, economically viable mixtures should not exceed a 1:1 C/L ratio. Despite

first using a 2:3 ratio, and adjusted ratio post-inital trials enhanced the economic feasibility without significantly compromising the visual quality. In fact, with a more balanced ratio the appearance of the newspaper cellulose shreds is quite favourable.

In regards to the reproducibility, it could be confirmed that visual qualities are able to be reproduced across sample types. Mainly the fibre wetting with lignin was reliant how the mould is filled. If the fibres were not spread out evenly with the mixing tool, the samples would show a more spotty appearance showing different levels of fibre wetting. Also, some preliminary indications suggest visual consistency does not directly correlate with mechanical performance—mechanical testing to be explored in Chapter 4. Cutting the samples into strips also revealed that the glossiness, or more the matteness does not necessarily imply that there is not enough lignin flow within the samples, as the cross section mostly showed a deep brown and glassy appearance.

Unexpectedly the organosolv lignin, despite its described superiority in the literature, had very poor performance, for mixing, pressing and later also the mechanical results. This is potentially linked to the initial high moisture content and uneven lignin particle size post-grinding.

The trials clearly demonstrate the critical importance of moisture management, controlled temperature processing, and precise cool-down phases in achieving desirable surface finishes and consistent material behaviour. The extensive documentation in Excel, supported by visual analysis and literature correlations, provides a robust foundation for optimizing the lignin-cellulose composite formulation. Despite successful visual consistency, further mechanical testing (addressed in Chapter 4) is required to fully understand the structural performance implications of these adjustments.

This experimental section has clearly demonstrated that the flow of lignin is achievable in a hot-pressing process. The experiments addressed the main research question by developing optimized mixtures and refining the suitable hot-press production methods. The controlled moisture management and careful adjustments of pressing parameters successfully made use of lignin's binding properties through controlled polymerization.

However, several sub-research questions remain only partially addressed or unanswered:

- **Computational Integration:** The integration and contribution of computational software for flexible material design have not yet been thoroughly explored.
- **Limits of Cellulose and Lignin Mixtures:** Further mechanical testing required to clearly define structural limits.
- **Additives or Treatments for Quality Improvement:** Specific additives to enhance mechanical and visual qualities are not yet fully tested or explored.
- **Scalability and Batch Size Issues**: Addressing batch-based production limitations and transitioning toward continuous processes like hot extrusion remains unresolved.
- **Computational Design for Variability:** Methods to achieve controlled variability using computational tools still need detailed exploration.
- **Design Implications:** Specific design implications based on material composition and production processes are yet to be systematically investigated.

These remaining aspects will guide further experimentation and analysis in subsequent Chapters.

Chapter 4

Material Analysis

4.1 Mechanical Tests 77

4.1.1 Flexural Tests 77

4.1.2 Tensile Tests 79

4.1.3 Compressive Tests 80

4.1.4 Cellulose/Lignin Trial Test Results 81

4.1.5 Moisture Trial Test Results 86

4.1.6 Lignin Variation Trial Test Results 87

4.1.7 Cellulose Pre-treatment Trial Test Results 89

4.1.8 DIC Analysis of Tensile Tests 90

4.2 Microscopy 92

4.2.1 Inspection of Mixture Trials 93

4.2.2 Review of Composite Failure Modes 96

4.2.3 Overview of the Observed Failure Types of the Material Trials 98

4.3 Material Relationships 104

4.4 Material Analysis Discussion 106

4. Material Analysis

4.1 Mechanical Testing

The material trials described in Chapter 3 yielded 47 hot-pressed plates covering the key variables of the study: moisture content, cellulose-to-lignin ratio, lignin type and cellulose pretreatment. From each plate, standardized test pieces were sawn, labelled and conditioned to remove any possible remaining moisture in the samples. These specimens form the basis of the present mechanical testing results.

Link to the digital model

In the architectural proof-of-concept, global load-paths and serviceability checks will be carried out in Rhino + Grasshopper with the Karamba3D plug-in. Karamba requires a concise orthotropic material card:

- E modulus in the principal plate directions
- G in-plane shear modulus
- $v_{1,2}$ major Poisson ratio
- f_t, f_c, f_b tension, compression and bending strengths

Because the experimental plates are essentially quasi-isotropic in plane (short fibre network, random orientation) but potentially weaker through-thickness, three classical tests cover the full data set efficiently. The specimen dimension are not in accordance with the standards, in length, but in width:

Table 5. Description of test types and according standards.

Property group	Test type	Specimen Dimension	Standard
f_b	Flexural four-point bending, using custom load cell for short spanning specimen	150 x 13 x 3 mm	EN 310, ASTM D7264
f_t, E_t	Tension parallel to plane	150 x 16 x 3 mm	ISO 527-4, EN 319 /EN 789
f_c, E_c	Compression parallel to plane, using anti buck-ling fixture	150 x 12 x 3 mm	EN 789 / ASTM D6641

The Shear modulus (G) is derived using the Poisson ratio and the and the Young's modulus.

For the sample preparation and chosen methods the following rationale is applied:

- **Specimen efficiency:** All three tests need to be able to be machined from the 150 x 90mm plate with minimal waste-cuts. At the same time as many data points per specimen type should be crated for more confidence in the data. Therefore the width is chosen according to the minimal necessary requirements in the norms.
- **Production process sensitivity:** The Flexural strength and modulus are governed by the outer fibre zone and thus reveal lignin flow / fibre anchorage. Compression highlights densification and potential brittle to ductile transition close to the lignin T_g.
- **Software compatibility:** The resulting parameters are supposed to be fed directly into Karamba's isotropic material definition.

4.1.1 Flexural Tests

Objective:

Determining the flexural strength and flexural modulus of the specimen types. This allows comparison to other wood-based or wood-like material types and composites. From the resulting flexural stress σ_b the flexural strength f_b is determined through:

$$f_b = \frac{3PL}{4bh^3}$$

where L (mm) is the support span and P the total load at fracture (N).

Specimen:

150 x 13 x 3 mm specimen size of the C/L ratio, lignin type and cellulose pre-treatment material trials. Due to warping out of plane of some of the specimen, the measured flexural strength might show inaccuracies. The specimen was placed on the support pins so that the curvature points upwards, against the loading direction.

Test Equipment:

- Zwick Z010 10kN testing machine
- 4-point bending fixture
- Custom insert for a narrower loading point distance

Test procedure:

The specimen are placed on the support pins that are centred 10cm apart, leaving 2.5cm overlap on each side. In the software *testXpret III* a new test is defined, and the specimen dimension are documented. The loading speed is set to 5 mm/min. The test will end once a drop in resistance to the applied force of 40% is registered.

Four-point bending creates a constant moment zone free of shear between the loading noses, so shear-sensitive composites or wood-based plates fail in pure flexure. The uniform stress field yields a more accurate flexural modulus and strength than three-point tests (Euclides, 2025).

Figure 61. Photograph of 4-point bending test setup and of the deformed samples (C/L ratio trial) after testing.

4.1.2 Tensile Test

Objective:

Determining the tensile strength, the Young's modulus and the Poisson ratio of the specimen types. The test results are used for mechanical performance calculation and to be fed into the material definition in Karamba3D in Rhino 8. Additionally, the results are used to create comparisons to other wood-based or wood-like material types and composites. The resulting maximum tensile stress is considered the tensile strength and denoted that way $\sigma_t = f_t$.

Specimen:

150 x 16 x 3 mm specimen size of the C/L ratio, lignin type and cellulose pre-treatment material trials. The samples are prepared for the DIC analysis according to Chapter 3.2.3.

Test Equipment:

- Zwick Z010 10kN testing machine
- Specimen Tensile Grip 10kN
- Emery Cloth for more friction while gripping the specimen, prevents slipping.
- DIC System, 80mm lens, VIC 3D system, 9MP DIC camera, light fixture, black backdrop.

Test procedure:

The starting position of the machine is set to 85mm distance. This leaves 32.5mm gripping length on each side of the specimen. The emery cloth is wrapped around the end of the specimen and then slid into the opened grip. Vertical alignment of the specimen is ensured and the grip is closed. In the software *testXpret III* a new test is defined, and the specimen dimension are documented. The loading speed is set to 5 mm/min. The test will end once a drop in resistance to the applied force of 40% is registered.

The DIC system is setup according to the software specification and a recording begin trigger is set when the test is initialized on the other computer. For analysing the images of the DIC system, an open-source code for python called µDIC (Olufsen et al., 2020) was used.

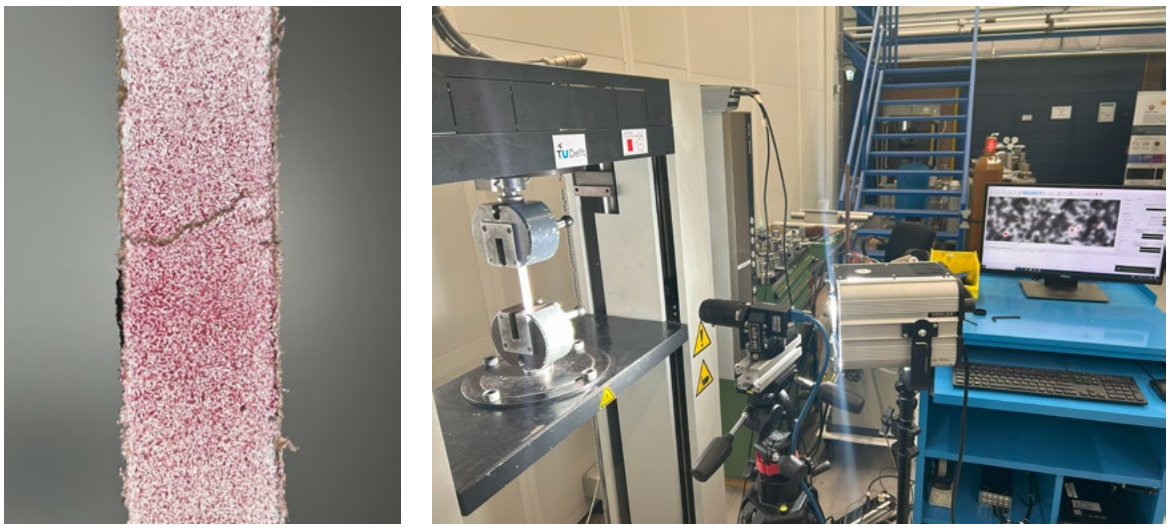

Figure 62. Close-up of speckle pattern on specimen and Testing setup including DIC System.

4.1.3 Compressive Test

Objective:

Determining the compressive strength of the specimen types. The test results are used for mechanical performance calculation and to be fed into the material definition in Karamba3D in Rhino 8. Additionally, the results are used to create comparisons to other wood-based or wood-like material types and composites. The resulting maximum compressive stress is considered the compressive strength and denoted that way $\sigma_c = f_c$.

Specimen:

Specimen type:

150 x 12 x 3 mm specimen size of the C/L ratio, lignin type and cellulose pre-treatment material trials.

Test Equipment:

- Zwick Z010 10kN testing machine
- Compression load cell
- Anti-buckling fixture according to ASTM D664, Torque Wrench (10 Nm)

Test procedure:

The compression fixture is slid apart and the bolts (left side of fixture in Figure 63) are unscrewed. The specimen is placed centred in the lower half and the clamping screws are tightened loosely. The upper half is slid on the guide rods until the specimens top edge is aligned with the edge of the fixture. The clamping screws are tightened using a torque wrench with a bolt torque between 2.5 - 3.0 Nm. In the software *testXpret III* a new test is defined, and the specimen dimension are documented. The loading speed is set to 2 mm/min. The test will end once a drop in resistance to the applied force of 40% is registered.

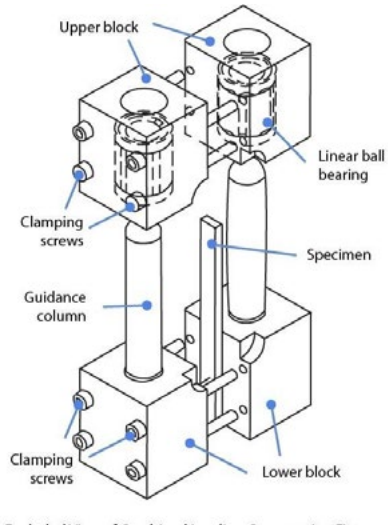

Figure 63. Photograph of compression test setup and diagram of compression fixture from ASTM D6641

4.1.4 Cellulose/Lignin Trial Test Results

This section will describe the results of the three mechanical test types performed on the specimen of the Cellulose/ Lignin material trial. The other material trials have yet to be tested for their mechanical performance

Figure 64 - Figure 66 show exemplary plots of the force/deformation curves of the strongest sample group per test type. In total 5 groups were tested in each of the tests, resulting in 15 overall grouped graphs.

Visual Description of the Graphs:

The graphs all demonstrate dissimilarities of the loading behaviour and reveal clear differences in stiffness, ductility and ultimate capacity:

In Figure 63 the flexural load climbs gradually, peaking between **~30 N and ~45 N** at 6–11 mm deflection. Two curves top out much lower (15–20 N) and soften early, indicating both lower flexural strength and reduced ductility in those specimens. The curves of the specimen cut from the edges of the plates also differ, one with a peak of 30N, another with 40N. Additionally, the tests specimens displayed very large amount of deformation, in comparison to the other test types.

In Figure 64 all compressive curves rise very steeply from zero, reaching **1200 - 1500 N** by about 0.8 - 1.0 mm displacement. Some specimens then plateau, showing a plastic-like yield, while others soften abruptly, indicating brittle failure.

In Figure 65 the tensile load reaches **650–720 N** at ~3% strain — which translates into 4mm of deformation with 150mm of initial specimen length — in the strongest samples before a sharp drop, while weaker ones peak at 490–550 N and then decline more gradually.

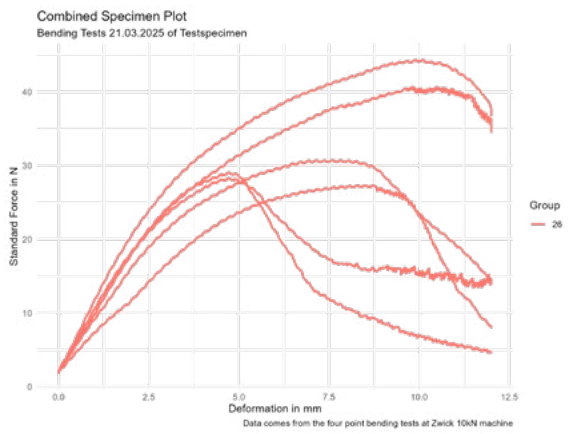

Figure 64. Exemplary Force/Deformation Plot of the strongest specimen group (C/L ratio). Bending Test

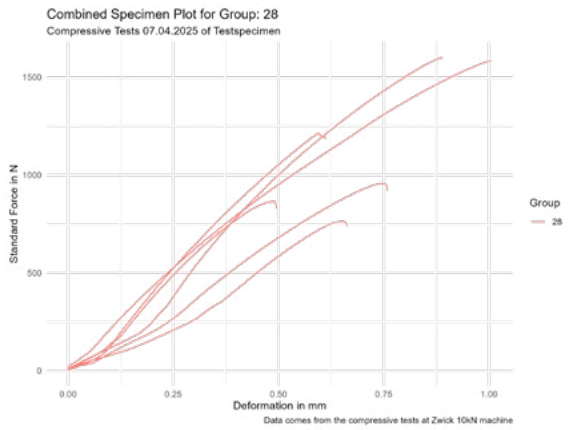

Figure 65. Exemplary Force/Deformation Plot of the strongest specimen group (C/L ratio). Compression Test

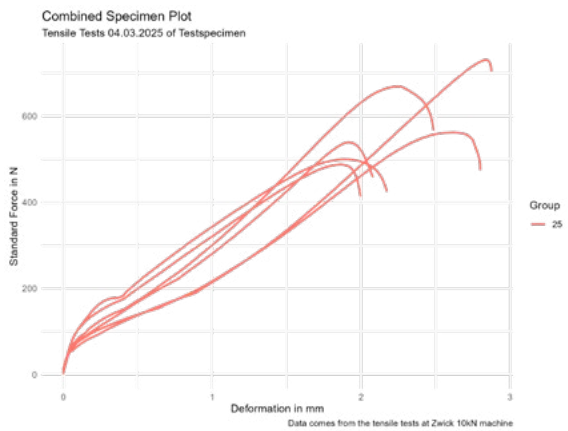

Figure 66. Exemplary Force/Deformation Plot of the strongest specimen group (C/L ratio). Tension Test

Translation of Standard Force to Material Strengths:

Each of these testing results now only represents the value of applied force at which the material fails. The first step in understanding the material performance is to determine the material strength based on the cross-section of the respective specimen. The groups that are in the legend of the plots refer to the sample number. The according C/L ratio is plotted on the mean position of each box. This ratio ranges from 0.66 to 4 which is the numeric value of the used mixture, for example a ratio of 0.5 means one part cellulose on two parts lignin, or a ratio of 2 means 2 parts cellulose 1 part lignin.

During the plotting of the compressive strengths an observation in regards to the specimen origin was made. The plot of the compressive strength f_t is faceted into two plots, separated

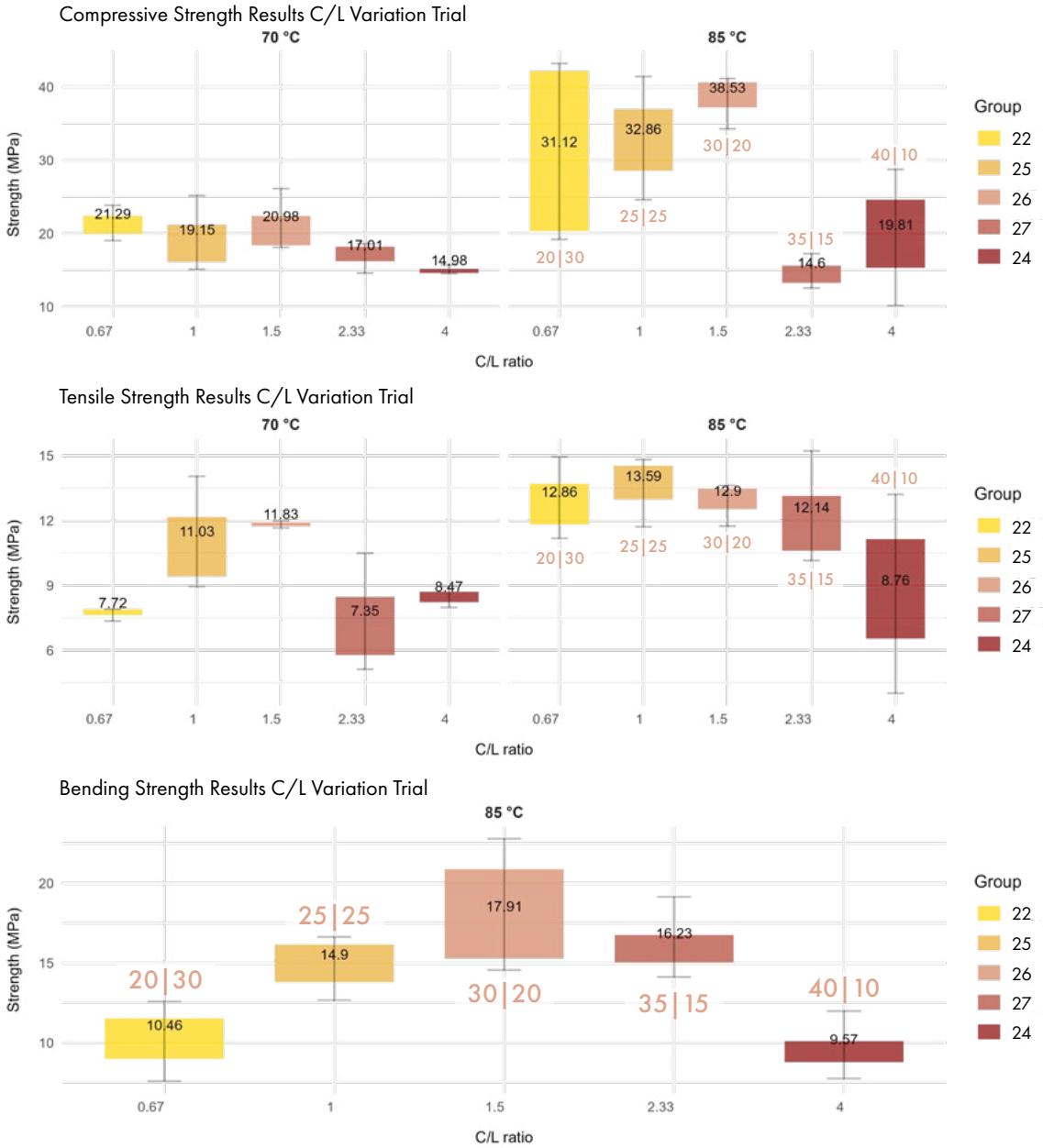

Figure 67. Box-plots of Bending, Compression and Tensile Strength Results of the C/L ratio analysis

by the sample that the specimen were cut from. Per test the 6 specimen per group were cut from two different plates in order to even out sample specific material behaviour.

In the production of the samples of the right group, a methodological error was found during the hot-pressing process. The samples were mistakenly pressed at 70°C, instead of the 85°C used for the other samples of the C/L material trial. This requires the plots to be separated.

While this means that the results of the compressive tests that can be set in relation with the other test types have less data points and possibly less certainty, the lower pressing temperature, shows quantitative data on how f_t is also depending on the processing temperature at constant moisture level.

Above a C/L ratio of 7:3 the strength of the 70°C samples is constantly lower than the 85°C samples. The 70°C samples also demonstrate a relationship of increasing f_t with increasing lignin content.

The tensile strength consists only of three data points for one C/L mixture ratio, this explains the change of the plot.

The bending strength displays the highest values for the 3:2 ratio of cellulose and lignin. Beyond this ratio the strength appears to drop both in positive and negative direction.

Elastic Moduli:

The Young's modulus (often denoted E_E) is the fundamental elastic modulus of a material and is derived from the ratio of uni-axial stress to uni-axial strain for small deformations.

In an ideal elastic, isotropic material, the slope of $\sigma - \varepsilon$ is identical in tension or compression, so "tensile" and "compressive" modulus are the same E_E. In real tests, friction, end-constraints, buckling, or micro-damage can cause slight differences.

For the following display of the Young's modulus the material is assumed to be isotropic, in order to simply the further steps of the data analysis and rule out imperfections of the material and inconsistencies during the production process.

In the determination of the bending modulus it has to be taken into account that the specimen experiences a non-uniform stress distribution (zero at the neutral axis, maximum at the surfaces), so the derived slope of load vs. deflection gives an effective modulus E_{eff}. It is related to E_E via beam theory, but sensitive to the specimen geometry, surface quality, and shear deformations. Additionally, without knowing the specimen deformation, but only the probe head deformation of the testing machine the bending modulus can also not directly be derived from these measurements.

In order to find the strength modulus of any kind, the slope of the stress/ strain curve has to be determined. Appendix Figure 6 demonstrates how for the compressive tests each graphs has the selected slope that is the most linear section of that curve. In Figure 68 the Moduli (in GPa) of the compressive and tensile and bending test are plotted. There is still quite a disparity in the strength of the samples, that indicates that the material not behaving isotropic.

Despite the systematic error of determining the bending modulus without knowing the deflection of the specimen, but only the position of the probe head, the bending modulus can be determined by dividing by a general factor of. These values are plotted in Figure 63. In the other material trials, the deflection of the sample should also be determined for a more reliable result.

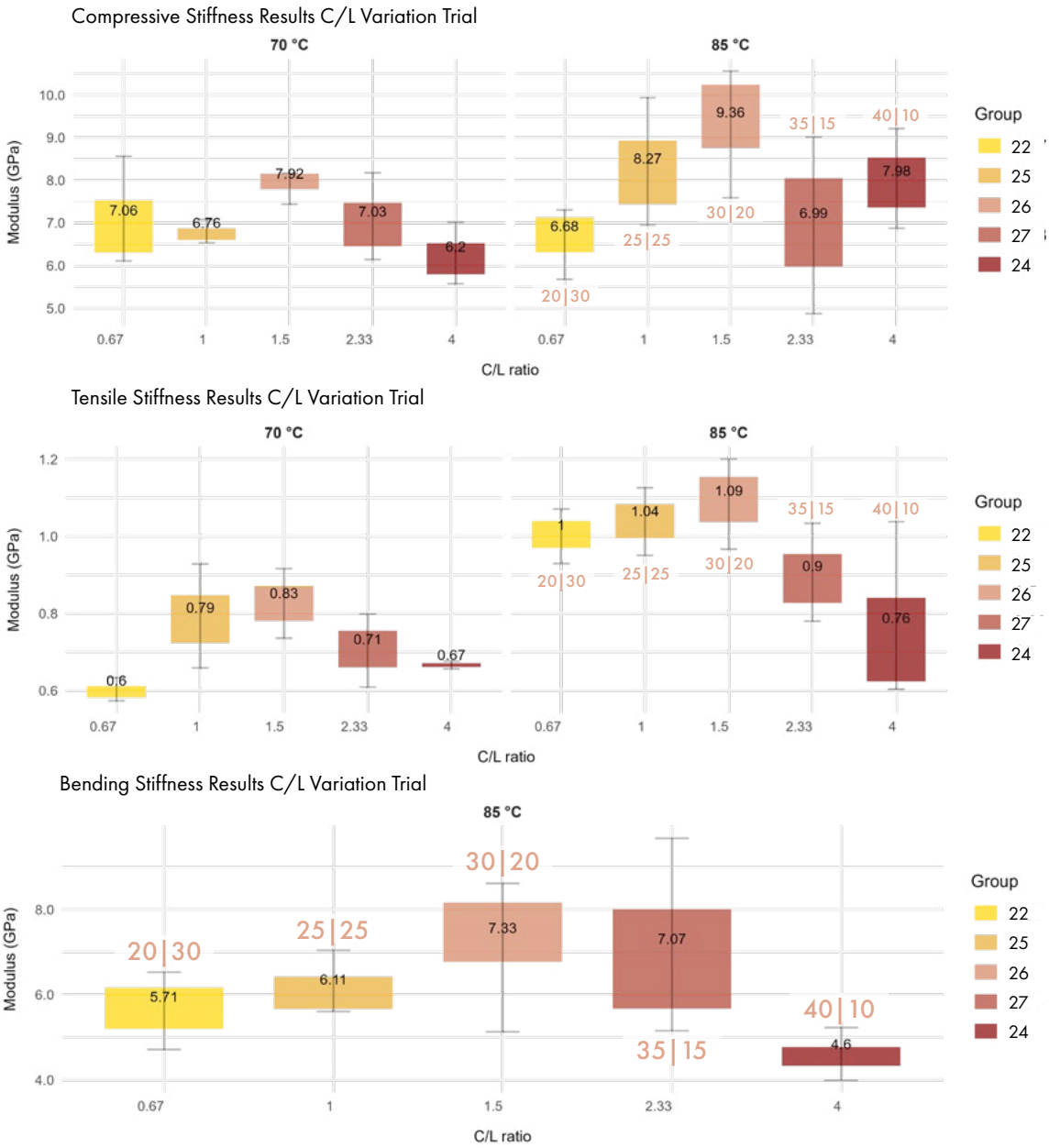

Figure 68. Box-plots of Compressive,Tensile and Bending Modulus, Results of the C/L ratio analysis

Table 6. Mean Strengths and Stiffness values from the C/L trial

Mixture Ratio in g	F_T	F_C	F_B	E_T	E_C	E_B
40 / 10	8.76 MPa	19.80 MPa	9.56 MPa	0.76 GPa	7.97 GPa	4.60 GPa
35 / 15	12.14 MPa	v14.60 MPa	16.22 MPa	0.89 GPa	6.98 GPa	7.07 GPa
30 / 20	12.89 MPa	38.52 MPa	17.90 MPa	1.09 GPa	9.35 GPa	7.32 GPa
25 / 25	13.59 MPa	32.86 MPa	14.89 MPa	1.04 GPa	8.27 GPa	6.11 GPa
20/ 30	12.86 MPa	38.68 MPa	9.34 MPa	1.00 GPa	6.66 GPa	5.81 GPa

Testing Results C/L Trial:

In Table 6 the means of the material strengths and strength moduli of the cellulose and lignin trial are combined. The tensile tests have yet to be successfully performed to include them in combined conclusion about the material trial. The strongest C/L ratio in compression is the 2:3 ratio, in bending it is the 3:2 ratio. The stiffest C/L ratio is 3:2 ratio in compression and presumably as well in bending.

Figure 69 depicts the data points for strength and stiffness of Table X combined and a polynomial regression is applied to study the material behaviour in relation to the change in ratio. In this study, a second-degree polynomial (quadratic) model of the form:

$$y = ax + bx^2 + c$$

was fitted to each series of C/L ratios and the corresponding strength or stiffness values. Ordinary least-squares estimation yields coefficients that minimise the sum of squared deviations between observed and predicted values, allowing the curve to accommodate both linear and quadratic trends.

The coefficient of determination, R^2, quantifies the proportion of total variance in the response explained by the model: values approaching 1 signal that the quadratic curve closely captures the pattern of the overall data, whereas lower values indicate that the curve misses a lot of values.

With the p-value it is possible to assess whether the combined linear (x) and quadratic (x^2) terms improve prediction relative to linear model. A p-value below 0.05 indicates that at least one of the regression coefficients differs significantly from zero, and it confirms that the fitted curvature is unlikely to result from pure chance. The p value also ranges from 0 to 1.

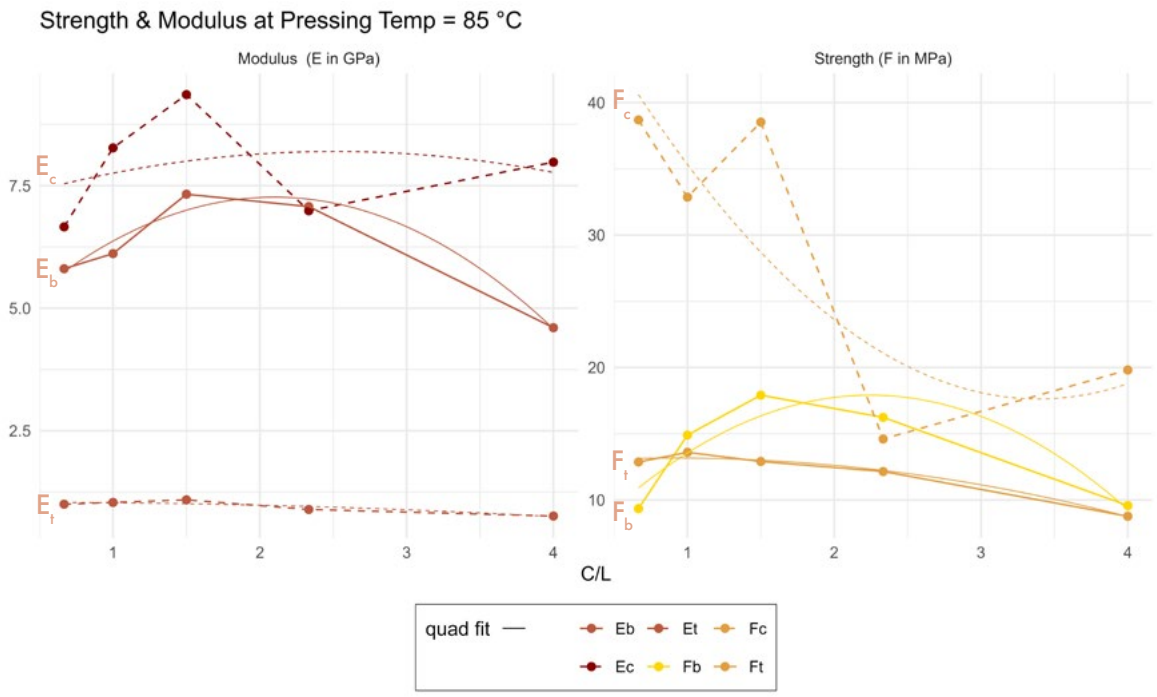

Figure 69. Scatterplots of the F_C, F_B, F_T and E_C, E_B, E_T values and functions based on polynomial regression.

Table 7. r^2 and p values of the 4 regressions.

Function	r^2 value	p value	Function of E/F to C-L
E_b	0.958	0.0419	$E_b(C/L) = 3.997 + 3.116 \times x + -0.742 \times x^2$
E_c	0.0544	0.946	$E_c(C/L) = 6.976 + 0.973 \times x + -0.194 \times x^2$
E_t	0.837	0.163	$E_t(C/L) = 1.035 + 0.02 \times x + -0.023 \times x^2$
F_b	0.845	0.155	$F_b(C/L) = 3.735 + 12.622 \times x + -2.81 \times x^2$
F_c	0.696	0.304	$F_c(C/L) = 53.228 + -20.999 \times x + 3.096 \times x^2$
F_t	0.981	0.0192	$F_t(C/L) = 12.783 + 0.839 \times x + -0.462 \times x^2$

Table 7 demonstrates all the r^2 and p values of the fitted regressions to the strength/ stiffness in relation to the C/L ratio. Two functions reveal to be of statistical significance. The function describing the bending stiffness E_b in relation to the C/L ratio has a p-value of 0.042 and a r^2 -value that tells us that almost 96% are explained by the applied model Additionally, with an even lower p-value of 0.0192 the regression is fitted over the data to create the F_t function. Also its coefficient of determination (r^2) shows large coverage of the variability.

In summary this means that those two functions used to describe the respective relationship are with a significant probability an accurate description for this relationship and at the same time a large share of their variability is explained by the function. The other applied regressions do not appear to be of enough significance to yet conclude a relationship from them.

4.1.5 Moisture Trial Test Result

The aim of the moisture variation trial was to investigate how the contained amount of moisture in a sample has an affect on the adhesive qualities of the lignin. The visual results of the hot-pressing already revealed that there is a gradual change in the surface finish of the samples from matt, light brown with isolated dark brown sheen spots to the full surface being dark brown and lustrous. Due to the blistering that occurred at the higher moisture content—which is a result of the improper cool-down step to only 60°C— the material performance might be impaired. The mechanical testing is used to gain more insight into mechanical properties.

In contrast to the other trials, these plates were only tested in their flexural performance. This approach is sufficient because a bending test simultaneously subjects one surface to tensile stresses and the opposite surface to compressive stresses, capturing both failure modes in a single experiment. Moreover the flexural loading more closely mimics real-world service conditions so the flexural modulus and strength measured provide the most comprehensive indication of the performance.

Testing Results Moisture Trial:

The results of this trial are plotted in Figure 70. The sample that was pressed without any additional water added to the mixture performed the weakest. The cohesion of the specimen was in fact so weak that some specimen did not exhibit any strength or stiffness. Past the initial sample, in both stiffness and strength there is a clear “dip-and-recover” trend visible. The strength first experiences a 16% decrease from 14.8 MPa to 12.7 MPa (5% to 15% added water) to only rise back to 14.9 MPa.

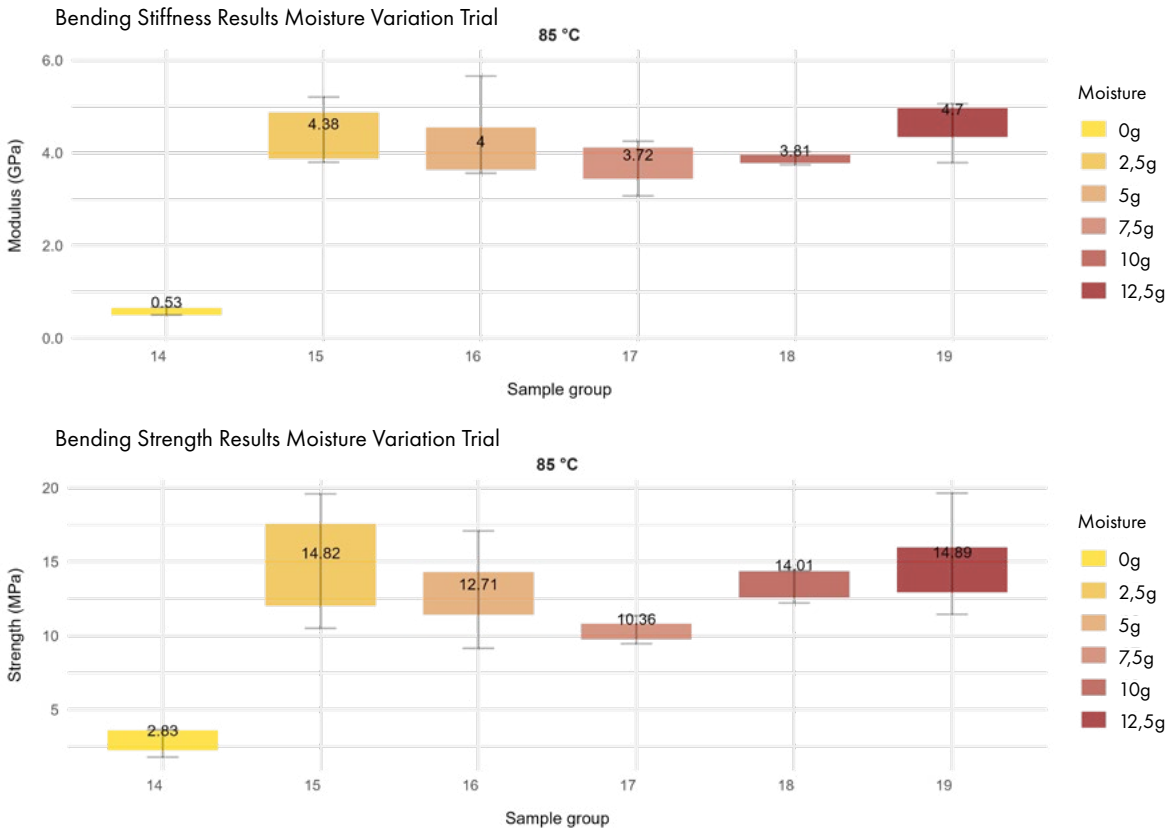

Figure 70. Boxplot of the Material Strength and Stiffness in Bending of the Moisture Variation Trial.

Also noticeable is that the spread (IQR) is smallest at Sample 17 (when strength is lowest) and then widens again as strength recovers.

The trend for the stiffness behaves similarly, with a 17% drop from 4.38 GPa to 3.72 GPa and a stronger recovery to 4.7 GPa. The smallest spread of data is measured for the Sample 18.

In comparison to the 3/2 ratio sample (using 25% moisture) of the C/L trials, which has similar processing conditions, the results from sample 19 that has the same moisture content outperforms that sample with a difference of 5.5 MPa in strength but is less stiff of 1 GPa.

These differences in the material are explainable by the change in processing conditions and refinement of the entire process. For example the moisture samples were tested much later in the process of the research and were dried more thoroughly after pressing. The large contrast in strength however, hints that either the material itself shows a lot of variability of the results or that the samples were not prepared properly. This underlines that many more tests are necessary to gain really reliable results.

4.1.6 Lignin Variation Trial Test Results

As a reminder, the variation in the lignin source is chosen to discover the potential differences in the adhesive qualities per lignin extraction process. Performing mechanical tests is useful to verify the conclusions from the literature, such that the sulphur contents affect the cross-linking capabilities of lignin, or broader claims that Organosolv lignin has a higher reactivity —there is usually no mention by which qualifier the reactivity is measured— than for example soda lignin. The results from the tests can then also be combined with factors like costs to

narrow down or rule out lignin types for future large scale adoption of the process. In contrast to the previous trial samples, this set of plates had 10wt% of added water and were hot-pressed at 140 °C, with thorough cool-down to 35°C.

Results Lignin Trial:

Under bending the lignin types exhibit the same relation in stiffness and strength, with Kraft lignin being the weakest, Organosolv lignin in the middle and Soda lignin being the strongest (34.7 MPa) and stiffest (14.07 GPa). In compression, Soda lignin had achieved an exception strength of 62.84 MPa and the other types in the range of 30 to 40 MPa. The kraft lignin simple had shown the highest compressive stiffness of the three, with only a slightly higher mean value than Soda lignin, of 7.96 GPa. The tensile stiffness of all samples is low and ranges from 0.6 to 1.36 GPa, implying the material is quite compliant. Also in the tensile strength the materials perform less than in compression (Figure 71).

A look at the deformations of the samples also reveals that the measured deformation is almost double in tension with 2 to 2.5mm and in compression —not including the outlier— around 1.2mm (Figure 72).

The samples for this trial were produced towards the end of the development process, were the process of mixing and hot-pressing was fine tuned. Indicatively, the spread of the boxplots has become smaller, suggesting more precise results and a more consistent, overall process. The difference in compressive and tensile performance is another indicator

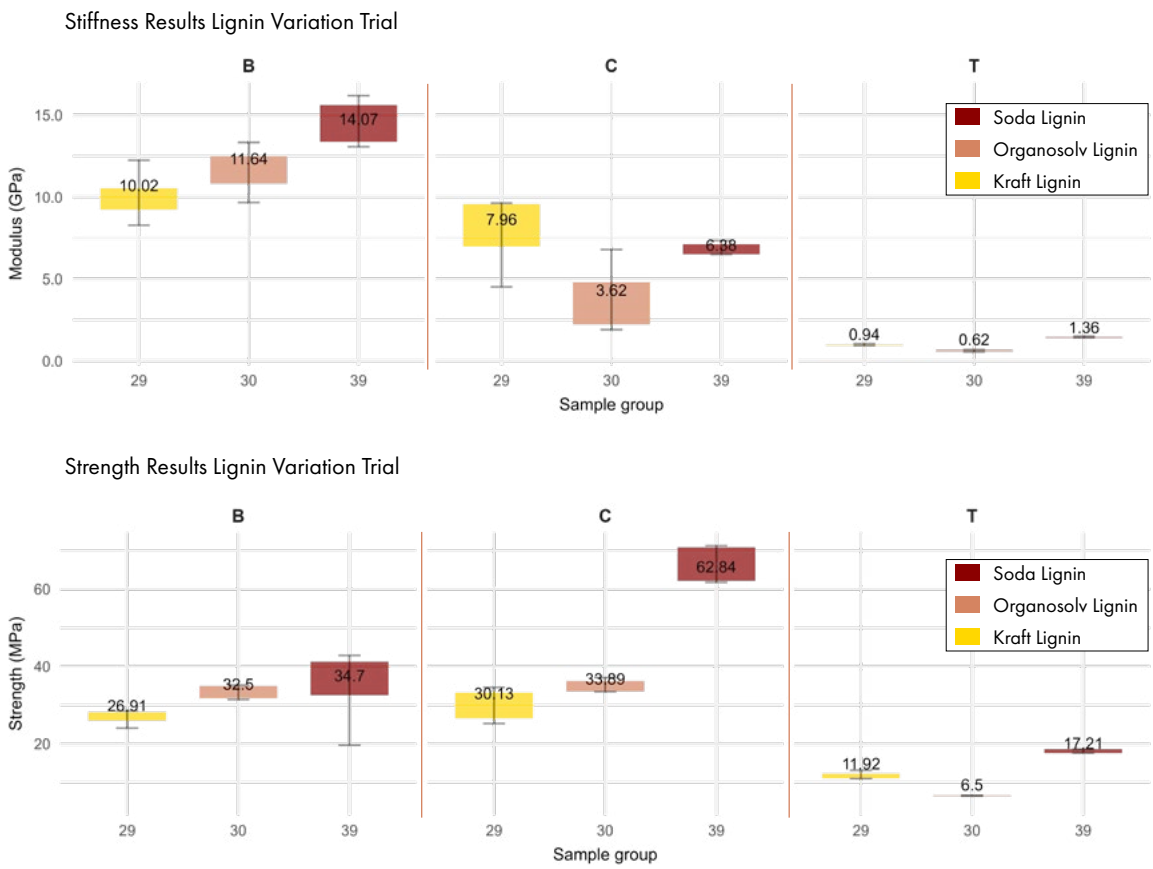

Figure 71. Boxplot of the Material Strength and Stiffness in Bending, Compression and Tension of the Lignin Variation Trial.

that the hot-pressed cellulose-lignin material does not behave isotropic. Through this trial it could be confirmed that the choice of lignin has quite significant impacts on the mechanical performance of the material.

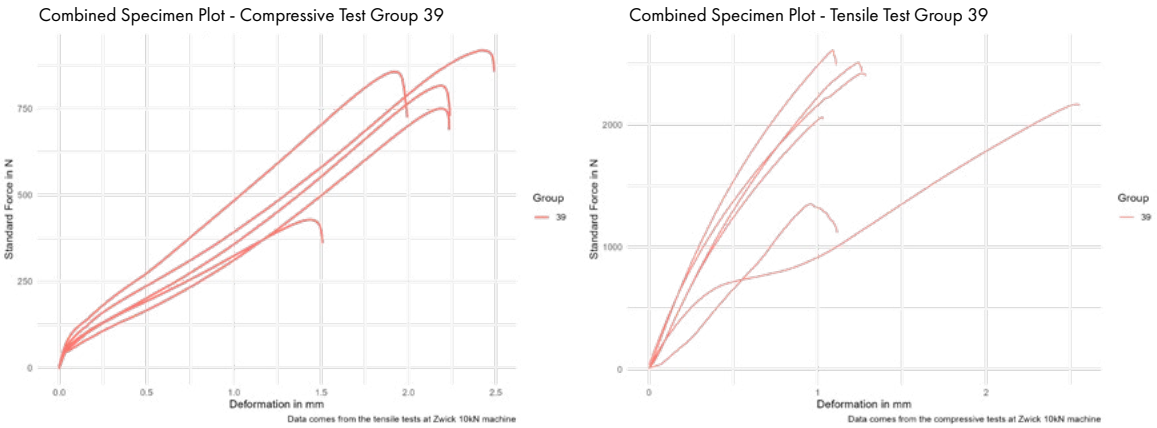

Figure 72. Comparison of deformation of tensile and compressive samples of sample 39 (Soda) in the lignin variation trial

4.1.7 Cellulose Pre-Treatment Trial

Aim of the pre-treatment trial of the cellulose was to verify the assumption from the literature that removal of the in-situ lignin and hemicellulose exposes more surface of the cellulose fibres to be available for cross-linking of the added lignin, potentially resulting in higher material performance. For this sample Soda lignin was used.

Results Cellulose Pre-Treatment Trial:

The sample that is directly comparable with the Soda lignin sample from the previous trial. In stiffness, the pre-treatment sample exhibits very similar results, being slightly weaker in bending (▼17%) and slightly stiffer in compression (▲8.7%) and tension (▲4.6%) . In strength, the pre-treatment sample is again slightly weaker in bending (▼6.1%), and stronger in compression (▲4.2%) and tension (▲16.4%).

Taking into account the spread of the data and overall variance, the pre-treatment does not seem to significantly effect the mechanical performance.

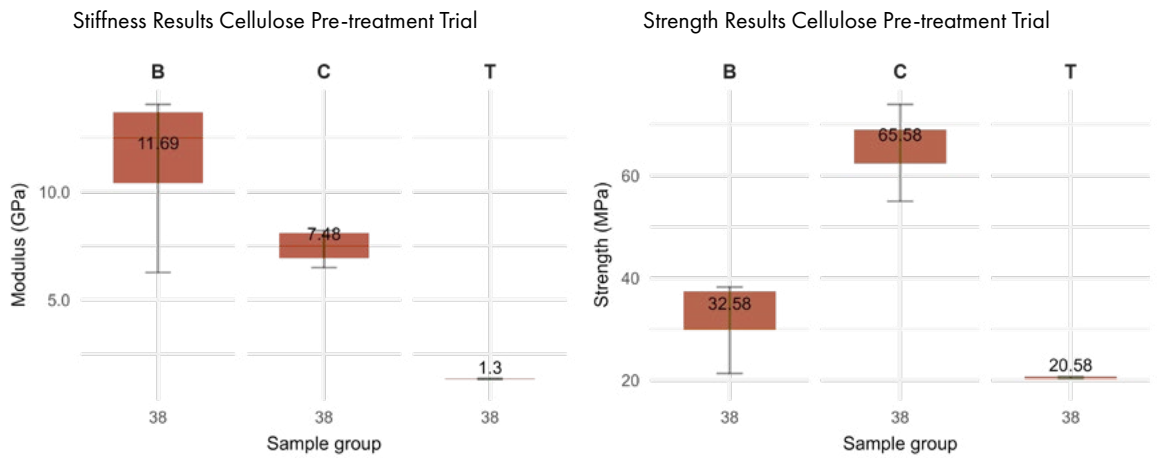

Figure 73. Boxplot of the Material Strength and Stiffness in Bending, Compression and Tension of the Cellulose-Pre-Treatment Trial

4.1.8 DIC Analysis of Tensile Tests

Along with the tensile tests, a digital image correlation (DIC) analysis was used to determine the full-field strains occurring across each specimen while they are being tested. From those measurements the transverse (lateral) and axial strains are extracted to compute the Poisson's ratio ν, and then the formula from Chapter 2.11 is used to obtain the shear modulus G.

The shear modulus is a fundamental material parameter that quantifies the resistance to shape-change under shear loading and is critical for accurately predicting the specimen's response in applications where torsion or off-axis stresses are present — for example an I-beam supporting a cantilevered balcony can experience shear stresses when the load is not applied exactly along its strong axis. The shear modulus G tells how much the cross-section will distort in that scenario.

This workflow using μDIC the visualisation of the engineering strain (eng_strain) is used because it directly corresponds to the "strain" reported by most mechanical test machines—small-strain values that are additive and easy to compare with the force–deformation curve. By interactively selecting the elastic limit on that curve and restricting the DIC run to frames up through that point, it is ensured that the calculated Poisson's ratio ν reflects only the elastic deformation and isn't biased by plastic flow or fracture (Figure 74). At the final elastic frame, the script extracts both the lateral (ε_{xx}) and axial (ε_{yy}) (Figure 76) strain fields across the selected region of interest (ROI) mesh (Figure 75). Then a local ν map is formed by computing $-\varepsilon_{xx}/\varepsilon_{yy}$ at each element center—masking out points where ε_{yy} falls below a small threshold to prevent division-by-near-zero errors that would produce unrealistically large or non-physical ν values. The map is then summarized with a histogram of all valid ν values, overlaid with vertical lines marking the mean, median, and one-sigma scatter. Because the median is least sensitive

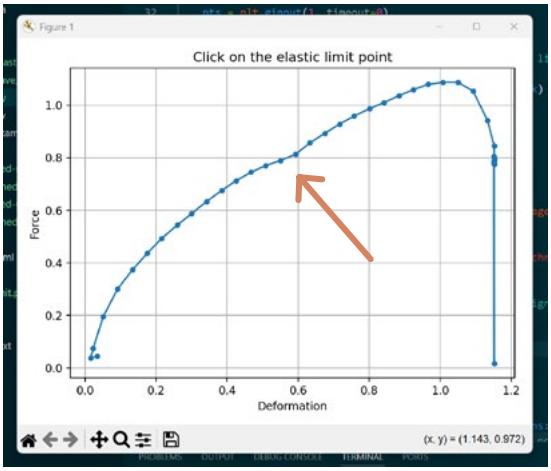

Figure 74. Window in Python for selection the elastic region along the force/deformation curve (custom addition).

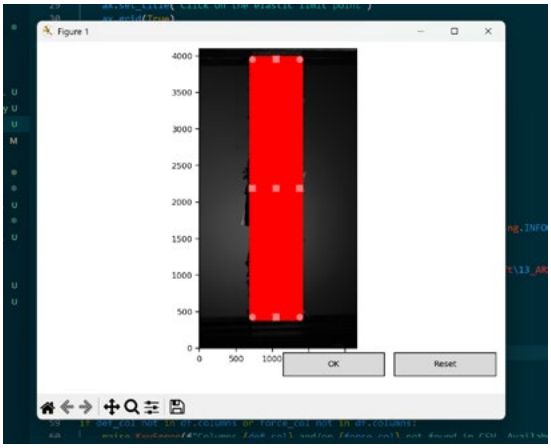

Figure 75. Window in Python for selection the region of interest (ROI) on the specimen (from μDIC).

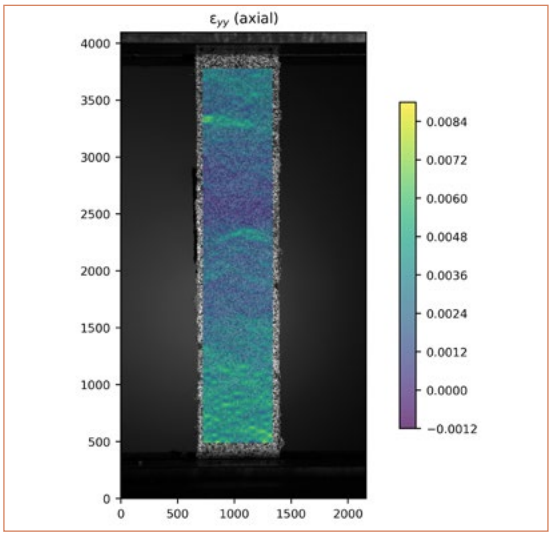

Figure 76. Output map of axial engineering strain on the surface of specimen 39 (from μDIC).

to outliers, it is chosen as the single v value for subsequent shear-modulus (G) calculations (Figure 77). It is still useful, however, to note the mean: when mean and median diverge significantly, it indicates that the v map is being skewed by a handful of extreme local values and that additional filtering or a tighter elastic-region selection may be warranted. In this demonstrated case the output values are:

Poisson's ratio (mean) = 0.562
Poisson's ratio (median) = 0.479
Poisson's ratio (sigma) = 0.429

As the linear elastic region of the testing curve was selected for determining the Poisson's ratio the equation for the standard elastic-moduli relationship — called the modulus conversion formula, or Lame-Hooke relation— is used: $G = \frac{E}{2(1+\nu)}$. The results per all specimen using the tensile modulus E are documented in Table 8 which is indicating a lowering shear stiffness with rising fibre content. Figure 78 shows the resulting shear modulus for the C/L Trial. A shear modulus of 0.4 GPa is comparable to pinewoood.

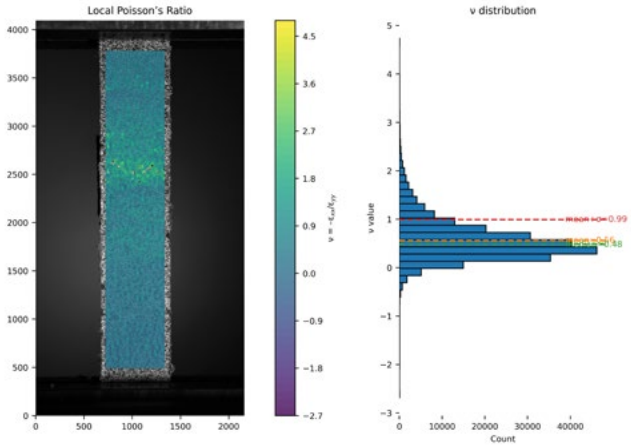

Figure 77. Output map of v-map and plotting of histogram that shows the mean, median and standard deviation of the local measurment (sigma) of specimen 39 (custom addition).

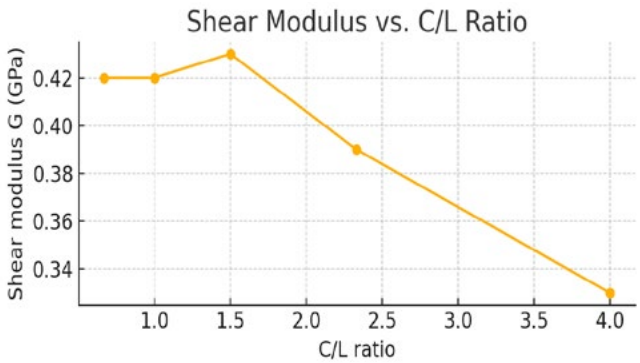

Figure 78. Shear modulus vs C/L ratio of samples from C/L Trials.

Table 8. Results of DIC measurements and calculation results of shear modulus G.

Trial	C/L ratio	v_{mean}	v_{med}	v_{σ}	E_T	G
C/L Trial	4.0	0.194	0.141	0.349	0.76 GPa	0.33 GPa
C/L Trial	2.33	0.156	0.145	0.347	0.89 GPa	0.39 GPa
C/L Trial	1.5	0.397	0.262	0.462	1.09 GPa	0.43 GPa
C/L Trial	1.0	0.246	0.229	0.3	1.04 GPa	0.42 GPa
C/L Trial	0.67	0.194	0.179	0.514	1.00 GPa	0.42 GPa
Lignin Trial (Soda)	1.0	0.562	0.479	0.429	1.36 GPa	0.46 GPa
Lignin Trial (Organosolv)	1.0	0.03	0.003	0.313	0.62 GPa	0.31 GPa
Lignin Trial(Kraft)	1.0	0.043	0.045	0.434	0.94 GPa	0.45 GPa
C-Pre-Treatment Trial	1.0	0.304	0.318	0.735	1.3 GPa	0.49 GPa

4.2 Microscopy

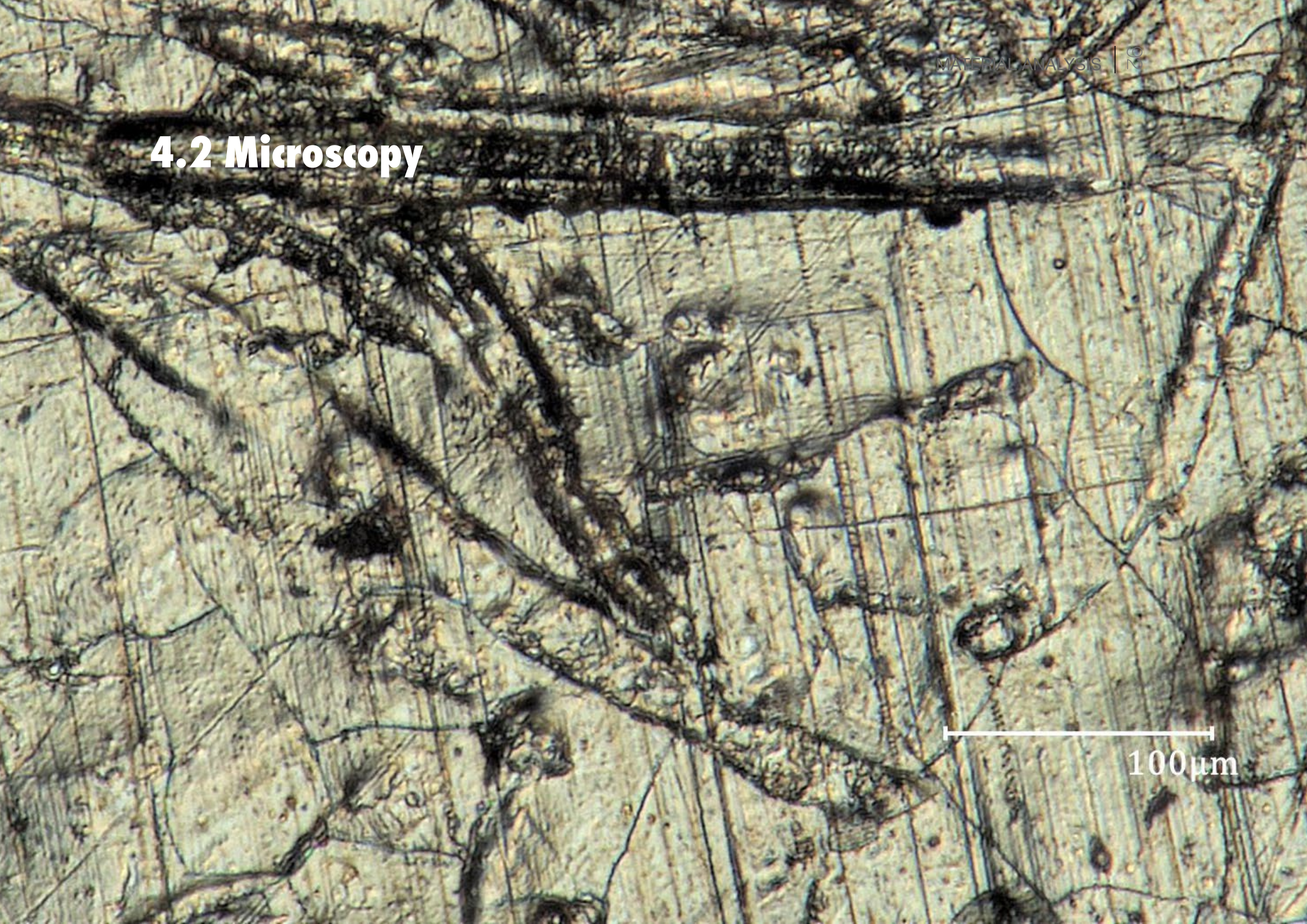

4.2 Microscopy

4.2.1 Inspection of Mixture Trials

This section will take a step back and investigate the surface qualities of the samples, that were produced in the material trials. With different ratios of cellulose and lignin, the impregnation of fibres with lignin might differ, so can also have lignin types, moisture levels and temperature differences an influence on the extend of lignin flow in the samples.

C/L Variation Trial

Figures 67-71 demonstrate the gradual change of the incorporation of the cellulose fibres within the lignin matrix. In all of the samples, it is visible that the fibres are all randomly bundled together while laying flat along the plane of the sample.

Starting from four parts cellulose and one part lignin the surface of the hot-pressed sample appears the most matt without any magnification. Under the microscope it is apparent that the lignin has flown throughout the sample and is in the gaps between the fibres but the comparative bulky cellulose fibres are exposed, making the surface less reflective than the following samples. Discolouration from the newspaper ink is also visible.

The 35/15 sample (Figure 69) has a similar appearance as the previous one, but shows larger segments of lignin on the surface of the sample. Still many fibres are protruding out of the surface.

From Figure 81 to 71 the incorporation of fibres under the surface of the matrix increases until the surface of the sample is the smoothest in the last sample that is only two parts cellulose and one part lignin. Also the amount and size of surface voids around the fibres gradually decreases until the surface is almost free of defects and also demonstrates the most reflecting and deep brown-black surface.

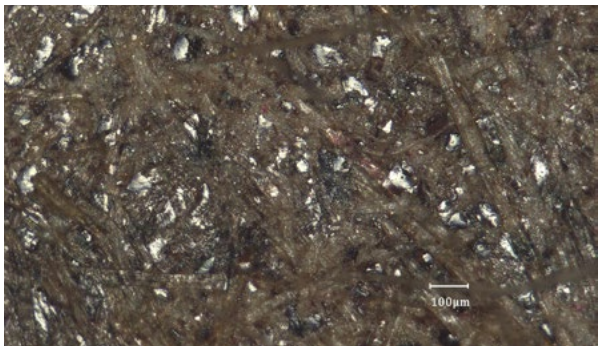

Figure 79. C/L Sample - 40/10 x200

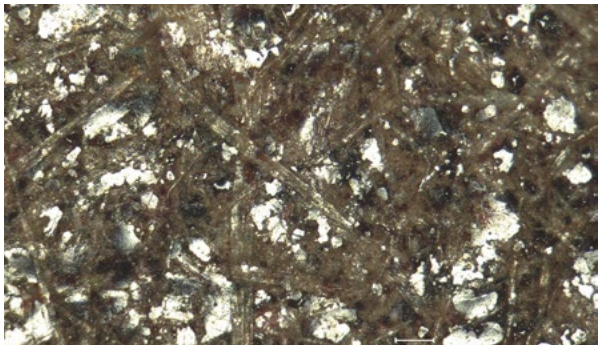
Figure 80. C/L Sample - 35/15 x200

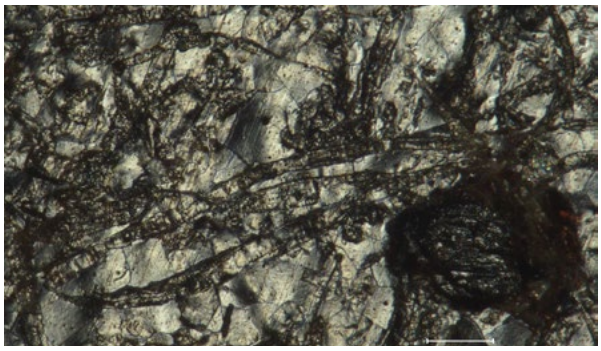
Figure 81. C/L Sample - 30/20 x350

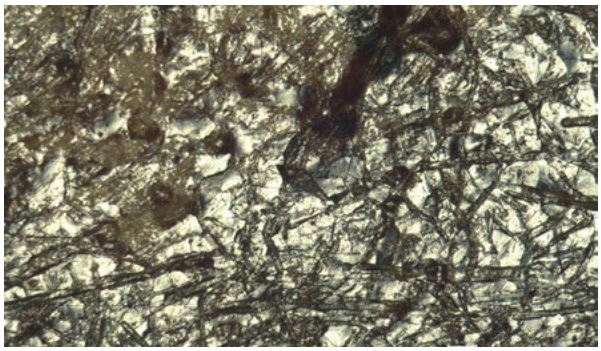
Figure 82. C/L Sample - 25/25 x150

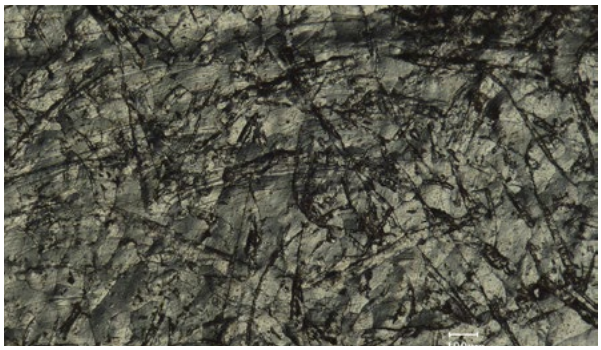
Figure 83. C/L Sample - 20/30 x150

Moisture Content Trial

The moisture content trial revealed that the lignin flow within the same material mixture (30/20) at constant temperatures is affected by the amount of water that is present during the hot-pressing process. Under the microscope it is also visible that the level that the lignin changes texture and becomes more glossy seems to be impacted by the change in moisture. Especially in the 0wt% sample (Figure 88) the lignin particles seem to be of the same grain size as before the pressing (when compared to the powder under the microscope), but now simply more clumped together. With only 5 wt% of moisture this image significantly changes showing the lignin in much larger, flat segments while already incorporating the fibres. From 10 wt% onward, the fibre incorporation seems to only slightly increase each step. The blisters or bubbles appear to be under the surface of the sample and no visible cracking or ripping can be seen.

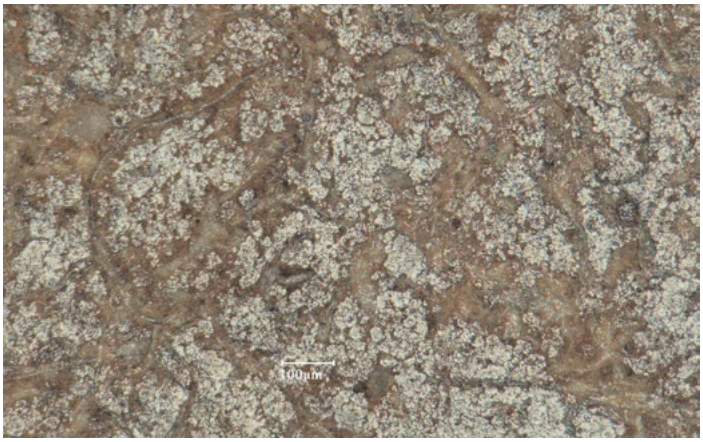

Figure 88. Moisture Sample - 0wt% x250

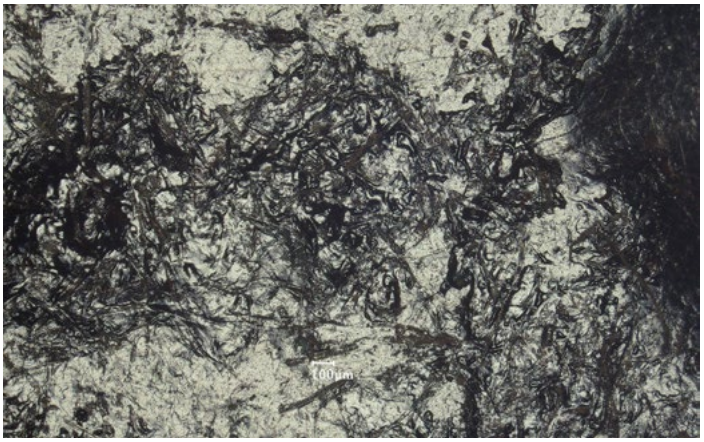

Figure 89. Moisture Sample - 15wt% x100

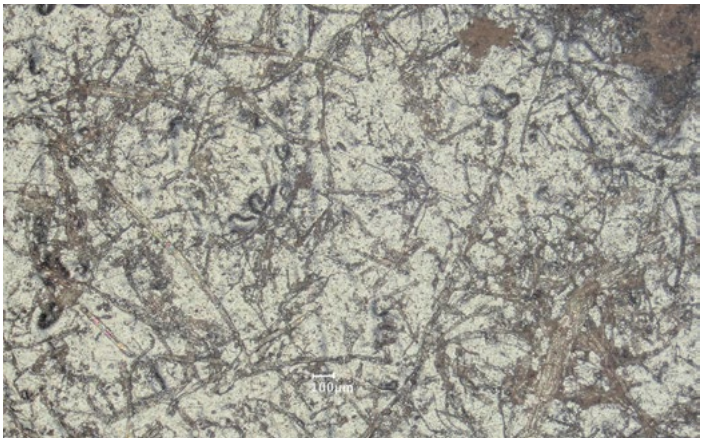

Figure 86. Moisture Sample - 5wt% x100

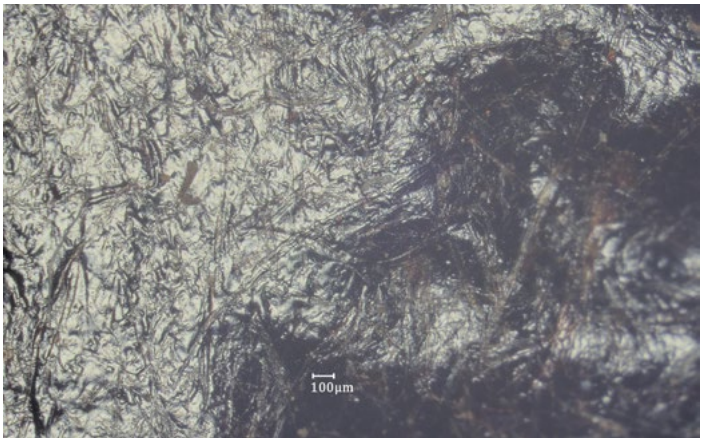

Figure 87. Moisture Sample - 20wt% x100

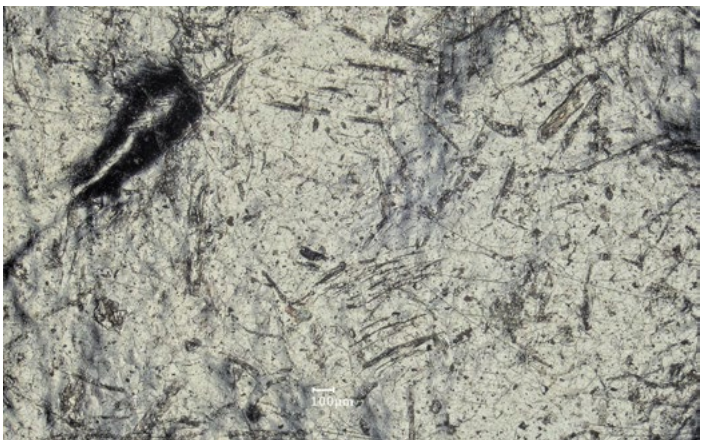

Figure 84. Moisture Sample - 10wt% x100

Figure 85. Moisture Sample - 25wt% x 100

Lignin Variation Trial

Figure 90 - Figure 92 compare the surface finish of the samples with different lignin types. The flow behaviour of the Kraft and Soda lignin type are comparable, with both of them creating a smooth and glossy finish. The Organosolv lignin sample however, has very patchy areas were the lignin seemed to have clumped together. It also the only sample that has fibres that are visibly exposed at the surface, which makes the finish appear less glossy.

Cellulose Pre-Treatment Trial

Figure 93 and Figure 94 show the surface finish and the cut section of the cellulose pre-treatment sample. The finishing of the surface is similarly to the Lignin trials very smooth. In this case however, there are almost now fibres directly visible included in the lignin. This could be explained by the extra processing steps, namely the multiple times the treated cellulose pulp is being blended. The fibres become shorter, finer and are less visible at the surface of- The lignin itself appears to have flown very thoroughly throughout the sample. The indentations, marks and creases from the releasefilm and the moulds surface are imprinted in the sample. Some clumping remains.

In the cut section a speckled pattern appears. What was previously not visible from the top is that within the sample clusters of the pre-treated cellulose remain un-wetted by the lignin. A possible reason of this can be found in the process of the pre-treatment. The dried treated pulp clumps together a lot and even though these clumps are blended again while they are mixed with the lignin, they do not fully break up in the process. Increasing the processing time could be an approach to address this.

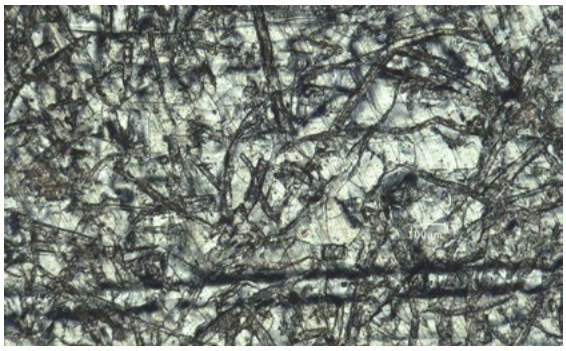

Figure 90. Kraft Lignin Sample x150

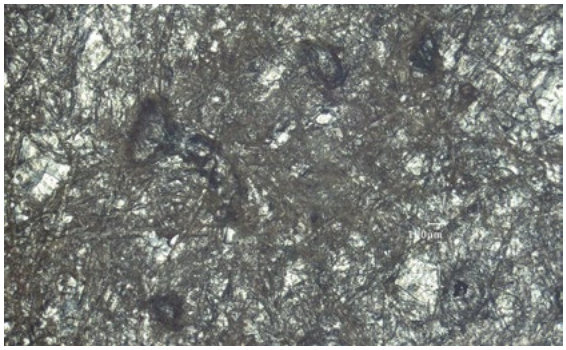

Figure 91. Organosolv Lignin Sample x100

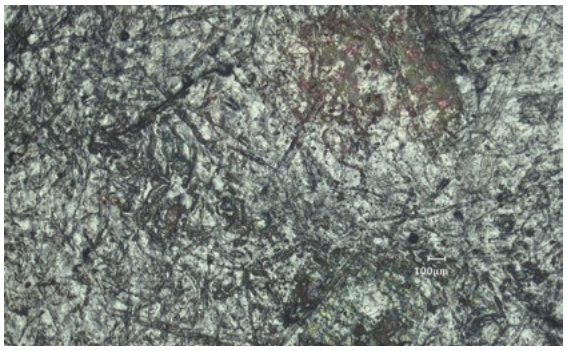

Figure 92. Soda Lignin Sample x100

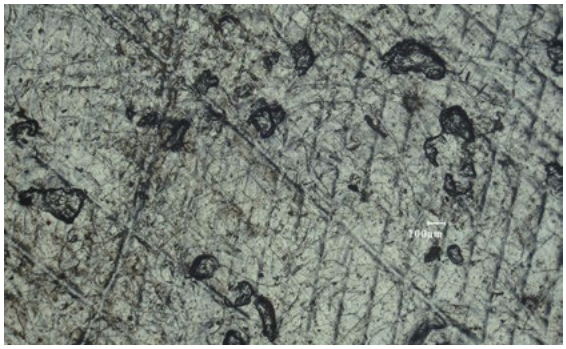

Figure 93. Cellulose Pre-Treatment Sample x100

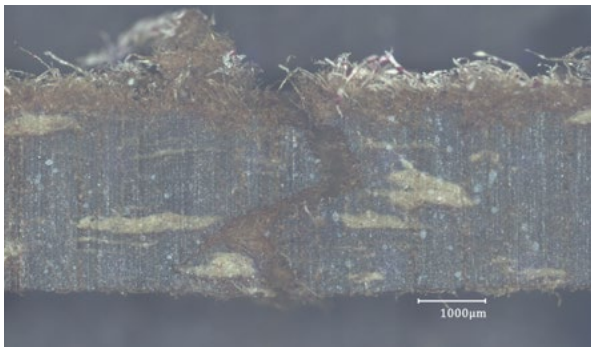

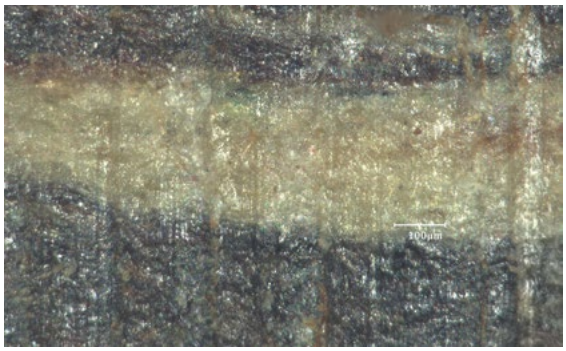

Figure 94. Cellulose Pre-Treatment Sample Cut Section x100. Larger frame and close-up.

4.2.2 Review of Composite Failure Modes

For understanding the type of failures that occur during the three mechanical testing types, this section will summarize the relevant mechanisms and failure modes for fibre reinforced composites.

Compressive Failure

Due two the differences of properties of the fibres and matrix the failure of the composite is typically initiated by one of these micro-mechanisms:

- The Poisson-ratio between the fibre and the matrix are mismatched, this creates a transverse tensile stress in the material and promotes cracks at the fibre matrix interface (Hahn & Williams, 1984).
- A localised stress concentration that appears around voids or poor bonding can also trigger interfacial shear cracking.
- Small misalignments between the fibres (in respect to unidirectional fibres) promotes microbuckling.

Also on a microscopic level the resulting mechanisms are elastic microbuckling, where the fibres buckle elastically within the matrix. Fibre kinking occurs when the fibres fracture within the matrix with irreversible kinks. Fibre crushing occurs in a very stiff matrix or when fibres are perfectly aligned and matrix cracking (Thomsen & Kratmann, 2010) (Figure 96).

This results in the three major failure modes on a macroscopic level (Figure 95). Shear crippling is the predominant macroscopic mode. In longitudinal direction splitting occurs

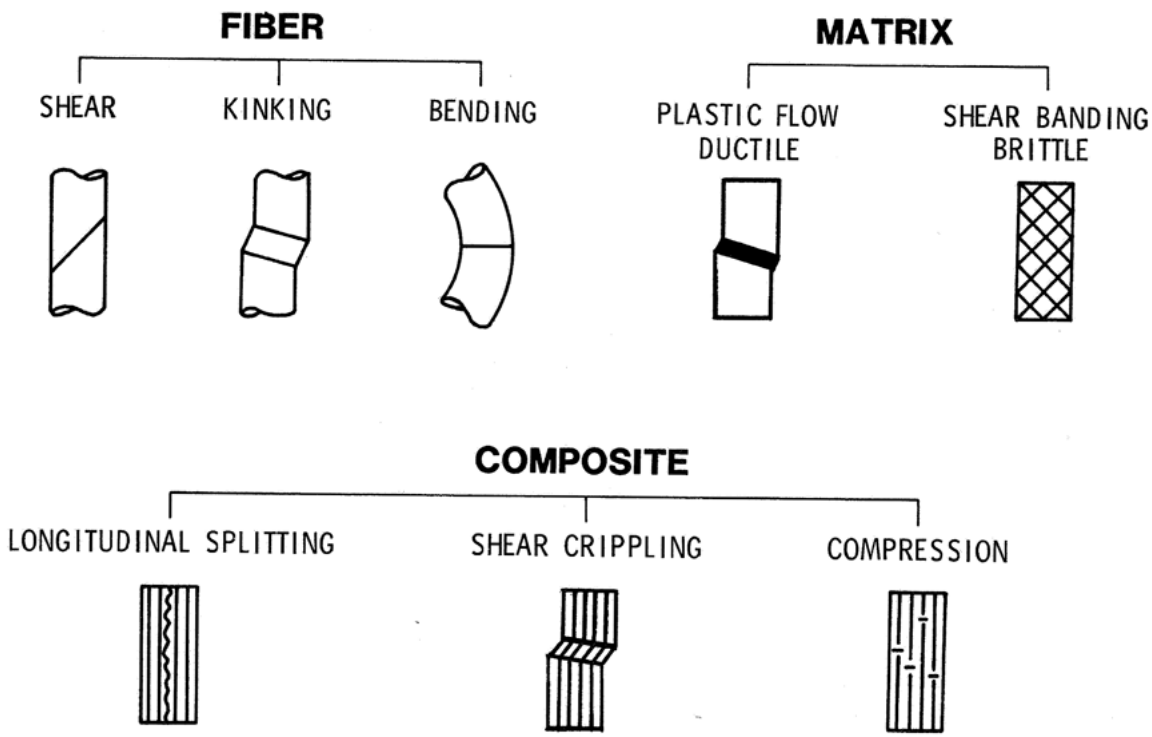

Figure 95. Composite compression failure modes. From Hahn & Williams, 1984

due to buckling of a failed fibre segment between intact fibres and can drive splitting along the fibre direction. Lastly buckle-delamination occurs when in a multi-laminate or sandwich configuration, a kink band induces delamination through-thickness (Figure 96).

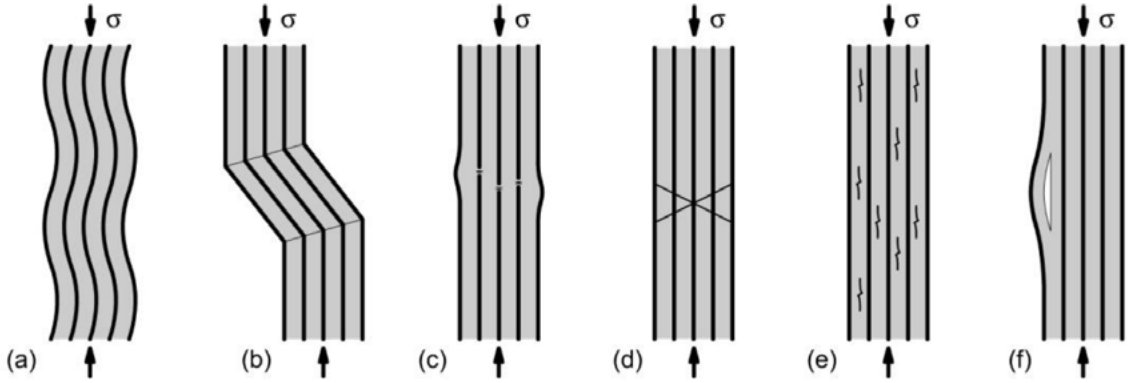

Figure 96. Compressive failure modes of fibre composites. (a) Elastic micro buckling. (b) Fibre kinking. (c) Fibre crushing. (d) Shear band formation. (e) Matrix cracking. (f) Buckle delamination. From Thomsen & Kratmann, 2010

Tensile Failure

Natural fibre composites experience failure modes that are similar to conventional fibre-reinforced polymers, with key failure mechanisms like matrix cracking, fibre/matrix interfacial debonding, fibre pull-out, fibre fracture and delamination between layers. These often occur in combination with increasing force and each of them influences the overall integrity and toughness of the composite.

It is important to note the role of the fibre-matrix interface. The quality of the interfacial bond (IFB) largely determines how load is transferred and how failure propagates. If the interface is extremely strong, the composite may behave in a brittle manner — cracks may cut straight through without engaging toughening mechanisms (Mohammed et al., 2022). Conversely, if the interface is too weak, the fibres cannot carry the load effectively, resulting in premature debonding and loss of strength. And optimal balance is achieved when the composite can absorb the energy via mechanisms like fibre pull-out or crack deflection, rather than catastrophic failure (e.g. Ripping of fibres). The tensile failure modes consist largely of the following types.

- Matrix Cracking

This is often the first mode of damage to appear in a composite under tensile stress. This is due to the matrix having the lower strain-to-failure value than the fibres, so it cracks once its tensile strength or fracture strain is exceeded. It is the pivotal first damage that can lead to other modes of damages, depending how the damage propagates (Mechanical Testing of Composites, 2024).

- Fibre-Matrix Interfacial Debonding

This failure type refers to the separation of the fibres from the surrounding matrix at their interface and indicates a loss of adhesion between fibre and matrix. Good mechanical and chemical adhesion between fibres and matrix govern how this failure type occurs This can be challenging to achieve for natural fibre composites. Untreated plant fibres are often hydrophilic

and do not bond strongly to hydrophobic polymer matrices As a result, interfacial debonding is a commonly observed failure mechanism in NFCs (Kala et al., 2021).

This debonding typically precedes fibre pull-out. When the matrix crack occurs and the fibre bridges the gap, either the fibre will break or the interface will fail, depending on their relative strengths (Mohammed et al., 2022). When the interface fails then the fibre begins to slip, resulting in pull-out of the fibre. Visible signs of interfacial debonding in fracture surfaces include fibre imprints or tunnels in the matrix and fibres with smooth surfaces (stripped of matrix), indicating they were pulled out from the matrix socket after debonding.

- Fibre Pull-out

As mentioned fibre pull-out occurs due to the failing of the interfacial bond between fibres and matrix. But another mechanism is needed for the fibre to pull out of the matrix and leave behind hollow sockets in the matrix and exposed fibre surfaces: the fibre must have at least one break so that a free end can withdraw from the matrix. The pull-out always takes place after interfacial debonding and failure of a fibre.

- Fibre Fracture/ Breakage

Fibre fracture is the failure mode where the reinforcing fibres themselves break (snap) under the applied tensile stress. This is a fibre-dominated failure and is often associated with a more brittle, catastrophic failure of the composite if it happens extensively, since breaking the fibres removes the primary load-carrying elements. In natural composites the fibre strength can vary, so some fibres will fracture at lower strains than others. If fibres are less aligned or present in lower volume, other modes like matrix cracking and debonding might dominate before fibre breakage is widespread.

- Delamination

Delamination only occurs in fibre composites that are made of individual (e.g. woven) mats and it means that these layers separate. Under tensile loading, delamination can occur if a crack propagates out of one layer and into the interface between layers, causing those layers to split apart. It is typically present as a planar crack between the layers.

4.2.3 Overview of the Observed Failure Types of the Material Trials

C/L- Trial Compression Test

In almost all natural-fibre composites the reinforcing fibres are significantly stiffer than the surrounding matrix. For example, cellulose microfibres typically have a tensile Young's modulus on the order of 70–140 GPa, whereas a lignin-rich polymer matrix will be in the single-digit GPa range. That large stiffness difference is why, under compression, the matrix is the "weak link". It yields or cracks first, allowing the fibres to buckle or kink inside a softer surrounding for support.

Figure 97 - Figure 101 show the failure on the short side of the C/L Trial samples. Through the hot-pressing process the fibres are being compacted into flat mats. While they have random orientations in the horizontal plane of the sample, they are mostly not arranged through the thickness of the sample. This is well observable in Figure 98, that shows some kind of marbling effect, where the fibres are less wetted with lignin or show discolouration.

In the 4:1 C/L Sample little deformation is visible in comparison to the other samples. The dominant failure feature is a longitudinal split of the fibres and delamination that creates bulging on the samples surface. Little or almost no matrix cracking is visible.

In the 35:15 sample a connected split that runs diagonally across the thickness of the sample is visible. Most fibres along the split appear to not have split but they have disconnected from the lignin matrix or kinked along the crack.

The remaining samples show classing signs of shear crippling failure that is dominated by plastic micro-buckling and shear-band formation rather than pure fibre crushing. The higher the lignin content, the more pronounced matrix cracking along the splits is visible — showing that the material becomes more brittle.

This effect can also be paired with the abruptness of the failure. The individual displacement / applied force mappings show a much pointier curve peak the higher the lignin content in the sample

C/L- Trial Tension Test

The sequence of micrographs (Figure 102) reveals a visible change in failure morphology as the cellulose-lignin ratio shifts in the C/L Trial samples. In all images, the orange trace highlights the crack path across the thickness. In the cellulose-rich sample (top image), the crack path is very wandering, propagating through fibre bundles rather than propagating in a straight line. This indicates that a combination of tensile and shear failure mechanisms is at play, rather than a purely axial tensile failure. The diagonal path may point to weaker fibre-matrix adhesion, causing cracks to deviate along interfacial zones rather than cleanly through fibres or matrix (Fibre-Matrix Interfacial Debonding). Within the crack numerous cellulose fibre protrude from the crack and signs of fibre pull-out are visible. The little amount of matrix material binding the fibres together, relies on the mechanical bonding of the entangled fibres

As lignin content increases in the next sample (top row, left), the crack path remains irregular but exhibits slightly reduced zig-zag pattern. Although still winding through fibre bundles, the amplitude of the zig-zags is less pronounced. The fibre continue to pull out and bridge the crack. With the crack cutting partly through the lignin-richer regions of the matrix and partly through residual fibre clusters, a mixed failure mode is evident. This intermediate behaviour illustrates how the addition of lignin begins to alter the balance between tensile opening and local shear stresses in the composite. In none of the sample pure failure of the fibres can be observed.

For the following samples the amount of zig-zags continuously decreases, however does not disappear. The final sample, with the highest lignin content portraits the cleanest fracture with the least amount of visible fibres bridging the crack. The failure mode remains similar to the previous samples, as the fibre content is still significant with 40%, no perfect matrix cracking with a perfect perpendicular line towards the loading axis will be visible. Mainly the fibres still appear to be debonding from the lignin interface.

Taking into account the result of the tensile test, the best performing sample seems to have found the most ideal mixture ratio where the fibres are bonded together by the lignin matrix. As the main failure type appears to be interfacial debonding of the two, the strength created by the cross-linking of lignin to cellulose seems to be the most limiting factor for the material performance.

Figure 97. C/L Sample - 40/10 x50

Figure 98. C/L Sample - 35/15 x50

Figure 99. C/L Sample - 30/20 x50

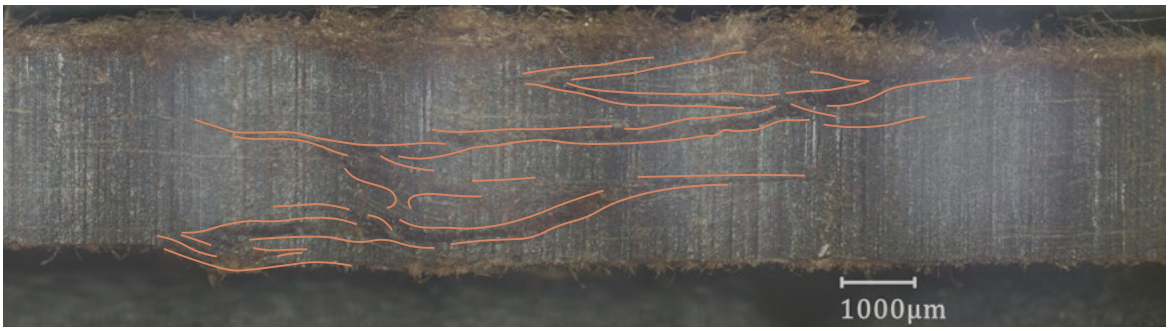

Figure 100. C/L Sample - 25/25 x50

Figure 101. C/L Sample - 20/30 x50

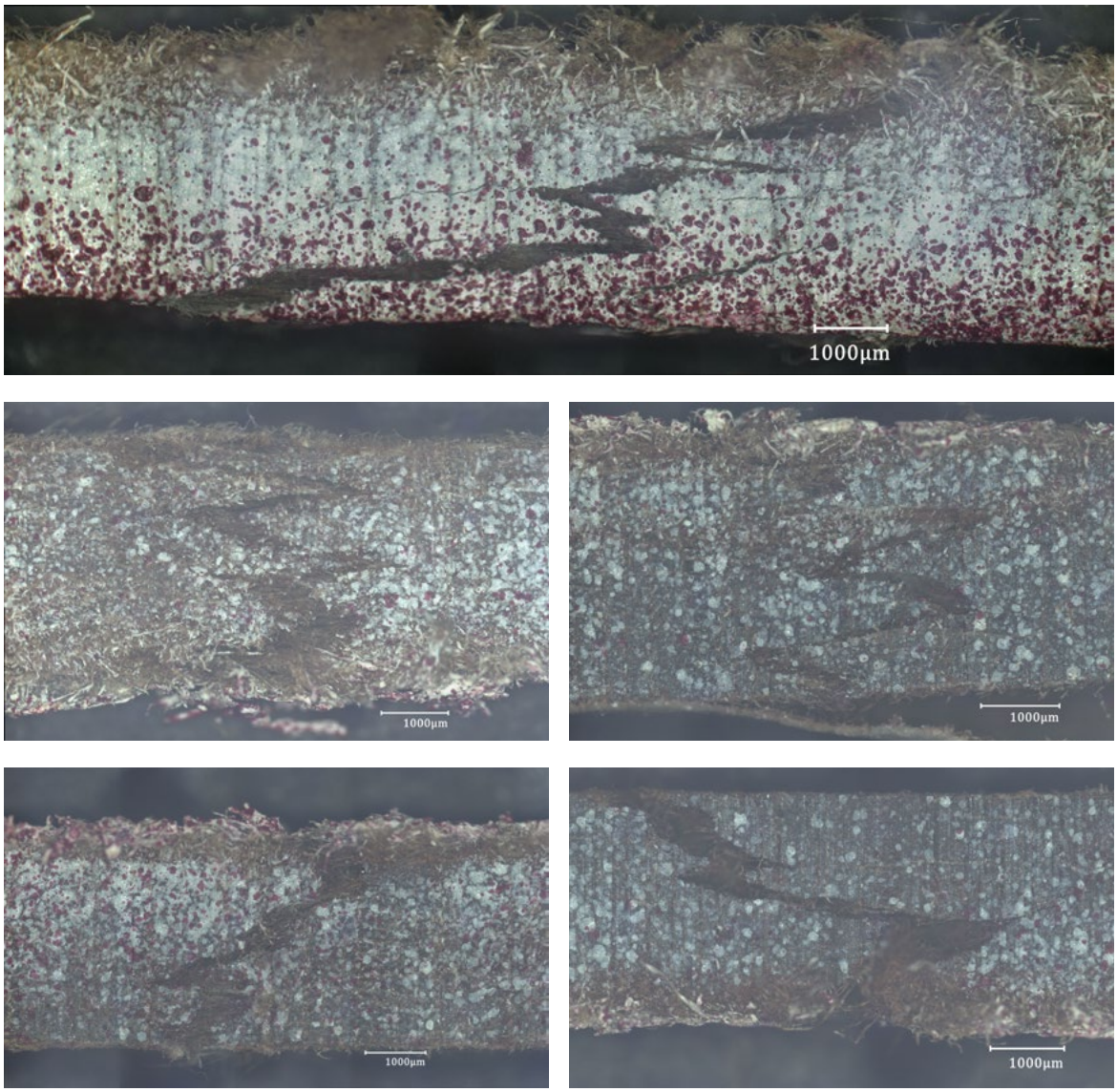

Figure 102. C/L Sample - 40/10 to 30/20 a) to e) - Tensile failure

Lignin Variation Trial Test Results

Figure 103 depicts both the characteristic compressive and tensile failure behaviour of the lignin variation samples.

The compression tests revealed distinct failure modes for each lignin type, despite all samples sharing a 1:1 cellulose-to-lignin ratio and having been pressed at the higher end of the temperature range. In the Kraft lignin specimen, multiple long, slender cracks formed parallel to the loading axis. One region appears to have buckled outward, initiating a crack that then propagated along the length. This indicates combined shear crippling and matrix cracking. Buckle delamination likely occurred where local compressive stresses forced layers of the composite to separate slightly before the matrix fractured. The principal crack reached almost 7 mm in length, tracing the path of least resistance through the weakened matrix. By contrast, the Organosolv lignin specimen exhibited a single, large crack in which cellulose fibres continued to bridge the gap at several points. This behaviour suggests that buckle delamination was also present. Fibre bridging delayed complete separation and limited crack

branching to a network of roughly 5–6 mm. The comparatively modest crack map reflects a partly tougher response, although it was still dominated by matrix cracking. In the Soda lignin specimen, an even longer crack—between 8 mm and 10 mm—ran diagonally across the cross section, almost fully separating the sample. The crack surface showed clear signs of brittle shear cracking of the matrix. The fracture was abrupt and explosive, with minimal fibre pull-out. It appears as if fibres were ripped rather than gradually de-bonded. The absence of significant fibre bridging suggests that the sudden, brittle failure overcame any residual adhesion between fibres and matrix. In both the Kraft and Organosolv specimens, fibres visible within cracks appeared bright brown, indicating incomplete wetting by lignin. In the Soda lignin specimen, the exposed fibres were uniformly dark brown. None of the cracks in this sample ran vertically; each followed a pronounced diagonal or even multiple diagonal paths. This reflects the anisotropic nature of shear stresses under compression.

Tensile failures further underscored these material differences. In the Kraft lignin sample, a slight zigzag crack traversed the cross section diagonally. Few fibres bridged the opened void. This implies that matrix–fibre debonding was minimal and that failure likely occurred by fibre fracture rather than extensive interfacial separation. This contrasts with the basic cellulose–lignin reference, where interfacial failure was more pronounced. Nonetheless, the tensile strength did not improve significantly. The Organosolv lignin specimen presented a similarly zigzag pattern, but the crack remained largely vertical across the section. A moderate number of exposed fibres were visible. Their coloration and the lack of deeper staining imply that lignin flow during pressing was insufficient to fully impregnate the fibre bundles. This observation is consistent with this sample's low tensile strength. Finally, the Soda lignin sample exhibited a clean, sharply diagonal rip across the cross section, with a moderate number of intact

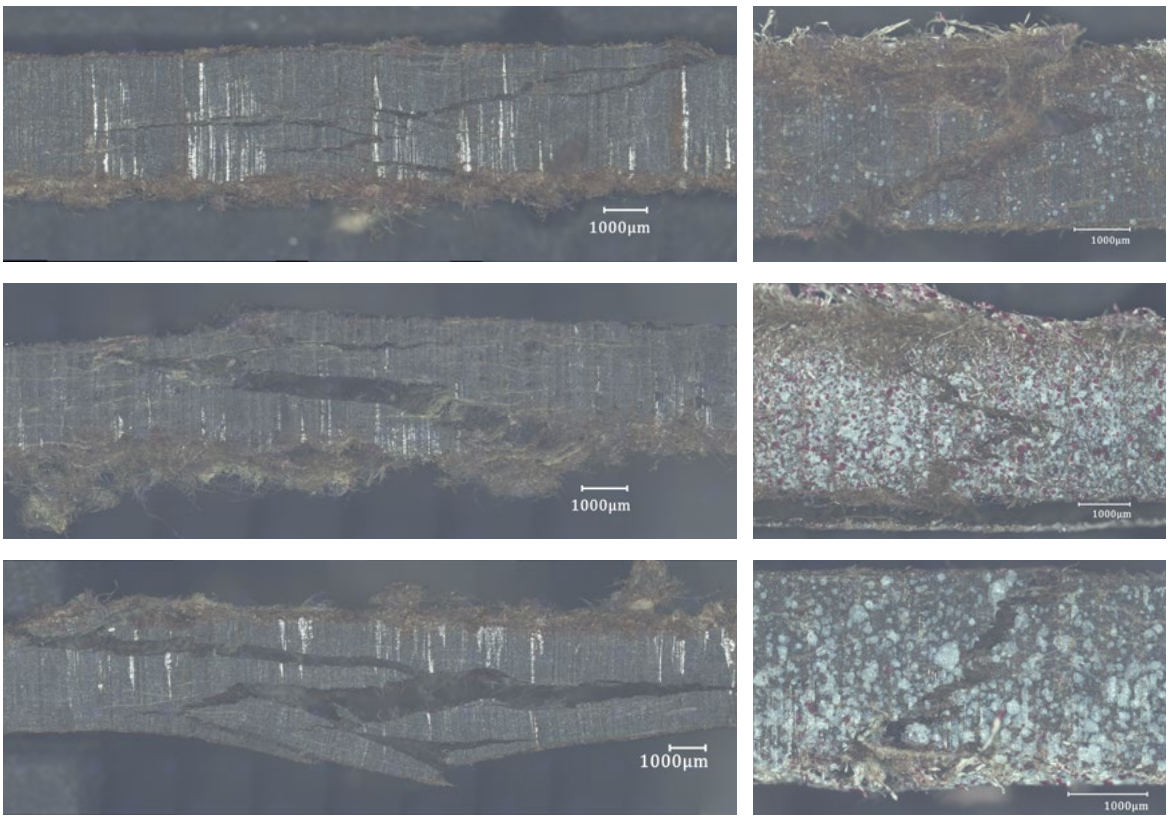

Figure 103. Lignin Trial Specimen. left) compressive, right) tensile specimen. From up to down: Kraft lignin, Organosolv lignin, Soda lignin

fibres bridging the crack. Matrix cracking was more evident, but there were no clear signs of interfacial debonding or extensive fibre pull-out. The crack cut cleanly through both matrix and fibre, suggesting that the composite failed in a more cohesive manner, with fibre fracture and matrix cracking occurring together.

Together, these observations indicate that Kraft lignin promotes greater fibre retention under tension. Organosolv lignin yields moderate fibre exposure but poor matrix impregnation. Soda lignin produces the most brittle, matrix-dominated response despite some fibre bridging.

Bending Test Results

Figure 104 presents representative failure images of the two specimens exhibiting the highest bending strength and stiffness. In both images, the fracture is clearly located in the tensile zone of the beam. A zigzag crack path propagates upward into the sample, ending at approximately two-thirds of its thickness. No noticeable deformation occurs in the compressive zone, which is unsurprising given that the compressive strength of these composites is considerably higher than their tensile strength.

The crack path consistently avoids larger fibre bundles, visible as white clusters in the pre-treatment sample cross-section. Instead, the fracture line jumps around these un-wetted cellulose packages. This behaviour suggests that the matrix failed first—its tensile capacity is lower than that of the fibres—causing the crack to initiate and grow through the weaker binder. The near-horizontal zigzag pattern indicates that the crack is following the plane of maximum tensile stress while being deflected by the fibre bundles. In other words, the fibres act as local obstacles, forcing the crack to change direction repeatedly rather than cutting straight through (especially visible in the lower image).

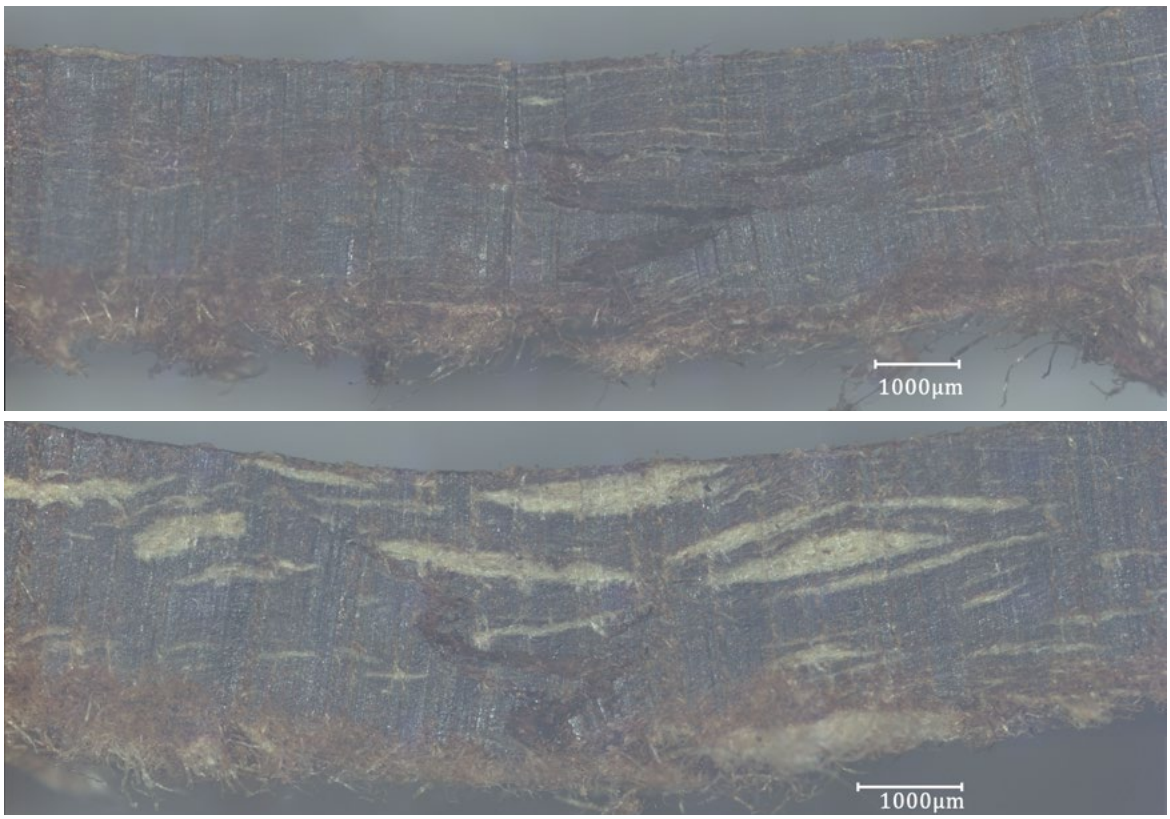

Figure 104. Four/Point bending test specimen with breaking point at center. Top Kraft lignin specimen, bottom Cellulose pre-treatment specimen

4.3 Material Relationships

During the development of a new construction material, in this case a composite material mixture, without any previously known characteristics, quickly understanding what behaviours and relationships are present is key for fast development of deployable products. These material relationships do include the mechanical performances but are in no way limited to those. The qualitative, soft values of the material are equally important to keep track of, and material trials and experiments in Chapter 3 have revealed that there exists a web of interconnected material properties. Identifying a material behaviour to a specific change in conditions is fairly simple, however keeping track of all of possible effects and at the same time understanding their relationship is not feasible when the analysis of the experiment is evaluated manually.

To be able to make use of the materials properties without a too long lasting trial-and-error process to just figure individual relationships, it is valuable to use methods that are able to identify these connections in the recorded data.

In this Chapter, the mechanical properties and their relationship to material composition have been investigated. And using a regression model has already identified at least one strength to mixture relationship with statistical significance ($p \leq 0.05$). Also the micro-mechanical failure behaviour has been investigated in regards to the different material trials, as well as surface changes on a microscopic change based on changes in mixtures or processing conditions.

The exploration of the non-mechanical qualities and performances of the material is less straight forward to map out, especially if they are dependent on many variables involved in the mixing and pressing process. Therefore, it is valuable to examine different approaches to interpret the resulting variations in material strength and appearance

In Figure 105 the entirety of the material properties are laid out. From left to right the properties transition from the mixture related variables, to process variables and to the final mechanical

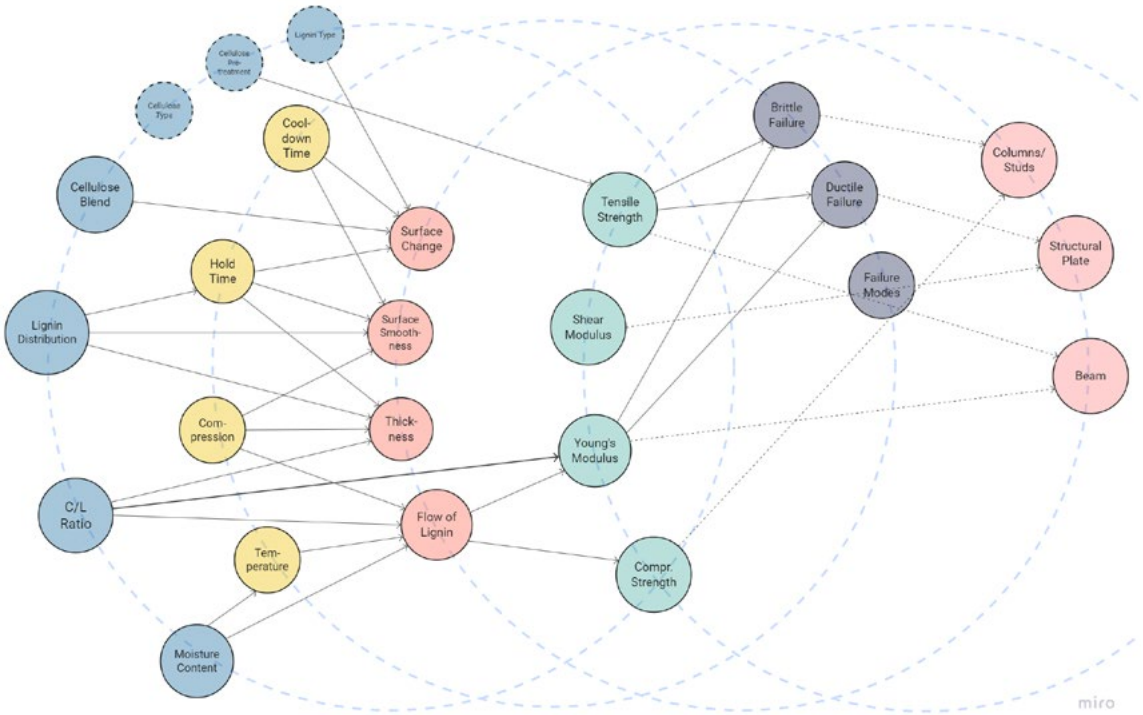

Figure 105. Mapping out of interconnectedness of the qualitative and quantitative material properties

results, which can ultimately have an impact on the applicable use case — for example a beam demonstrating brittle failure without any visible strain is less suitable, as there are no warning signs of failure.

Over the course of the experiments these relationships were kept track of. Figure 106 shows how the changes of the identified variables has an affect on the material properties, in a continuous slope diagram. For example as the cellulose-to-lignin (C/L) ratio increases—that is, as samples become richer in cellulose—the amount of blister formation, the extent of lignin flow, and the degree of plate warping all diminish. Mechanical testing further shows a corresponding decrease in compressive strength. While this loss of strength may stem directly from the higher C/L ratio, it can also be influenced by the reduced mobility of lignin within the matrix. Although the diagram highlights only the variables we control and the properties we observe, it's important to remember that these properties often interact causally rather than independently.

This initial effort maps and tracks interdependencies across the entire process chain. However, doing so manually is time-consuming and prone to user bias. An alternative is to employ computational techniques—such as metric/non-metric multidimensional scaling or principal component analysis—to visualize and interpret these complex datasets more objectively.

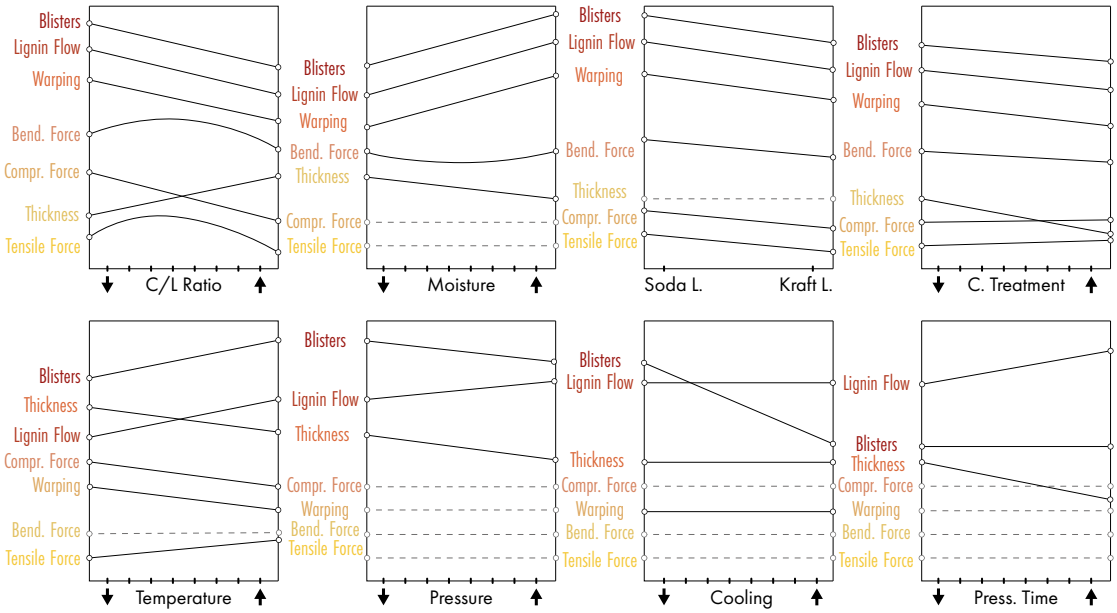

Principal component analysis (PCA) is a dimensionality-reduction technique that transforms a dataset into a new coordinate system whose axes (principal components) capture the directions of greatest variance. Each successive principal component is orthogonal to the previous ones, ensuring they represent independent patterns in the data. By projecting high-dimensional observations onto the first few components, PCA often reveals dominant trends and clusters with minimal loss of information (Jolliffe, 2002).

Metric multidimensional scaling (MDS) is an ordination technique that projects high-dimensional data into a low-dimensional space by preserving the actual pairwise distances between samples (Pedregosa et al., 2011).

Non-metric multidimensional scaling (NMDS), in contrast, preserves only the rank order of those distances rather than their absolute magnitudes, making it more robust to non-linear relationships and varying measurement scales. By optimizing the spatial configuration based on these ranks, NMDS reveals relative proximities among samples without assuming linearity in the data (Jacoby & Ciuk, 2018), (Saeed et al., 2018).

In this particular case, taking into account the data available from the tests and protocols, the use of a MDS method is the most suitable, because what this analysis is after is understanding how each variable of concern (strength, pressing temperature etc.) trades off against the others —and which combinations give you the best mechanical performance. In contrast to the NMDS this method preserves the option to directly read relationships off the axes. The below, brief overview shows how the MDS uses the mathematical technique called Eigen-Decomposition to produce coordinates for a 2d coordinate system, how much variation the axes of the graph account for and how the loading score shows what the axes mean.

The selected conditions and results that showed to have the highest significance throughout the analysis were the pressing temperature, the mixture moisture content (which helps with lignin flow and compaction in press), the mechanical strength and stiffness.

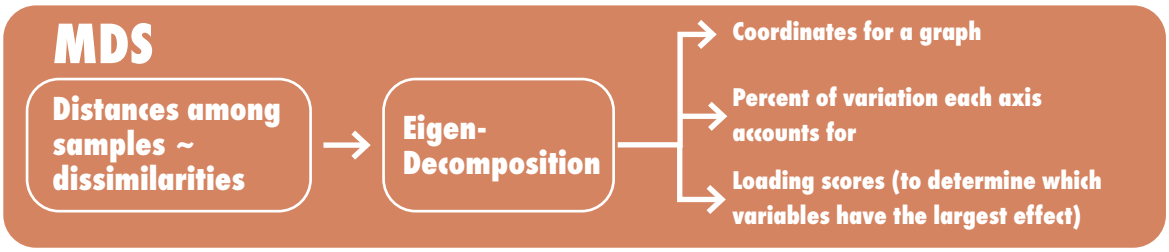

What follows is a step by step interpretation of the final within-model-scaled MDS plot with Envfit vectors (Figure 107) that was created in R.

The loading scores which are the computed relations between the four z-scored variables and the two MDS axes are documented in Table 9. They display the spew of the two axes and allow to annotate them accordingly. Dimension 1 covers 85% of the variance in the samples which makes it the dominant axis. As there is a strong positive with the pressing temperature (+0.96) and a strong negative with the moisture content (-0.97) and only moderate positives with strength&modulus this dimension can be read from left to right as:

Table 9. Loading Scores: Computed correlations between the four z-scored variables.

Variable	Dimension 1	Dimension 2
strength	+0.737	+0.380
modulus	+0.457	+0.820
moisture content	-0.969	+0.220
pressing temperature	+.0961	-0.182

- Left = cooler presses with wetter dough
- Right = recipes pressed at higher temp. from drier dough, yielding higher mechanical performance

Thus, the label of the axis is described as “Dim 1: Strength & Pressing-Temp vs. Moisture”.

The second dimension covers 21.4% of the variance. With a strong positive with the modulus (+0.82), moderate positive strength & moisture and slight negative pressing temperature the axis can be read as:

- Upward= samples whose stiffness (modulus) drives their position
- Downward = specimens driven primarily by heat (even if they stiffen less).

With this in mind the axis is labelled as "Dim 2: Modulus vs. Pressing-Temperature Dominance".

The plot itself is scaled within each testing type (bending, compression, tension) so that all three average at the (0,0) point. Therefore, the plot reveals the within-type differences only — so each point shows how a specimen compares to its own test-type average rather than to specimens from other types.

The arrows of the Envfit function are displaying the directions that correspond to a different variable in the plot. For example the arrow of Pressing.temp. pointing down right means that datapoints along that direction correspond to a higher pressing temperature (with a slight trade-off in stiffness). Or the arrow pointing up-right means that points in this direction experience a combined effect of heat and stiffness on the ultimate strength.

The specimen positions reveal therefore the following:

- Far right = the hottest processing and driest dough recipe used results in maximum strength/modulus.
- Far left = cooler and wetter dough and processing used results in weaker and more ductile materials.
- Higher up = the recipes emphasize stiffness (largest modulus)
- Low down = the recipe that relied almost solely on temperature to bind but without as much stiffness gain.

The C/L trials (circles) consistently sit towards the left (high-moisture) and lower strength/ pressing temperature. The pre-treated samples (squares) sit on the right (high pressing-temp & strength), often with middling-to-high modulus. And the Lignin trials (triangles) fall in between, sometimes overlapping both clusters. While these observations would also be visible with a good familiarity of the data, just from the data alone, the MDS does give direct insight that:

- Increasing pressing temperature reliably boosts strength (rightward shift) but can pull modulus downward (arrows for modulus point upward).
- Higher moisture content pushes samples leftward, away from both strength and modulus peaks.

In conclusion, the MDS allows to make the following take-aways, which not only validate the correlations that were manually observed while running the tests, but also allow to simplify displaying these multidimensional relationships in an understandable way:

The formulation shows the trade-off that pushing the pressing temperature and reducing the moisture content boosts the strength of the sample but it can compromise the stiffness (the arrows show this really well). This is a new observation that was not yet visible (or obvious) just from observing the test results alone.

The displayed sample IDs can be targeted as their extremes (e.g. 29.1.2 for top modulus in bending, 38.2.3 for top strength in compression, 27.3.1 for top stiffness in tension) are worth digging into chemically or micro structurally to see why they outperform.

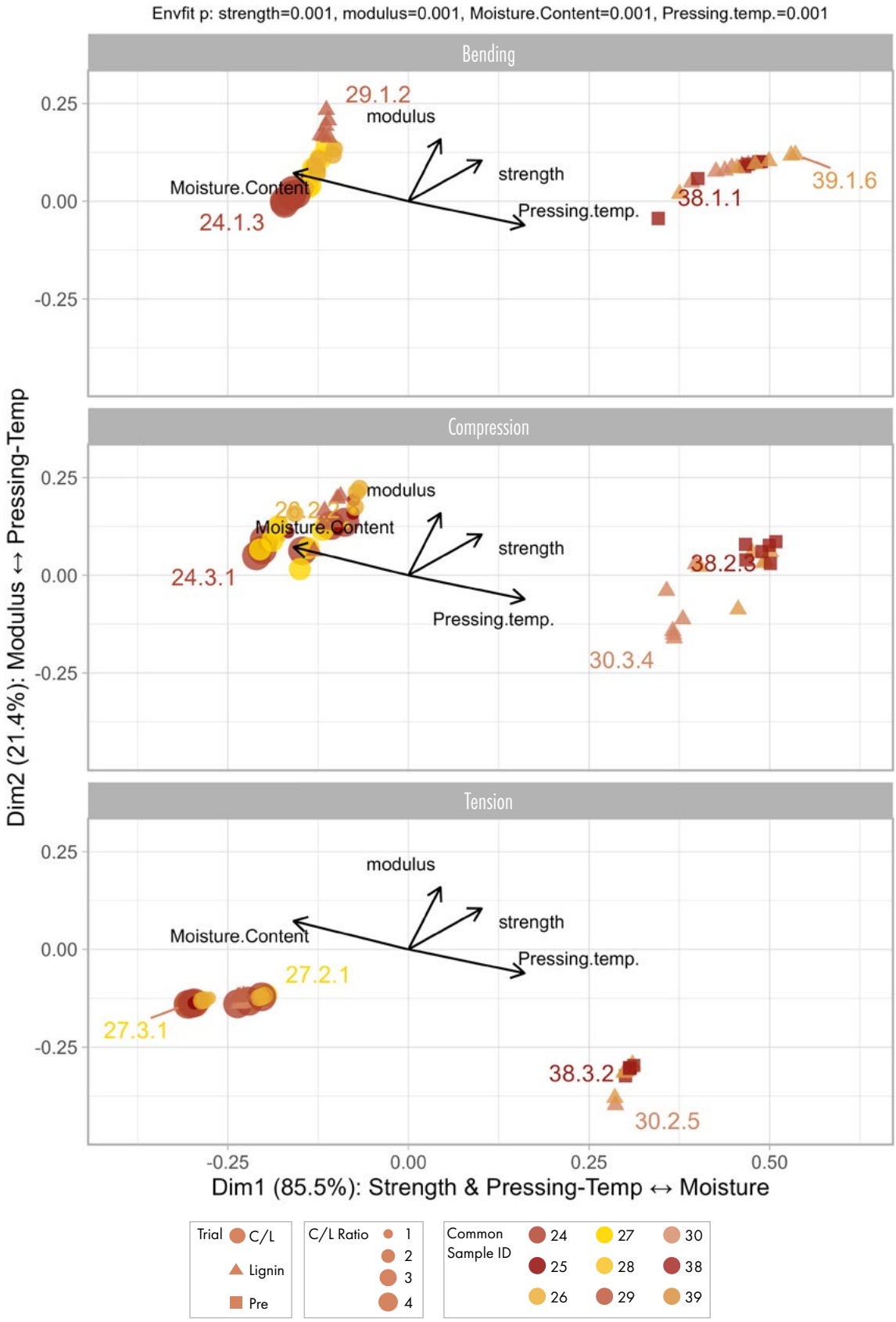

Figure 107. Classical MDS (within-mode scaled) with Envfit vectors of test specimen data

In terms of consistency the pre-treated cellulose samples always sit at the strength/temperature end. The C/L trial samples are always at the moisture end and the Lignin types are intermediate —with one exception, the 29 sample (Kraft lignin) which was pressed at 80°C rather than 120. That suggests the hot-pressing protocol has a reliable, predictable effect, regardless of bending vs. compression vs. tension. These insights can be used to further fine-tune your C/L ratios, pressing conditions, or material recipes—either by aiming for a "sweet spot" in the middle or by specifically targeting one of those extreme performers for further study. Having those different extremes is also favourable for further developing the controlled variability aspect of the mixture.

4.4 Material Analysis Discussion

In relation to the optimisation of mixture ratios and hot-pressing conditions, the mechanical testing has helped providing crucial information on understanding the variation in the material mixture. Through the testing of the moisture trial samples, in addition to the visual observations, demonstrates that without any added moisture to the sample, the pressing conditions of 85°C pressing temperature is not enough to achieve flow of lignin. As soon as moisture is added to the mixture the assuringly lowered T_g of lignin and induced flow drastically improve performance.

The C/L Trial has resulted in a variation of optimal flexural, compressive, and tensile strengths, where two ratios stood out for the C/L mixture. An ideal ratio for the bending and tensile properties is 3 to 2 and in compression 2 to 3 (cellulose to lignin). From the microscopy findings, it is evident that higher lignin contents improve fibre impregnation. In samples with elevated lignin content, marbling effects were observed where fibres appeared less wetted by lignin, indicating local regions of matrix weakness.

Changing the hot-pressing conditions has revealed that there are many changes occurring in lignin flow, strength, and surface characteristics with varying pressing temperature and the moisture content has been proven to influence the lignin mobility and fibre impregnation, correlating this directly with mechanical performance and material appearance. In the end an optimal condition was found, with a pressing temperature of 120°C at 3.7MPa and a moisture content of 10wt%.

The testing results of the lignin variation trial show that the selection of the added technical lignin has strong implications on the performance values, which correlates with the findings in the literature about varying qualities of lignin types. For example, the Kraft lignin specimen exhibited long, slender cracks indicative of shear crippling and matrix cracking, whereas the Organosolv lignin sample displayed fibre bridging along a 5–6 mm crack, suggesting partially tougher behaviour. In the Soda lignin specimen, brittle shear fractures of 8–10 mm length occurred with minimal fibre pull-out, indicating a matrix-dominated failure mode The pre-treatment trial of the cellulose does not appear to result in significant changes of the performance. The additional effort needed for the fibre treatment, does therefore not appear to be needed.

The material-trial results can already be benchmarked against established construction materials. Figure 108 and Figure 109 plot specific bending, compressive and tensile strengths and stiffnesses. The orange circles with a digit map out the C/L trial results, and the letters mark the lignin variation and pretreatment results, creating a new material zone for this new bio-based material. Generally, the presence of the material amidst other common construction

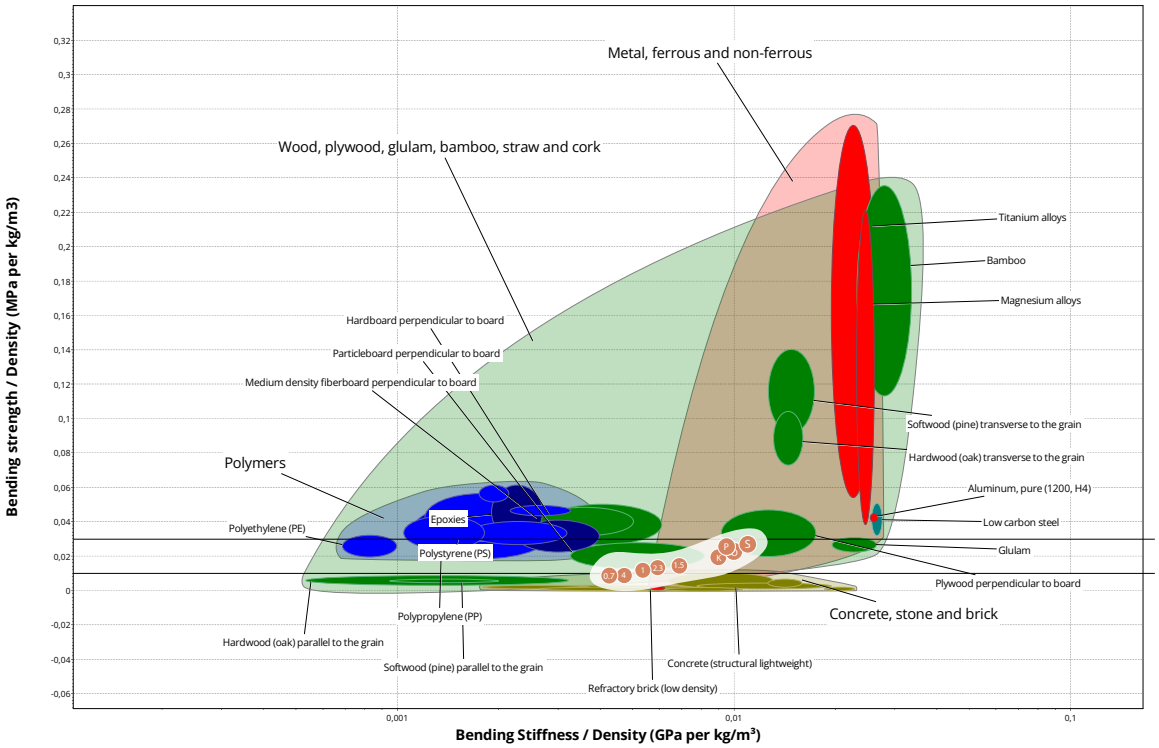

Figure 108. Ashby diagram of Specific Bending Strength/ Specific Bending Stiffness of selected Wood Products, Plastics, Metals, Concrete & Bricks with the Trial Results..

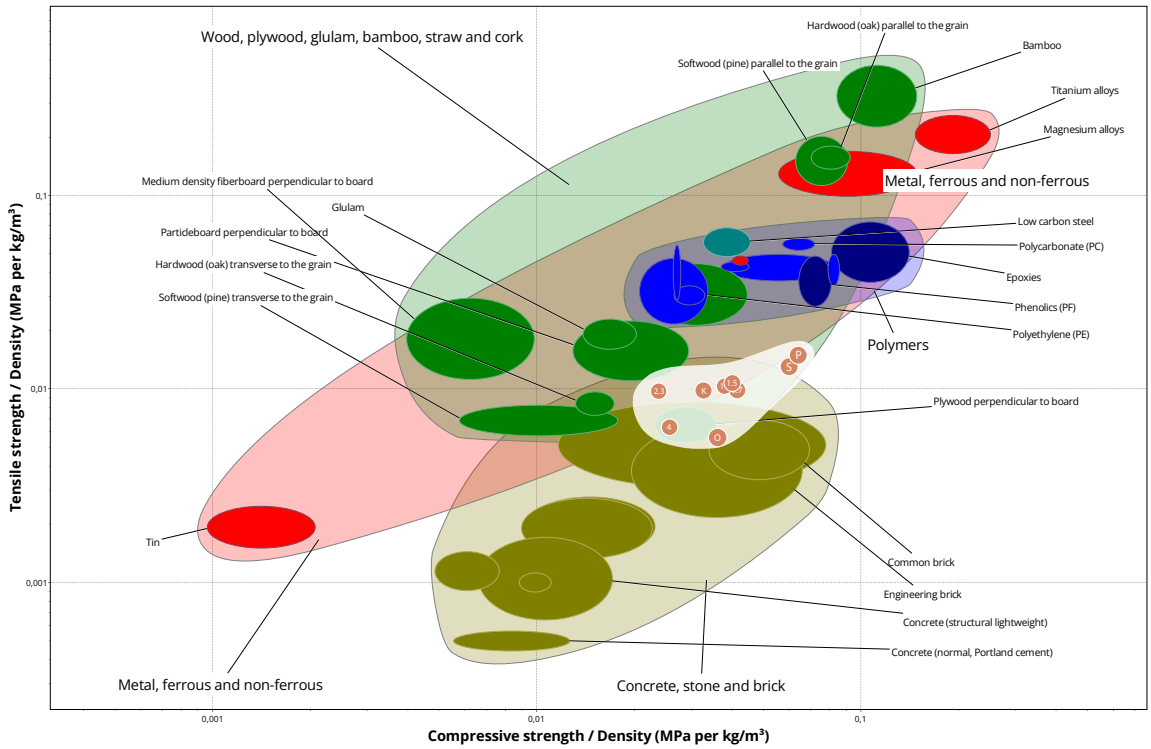

Figure 109. Ashby diagram of Specific Tensile Strength/ Specific Compressive of selected Wood Products, Plastics, Metals, Concrete & Bricks with the Trial Results..

materials is a sign of a successful material development with real-life potential for structural application. While the performance of the material in bending

The variation in the material properties underlines that no one material is universally suited to every application; designers must select materials in light of their mechanical profiles. Demonstrating how novel formulations compare with standard materials is therefore crucial—it steers further development towards those mixtures most likely to succeed in practice.

Here, the variability of mechanical properties across different C-L mixtures can be turned to advantage in the design phase. By tailoring both composition and component geometry in tandem, one can target each mixture's strengths and minimise ecological impact. Since density is a proxy for material quantity—and thus embodied energy and emissions—the plots also guide choices that optimise performance while reducing environmental impact.

At this moment, the density of the C-L mixture is higher than the other wood based product. Through displaying the specific strength or stiffness (normalised by the density) the effect of this is especially visible in Figure 108 in which the specific bending strength is considerably reduced by the high density. The peak bending strength of all samples is around 35 MPa. In comparison Glulam, with a bending strength of 12-14 MPa[1], performs much better due to its almost half as high density with 500-650 kg/m^3[1]. Considering the environmental impact, using constituents from waste streams can offset the impact, reducing the density while maintaining the strength can still be a point of improvement in future research.

The use of statistical methods (polynomial regression, PCA, MDS, NMDS) can be used in the future to better understand these material relationships between the composition, processing conditions, and mechanical performance. Such computational methods could streamline iterative experimental processes and guide the material selection for a more efficient development process.

With the mechanical testing, this chapter has provided data on the structural limits of the materials in regards to their mixture specifications and has attempted to create mathematical functions to describe these relationships. With the structural constrains at hand the results can now directly be used to inform a material driven design. The design strategies that can be applied can exploit the unique material properties rather them considering them as limitations (e.g., Leveraging ductility for flexible components or brittleness for compressive structures) and the variability in the material mixture can be used to produce customised structural products based on their loading condition.

Microscopy of the C/L Trial compression samples revealed that, under load, the matrix acted as the weak link: fibres were seen to buckle or kink within the softened lignin-rich matrix. In the 4 : 1 sample, a longitudinal split and delamination created surface bulging, with minimal matrix cracking visible. In the 3 : 2 sample, a diagonal split ran through the thickness, where fibres remained largely intact but disconnected from the matrix by kinking along the crack. In samples with higher lignin content, shear crippling dominated, with pronounced matrix cracking along the splits—evidence that increased lignin content yields more brittle behaviour. Correspondingly, force–displacement curves exhibited sharper peak profiles as lignin concentration rose, indicating more abrupt failure.

In tensile microscopy, the crack path evolved from meandering through fibre bundles in cellulose-rich specimens to a cleaner diagonal orientation in lignin-rich ones. Early samples showed significant fibre pull-out and interfacial debonding, whereas the highest-lignin specimens exhibited predominantly matrix cracking with only moderate fibre bridging. These

1. Ansys® Granta EduPack 2024 R2 Version: 24.2.1, Glulam

observations confirm that interfacial bonding between lignin and cellulose is the limiting factor in tensile performance, and that an optimal blend maximises adhesion without sacrificing ductility.

However, the batch-based production still has an effect on the scalability of the process for manufacturing. The current process at this scale has a limited plate size that might impact the statistical robustness of the collected data. As it was presented earlier in the methodologies the transition to other processing methods like hot-extrusion can therefore still be considered if they would result in more freedom of design or larger scales. Common practices of the plate manufacturing industry can also be used to develop larger scale manufacturing. Structural wood-based plates like MDF or OSB are also hot-pressed in much larger sizes and quantities, or in continuous processes using rolls and conveyor belts.

Besides the challenges of large scale application, the material properties have to further investigated in terms of their non-structural performances. Considering various application cases as cladding or structural plates the following aspects are still crucial for consideration.

In terms of the thermal and fire behaviour, the flammability rating and fire resistance are crucial

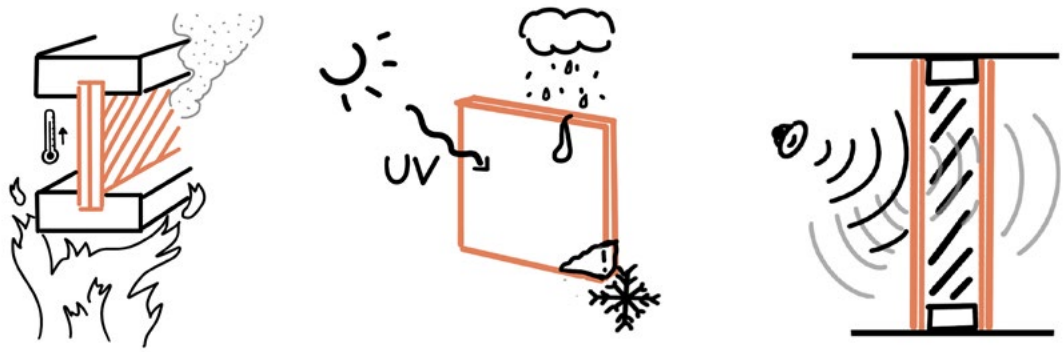

Thermal and Fire Behaviour Environmental Response Indoor Performance

to determine, next to that are heat release and smoke development. But also, the thermal conductivity and thermal expansion/contraction are big factors to determine the quality of the construction material— to much movement when exposed to heat (solar, appliances) or even reduction of stiffness (considering the T_g of lignin) can be detrimental to the quality. Next, the moisture sensitivity, absorption and vapour permeability need to be investigated to consider the applicability in indoor or outdoor conditions. The general durability against UV irradiation, abrasion and surface toughness or biological affect are points of concern specifically for bio-based materials. Promising qualities could be revealed when it comes to sound transmission or noise absorption. Due to the high density vibrations are usually dampened more effectively, varying levels of fibre content and surface finishing can also be a manipulated to affect the reflectivity of sound.

In summary this Chapter has provided the needed data to continue with the research proposal and apply a computational tool for modelling and analysis of a component design using this new material. In the next steps the generated relationships can be used to verify the controlled variability of the polymerisation of lignin in a prototype design. The investigation of a application will also help to provide more insight into the production limitations of this material and how process can be improved.

Hauptschalter
Autom. 0 Main
BUCHER - GUYER
Niederwenigen
0
100
200
300
400
500
Tonnen

Chapter 5
Design and Application

5.1 Computational Framework Description, Requirements and Goals 115

5.1.1 Data Structure 116

5.1.2 R-Based Pipeline: From Excel Import to Curve-Fit Modelling of Mechanical Test Results 118

5.1.3 Pipeline Continuation: Rhino & Grasshopper Implementation 119

5.2 Prototype Design 122

5.2.1 Structural System 124

5.2.2 Environmental Impact 128

5.2.3 Mixture and Design Optimisation 130

5.2.4 Resource-Aware Local Material Optimization 133

5.3 Application Potential and Manufacturing Proposals 134

5. Design and Application

5.1 Computational Framework Description, Requirements and Goals

After conducting the experiments and material tests the data that was gathered on the material trials, pressing conditions on stress/strain behaviour of the respective materials. Also, as it is laid out in the project workflow, the integration of the data into a computational software was done in parallel to the material design.

The goal of the computational framework is to use the gathered information on the material behaviour and apply it to a component design. Specifically the workflow will focus on the material functions and their application to a virtual structural model.

The information of the material process was gathered and saved to multiple excel files, as the data bases of all steps. In the previous Chapters a majority of the steps —shown in the diagram below— were already shown in Chapter 4 but not yet put into context with the computational aspect of the project. These steps are the samples trials, mechanical testing plots, determining of material strengths and moduli, regression and mapping out relationships in graphs, as well as creating the Ashby charts for material comparisons (Figure 111). This entire workflow was done in R – a programming language similar to Python, that is specialized on data analysis and statistical computing – to ensure that the workflow is based on a automated process and that it is also easy to produce visual outcomes in between.

In this Chapter, the workflow for data capture, transformation and calculation during material production is described. The subsequent stages—parametric design and

Figure 111. Diagram of proposed computational Framework[1]

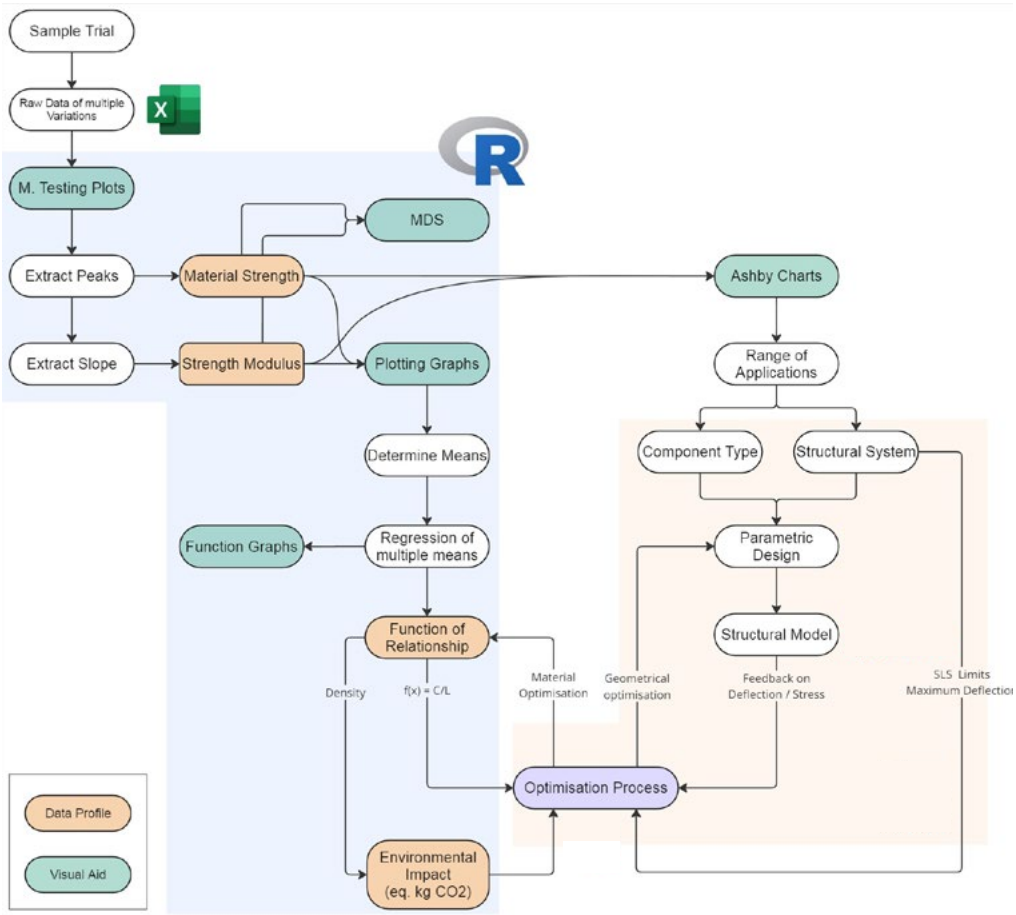

1. "Excel" logo from: https://www.google.com/url?sa=i&url=https%3A%2F%2Fals.wikipedia.org%2Fwiki%2FMicrosoft_Excel&psig=AOvVaw2-LN_YtiCs1UIEBrlV5njx&ust=1750326496796000&source=images&opi=89978449
2. "R" logo from: https://www.google.com/url?sa=i&url=https%3A%2F%2Fen.wikipedia.org%2Fwiki%2FR_%2528programming_language%2529&psig=AOvVaw1GkQDlyh-MaBH2FOY5SQ5F&ust=1750326588423000&source=images&opi=89978449

optimisation—are then demonstrated, including the tools and methods used. It also explains how each phase links to the next and specifies the data formats exchanged between steps.

For the following parts the requirements and objectives are to be kept in mind:

Framework Description

- A parametrized system that links material-mix variables, processing parameters and final component geometry
- Real-time feedback loops: measurement data from each experimental batch update the model's material property database automatically.
- Robust and adaptable core program that does not require proprietary software
- Clear interfaces between the data-capture, transformation, analysis, simulation and optimisation for a coherent pipeline

Requirements:

- All data transformations and model decisions are logged and exposed, so users can trace how inputs propagate through each step.
- Scalability of the systems, so that it can handle "what-if" runs to full factorial DOE (hundreds of runs) without manual intervention.

Goals:

- Accelerated R&D that cuts down the delay time from prototyping to application design
- Find "sweet-spots" between density, strength, and ease-of-processing with singular runs
- Pinpoint the 2–3 most promising material/process combinations for the physical validation in each cycle, rather than trial-and-error.

5.1.1 Data Structure

Before continuing with the workflow outside of R, the specimen, mixture and sample nomenclature and data structure needs to be explained. The naming of the mixtures governs the entirety workflow and considerations when handing from one step to the next.

As in Figure 112 visible, each mixture produced receives its own unique number. This works with the aspect in mind that one mixture produced results in one hot-pressed plate. In combination with the thorough documentation of the entire process having unique numbers per mixture ensures that every step can be traced back — in case errors or large deviations appear in the analysis. The hot-pressing conditions are also included in the mixture number. For the mechanical tests identical plates are needed, so for each repeated and identical production process a sub-number is added, to keep the identical plates apart.

As further processing the plates are cut into sample pieces. As each mechanical test requires a specific specimen width, the specimen will be identified with a letter in front of the mixture. After the Mixture and Sample number another sub-number is added for the specimen number cut from the plate. As mentioned earlier the specimen number (index) also indicates the position that the strip is cut from (1-edge, 2,3 - inner).

The entire numbering sequence is then typed into the mechanical testing software. The spreadsheets in the excel file will be named with this specific number. The data that is included with this number is the specimen length, width, thickness and weight.

Once imported in R a data frame is created in which the entire sequence of deformation and applied force data is first mutated to strain and stress — this means cross section and length are included in the numbers, saving extra columns — and then appended to one combined

Figure 112. Specimen Nomenclature and Data Structure throughout the steps in R

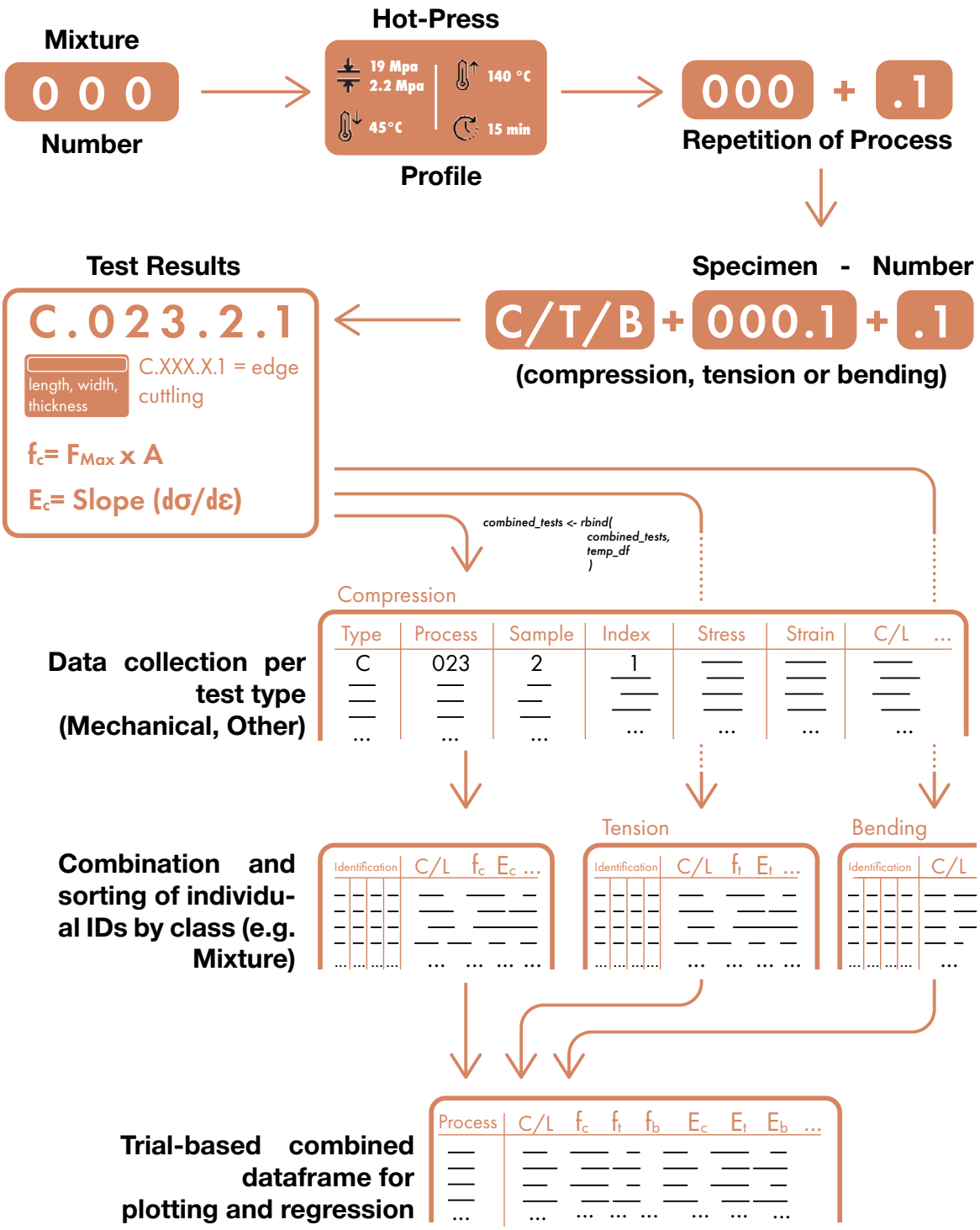

data frame containing all measurements from the test type. Additionally, the specimen number is deciphered into columns called type (test type), process, sample and index. This way identification, isolation and grouping by those numbers becomes simpler. Other data that is included in this overall collection of data is the variable that is related to the material trial, for example the cellulose and lignin ratio in form of a numerical value like “2.66”.

From this entire collection the next processing is done, strength and modulus or other properties are determined. These values are stored including their respective identification into a data frame. From this collection of single row values per specimen, the plotting from Figure 113, Step 5 can be done. As an example, when creating a box plot that distinguishes by Process number, all samples and indices are combined to create one box, showing outliers, mean, median and interquartile range.

From each box plot the mean values will then be saved, only keeping the process number and the trial variable, and saved into an individual dataframe per trial type. Within that data frame, the regressions can be performed and exported.

5.1.2 R-Based Pipeline: From Excel Import to Curve-Fit Modelling of Mechanical Test Results

The process up until the extraction of material relationships, based on the mechanical testing of material trials, was as previously mentioned all performed in R (Figure 113). The mechanical testing data is exported from the software used by the testing machine as an excel file, that contains multiple worksheets with the specimen data. Included is another spreadsheet containing the specimen dimension, that were specified while performing the tests. Those spreadsheets are imported into R using the “readxl” library.

Next the applied/force graphs are plotted, individually, per mixture group and all together, this is the first way to qualitatively evaluated the experiments. Following that is the determination of strength values and moduli and plotted, as described in Chapter 4. As one mixture consists of multiple specimen the combined mean value of strength and modulus are extracted and added to a new data frame. As new specimens are tested, their results are appended to the dataset and the aggregate values are recalculated automatically, ensuring that the database remains current.

With the global data frame in place, plots are generated to relate material strength (or modulus) to the corresponding mixture or process variable. For each relationship, a suite of candidate regression models—linear, polynomial of low order, exponential or power-law—is fitted, and the optimal form is selected according to goodness-of-fit metrics such as the coefficient of determination. The chosen regression curve is then superimposed on the scatter plot, facilitating a quantitative interpretation of how changes in composition or processing parameters drive mechanical performance. The accuracy of the regression is taken into account (r^2 and p values) and then the functions are exported as a readable .txt file for the following step.

In addition to the functions based on the material variable, the .txt file also includes the more static data required by the modelling software like density and thermal expansion coefficient.

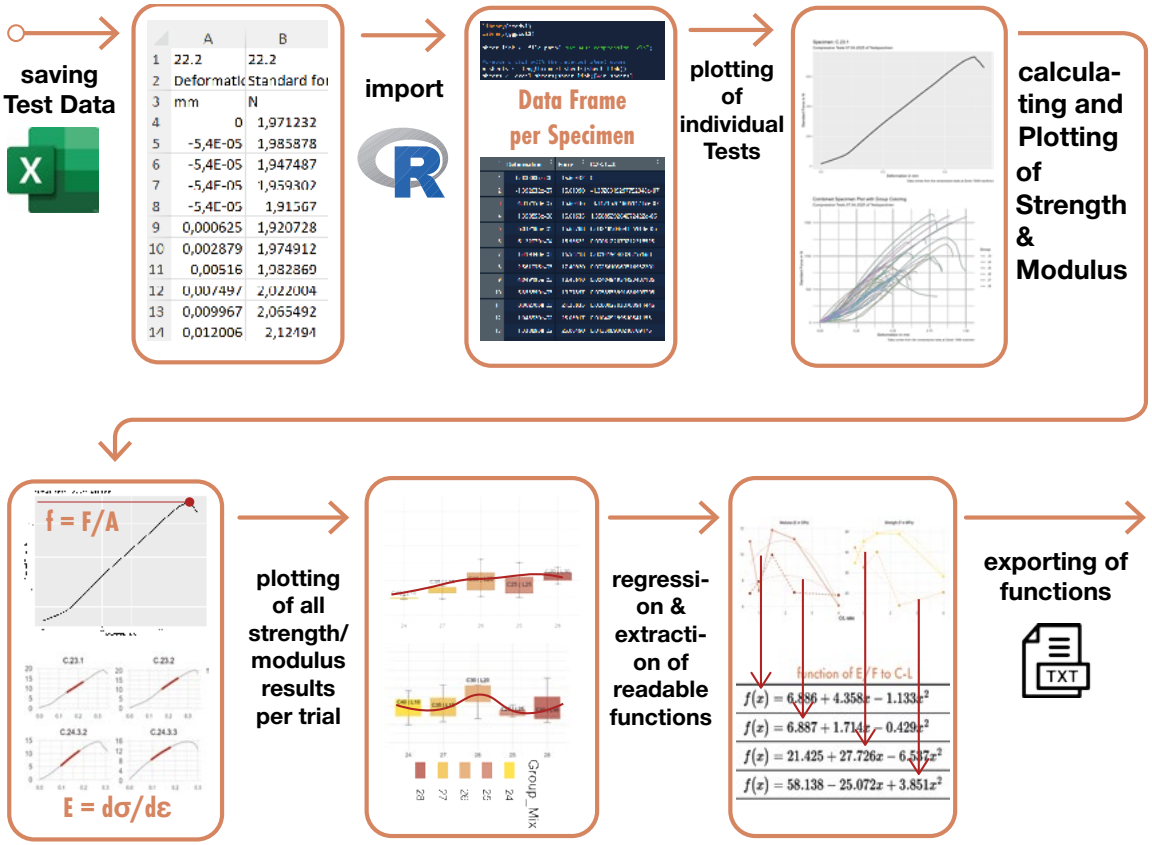

Figure 113. R-based pipeline to compute the material testing data[1]

5.1.3 Pipeline Continuation: Rhino and Grasshopper Implementation

What follows is the process of using the material functions in the 3d modelling software Rhino 8 with the use of a Grasshopper program.

The exported .txt file from R contains material functions derived from variables that influence the mechanical properties defined in the Karamba custom material component. Figure 114 shows the Grasshopper component that imports this file: a Python script reads each line, interprets the functions, and evaluates them for a given variable value. Here both the functions for compressive and tensile strength are extracted (to be remembered that f_c had no p≤0.05).

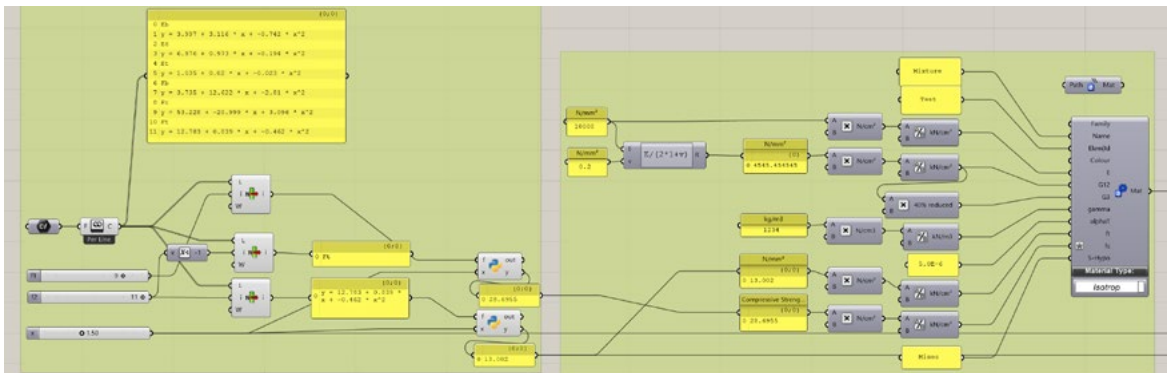

Figure 114. Screenshot of the linked .txt file and the extraction of the functions using a python component.

1. "Excel" logo from: https://www.google.com/url?sa=i&url=https%3A%2F%2Fals.wikipedia.org%2Fwiki%2FMicrosoft_Excel&psig=AOvVaw2-LN_YtiCs1UIEBrlV5njx&ust=1750326496796000&source=images&opi=89978449
2. "R" logo from: https://www.google.com/url?sa=i&url=https%3A%2F%2Fen.wikipedia.org%2Fwiki%2FR_%2528programming_language%2529&psig=AOvVaw1GkQDlyh-MaBH2FOY5SQ5F&ust=1750326588423000&source=images&opi=89978449

In Figure 117, the variable (denoted as x) is controlled by a slider whose range matches the limits of the material functions. For simplicity, we currently assume an isotropic material. To ensure the simulation mirrors real-world behaviour, the model preserves the original plate geometry and thickness, and applies loads identical to those used during mechanical testing. The parametric model, to be analysed, also provides several controls that the optimisation tool can tune. According to the model and its use-case, the loading situation and support types are defined and assembled with the geometry for the structural analysis.

The analysis itself provides information and values on results like deflection, stress/strength behaviour and the resulting forces within the component and supports. And the grasshopper script presents these outcomes in the rhino 3d environment to visually inspect the outcome of the analysis. For structural components, specifically a beam or floor joist, the load-bearing capacities can be ensured through the deflection limit. Dimensioning by deflection limit describes the serviceability design route. The beam's stiffness is sized (through its cross section and material) so that under everyday loads it will not sag more than the building code allows. In Figure 115 the results of this analysis are demonstrated. An arbitrary value for the variable x for the compressive strength to C/L ratio is set.

Figure 115. Axonometric view of exemplary modelling result of the presented workflow.

In addition to the deflection limit another assessment criterion for the structural model is the reduction of the equivalent CO_2 emissions. The added up green house gas emissions of all used components in the model are calculated so they can be part of the optimisation step. This also includes the mixture ratio. With the calculated of the respective carbon emissions per

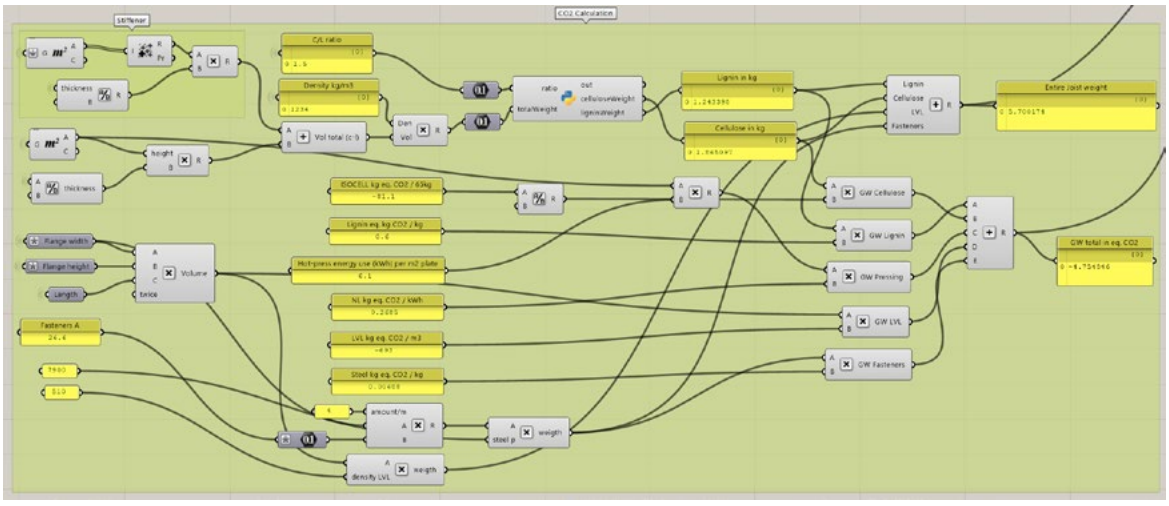

Figure 116. Screenshot of the Grasshoper script segment, calculating the equivalent CO_2 emissions of the model

constituent, in Chapter 3.5, increasing the cellulose content becomes much more desirable because of the extremely high negative values for the global warming potential.

Other materials like bolts or timber products are included in the equivalent CO_2 calculations using a plug-in called EPiC Grasshopper which provides the embodied environmental flows coefficients for construction materials into grasshopper[1].

At this step the optimisation tool comes into play, for determining the optimised combination of all the genomes that are provided (Figure 117), by assessment of the fitness, in this case the deflection limit and the carbon emissions.

One in-built optimisation tool from grasshopper is Galapagos, it provides an evolutionary algorithm for a single objective optimisation. Other possible optimisation tools are plug-ins like Wallacei[2] ,also using an evolutionary algorithm, or Octopus[3],which can make use of a genetic optimisations.

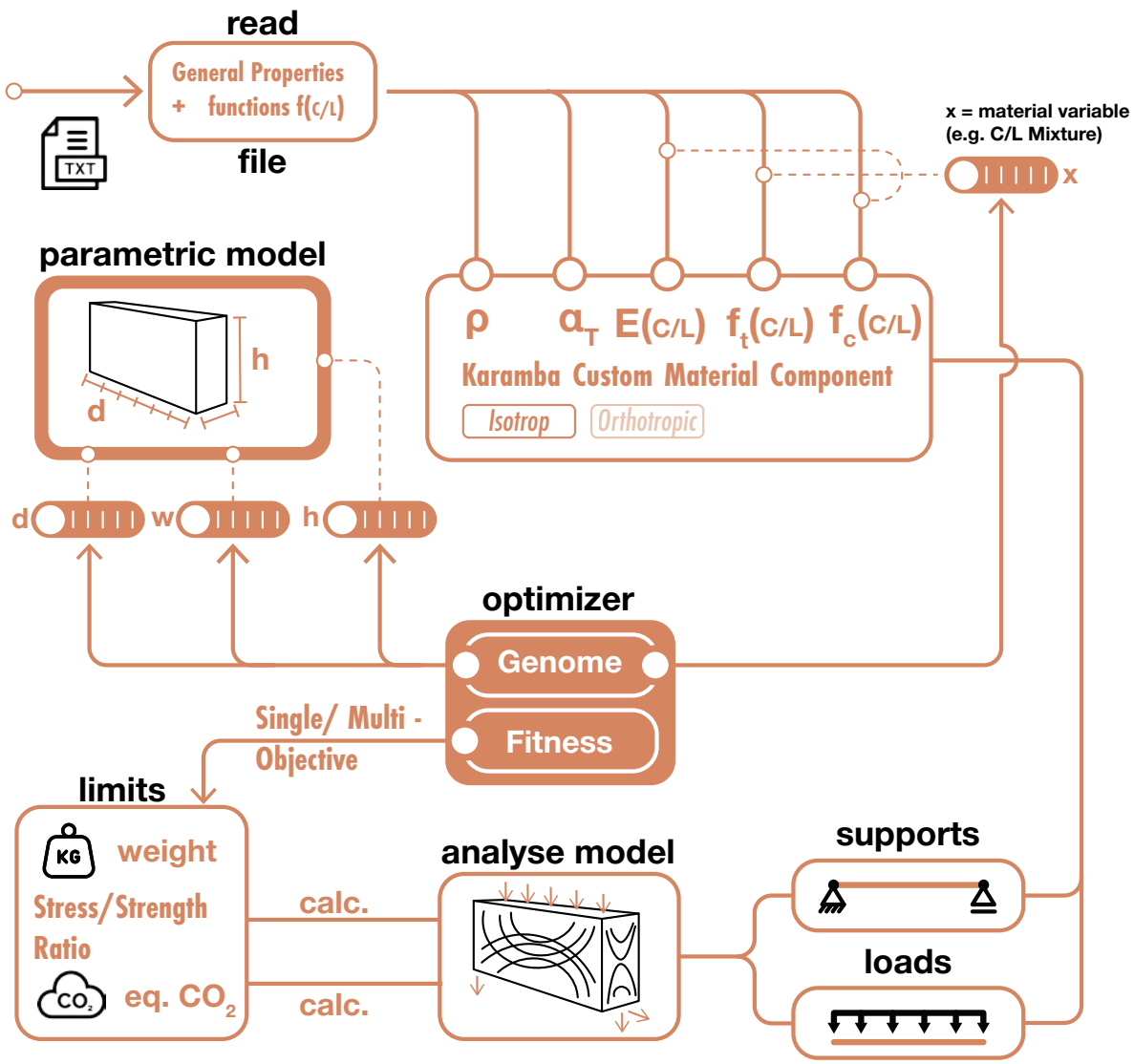

Figure 117. Diagram of proposed computational Framework

1. EPIC GRASSHOPPER, https://www.food4rhino.com/en/app/epic-grasshopper
2. WALLACEI, https://www.food4rhino.com/en/app/wallacei
3. OCTOPUS, https://www.food4rhino.com/en/app/octopus

5.2 Prototype Design

In the presentation of the material experiment results, the mechanical properties of the plate specimen were compared against common wood-based plate materials like MDF or OSB plates. The achieved properties are already now on par with those types of materials, with the slight drawback of the higher density. With these results the prototype design was chosen to make the best use of the mechanical properties. This way the feasibility of the material can be demonstrated without making to many changes to the production process.

As a structural case study, a Finn-joist was chosen because its I-shaped profile allows a straightforward substitution of the central web while retaining the familiar flange dimensions and through adjustments of the fastening details. By replacing only the timber web with the cellulose–lignin plate, the joist's load-bearing behaviour can be directly assessed under typical shear and bending actions, without re engineering the surrounding elements. This approach can therefore both validate the new material's performance in a well-understood structural system and underscores its compatibility with existing manufacturing and installation practices.

Finnjoist I-Beams (FJI) consist of laminated veneer lumber (LVL) for the flanges and a web

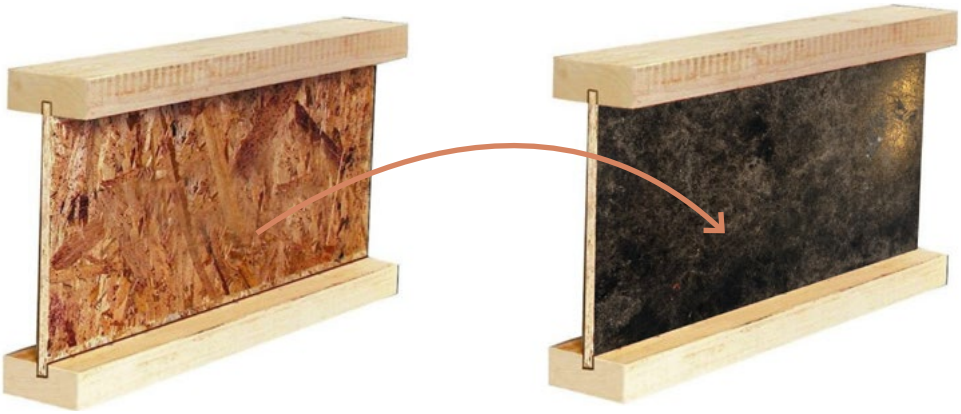

Figure 118. Conceptual depiction of the replacement of the web material of a Finnjoist[3].

made from oriented strand boards (OSB). They are used for flooring or roof beams for residential, educational and light-industrial as well as office buildings. Though their composite construction and assembly in factories, they can be produced with a high level of uniformity. Through the lightweight design they are also simpler to install in comparison to traditional solid wood construction. The main producer of Finnjoists in Europe is the Metsä Group[1], that also specialises on the production of the LVL lumber.

In the environmental product declaration (EDP) from the Metsä FInnjoists, the global warming potential (GWP) for 1kg of finnjoist, the total equivalent carbon emissions for the product stages A1 - A3, are -1.03 kg CO_2 eq [2].

For the design of the application multiple considerations have to be made considering the member assembly, design context (structural system layout), material and production restrictions or material availability. In the following parts these aspects will be presented.

Finnjoists are supplied with a variable joist height from 195 to 400mm and a flange width of 45 to 96mm. The span is also variable between 8 and 14m. The web-thickness is variable in accordance to the standard board types from 6 to 40mm.

1. https://www.metsagroup.com/en-gb/metsawood/products-and-services/products/finnjoist/finnjoist/
2. https://www.metsagroup.com/contentassets/bdd9a4385ba74645a0815d64c727455d/environmental_product_declaration_for_finnjoist.pdf
3. Image from: https://www.google.com/url?sa=i&url=https%3A%2F%2Fwww.homedepot.ca%2Fproduct%2F1001854928&psig=AOvVaw08vtIpbDeXu-NnMm-iYQuM&ust=1750326331826000&source=images&opi=89978449

For the reference strength that has to be met with the new cellulose-lignin boards the standard for oriented strand boards can be used. In Table 4 of NEN-EN 300:2006 (2006) the conditions for the OSB3 boards that are used in the Metsä Finnjoist are listed (Figure 119). To compare

Board type (technical class) OSB/3 Property	Test method	Unit	Requirement				
			Board thickness range (mm, nominal)				
			6 to 10	> 10 to < 18	18 to 25	> 25 to 32	> 32 to 40
Bending strength — major axis	EN 310	N/mm^2	22	20	18	16	14
Bending strength — minor axis	EN 310	N/mm^2	11	10	9	8	7
Modulus of elasticity in bending — major axis	EN 310	N/mm^2	3 500	3 500	3 500	3 500	3 500
Modulus of elasticity in bending — minor axis	EN 310	N/mm^2	1 400	1 400	1 400	1 400	1 400
Internal bond	EN 319	N/mm^2	0,34	0,32	0,30	0,29	0,26
Swelling in thickness — 24 h immersion	EN 317	%	15	15	15	15	15
If it is made known by the purchaser that the boards are intended for specific use in flooring, walls or roofing, the performance standard EN 12871 has also to be consulted. This can result in additional requirements having to be complied with.							

Figure 119. Load-bearing boards for use in humid conditions — Requirements for specified mechanical and swelling properties (NEN-EN 300:2006 (2006))

back to the mechanical performance results from Chapter 4.1 the peak material strengths are,

- max. Bending strength : 49.22 MPa (C/L - 3:2)

- max. Modulus of elasticity: 3.4. GPa (C/L - 3:2),

which appears to make the material strength on paper more than strong enough. Although, as mentioned in the conclusion of this Chapter, there are still major drawbacks, like warping and moisture sensitivity that require more optimisation of these secondary material qualities. The orthotropic behaviour also has to be studied more.

Design Requirements/ Adjustments

For the design, the following restrictions or requirements have to be respected:

- No use of adhesives or glues: to preserve the material purity by relying solely on removable mechanical fasteners, enabling “pure stream” separation and end-of-life recovery.
- Maximum plate thickness of 4 mm (due to production limit, mould thickness and pressable area) if a greater effective thickness is required, either stack two plates or introduce removable web stiffeners to control buckling.
- Preserve standard joist connections: retain the original Finnjoist interface geometry so that all connection types listed in the Finnframe flooring system catalogue remain fully compatible without modification.

Material Improvement

The application case of a structural component requires further improvements of the material performance in categories like,

- Achieve at least Euroclass B-s1, d0 (per EN 13501-1) to match or improve upon OSB fire ratings (D: no flash over within 20 minutes; s1: no smoke development; d0: no drooping)
- Investigation of hazardous emissions into the indoor air environment. As some of the lignin types contain sulphur and the newspaper waste could contain impurities.
- Lower target density ≤ 750 kg/m³ (to keep self-weight within 10 % of the original OSB-web joist)
- Moisture sensitivity of the surfaces and limiting of swelling and shrinkage to ≤ 0.5 % (to avoid flange-web gap formation)

5.2.1 Structural System

The floor joist has to be designed in a way so that it works in combination with other conventional building materials and components. Thus, the prototype design is planned within a structural system.

The prototype is conceived as part of a typical residential timber-frame structural system, in which cross-laminated timber (CLT) walls carry vertical loads and provide lateral stability. Within this context, the floor joists must satisfy both structural and acoustic criteria dictated

Table 10. Overview of structure serviceability and strength requirements (residential)

Type	Specification	Standard
Maximum deflection	≤ L/300; under characteristic (dead + live) loads	EN 1990:2002
Live load	2 kN/m² (residential area)	EN 1990-1-1:2002
Dead load	1.5 kN/m² (floor finishes, services, self-weight of joist and decking)	EN 1990-1-1:2002
Partial safety factors	γ_G = 1.35 (permanent), γ_Q =1.50 (variable)	EN 1991-1-1:2002
Minimum floor surface mass	200 kg/m² (to achieve $R_{n'}w \approx 50$ dB airborne sound insulation in a timber-framed floor)	EN ISO 12354-2:2017

by conventional building practice.

Specifically, the following table will summarize the structural serviceability and strength requirements within such a structure :

The structural grid in which the prototype joist is designed in has a primary span of 6m and a secondary span of 4m. This resembles a typical grid distance for residential (or office) uses. From secondary to secondary axis the floor joists are spanning with a centre distance of 60cm. The load bearing area per joist is therefore 0.6m by 4m or 2.4m² (Figure 120).

That results in 4.8kN total live loads and 3.6kN of dead loads, which are 7.2kN and 4.86kN respectively including the safety factor.

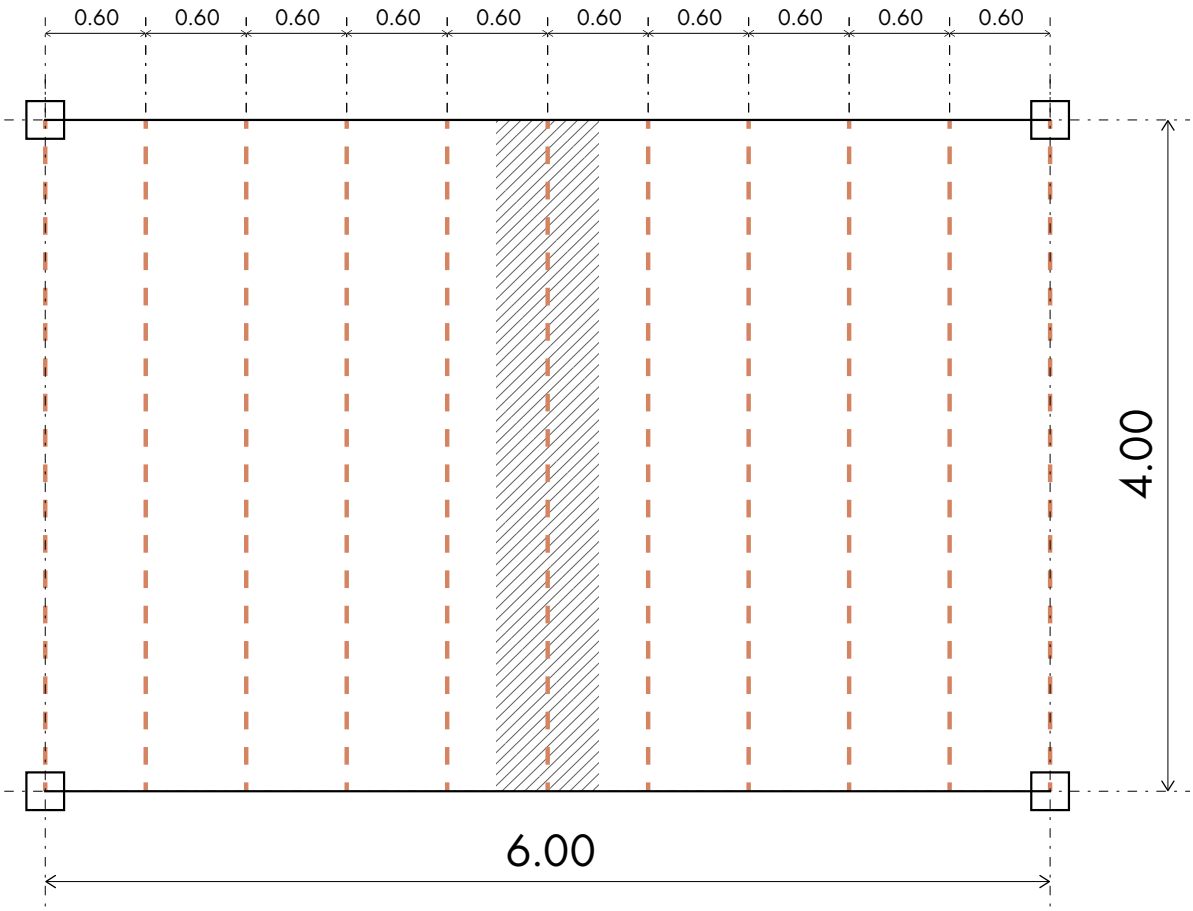

Figure 120. Structural grid plan view.

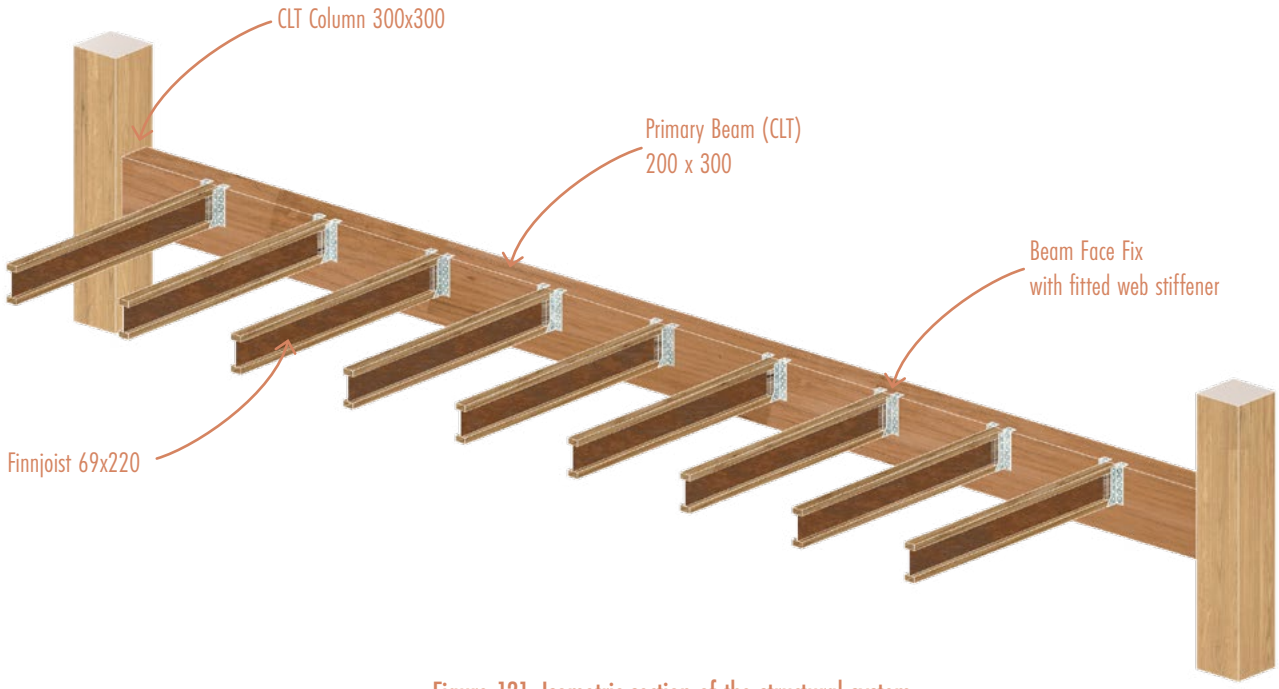

Figure 121. Isometric section of the structural system

Per square meter of flooring the surface mass of the floor reaches the minimum required mass due to the applied dead loads: $1.5\ kN/m^2\ \times 1.35\ =\ 2.025\ kN/m^2\ \approx\ 206\ kg/m^2$ ensuring the required sound insulation.

The connection detail of the Finnjoist, as the secondary structure, to the primary beam is created with a beam face fix. Between the metal bracket and the web a piece of web stiffening is fitted to create a strong joint and to improve the uplift capacity (Figure 121).

Cross-Section Detailing

In accordance to the design requirements/ adjustments, the cross-section of the typical Finnjoist was also altered. Figure 122 demonstrates how these alterations are worked in to the existing cross-section of the Finnjoist.

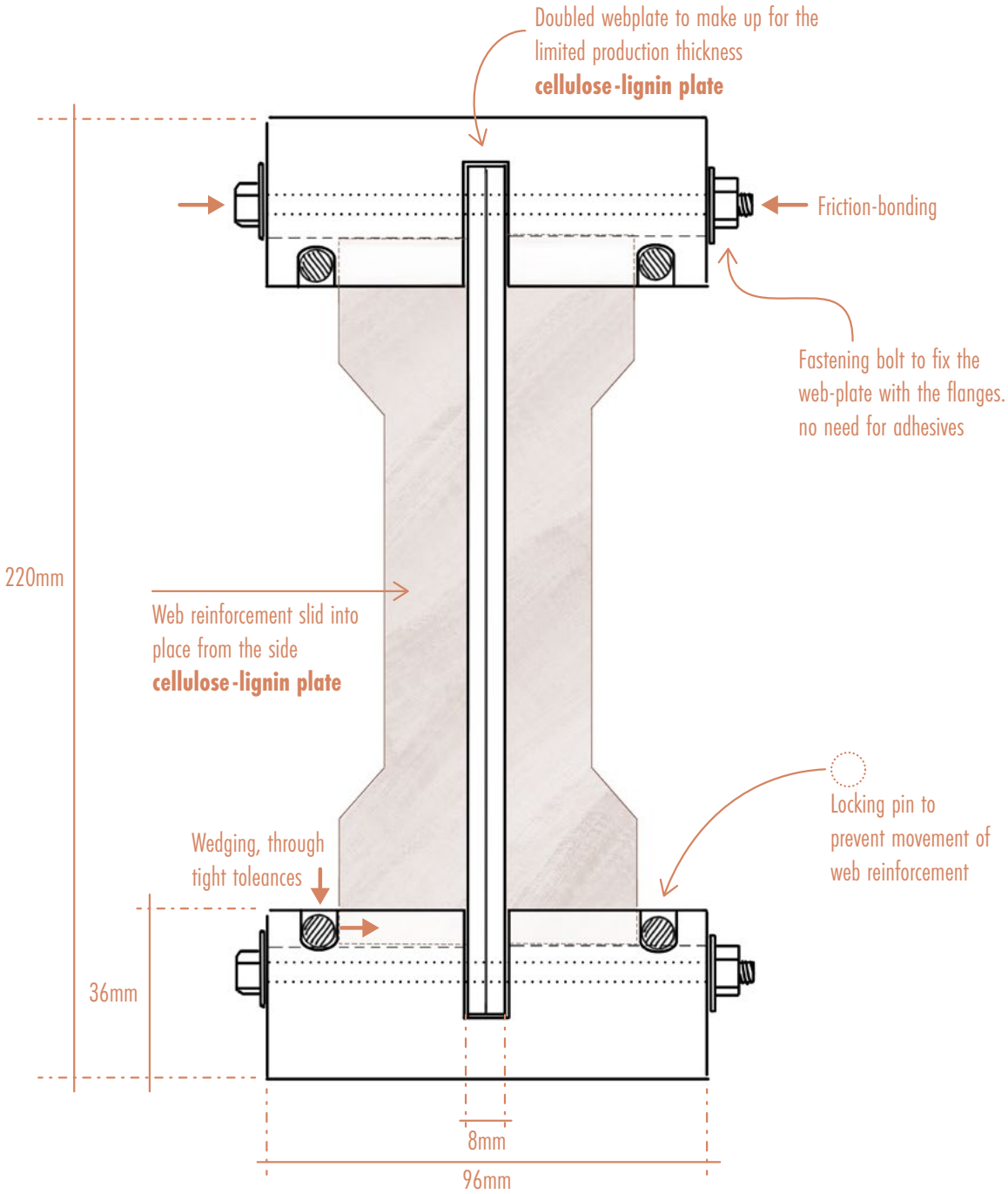

Figure 122. Schematic section of the Finnjoist using the cellulose-lignin plates.

Firstly, the web-plate is doubled up as the production limit for this project was 4mm. The web-thickness that will be used in Karamba will be 8mm.

In addition to the channels that are cut into the LVL flanges to place the web in, there are channels cut perpendicular to the main axis, although not as deep. In these channels the web reinforcements are slid. Their distancing is determined parametrically through structural analysis. The web reinforcements are introduced to counteract the materials relatively flexible behaviour. To fasten the reinforcement plates in the flanges another channel is cut into the flange right infront of the edge of the plate. A wedge is then pressed into the channel to create a tight connection and prevent the plate from sliding out.

To fix the web within the flange, bolts are used that are slid through holes that are drilled after the web and flanges are assembled. Tightening the bolts creates enough friction between the components to prevent any movement. The spacing of the bolts has yet to be determined.

Results:

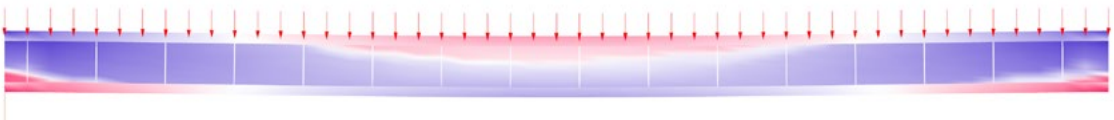

Figure 123. Overview of one isolated floor joist with the loads according to the load bearing area.

The simulation of a single floor joist (including the modelling of the web stiffeners) demonstrated that the cellulose–lignin plate is structurally feasible under the prescribed loading conditions (Figure 123). A closer look on the results reveals that the materials strength is utilized in compression to 55.9% (Figure 124), indicating a viable safety margin but also highlighting room for further optimization. Notably, the highest compressive stresses occurred in the flanges, suggesting that flange material selection (in this case, Glulam Timber grade 24h) and adjustments to web height could further reduce utilization. By applying an optimization algorithm to fine-tune both geometry and mixture parameters, structural performance is expected to improve. The specific global warming potential (GWP) results for this joist will be presented in the following segment. The results of the structural simulation and the presented workflow demonstrate that early integration of the analysis data into the design considerations is possible, keeping in mind that not every derived function is yet of statistical significance.

To also demonstrate that the controlled variability in the mixture design is possible, an optimisation algorithm will be applied to really harness the benefits from being able to optimise the mixture during the design process.

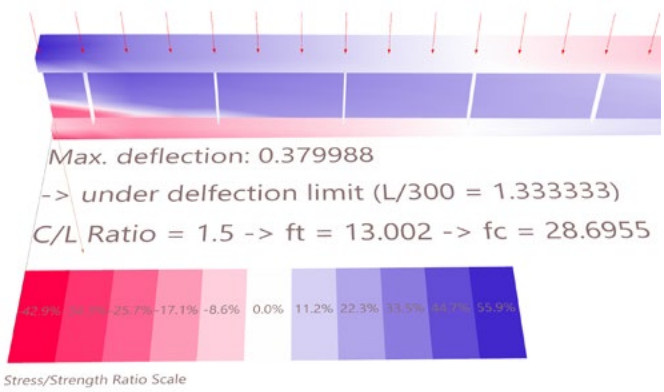

Figure 124. Result of joist under load - Overview panel

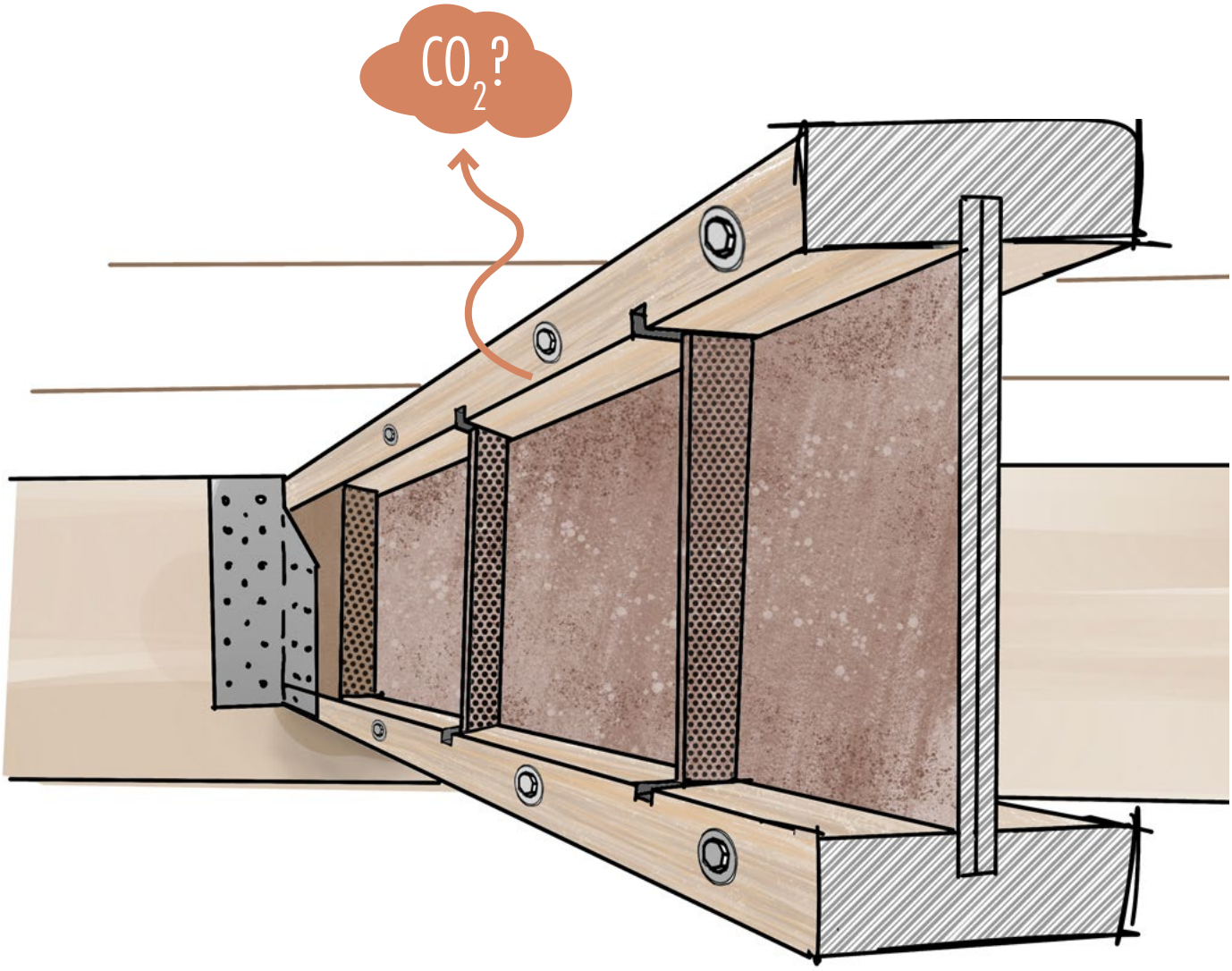

5.2.2 Environmental Impact

Assessing the environmental impact of innovative building materials is essential for ensuring sustainable design. In this section, the global warming potential (GWP) of the 4m Finnjoist with the cellulose–lignin web is evaluated for life cycle stages A1–A3 (raw material extraction, processing, and manufacturing). Downstream stages (transportation beyond the factory gate, installation, use, maintenance, and end-of-life) are excluded to avoid excessive speculation.

Care has been taken to report all numerical values explicitly. However, several variables remain that can drastically influence the GWP results: the source and purity of the lignin (e.g., soda vs. organosolv), cellulose feedstock quality (newspaper waste vs. virgin pulp), extraction and processing methods (energy intensity of pulping, drying techniques), and geographic location of material sourcing (grid electricity mix, transport distances). These factors can introduce considerable variation in the kilogram-CO_2-equivalents per kilogram of plate.

Disclaimer: The GWP values presented here are considered reasonable because they align closely with the documented A1–A3 GWP for a kilogram of conventional Finnjoist (–1.04 kg CO_2 eq; Metsä EPD). Although a direct, stage-for-stage comparison cannot be made (our scope is limited to A1–A3), the magnitude of our A1–A3 GWP result falls within the same order of magnitude as the total GWP reported for the Finnjoist, confirming that the calculations are consistent and credible.

For consideration in determining the GWP of the cellulose-lignin Finnjoist are the individual material scores and the energy demand for the production method. The following table lists the individual elements and their GWP. The values are based on a 4m long joist with the cross section specification according to Figure 122 with a web cellulose-lignin ratio of 3 to 2.

To determine the energy consumption of the hot-pressing process, the area under the power-vs-time curve shown in Figure 10 (page 1072) of Silva et al. (2020) was calculated. This integration yields the total energy consumption in kilowatt-hours (kWh) for one pressing cycle. The resulting value was interpreted as the energy required to press one square meter of plate material. To estimate the related carbon emissions, this energy value was multiplied by the Dutch electricity mix's emission factor. It should be noted that this approach introduces several sources of uncertainty. The press in the cited paper may differ from the one used in the actual production process (e.g., in scale, efficiency, insulation), and regional differences in electricity generation or machine specifications could significantly alter the energy footprint. Nonetheless, the result is considered plausible, as it aligns in magnitude with values reported for similar processes and materials.

All components combined result in a total weight of 22.8kg and a GWP of –19.02 kg CO_2-eq for the 4 m joist (Table 11). For comparison, the traditional Finnjoist has an A1–A3 GWP of –1.04 kg CO_2-eq per kilogram (Metsä Wood UK Ltd., 2023), while the bio-based prototype reaches –0.9 kg CO_2-eq per kilogram. Although the total GWP remains negative, the emissions per kilogram are currently slightly less favourable—mainly due to the processing impacts of the lignin source and electricity use.

However, with a more fine-tuned process chain tailored to the new material, including optimized sourcing and manufacturing methods, the carbon footprint could be reduced to levels comparable to that of conventional Finnjoists. One major advantage of the prototype is the complete avoidance of formaldehyde emissions, as the OSB web is replaced with a cellulose–lignin-based plate that does not rely on synthetic resins. This adds an important indoor air quality and health benefit alongside its structural and environmental potential.

Table 11. Summary of elements accounted for in the estimation of the GWP of a 4m Finnjoist using the cellulose-lignin material

Type	Equivalent kg CO_2	Amount	Source
Lignin	0.6 kg CO_2 /kg	4.97 kg	Bernier et al., 2013
Cellulose	-81.1kg CO_2 (65kg/kg)	7.46 kg	ISOCELL GmbH. (2014).
LVL	-693 kg CO_2/m^3	10.13 kg	Stora Enso. (2023)
Metal Fasteners	6.88 kg CO_2/1000kg	0.23 kg	Adolf Würth GmbH & Co. KG, 2024
Type	Specification		Source
Hot-pressing	6.1 kWh per m^2		Silva et al., 2020
Dutch Energy Mix	0.2685 kg CO_2/kWh		Statista, 2025
	Total kg CO_2 -19.02 (-0.9/kg)	Total weight: 22.80 kg	

5.2.3 Mixture and Design Optimisation

In order to achieve controlled variability in the mixture, the material tests conducted to date have been used to derive mathematical relationships linking mechanical performance to the cellulose–lignin (C/L) ratio. To frame the optimization process, the following question is posed:

"How can the optimal combination of cellulose-lignin ratio and web height be determined to simultaneously minimize compressive and tensile utilizations while respecting geometric constraints?"

To address this, a multi-objective optimization problem was formulated in the Grasshopper pipeline (see Figure 117), with Wallacei employed as the evolutionary solver. The decision variables (Genomes) consist of the cellulose-lignin ratio—which directly influences compressive and tensile strength—and the height of the web, since geometry constitutes one of the adjustable parameters. The fitness objectives (FOs) are defined to capture structural performance: specifically, reducing compressive utilization (FO3) and tensile utilization (FO4), while also considering weight and member height constraints (FO1 and FO2).

Table 12. Inputs into Wallacei X component in Grasshopper

Walleci inputs				
Fitness	Minimise equivalent CO2 emissions	Minimise weight	Minimise maximum compressive utilisation (red zone of stress/strength factor)	Minimise maximum tensile utilisation (blue zone of stress/strength factor)
Genomes	Web height (Finnjoist catalog)	C/L ratio -> affecting f_t and f_c (0.66-4.00)		

By integrating these variables and fitness definitions (Table 12) into the Wallacei X component, competing objectives for each candidate solution are evaluated. In the case study of the Finnjoist, a population size of 20 was selected and the algorithm was run for 60 generations, processing a total of 1,200 individuals. Although the single best-ranked solutions for FO3 and FO4 may not represent the absolute global optimum—due to the inherent trade-offs among objectives—they provide an initial insight into the performance envelope. For instance, one top-ranking candidate already exhibits compressive and tensile utilizations as low as 28% and 21%, respectively (Figure 125).

Next, in order to find the optimal solution between all of the iterations, the Wallacei tool offers an unsupervised machine learning algorithm that creates the Pareto front for any generation of results. Clustering the points of the selected generation forces Wallacei to group together all of those solutions with similar objective-values making trends in the points directly visible.

Wallacei's unsupervised machine learning algorithm applies clustering (e.g., K-means or hierarchical) to group solutions based on their objective values without needing predefined categories. This helps reveal how the different designs distribute in objective-space. The Pareto front consists of all solutions, for which no objective can be improved without worsening another and defines the trade-off surface. Within the Pareto front, the "knee" is the region where small gains in one objective cause large sacrifices in others, representing the

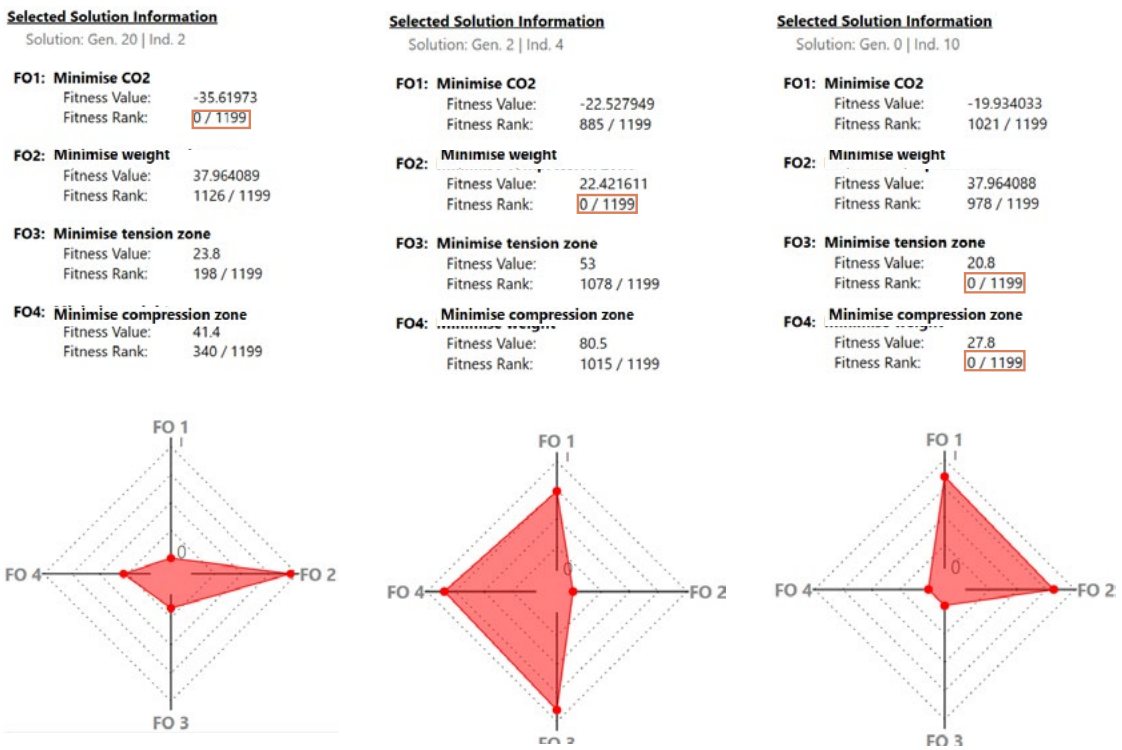

Figure 125. Top ranking solutions of optimisation process per fitness objective.

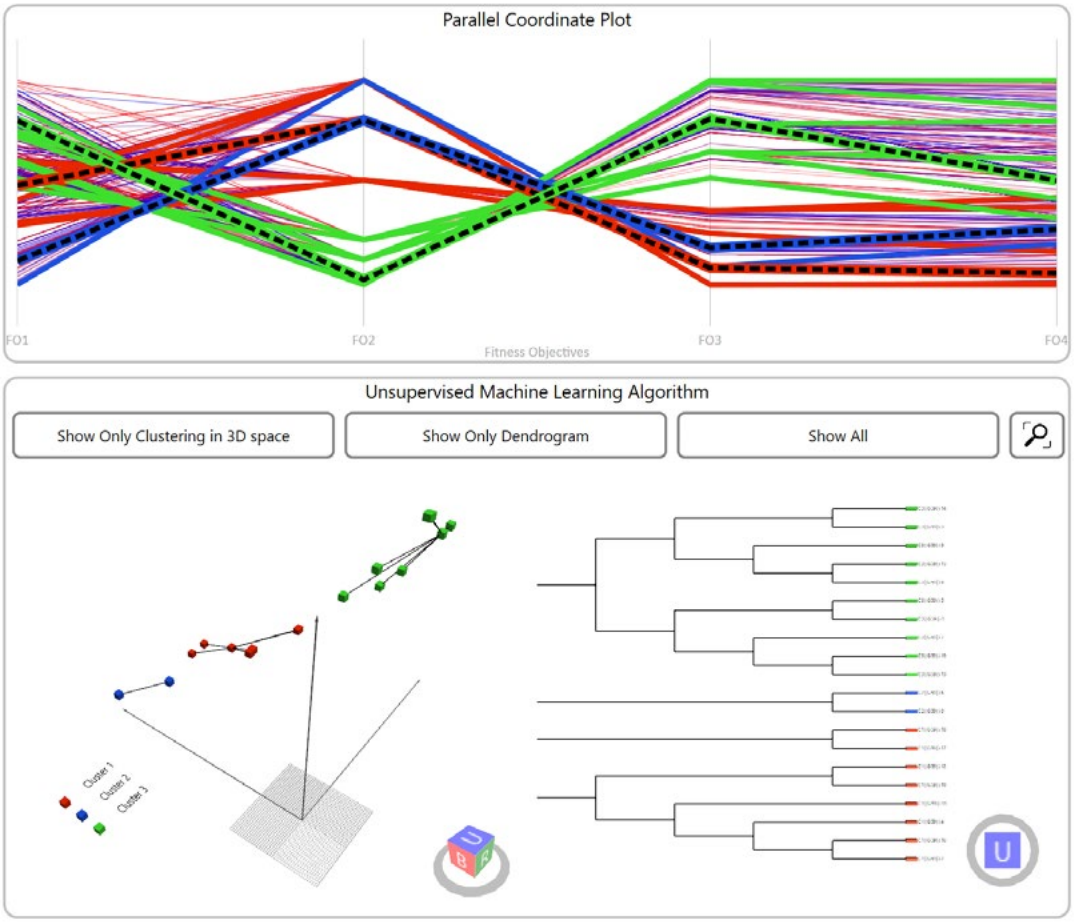

Figure 126. Parallel Coordinate Plot of optimisation process and clustering of Pareto front data points, including Dendogram.

best compromise among conflicting goals. Identifying the knee-directed cluster highlights the most balanced solution.

In Figure 126 the clusters are highlighted in the points of the clusters in the PC plot that are closest to the origin of the 3d coordinate system, also being the closest to the knee of the Pareto front. In this case these three points are exported back into the grasshopper environment to display the phenotype (e.g. volumetric representation) and the optimisation outcomes. Figure 127 shows the three exported solutions, their respective scores for all four fitness objectives and the variables chosen in the genome. All three solutions showcase a different chosen member height and different cellulose-lignin ratios. The upper solution is the most averaged between all FOs with higher weight and the least utilisation, the centre solution showcases the most lightweight approach with the highest utilisation and the lower solution is offering the best GWP.

A selection among these Pareto-optimal solutions allows a designer to choose the most appropriate configuration according to project-specific requirements. For example, if a limited installation height is imposed, one would select a solution from the Pareto front that satisfies that height constraint while still achieving low compressive and tensile utilizations. Conversely, if more conservative safety margins are desired for member utilisation—perhaps due to unusually high live loads or uncertain material properties—a solution exhibiting lower utilization values (at the expense of slightly increased weight or height) can be chosen. In this particular case, the MMO has delivered a family of non-dominated designs, each representing a different compromise between member height, material ratio, and structural performance. By inspecting these alternatives, the designer can make a fully informed decision that balances geometric restrictions, strength requirements, and safety considerations.

Figure 127. Exported solutions of optimisation process - 3 out of 1200

5.2.4 Resource-Aware Local Material Optimization

The adjustability of the mixture and the inclusion of the entire optimization process enable the creation of building products customized to specific design requirements. Previous material analysis has demonstrated that performance potentials vary according to mixture composition and processing conditions, indicating that no single blend is suitable for all applications.#

As demonstrated in the previous section, the multi-objective optimization (MOO) framework provided a set of Pareto-optimal Finnjoist designs, each representing a different compromise between cellulose-lignin ratio, web height, and structural performance. Developing this method further, the same MOO strategy can be extended to a finer scale: instead of optimizing only global variables for an entire member, localized objectives—based on principal stress distributions—can guide mixture adjustments segment by segment.

Moreover, resource availability becomes critical when scaling production of this material to volumes comparable to wood-based panels such as OSB or MDF. Annual production of comparable boards ranges from 3 million m^3/year (soft/hardboards) to 31 million m^3/year (particleboard) (Stubdrup et al., 2016). Regional price fluctuations for a square meter of MDF currently lie between 13.7 € and 22.8 € (15 – 25 USD)[1]. At present, lignin costs range from 91€ to 456 € per metric tonne—Soda lignin being at the lower end and Organosolv lignin at the higher end (Nadányi et al., 2022). Newspaper waste can be procured for approximately 124 – 153 € per tonne[2]. Assuming a 3:2 cellulose-lignin ratio, raw material costs for a 1 cm-thick plate would range from 16.9 € to 42 € per square meter. This expense renders the plates relatively costly, necessitating very deliberate use of mixture ingredients to achieve a competitive price point. Additionally, lignin extraction accounts for the largest share of carbon emissions among all constituents, making it imperative to employ the material purposefully and avoid over-dimensioning. The optimization process provides a structured approach to addressing these challenges.

In the Finnjoist case study, the web material experienced largely symmetrical loading, resulting in predominant compressive forces within the web and tensile forces in the flanges. This scenario proved ideal for optimizing the mixture toward compressive load resistance. As shown in Chapter 4.1.4, compressive and tensile force magnitudes vary inversely according to a quadratic function of deformation: when tensile force peaks, compressive force reaches its minimum.

When a building component undergoes non-uniform loading, the opportunity arises to adjust the mixture and locally tailor strength characteristics. For instance, consider a beam supporting a constant, non-uniformly distributed load—such as a cantilevered balcony with a heavy railing or a planter at its outer edge. In this case, the beam's first principal stress (σ_1) is tensile and increases toward the fixed support due to rising bending moments (Figure 128).

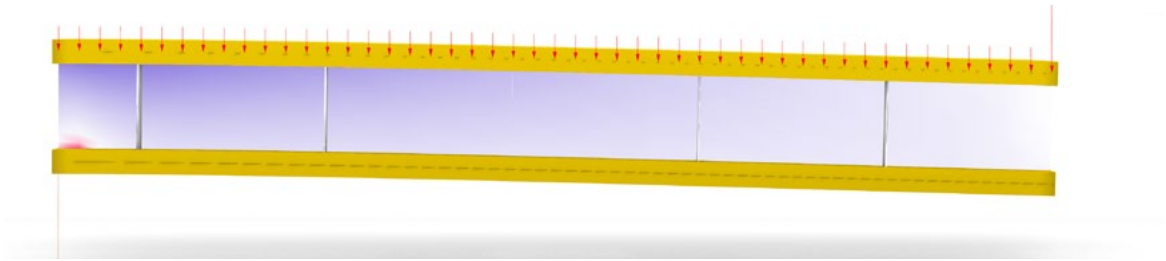

Figure 128. Cantilevered beam with linear load and point load at outer point, display of principal stress 1.

1. Which is more expensive, MDF board or HDF board? - Guang Dong DAEI New Material Co.Ltd. (2024, July 16). https://www.daeipetsheet.com/news/which-is-more-expensive-mdf-board-or-hdf-board
2025, from https://www.daeipetsheet.com/news/which-is-more-expensive-mdf-board-or-hdf-board
2. 2022 Domestic Mill Prices. (n.d.). Letsrecycle.Com. Retrieved June 2, 2025, from https://www.letsrecycle.com/prices/waste-paper/uk-domestic-mill-prices/2022-domestic-mill-prices/

Mapping the direction and magnitude of σ_1 thus guides localized mixture adjustments to reinforce regions under higher tensile demand.

By subdividing the component into discrete segments and evaluating principal stresses locally, the material formulation can be tailored to structural requirements (Figure 129). In areas with elevated tensile stress, variables such as lignin content, moisture level, or fiber orientation—which remains an unexplored but potentially influential parameter—could be modified to enhance tensile resistance. This stress-informed strategy paves the way for spatially optimized, performance-driven mixture design.

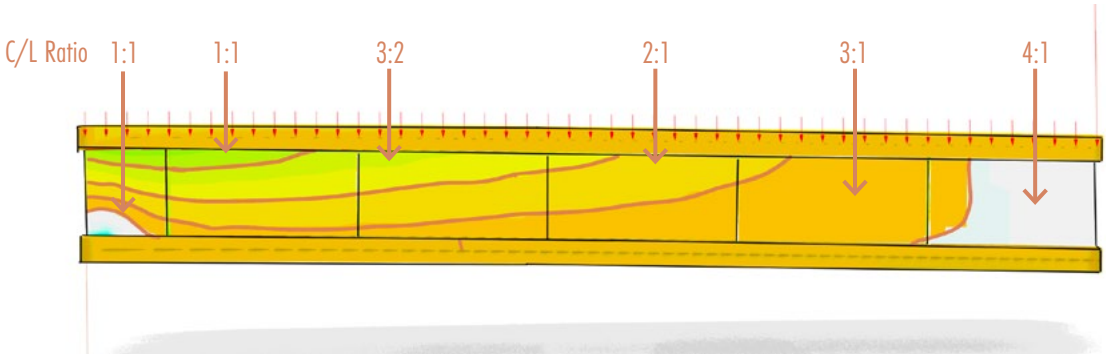

Figure 129. Segmentation of web into zones with different mixture ratios based on the occuring principle stress magnitude.

Implementing such localized adaptation in plated elements would involve guiding material tuning according to stress gradients, thereby balancing mechanical efficiency and material usage, and allowing to lower the potential prize. Realization of this approach will require further investigation into suitable manufacturing techniques.

5.3 Application Potential and Manufacturing Proposals

The development of the production technique and variable mixture and component design through the integration of a computational approach has opened up many possibilities how this knowledge can be used in several application scenarios (Figure 130). As of now the most-straight forward application case appears to be a replacement of traditional structural wood-based plates. The already intermediate to high structural qualities mean that plates could be used as stiffening of timber structures or simply used as cladding.

Having successfully re-manufactured a already hot-pressed plate into a new plate with seemingly very similar qualities implies that the dough that is used to produce the plates can be a further developed into pellets for an extrusion based process, which allows the production of much more complex geometries or bespoke applications like in heritage applications.

Besides extrusion, the re-manufacturability of the material makes the use of subtractive shaping techniques like CNC-milling an attractive potential application case, as the off-cuts cut simply be used to press new plates. With milling, also more customised structures can be created from plates. Paring the customisability of milling with the parametric structural modelling of panellised structures and the subsequent adjustment of the material mixture to the local structural demand of the panels can be the key to making very resource efficient designs.

A broader application scenario that can also make use of the customisable material mixture is the combination of thin plates to larger structural components like columns or beams.

Strips of the plates can be layered to make up a typical cross section of other mass timber construction, similar to CLT or LVL components. To retain the material purity, the layers could be combined through friction bonding with external reusable clamps. The benefit of customising the mixture per layer comes then into play when a component is exposed to different internal stresses. In a horizontal beam the layers could be optimised for high tensile capacities at the bottom layers and high compressive capacities at the top layer.

Similarly to the milling approach, a panellised structure could also be produced in a hot-press using a single mould that creates a discrete element. The mixture can then again be adjusted per panel in accordance to the structural demands. In Figure 131 the steps involved in producing the panels for a large structure is shown. In principle the production steps remain the same as the ones presented in chapter 3, as each mixture would have to be individually produced per panel. However, the use of larger, fully enclosed machinery for blending the fibres to control fibre length, cellulose-lignin homogenisation and moisture incorporation make this process far more efficient.

The production of large sheets can be similarly designed as the production line steps of modern sites for MDF-, Chip- or OSB boards. Continuous presses used as the major pressing type in Europe for OSB And MDF. The specific pressure of these continuous presses is 3 to

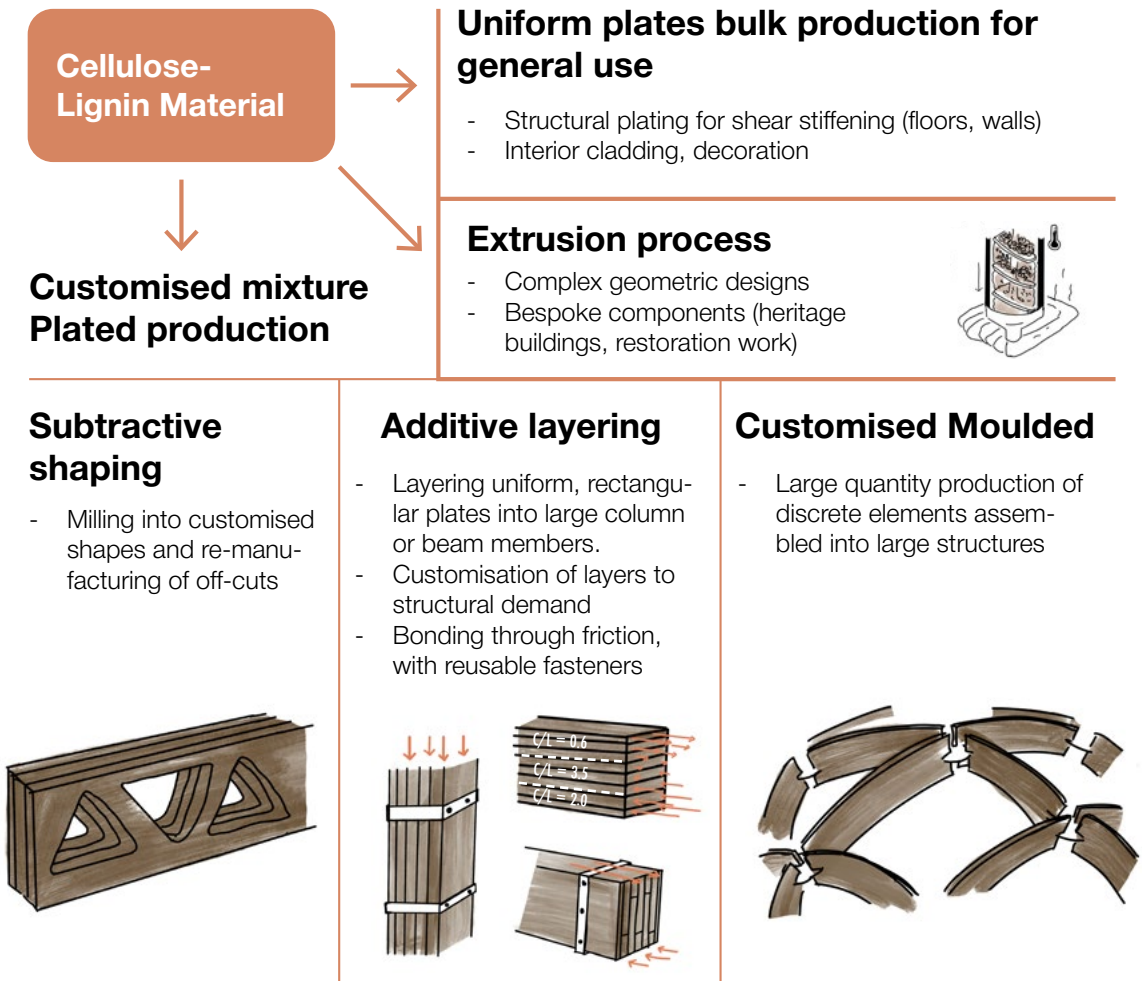

Figure 130. Potential material applications utilising the main learnings of the research project

5 MPa, with a temperature limit of 260°C (Stubdrup et al., 2016), both of which are also lying in the range that the plates have been pressed at in Chapter 3. From the storages to the dry-blowlines, to the forming stations and pressing, cutting belts most of the existing productions steps can be adapted very similarly for the cellulose lignin material (see Appendix Figure 12). As an optional addition in the processing chain, to accommodate the mixture variability that is proposed in Figure 129, the mixing of lignin and cellulose is done once the (lignin free-) cellulose dough is formed into a mat on the conveyor belt. This would also mean that the

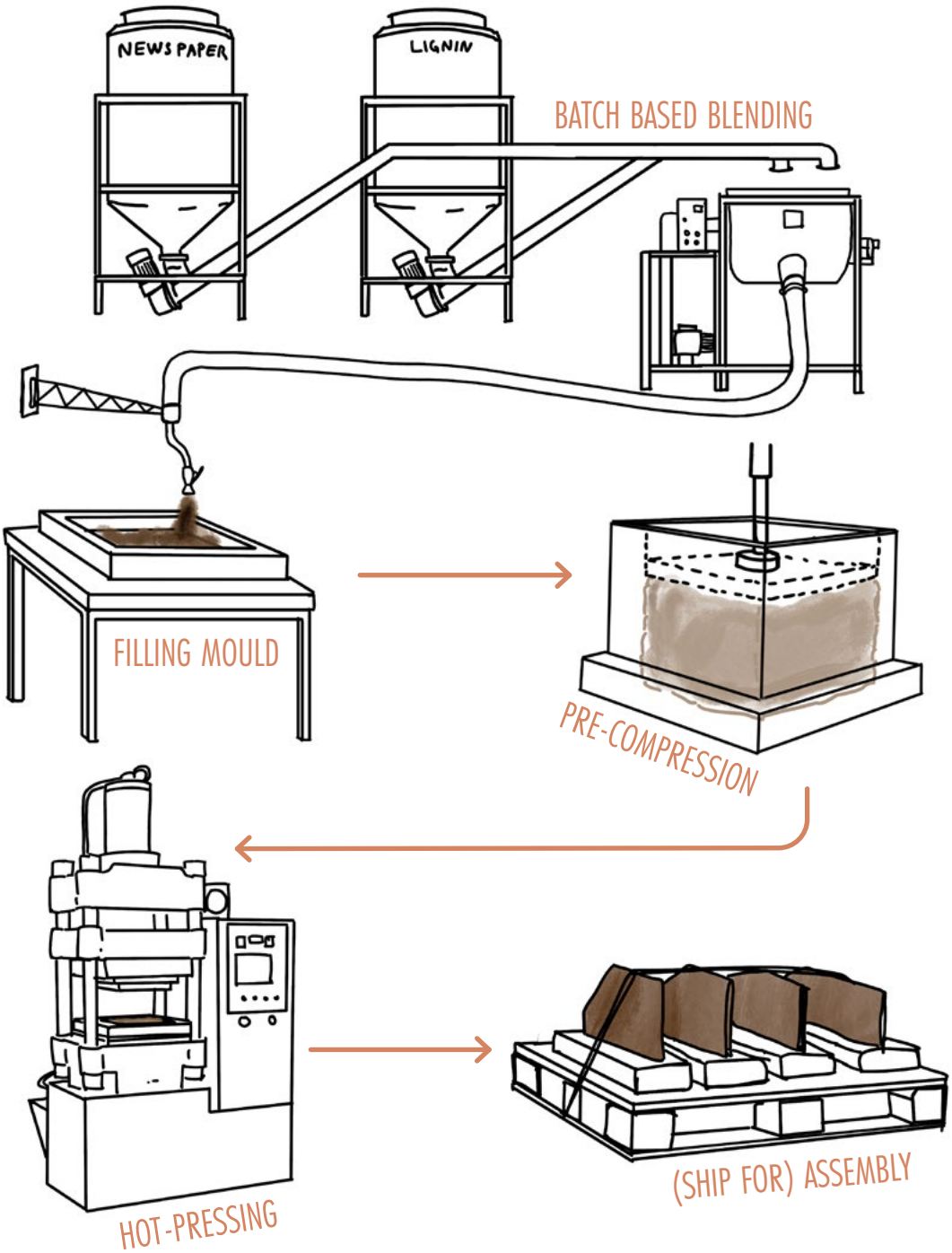

Figure 131. Schematic large scale hot-press production process of discrete elements

continuous plate is now segmented into plate lengths defined by the structural application. A robot arm with a spraying gun for powdered materials can then apply the desired amount of lignin in the respective zones and in another step the lignin powder is incorporated into the cellulose mat (pre compression with mixing tool). During the hot-pressing the lignin flows and wets the fibres and distributes evenly throughout the plate thickness. The plate is then be cut to size and assembled in the joist application (Figure 132)

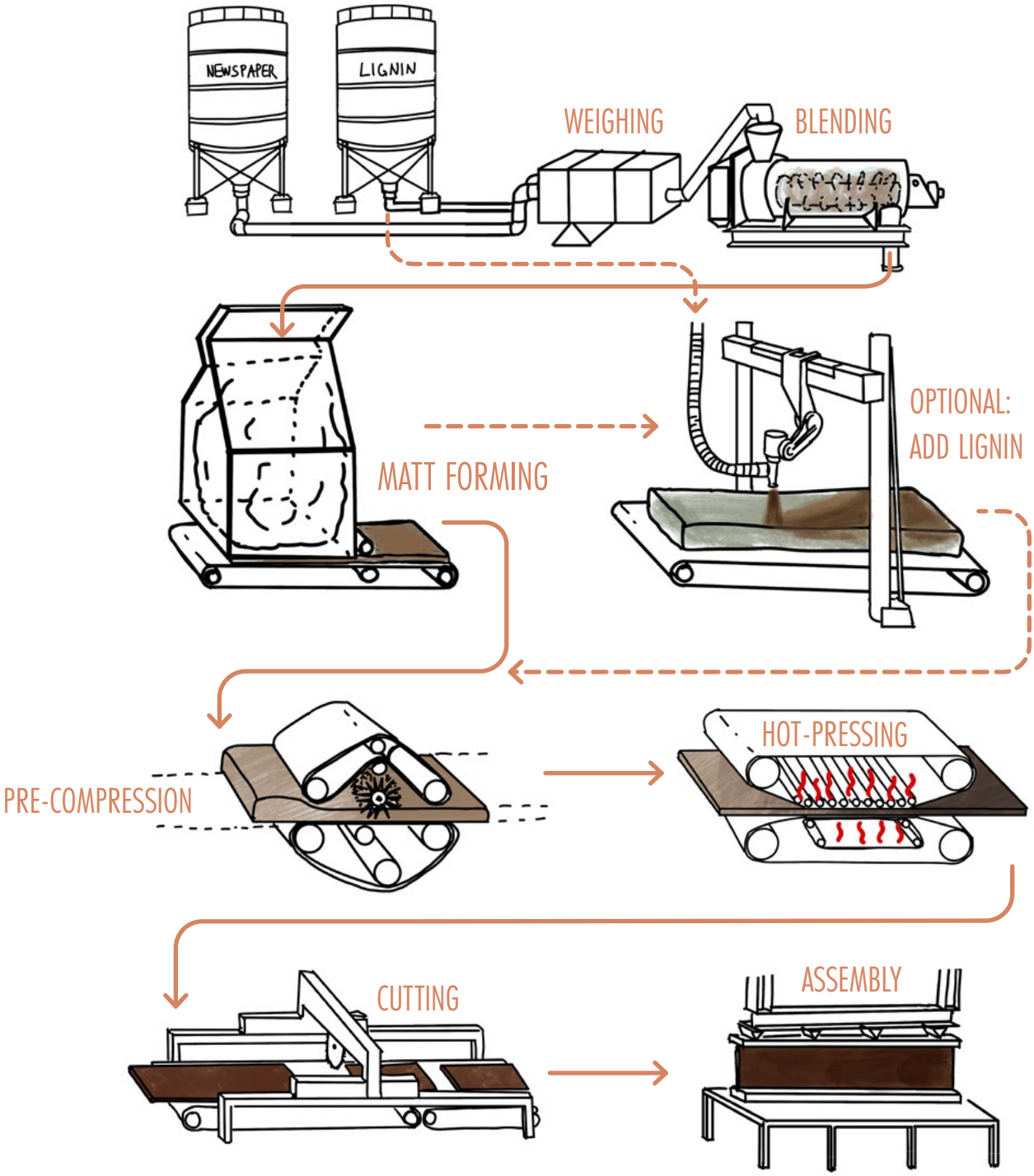

Figure 132. Schematic large scale continuous production line of cellulose-lignin plates.

Chapter 6
Conclusion and Recommendations

6. Conclusion and Recommendations

The primary goal of this research was to develop an optimized cellulose-lignin mixture combined with an appropriate hot-pressing production method, leveraging lignin's natural binding properties through controlled polymerization. By exploring cellulose and lignin from waste streams, this study addressed the urgent need for sustainable, bio-based construction materials within the building industry and achieved to produce a novel circular cellulose-lignin composite. Through an extensive experimental approach combined with innovative integration of computational techniques, the developed cellulose-lignin composite reveals significant promise for replacing conventional construction materials and addressing critical sustainability issues within the construction industry.

The systematic exploration of material mixtures, focusing on cellulose-to-lignin (C/L) ratios, has highlighted specific formulations with optimal mechanical performance. Ratios of 3:2 (cellulose to lignin) demonstrated superior flexural and tensile properties, while a reversed ratio of 2:3 was optimal for compressive strength. These ratios align with microscopic observations, confirming that higher lignin contents significantly improve fibre impregnation and adhesive bonding within the composite matrix. This underscores lignin's crucial role as a natural, effective adhesive, capable of replacing environmentally harmful synthetic binders typically found in conventional wood-based panels. Additionally, variations in hot-pressing conditions, especially temperature and moisture content, were found to be crucial in influencing the lignin flow and polymerization process, directly impacting the final mechanical and visual characteristics of the material.

Integration of computational design tools, particularly Rhino and Karamba3D, demonstrated substantial value in predicting mechanical performance, allowing early-stage adjustments in material composition and design to improve efficiency and reduce trial-and-error iterations. Employing statistical methods like polynomial regression and multi-objective optimization (MOO) streamlined the optimization process, offering a powerful framework for rapid exploration and refinement of material properties. Additionally, Multidimensional Scaling (MDS) analyses provided deeper insights into material behaviour across multiple mechanical and processing parameters, allowing a nuanced understanding and fast way of interpreting and visualising relationships between composition, processing conditions, and resultant properties.

Microscopic analysis highlighted critical insights into lignin distribution, polymerization quality, and fibre-matrix adhesion, underscoring lignin's potential as an effective natural adhesive. Nonetheless, it was also evident that purely cellulose-lignin compositions had inherent limitations, such as brittleness, susceptibility to warping, and reduced ductility, suggesting the necessity of targeted additives or treatment adjustments to enhance material performance comprehensively. Properties like moisture sensitivity, thermal behaviour and fire resistance have to be further investigated.

Differential Scanning Calorimetry analysis provided and initial attempt on clarifying the thermal behaviour of lignin, specifically identifying critical glass transition temperatures (T_g). These findings are instrumental in refining the hot-pressing conditions, choosing the most suitable lignin type and optimizing the lignin polymerization, and improving the resultant mechanical properties of the composite materials.

Already now, many application opportunities revealed themselves in which this material and the underlying data analysis and computational approach can be deployed. The application of the material to a prototype design has shown that the material is well on the way to be deployed in actual building components. Many characteristics are already suitable for a

structural member and the processability of the plates like cutting or drilling through, make it now a usable construction material. The redesigned Finnjoist with the altered web material and non-use of any adhesives has demonstrated a competitive alternative, that does not require the use of adhesives or OSB panels that emit formaldehyde. The tailoring of the mixture to the specific design and structural demands can make for incredibly efficient, resource-saving applications.

Ultimately, the variability in mechanical performance across different cellulose-lignin mixtures underscores that no single formulation is universally optimal. Instead, tailored mixtures aligned with specific design and structural applications provide the greatest potential for success. Future research should therefore focus on refining additive selections, exploring scalability through hot extrusion methods, and further validating computational predictions with practical structural applications. This approach will not only maximize performance but also significantly contribute to sustainability in construction.

Recommendations and Potential Development:

Future research on this particular topic should strive to push both the material development and design application in a direction of a market ready and competitive building product (Figure 133).The immediate steps that could follow this project can entail:

- Performing more material trials focusing on the accuracy of the mixing and pressing procedure to create reliable material data with statistical significance. Especially exploring the orthotropic nature of the material.
- Exploring of additives and treatments of the materials constituents to further improve the performance, on the mechanical side but also the functional performance characteristics, that are required for the safe use of the material in a building (fire, thermal, acoustic, moisture..).
- Address warping and blistering issues of the water containing mixtures.
- Advancing the production method to scale up the batch sizes or exploring alternative hot-processing methods, besides the hot-press, to create a production process that focuses on using lignin's adhesive properties.
- Further development of the computational integration and the use of analytical tools to gain deeper insights on the material relationship interdependencies.
- Incorporate industry partners and asses the material quality and availability. What impacts would changing cellulose and lignin sources have on the material?
- Assessing the environmental impact and economical aspects of the entire life cycle chain from material sourcing, production, use and end of life.

Future Roadmap of Research Topic

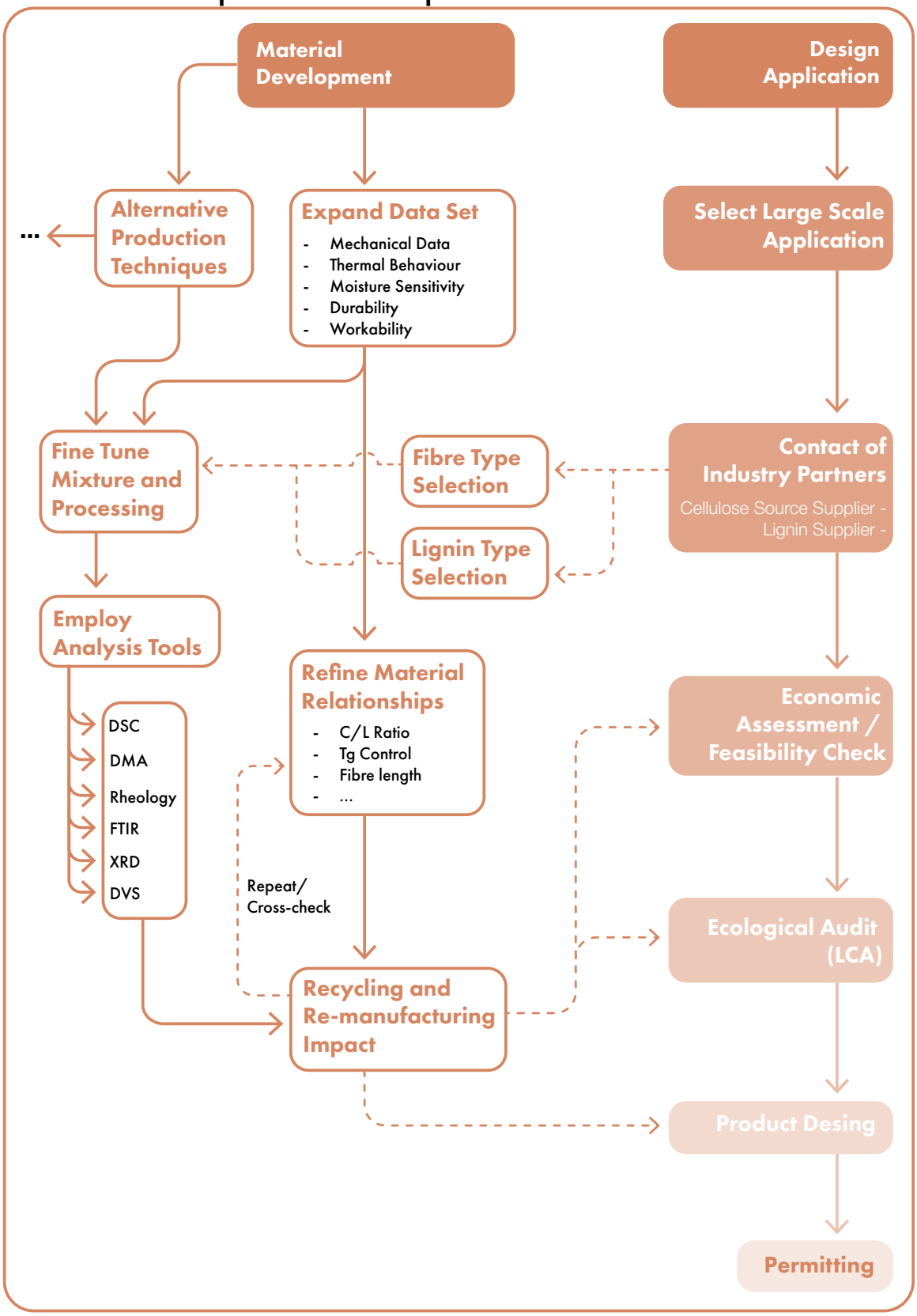

Figure 133. Future Roadmap

Chapter 7
Reflection

7. Reflection

1. What is the relation between your graduation project topic, your master track (A, U, BT, LA, MBE), and your master programme (MSc AUBS)?

In summary the proposed graduation topic focuses on the innovation of a new construction material. It merges multiple disciplines like structural and computational design, and also material science with the goal of creating an architectural component that can be a competitive alternative to the conventional catalogue of building materials and components.

Therefore, this research aligns seamlessly with the Building Technology track that encompasses a broad spectrum of architectural and engineering skills. The proposal demonstrates the design of an innovative and sustainable building component and provides ways past the initial development stage by providing a framework that can make use of the experimental results directly in the built environment.

2. How did your research influence your design/recommendations and how did the design/recommendations influence your research?

The approach taken for this thesis can be described as a "bottom-up" approach. The construction material and ultimately the construction product development starts with separate source materials that are combined to come up with a new material. This would mean that mostly all implications on the design come from the material performance.

However, the computational approach described in Chapter 1.7.3 is supposed to create an interaction between design and material development (research through design approach). As a new construction material is developed, the performance that is achieved of a singular optimisation process can determine the possible application to only one field. Creating the so called, controlled variability through the computational approach, in the material mixture would allow to explore multiple paths for the application.

The results from the mechanical testing have narrowed down the possible application of the developed material from a hot-press process. The current material strength is in bending on-par with common wood-based boards (MDF, OSB etc.), thus possible applications as interior cladding material can be investigated. The structural modelling has already proven that the application of the material in a structural member is possible, so the design of a Finnjoist was chosen due to the transferability of the current production method with the one needed for the web of the joist.

3. How do you assess the value of your way of working (your approach, your used methods, used methodology)?

For all my experiments, whether mixing, hot-pressing or testing I am documenting all relevant steps and variables in protocols to be able to back track all of my steps. This documentation has helped me a lot to quickly understand the effects of my adjustments during the hot-pressing and determining a very precise approach to achieve the current results for lignin-"flow" and surface finishing.

The use of the protocols for the analysis of relationships has also been very beneficial, for example in the computational approach to extract relationships that are not apparent just from looking at the data. In addition, the data collection from the mechanical experiments adds a significant overview and control of quality to the work. The variance of the data is key in determining how consistent the work on the plate is done. The statistical significance of the regression models is a very numerical way of assessing the value of the process. Methods like the Multidimensional scaling are additionally a tool to assign value to the work and the way of working.

4. How do you assess the academic and societal value, scope and implication of your graduation project, including ethical aspects?

While the final application of this material can still vary from the prototype design, it is already possible to say that the material can benefit the construction industry and environment at large. The construction industry is in desperate need of sustainable, viable and quickly deployed building materials that can replace what we build with every day. The use of virgin materials should not be possible in the near future according to the European plans for a circular economy, this also means considering the end-of-life scenario. This material can be a step in this direction with the use of only bio-based waste materials as the feedstock. Having successfully produced a recycled plate from the discarded hot-pressed scraps adds another valuable layer of sustainability.

In comparison with traditional wood based particle boards which often use harmful chemicals (formaldehydes) for the binding of wood, this material can stand out by first relying only on materials from existing waste streams and then making use of such chemicals. Also, in the finished building this will be beneficial as those chemicals are not at risk anymore of evaporating and affecting the indoor environment.

Bringing new materials to the market that can actually achieve the goals that plans like the European action plan towards a circular economy set as a goal, shows the shift in thinking that our building industry needs to take on.

5. How do you assess the value of the transferability of your project results?

The graduation work also plays a key role for the scientific context. It challenges the traditional way of conducting experiments on new materials as usual with a trial-and-error method. The inclusion of a computational method that aims to inform the experiments directly and make implications on the mixture of the material, is something rarely seen in scientific literature, especially for the development of construction materials.

The transferability of my graduation project is significant due to its structured documentation and interdisciplinary approach and collaboration with other faculties. The computational

framework to be developed can serve as a methodological basis for future research on bio-based composites, enabling reproducibility and scalability beyond this thesis' explored material. Ultimately, the computational approach, emphasizing controlled variability in material development, sets a valuable precedent for integrating structural engineering, computational design, and material science into architectural innovation. This approach can be applied to many other material investigations and can help in the investigation of new sustainable and biobased materials.

6. If given additional time and resources, which aspects of your research would you further develop or explore, and why?

I would further explore improving the structural properties of the material by adjusting the mixture ratios and processing parameters. More data points for the data analysis would allow more precise statements on the material behaviour. This can ultimately widen potential structural applications beyond the current interior cladding possibilities. Especially investigating the performance of the recycled plates is a significant aspect to the success of this material. Additionally, applying this research to additive manufacturing techniques would be one of the next steps taken with additional time and resources.

7. In what ways did technical difficulties or constraints during the material development process affect or limit the outcomes presented in your thesis?

The technical aspects created several practical challenges that influenced the results of my thesis significantly. For instance, obtaining the mould for the hot-pressing process was uncertain and heavily reliant on coincidence; without the generous support from my mentors contacts at aerospace engineering, none of the current experimental work would have been feasible. Moreover, the chemical pre-treatment initially proposed proved extremely demanding, requiring extensive lab preparation and detailed risk assessments. The restrictions on hazardous chemicals made these treatments practically impossible. Even gaining access to the Heritage and Technologies lab was unexpectedly difficult, as I needed to extensively document my procedures despite the minimal risks involved, mainly just dust exposure from non-hazardous bio-based materials. While these are necessary precautions to working in a laboratory, these practical constraints also limited my experimental freedom and shaped the direction of the thesis outcomes.

Chapter 8
References

8. References

- Arévalo, R., & Peijs, T. (2016). Binderless all-cellulose fibreboard from microfibrillated lignocellulosic natural fibres. Composites Part A: Applied Science and Manufacturing, 83, 38–46. https://doi.org/10.1016/j.compositesa.2015.11.027
- Bernier, E., Lavigne, C., & Robidoux, P. Y. (2013). Life cycle assessment of kraft lignin for polymer applications. The International Journal of Life Cycle Assessment, 18(2), 520–528. https://doi.org/10.1007/s11367-012-0503-y
- Bierach, C. B., Alberts Coelho, A. a. C., Turrin, M., Aşut, S., & Knaack, U. (2023). Wood-based 3D printing. https://doi.org/10.1007/s44150-023-00088-7
- Bilal, M., Qamar, S. A., Qamar, M., Yadav, V., Taherzadeh, M. J., Lam, S. S., & Iqbal, H. M. N. (2024). Bioprospecting lignin biomass into environmentally friendly polymers—Applied perspective to reconcile sustainable circular bioeconomy. Biomass Conversion and Biorefinery, 14(4), 4457–4483. https://doi.org/10.1007/s13399-022-02600-3
- Campos, T., Cruz, P. J. S., & Bruno, F. (2021). The Use of Natural Materials in Additive Manufacturing of Buildings Components—Towards a more sustainable architecture. Stojakovic, V and Tepavcevic, B (Eds.), Towards a New, Configurable Architecture - Proceedings of the 39th eCAADe Conference - Volume 1, University of Novi Sad, Novi Sad, Serbia, 8-10 September 2021, Pp. 355-364. https://papers.cumincad.org/cgi-bin/works/paper/ecaade2021_202
- Chen, C., Kuang, Y., Zhu, S., Burgert, I., Keplinger, T., Gong, A., Li, T., Berglund, L., Eichhorn, S. J., & Hu, L. (2020). Structure–property–function relationships of natural and engineered wood. Nature Reviews Materials, 5(9), 642–666. https://doi.org/10.1038/s41578-020-0195-z
- Chio, C., Sain, M., & Qin, W. (2019). Lignin utilization: A review of lignin depolymerization from various aspects. Renewable and Sustainable Energy Reviews, 107, 232–249. https://doi.org/10.1016/j.rser.2019.03.008
- Daniel, D., Khachatryan, L., Astete, C., Asatryan, R., Marculescu, C., & Boldor, D. (2019). Sulfur contaminations inhibit depolymerization of Kraft lignin. Bioresource Technology Reports, 8, 100341. https://doi.org/10.1016/j.biteb.2019.100341
- DeRousseau, M. A., Kasprzyk, J. R., & Srubar, W. V. (2021). Multi-Objective Optimization Methods for Designing Low-Carbon Concrete Mixtures. Frontiers in Materials, 8. https://doi.org/10.3389/fmats.2021.680895
- Dunky, M. (2003). Adhesives in the Wood Industry. Handbook of Adhesive Technology, Third Edition, 70. https://doi.org/10.1201/9780203912225.ch47
- Euclides, Q. (2025, February 21). Comparison of 3 and 4 Point Bending Tests. INSPENET. https://inspenet.com/en/articulo/3-and-4-point-bending-tests-comparison/
- European Commission. (2020). A new circular economy action plan: For a cleaner and more competitive Europe (COM(2020) 98 final). https://eur-lex.europa.eu/legal-content/EN/TXT/?uri=CELEX%3A52020DC0098
- Evdokimov, A. N., Kurzin, A. V., Fedorova, O. V., Lukanin, P. V., Kazakov, V. G., & Trifonova, A. D. (2018). Desulfurization of kraft lignin. Wood Science and Technology, 52(4), 1165–1174. https://doi.org/10.1007/s00226-018-1014-1
- Feng, Y., Hao, H., Lu, H., Chow, C. L., & Lau, D. (2024). Exploring the development and applications of sustainable natural fiber composites: A review from a nanoscale perspective. Composites Part B: Engineering, 276, 111369. https://doi.org/10.1016/j.compositesb.2024.111369

- Feng, Y., Mekhilef, S., Hui, D., Chow, C. L., & Lau, D. (2024). Machine learning-assisted wood materials: Applications and future prospects. Extreme Mechanics Letters, 71, 102209. https://doi.org/10.1016/j.eml.2024.102209
- Ganewatta, M. S., Lokupitiya, H. N., & Tang, C. (2019). Lignin Biopolymers in the Age of Controlled Polymerization. Polymers, 11(7), 1176. https://doi.org/10.3390/polym11071176
- Glass Transition Temperature. (2024, July 19). Corrosionpedia. https://www.corrosionpedia.com/definition/593/glass-transition-temperature-tg
- Hahn, H. T., & Williams, J. G. (1984, August 1). Compression failure mechanisms in unidirectional composites. ASTM Symp. on Composite Mater., Philadelphia, PA. https://ntrs.nasa.gov/citations/19840025452
- Harito, C., Bavykin, D., Yuliarto, B., Dipojono, H., & Walsh, F. (2019). Polymer Nanocomposites Having a High Filler Content: Synthesis, Structures, Properties, and Applications. Nanoscale, 11. https://doi.org/10.1039/C9NR00117D
- Hosseinaei, O., Wang, S., Enayati, A. A., & Rials, T. G. (2012). Effects of hemicellulose extraction on properties of wood flour and wood–plastic composites. Composites Part A: Applied Science and Manufacturing, 43(4), 686–694. https://doi.org/10.1016/j.compositesa.2012.01.007
- Huang, H., Zheng, C., Zhang, Z., & Huang, C. (2024). Adding lignin to bagasse cellulose-based materials increases the wet strength and reduces micro-nano scale wet low-temperature defects. Industrial Crops and Products, 222, 119750. https://doi.org/10.1016/j.indcrop.2024.119750
- Hubbe, M. A., Pizzi, A., Zhang, H., & Halis, R. (2017). Critical Links Governing Performance of Self-binding and Natural Binders for Hot-pressed Reconstituted Lignocellulosic Board without Added Formaldehyde: A Review. BioResources, 13(1), 2049–2115. https://doi.org/10.15376/biores.13.1.Hubbe
- International Organization for Standardization. (2024). ISO 22206:2024. Kraft lignin—Glass transition temperature by differential scanning calorimetry. https://www.iso.org/obp/ui/en/#iso:std:iso:22206:ed-1:v1:en
- Jacoby, W. G., & Ciuk, D. J. (2018). Multidimensional Scaling. In The Wiley Handbook of Psychometric Testing (pp. 375–412). John Wiley & Sons, Ltd. https://doi.org/10.1002/9781118489772.ch14
- Jakob, M., Mahendran, A. R., Gindl-Altmutter, W., Bliem, P., Konnerth, J., Müller, U., & Veigel, S. (2022). The strength and stiffness of oriented wood and cellulose-fibre materials: A review. Progress in Materials Science, 125, 100916. https://doi.org/10.1016/j.pmatsci.2021.100916
- Jolliffe, I. T. (2002). Principal Component Analysis (2nd edition). Springer-Verlag. https://doi.org/10.1007/b98835
- Kala, T., Maharshi, K., Patel, S., & Panwar, R. (2021). Electromagnetic and Mechanical Characterization of Iron Reinforced Natural Fiber Composites for Microwave Absorbing Applications. Advanced Composite Materials, 30, 1–11. https://doi.org/10.1080/09243046.2021.1904345
- Kenny, J. K., Medlin, J. W., & Beckham, G. T. (2023). Quantification of Phenolic Hydroxyl Groups in Lignin via19 F NMR Spectroscopy. ACS Sustainable Chemistry & Engineering, 11(14), 5644–5655. https://doi.org/10.1021/acssuschemeng.3c00115

- Kivikytö-Reponen, P., Fortino, S., Marttila, V., Khakalo, A., Kolari, K., Puisto, A., Nuvoli, D., & Mariani, A. (2024). An AI-driven multiscale methodology to develop transparent wood as sustainable functional material by using the SSbD concept. Computational and Structural Biotechnology Journal, 25, 205–210. https://doi.org/10.1016/j.csbj.2024.10.022
- Kumar, P., Barrett, D. M., Delwiche, M. J., & Stroeve, P. (2009). Methods for Pretreatment of Lignocellulosic Biomass for Efficient Hydrolysis and Biofuel Production. Industrial & Engineering Chemistry Research, 48(8), 3713–3729. https://doi.org/10.1021/ie801542g
- Kutnar, A., & Sernek, M. (2007). Densification of wood. Zbornik Gozdarstva in Lesarstva, 82, 53–62.
- Laurichesse, S., & Avérous, L. (2014). Chemical modification of lignins: Towards biobased polymers. Progress in Polymer Science, 39(7), 1266–1290. https://doi.org/10.1016/j.progpolymsci.2013.11.004
- Laycock, B. G., Chan, C. M., & Halley, P. J. (2024). A review of computational approaches used in the modelling, design, and manufacturing of biodegradable and biobased polymers. Progress in Polymer Science, 157, 101874. https://doi.org/10.1016/j.progpolymsci.2024.101874
- Leban, J.-M. (2005). Wood welding – an award-winning dicovery. Scandinavian Journal of Forest Research, 4, 370–371.
- Lee, N. A., Shen, S. C., & Buehler, M. J. (2022). An automated biomateriomics platform for sustainable programmable materials discovery. Matter, 5(11), 3597–3613. https://doi.org/10.1016/j.matt.2022.10.003
- Libretti, C., Correa, L. S., & R. Meier, M. A. (2024). From waste to resource: Advancements in sustainable lignin modification. Green Chemistry, 26(8), 4358–4386. https://doi.org/10.1039/D4GC00745J
- Liebrand, T. R. H. (2018). 3D printed fiber reinforced lignin. https://repository.tudelft.nl/record/uuid:2856a86c-d862-48b1-924e-1f3ce74647b3
- Madurwar, M., Sakhare, V., & Ralegaonkar, R. (2015). Multi Objective Optimization of Mix Proportion for a Sustainable Construction Material. Procedia Engineering, 118, 276–283. https://doi.org/10.1016/j.proeng.2015.08.427
- Mathew, A. K., Abraham, A., Mallapureddy, K. K., & Sukumaran, R. K. (2018). Lignocellulosic Biorefinery Wastes, or Resources? In Waste Biorefinery (pp. 267–297). Elsevier. https://doi.org/10.1016/B978-0-444-63992-9.00009-4
- Mechanical Testing of Composites. (2024, October 8). https://www.addcomposites.com/post/mechanical-testing-of-composites#headline2
- Mitteldichte Faserplatten | Material-Archiv. (n.d.). Retrieved January 20, 2025, from https://materialarchiv.ch/de/ma:material_657?type=all&n=Nachhaltigkeit
- Mohammed, M., Rasidi, M., Mohammed, A., Rahman, R., Osman, A., Adam, T., Betar, B., & Dahham, O. (2022). Interfacial bonding mechanisms of natural fibre-matrix composites: An overview. BioResources, 17(4). https://doi.org/10.15376/biores.17.4.Mohammed
- Morsing, N. (1998). Densification of Wood.: The influence of hygrothermal treatment on compression of beech perpendicular to gain. Technical University of Denmark.
- Mukhtar, A., Zaheer, M., Saeed, M., & Voelter, W. (2017). Synthesis of lignin model compound containing a β-O-4 linkage. Zeitschrift Für Naturforschung B, 72(2), 119–124. https://doi.org/10.1515/znb-2016-0201

- Nachhaltige Wärmedämmung aus Zellulosefaser | ISOCELL. (2025). https://www.isocell.com/de-at/zellulosedaemmung
- Nadányi, R., Ház, A., Lisý, A., Jablonský, M., Šurina, I., Majová, V., & Baco, A. (2022). Lignin Modifications, Applications, and Possible Market Prices. Energies, 15(18), Article 18. https://doi.org/10.3390/en15186520
- NWO-SIA. (2025). Project Wood without Trees. SIA Projectenbank. Retrieved January 20, 2025, from https://www.sia-projecten.nl/project/wood-without-trees
- Olufsen, S. N., Andersen, M. E., & Fagerholt, E. (2020). μDIC: An open-source toolkit for digital image correlation. SoftwareX, 11, 100391. https://doi.org/10.1016/j.softx.2019.100391
- Oriented Strand Boards (OSB)—Definitions, classification and specifications (NEN-EN 300:2006 en). (2006). https://connect.nen.nl/Standard/Detail/108785?compId=10037&collectionId=0
- Parveen, S., Rana, S., & Fangueiro, R. (2017). 13—Macro- and nanodimensional plant fiber reinforcements for cementitious composites. In H. Savastano Junior, J. Fiorelli, & S. F. dos Santos (Eds.), Sustainable and Nonconventional Construction Materials using Inorganic Bonded Fiber Composites (pp. 343–382). Woodhead Publishing. https://doi.org/10.1016/B978-0-08-102001-2.00020-6
- Pedregosa, F., Varoquaux, G., Gramfort, A., Michel, V., Thirion, B., Grisel, O., Blondel, M., Prettenhofer, P., Weiss, R., Dubourg, V., Vanderplas, J., Passos, A., Cournapeau, D., Brucher, M., Perrot, M., & Duchesnay, E. (2011). Scikit-learn: Machine Learning in Python. Journal of Machine Learning Research, 12, 2825–2830.
- Qianli, W. (2022). Studies on Fabrication of High-Strength Material from Residue of Hot-Compressed Water Extraction of Biomass. Kyushu University.
- Qin, S., Liu, K., Ren, D., Zhai, Y., Zhang, S., Liu, H., Ma, H., Zhao, C., Huang, F., & Zhou, X. (2023). All-natural and high-performance structural material based on lignin-reinforced cellulose. Materials Today Communications, 36, 106559. https://doi.org/10.1016/j.mtcomm.2023.106559
- Rowell, R. M. (2005). Handbook of Wood Chemistry and Wood Composites. CRC Press.
- Saeed, N., Nam, H., Haq, M. I. U., & Muhammad Saqib, D. B. (2018). A Survey on Multidimensional Scaling. ACM Comput. Surv., 51(3), 47:1-47:25. https://doi.org/10.1145/3178155
- Sandanayake, M., Bouras, Y., & Vrcelj, Z. (2022). A feasibility study of using coffee cup waste as a building material—Life cycle assessment and multi-objective optimisation. Journal of Cleaner Production, 339, 130498. https://doi.org/10.1016/j.jclepro.2022.130498
- Silva, D., Firmino, A., Ferro, F., Christoforo, A., Rezende Leite, F., Rocco Lahr, F., & Kellens, K. (2020). Life cycle assessment of a hot-pressing machine to manufacture particleboards: Hotspots, environmental indicators, and solutions. The International Journal of Life Cycle Assessment. https://doi.org/10.1007/s11367-020-01755-3
- Singh, G., Kaur, S., Khatri, M., & Arya, S. K. (2019). Biobleaching for pulp and paper industry in India: Emerging enzyme technology. Biocatalysis and Agricultural Biotechnology, 17, 558–565. https://doi.org/10.1016/j.bcab.2019.01.019
- Stappers, P. J., & Giaccardi, E. (2017). Research through Design. In M. Soegaard & R. Friis-Dam (Eds.), The Encyclopedia of Human-Computer Interaction (pp. 1–94). The Interaction Design Foundation. https://www.interaction-design.org/literature/book/the-encyclopedia-of-human-computer-interaction-2nd-ed/research-through-design

- Stefania Chiujdea, R., & Nicholas, P. (2020). Design and 3D Printing Methodologies for Cellulosebased Composite Materials. 1, 547–554. Scopus.
- Stubdrup, K. R., Karlis, P., Roudier, S., & Delgado Sancho, L. (2016). Best available techniques (BAT) reference document for the production of wood-based panels. Joint Research Centre, European Commission.
- Thakur, M. S. H., Shi, C., Kearney, L. T., Saadi, M. A. S. R., Meyer, M. D., Naskar, A. K., Ajayan, P. M., & Rahman, M. M. (2024). Three-dimensional printing of wood. Science Advances, 10(11), eadk3250. https://doi.org/10.1126/sciadv.adk3250
- Thomsen, O., & Kratmann, K. K. (2010). Experimental Characterisation of Parameters Controlling the Compressive Failure of Pultruded Unidirectional Carbon Fibre Composites. Applied Mechanics and Materials, 24–25, 15–22. https://doi.org/10.4028/www.scientific.net/AMM.24-25.15
- Thum, M. (2023, April). Direct-Ink-Writing (DIW). 3D-grenzenlos – Deutschlands Magazin zum 3D-Druck! https://www.3d-grenzenlos.de/3d-druckverfahren/direct-ink-writing-diw/
- UNEP. (2024). 2023 Global Status Report for Buildings and Construction: Beyond foundations - Mainstreaming sustainable solutions to cut emissions from the buildings sector. United Nations Environment Programme. https://doi.org/10.59117/20.500.11822/45095
- Xia, G., Yu, S., Yang, Z., Lian, J., Xie, Y., & Feng, Q. (2024). Reconstructed wood with high water stability from bark cellulose and corncob lignin. International Journal of Biological Macromolecules, 281. Scopus. https://doi.org/10.1016/j.ijbiomac.2024.136187
- XYZAidan. (2020, June). Recycle Cardboard Into Anything With 3D Printing! Instructables. https://www.instructables.com/Recycle-Cardboard-Into-Anything-With-3D-Printing/
- Yang, Y., Zhang, L., Zhang, J., Ren, Y., Huo, H., Zhang, X., Huang, K., Rezakazemi, M., & Zhang, Z. (2023). Fabrication of environmentally, high-strength, fire-retardant biocomposites from small-diameter wood lignin in situ reinforced cellulose matrix. ADVANCED COMPOSITES AND HYBRID MATERIALS, 6(4), 140. https://doi.org/10.1007/s42114-023-00721-5
- Zhang, Y., Wu, J.-Q., Li, H., Yuan, T.-Q., Wang, Y.-Y., & Sun, R.-C. (2017). Heat Treatment of Industrial Alkaline Lignin and its Potential Application as an Adhesive for Green Wood–Lignin Composites. ACS Sustainable Chemistry & Engineering, 5(8), 7269–7277. https://doi.org/10.1021/acssuschemeng.7b01485
- Zhao, C., Huang, J., Yang, L., Yue, F., & Lu, F. (2019). Revealing Structural Differences between Alkaline and Kraft Lignins by HSQC NMR. Industrial & Engineering Chemistry Research, 58(14), 5707–5714. https://doi.org/10.1021/acs.iecr.9b00499
- Zheng, G., Ye, H., Liang, Y., Jin, X., Xia, C., Fan, W., Shi, Y., Xie, Y., Li, J., & Ge, S. (2023). Pre-treatment of natural bamboo for use as a high-performance bio-composites via acetic acid ball milling technology. Construction and Building Materials, 367, 130350. https://doi.org/10.1016/j.conbuildmat.2023.130350
- Some Figures have been designed using resources from Flaticon.com see Table 13.

Table 13. Pictogram Resource Reference List

Icon Title	Author	Used on Page:	Flaticon URL
Weather	Ivan Abirawa	60,61,62,64,69	https://www.flaticon.com/free-icon/weather_13936209
Cell	Nadiinko	60,61,62,64,69	https://www.flaticon.com/free-icon/cell_4299855
Horizontal Merge	Freepik	60,61,62,64,69	https://www.flaticon.com/free-icon/horizontal-merge_80716
Textile	Freepik	60,61,62,64,69	https://www.flaticon.com/free-icon/textile_5482820
Humidity	Freepik	60,61,62,64,69	https://www.flaticon.com/free-icon/humidity_8678233
Time	Ilham Fitrotul Hayat	60,61,62,64,69	https://www.flaticon.com/free-icon/time_3395452
Non-Toxic	Freepik	5	https://www.flaticon.com/free-icon/non-toxic_4876347?term=non+toxic&page=1&position=4&origin=search&related_id=4876347
Recycle Sign	Hilmy Abiyyu A.	5	https://www.flaticon.com/free-icon/recycle-sign_4361302?term=recycle-sign&page=1&position=44&origin=search&related_id=4361302
Copy Paste	I Wayan Wika	5	https://www.flaticon.com/free-icon/cut_4429996?term=copy+paste&page=1&position=63&origin=search&related_id=4429996
Time	Ilham Fitrotul Hayat	5	https://www.flaticon.com/free-icon/time_3395452?term=time&page=1&position=35&origin=search&related_id=3395452
Success	Parzival' 1997	7,8	https://www.flaticon.com/free-icon/success_7508545?term=trial+and+error&page=1&position=3&origin=search&related_id=7508545
Pie Chart	bsd	8	https://www.flaticon.com/free-icon/pie-chart_8972636?term=pie+chart+data&page=1&position=2&origin=search&related_id=8972636
3D-Modeling	Freepik	8	https://www.flaticon.com/free-icon/3d-modeling_12008058?term=modeling+cube&page=1&position=31&origin=search&related_id=12008058
TXT-file	Freepik	119,121	https://www.flaticon.com/free-icon/txt-file_104647
Weight	Freepik	121,130	https://www.flaticon.com/free-icon/weight_847345?term=weight&page=1&position=1&origin=search&related_id=847345
Carbon Dioxide	Freepik	121,130	https://www.flaticon.com/free-icon/carbon-dioxide_550250?term=co2&page=1&position=20&origin=search&related_id=550250
Analysis	mynamepong	8	https://www.flaticon.com/free-icon/analysis_809497

Chapter 9
Appendix

9. Appendix

Appendix Table 1. Summary of all relevant additives from the literature review

Name	Description	Role	Sources:
Sodium Hydroxide (NaOH)	Strong alkali	Used to remove lignin and hemicellulose from cellulose, exposing microfibrils for bonding; degreasing	Qin et al. (2023), Yang et al. (2023), Xia et al. (2024)
Sodium Sulphite (Na_2SO_3)	Sulphur-based delignification agent	Assists in breaking lignin bonds to make cellulose more accessible	Qin et al. (2023), Xia et al. (2024)
Sodium Silicate (Na_2SiO_3)	Inorganic flame retardant and binder enhancer	Improves structural bonding and fire resistance	Yang et al. (2023)
Sodium Chlorite ($NaClO_2$)	Oxidising agent	Removes residual lignin and hemicellulose, improving fibre purity for mechanical bonding.	Xia et al. (2024)
Acetic Acid (CH_3COOH)	Organic acid	Pre-treatment to disrupt cell structure, enhancing lignin accessibility.	Zheng et al. (2023), Xia et al. (2024)
Hydrogen Peroxide (H_2O_2)	Oxidising agent	Removes surface impurities and facilitates fibre bonding	Yang et al. (2023)
Deep Eutectic Solvent (DES)	Solvent system (e.g., choline chloride and oxalic acid).	Dissolves and re-polymerises lignin for better fibre adhesion	Qi et al. (2024)
TEMPO Catalyst	Oxidation catalyst	Facilitates selective oxidation of cellulose, enhancing lignin-cellulose interaction.	Xia et al. (2024)
Guar & Xanthan Gum	Organic binding agents	Adds elasticity and malleability to cellulose composites during extrusion	Chiujdea and Nicholas (2020)
Glycerin	Plasticiser	Reduces brittleness and enhances flexibility in printed composites	Campos et al. (2021), Chiujdea and Nicholas (2020)
PVA Glue	Synthetic water-soluble polymer	Provides structural integrity and prevents delamination in molded paper objects	XYZAidan(2020)
Rice Paste	Organic starch-based adhesive	Strengthens paper pulp composites while maintaining biodegradability.	XYZAidan(2020)
Corn Starch	Plant based thickening agent	Provides moderate bonding strength while being eco-friendly.	XYZAidan(2020)
Methylcellulose	Gelatinising agent	Improves viscosity and stability for extrusion processes	Bierach et al. (2023)
Dimethyl Sulfooxide (DMSO)	Solvent	Acts as a binding agent that helps to create a homogeneous and adhesive matrix when combined with lignin and cellulose.	Bierach et al. (2023)
Bentonite	Mineral gelatinising agent	Improves viscosity and extrudability of the material, making it more suitable for 3D printing. Increases density and enhances the material's workability while reducing its crumbliness.	Bierach et al. (2023)
Alginate	Natural biopolymer derived from brown algae, Gelling agent or viscosifying	Used as a binder in the mixture to provide viscosity and adhesion. Creates homogeneous pastes when mixed with lignin and cellulose. When dried brittle or too dry.	Bierach et al. (2023)

Appendix Table 2. Cellulose-Lignin Composition of Mixtures presented in the Literature

Reference Name	Material Description	Cellulose Type	Lignin Type	Comments
Arévalo & Peijs, 2016	Binderless all-cellulose fibre board	Flax fibres	Qin et al. (2023), Yang et al. (2023), Xia et al. (2024)	
70% cellulose, 16% hemicellulose and 2% lignin	None		Qin et al. (2023), Xia et al. (2024)	
Bierach & Coelho, 2023	Cellulose-lignin with methyl-cellulose binder	Kraft Cellulose Sheets	Kraft Lignin	Solved in Acetone
Campos Arevalo & Peijs, 2016	Lignin-based fibre composite	Microcrystalline cellulose powder (CNC)	None	
Huang et al., 2024	Bagasse cellulose with lignin reinforcement	Bleached Bagasse Cellulose	Zheng et al. (2023), Xia et al. (2024)	
0.8 wt% lignin	Lignin	Dry mixed	Yang et al. (2023)	
Hubbe et al., 2017	Analysis: Binder-free wood-lignin composite			
Liebrand, 2018	Fibre-reinforced lignin (acetone-water mix)	skogcell 90Z bleached kraft WFbR	Kraft Lignin, type Indulin AT	
Qi et al., 2024	Wood-Plastic Composite with HDPE	corn stover		in-situ lignin
Qianli, 2022	High-Strength Material through Hot-Compressed Water Extraction	Rice Husk/ Bamboo Powder		in-situ lignin
Qin, 2023	Lignin-reinforced cellulose bamboo composite	Natural bamboo particles		in-situ lignin
Stefania Chiujdea, 2020	Densified wood-cellulose mix	Recycled Paper, Cardboard	None	
Thakur et al., 2024	Wood-like material from lignin and cellulose	tempo-oxidized CNFs and CNCs	Organosolv fractionated hardwood lignin, mixed biomass	
Xia et al., 2024	Lignin-infused Paper Mulberry bark	Bark of Broussonetia papyrifera		in-situ lignin
XYZAidan, 2020	Recycled Cardboard shapes from 3D- printed moulds.	Recycled Paper, Cardboard	None	
Yang et al., 2023	High strength bio-composite	Buxus sinica Wood		in-situ lignin
Yao, 2023	Microwaved lignin PLA and resin prints	None	Lignin, Sodium lignosulfonate, microwaved	
Zhang et al., 2017	Hot-pressed wood-lignin composite	Poplar Wood particles cellulose (43.1%), hemicelluloses (22.8%), acid-insoluble lignin (19.0%)	alkaline lignin 90.81% Klason lignin, 3.61% acid-soluble lignin, 0.63% sugars, 2.16% ash, and 2.79% others	
Zheng et al., 2023	Bamboo composite with in-situ lignin polymerization	Nature Moso bamboo (Phyllostachys heterocycle)		in-situ lignin

Appendix Table 3. Summary of all Strength Values of the Materials in the Literature

Reference Name	Material Description	Tensile Strength (MPa)	Compressive Strength (MPa)	Flexural Strength (MPa)	Shear Strength (MPa)	Young's Modulus (MPa)	Bending Modulus (MPa)	Other Strengths	Method	Production Method
Bierach & Coelho, 2023	Cellulose-lignin with methyl-cellulose binder	3,64		9,59		445	860	Prototypes: window frame, structural node	Cold Mixture	Cold Mixture
Arevalo & Peijs, 2016	Lignin-based fibre composite			120			1800	High tensile strength composite material (10mm flax fibres)	Unspecified	Polymerization with Temperature
Huang et al., 2024	Bagasse cellulose with lignin reinforcement (thin-film)	5						Improved wet strength	Unspecified	Hot-pressing
Qi et al., 2024	Wood-Plastic Composite with HDPE							Improved interfacial strength	Unspecified	Hot-pressing
Qianli, 2022	Densified bamboo material	29,5		58,5			7300	Tensile strength 2.8x improvement	Unspecified	Hot-pressing
Qin, 2023	Lignin-reinforced cellulose bamboo composite		178	162				High flame and water resistance	Unspecified	Hot-pressing
Stefania Chiujdea, 2020	Densified wood-cellulose mix							Increased density and bonding strength	Unspecified	Hot-pressing
Thakur et al., 2024	Wood-like material from lignin and cellulose		33	1,8		2400	1180	Enhanced UV resistance	Unspecified	Cold Mixture
Xia et al., 2024	Lignin-infused Paper Mulberry bark	110		59,64				High water stability, UV resistance	Unspecified	Hot-pressing
Yang et al., 2023	High strength bio-composite	106		T		3720	8930	Flame retardant	Unspecified	Hot-pressing
Yao, 2023	Bio-based lignin-cellulose composite	47		35		2,8		Eco-friendly with improved durability	Unspecified	Polymerization with Temperature
Zhang et al., 2017	Hot-pressed wood-lignin composite							Optimised cross-linking at 160°C	Hot Pressing	Hot-pressing
Zheng et al., 2023	Bamboo composite with in-situ lignin polymerization	286		56,5	925	11800	9000	Water resistance 8.9% absorption	Unspecified	Hot-pressing

Spezifikation

Artikelnummer: 25XN

Soda Lignin

>90 %

CAS-Nummer: 9005-53-2 Druckdatum: 01.01.2025

Formel:

Dichte:

Molekulargewicht:

Typanalyse

Aussehen	braunes Pulver
pH (10 %, Suspension)	2,2-4,2
Feuchtegehalt	≤3,0 %

Unsere Produkte sind für Laborzwecke geprüft.
Die Angaben beziehen sich auf den aktuellen Stand der Produktqualität.
Wir behalten uns vor, notwendige Änderungen durchzuführen.

Dr. R. Niemand
Head of Quality Assurance

S. Lorsee
Head of Quality Management

Dieses Dokument wurde maschinell erstellt und ist ohne Unterschrift gültig.

Carl Roth GmbH + Co. KG
Schoemperlenstraße 3-5
76185 Karlsruhe

Telefon 0721/5606-0
Telefax 0721/5606-149
E-Mail: info@carlroth.de

Die Firma ist eine Kommanditgesellschaft mit Sitz in Karlsruhe, Reg. Gericht Mannheim HRA 100055. Persönlich haftende Gesellschafterin ist die Firma Roth Chemie GmbH mit Sitz in Karlsruhe, Reg. Gericht Mannheim HRB 100428. Geschäftsführer: André Houdelet

Appendix Figure 1. Datasheet of newly ordered Kraft Lignin

chemicalpoint
www.chemicalpoint.eu

Certificate of Analysis

Product name	Lignin,organosolv	
Product number	CP8068-03-9-BULK	
Batch	CP9191	
CAS	8068-03-9	
Mfg. Date	May 2024	
Retest Date	May 2026	
Item	**Specification**	**Results**
Appearance	Brown solid powder	Conforms
Moisture	≤40%	32.7%
Residual sugar	≤5.0%	0.07%
Ash	≤5.0%	0.5%
Lignin	≥80.0%	89.2%

This document has been generated electronically and is valid without a signature

June 2024

Chemical Point UG • Gleißentalstr. 16 • 82041 Deisenhofen, Germany • Tel.: + 49 (0)89 41 61 599 - 30 • Fax: + 49 (0)89 41 61 599 - 39

Appendix Figure 2. Datasheet of newly ordered Organosolv Lignin

Appendix Table 4. Specimen mixture and hot-pressing tracking sheet

Name	date_mix	Cellulose (g)	ISCOELL	FPC	KP	Other Name	Other Amount	Lignin (g)	Type	Water amount	Mix-Type	wet-weight	dry-weight	Hot-Pressing	date_press	time (min)	pressure (Mpa)	temperature (°C)	pre-weight (g)	post-weight (g)	compress (kN)	extra hold (min)
1	24.02.2025	40	40	0	0		0	0	None	350	wet		50,9									
2	24.02.2025	30	15	15	0		0	0	None	250	wet		136									
3	24.02.2025	30	15	0	15		0	0	None	350	wet	331	30,5									
4	24.02.2025	22	10	2	10		0	0	None	275	wet	275	47									
5	24.02.2025	20	10	0,5	9		0	0	None	256,25	wet	266	26									
6	25.02.2025	30	15	0	15		0	15	Soda	300	wet	161,85	57,1		03. Mrz	30	5	220	40	39,4		
7	25.02.2025	19,5	10	0,5	9		0	10	Soda	225	wet	147	44,3									
8	25.02.2025	30	15	0	15		0	30	Soda	250	wet	187,4	85,2		27. Feb	22	1	160	53,8	55,03		
9	25.02.2025	30	15	0	15		0	30	Soda	260	wet	192,66	57,9									
10	25.02.2025	30	15	0	15		0	30	Soda	260	wet	212	57,57									
11	28.02.2025	20	20	0	0		0	20	Soda	14	dry		59,6		03. Mrz	30	1	85	44	42,6		
12	28.02.2025	20	20	0	0		0	40	Soda	55,3	dry	112,5	86	FAILED	03. Mrz	30	5	140	86			
13	28.02.2025	20,8	20	0,8	0		0	20,8	Soda	53,6	dry	59,4	40,7									
14	06.03.2025	20	20	0	0		0	30	Soda	0	dry		48,5		07. Mrz	15	2	85	48,5	47,1		
15	06.03.2025	20	20	0	0		0	30	Soda	2,5	dry		51,3		07. Mrz	15	2	85	51,3	50,5		
16	06.03.2025	20	20	0	0		0	30	Soda	5	dry		53,5		07. Mrz	15	2	85	53,5	52,2		
17	06.03.2025	20	20	0	0		0	30	Soda	7,5	dry		55,6		07. Mrz	15	2	85	55,6	53,9		
18	06.03.2025	20	20	0	0		0	30	Soda	10	dry		60,1		07. Mrz	15	2	85	60,1	58,1		
19	06.03.2025	20	20	0	0		0	30	Soda	12,5	dry		60,7		07. Mrz	15	2	85	60,7	58,3		
20	06.03.2025	20	20	0	0		0	30	Soda	15	dry		64,5									
21	06.03.2025	20	19	1	0		0	30	Soda	12,5	dry		61,6									
22	11.03.2025	20	20	0	0		0	30	Soda	12,5	dry		59,9		13. Mrz	15	3	85	59,9	56		
23	06.03.2025	20	20	0	0		0	30	Soda	12,5	dry		61,1		13. Mrz	120	2	85	61,1	58,2		
24.1	06.03.2025	40	40	0	0		0	10	Soda	12,5	dry		60,65		14. Mrz	15	2	85	60,65	57,8	270	
24.2	06.03.2025	40	40	0	0		0	10	Soda	12,5	dry		59,5		18. Mrz	15	2	85	59,5	57,4	250	
24.3	20.03.2025	40	40	0	0		0	10	Soda	12,5	dry		61,9		28. Mrz	15	2,22	70	61,9	59,1	250	10
25.1	06.03.2025	25	25	0	0		0	25	Soda	12,5	dry		61,16		14. Mrz	15	2	85	61,16	58,4	200	
25.2	06.03.2025	25	25	0	0		0	25	Soda	12,5	dry		60,8		18. Mrz	15	2	85	60,8	58,8	200	
25.3	20.03.2025	25	25	0	0		0	25	Soda	12,5	dry		60,8		28. Mrz	15	2,22	70	61,85	58,7	250	10
26.1	06.03.2025	30	30	0	0		0	20	Soda	12,5	dry		60,3	overnight	18. Mrz	15	2	85	59,3	57,9	200	
26.2	06.03.2025	30	30	0	0		0	20	Soda	12,5	dry		60		18. Mrz	15	2	85	60	58,3	200	
26.3	20.03.2025	30	30	0	0		0	20	Soda	12,5	dry		61,2		28. Mrz	15	2,22	70	61,2	58,8	250	10
27.1	06.03.2025	35	35	0	0		0	15	Soda	12,5	dry		59,3									
27.2	06.03.2025	35	35	0	0		0	15	Soda	12,5	dry		60,8		18. Mrz	15	2	85	60,8	58,6	200	
27.3	20.03.2025	35	35	0	0		0	15	Soda	12,5	dry		61,2		28. Mrz	15	2,22	70	61,75	59,1	200	10
28.1	06.03.2025	20	20	0	0		0	30	Soda	12,5	dry		62,2		14. Mrz	15	2	85	59,2	58,1	135	
28.2	06.03.2025	20	20	0	0		0	30	Soda	12,5	dry		61,9	overnight	13. Mrz	15	2	85	61,9	59,9	135	
28.3	20.03.2025	20	20	0	0		0	30	Soda	12,5	dry		61,85		28. Mrz	15	2,22	70	61,85	59,5	250	10
29.1	20.03.2025	25	25	0	0		0	25	None	12,5	dry		61,48									
29.2	20.03.2025	25	25	0	0		0	25	None	12,5	dry		61,94									
29.3	20.03.2025	25	25	0	0		0	25	None	12,5	dry		62,28									
29.4	20.03.2025	25	25	0	0		0	25	None	12,5	dry		60,8									
30	20.03.2025	25	25	0	0		0	25	Organosolv	12,5	dry		57,98	no flow	28. Mrz	15	2,22	70	57,98	54,8	250	10
31	20.03.2025	25	12	1	12		0	25	Soda	12,5	dry		60,63		07. Apr	15	3,70	80	59,4	58	250	10
32	20.03.2025	25	12,5	0	0	Flax	12,5	25	Soda	12,5	dry		55,15		27. Mrz	15	2,22	70	55,15	52,9	250	
33	20.03.2025	25	12,5	0	0	Jute	12,5	25	Soda	12,5	dry		58,67									
34	20.03.2025	25	0	0	0	MC	2	25	Soda	12,5	dry		61,1									
35	27.03.2025	30	30	0	0		0	20	Soda	2,5	dry		52,3	overnight	27. Mrz	15	2,22	140	52,3	50,3	250	
36	27.03.2025	30	30	0	0		0	20	Soda	5	dry		54,2		27. Mrz	15	2,22	90	54,2	52,2	250	
37	27.03.2025	30	30	0	0		0	20	Soda	12,5	dry		61,9		27. Mrz	15	2,22	70	61,9	60,1	250	
38.1	14.04.2025	25	0	0	0	treated ISO	25	25	Soda	6,5	dry		53,5		24. Apr	15	3,70	120	53,5	51,2	250	10
38.2	14.04.2025	25	0	0	0	treated ISO	25	25	Soda	6,5	dry		56,9		24. Apr	15	3,70	120	46,9	55	250	10
38.3	14.04.2025	25	0	0	0	treated ISO	25	25	Soda	6,5	dry		56,9		24. Apr	15	3,70	120	56,9	55,05	250	10
39.1	14.04.2025	25	25	0	0		0	25	Soda	12,5	dry		61,1		28. Apr	15	3,70	120	53,7	52,5	250	10
39.2	14.04.2025	25	25	0	0		0	25	Soda	12,5	dry		61		28. Apr	15	3,70	120	53,7	52,8	250	10
39.3	14.04.2025	25	25	0	0		0	25	Soda	12,5	dry		62,19		28. Apr	15	3,70	120	54,9	51,5	250	10
30.1	14.04.2025	25	25	0	0		0	25	Organosolv	13,5	dry		61,24		24. Apr	15	3,70	85			250	10
30.2	14.04.2025	25	25	0	0		0	25	Organosolv	14,5	dry		61,2		28. Apr	15	3,70	120	53,6	52	250	10
30.3	14.04.2025	25	25	0	0		0	25	Organosolv	15,5	dry		61		28. Apr	15	3,70	120	53,5	50,9	250	10

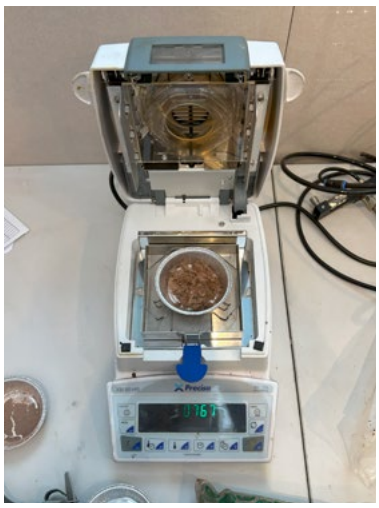

1 gram of cellulose-lignin mixture with 10wt% added water content

Heating cycle while measurement of loss of weight

Final result: 100% - 79.57% = 20.43% moisture

Appendix Figure 3. Measurement of moisture inside the cellulose-lignin mixture using a moisture metre.

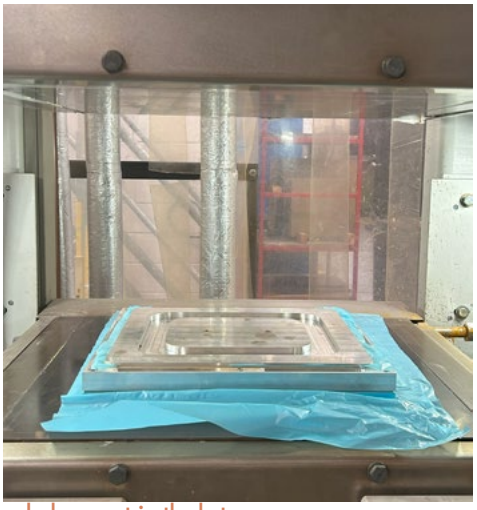

Appendix Figure 4. Photographs of large mould filling and placement in the hot-press

Appendix Figure 5. Photographs of large mould filling and placement in the hot-press

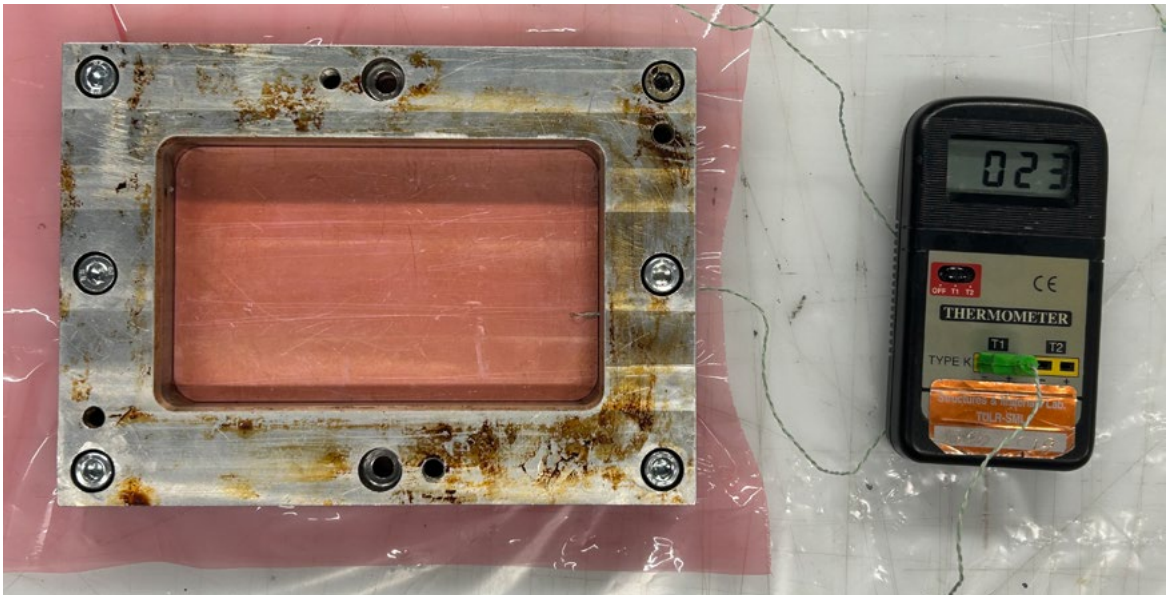

Appendix Figure 6. Installation of Thermal Couple in Mould

Appendix Figure 7. Preparation of crucible pans for DSC analysis.

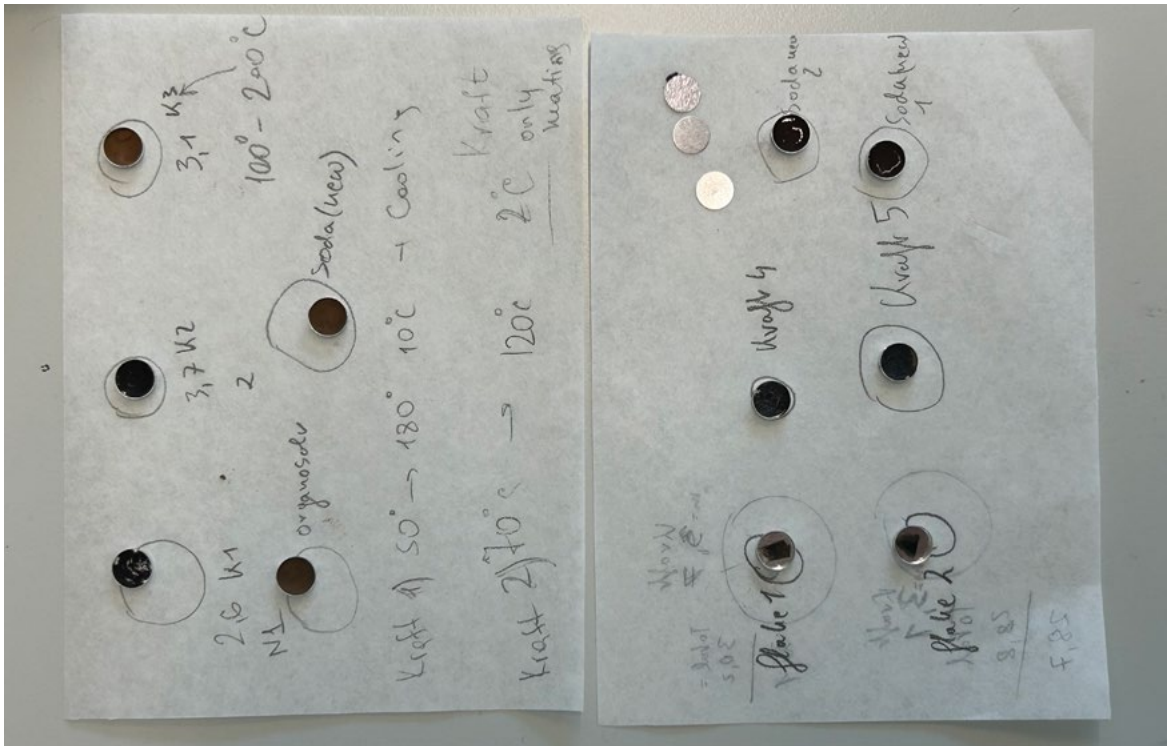

Appendix Figure 8. Crucible pans with samples after DSC Analysis

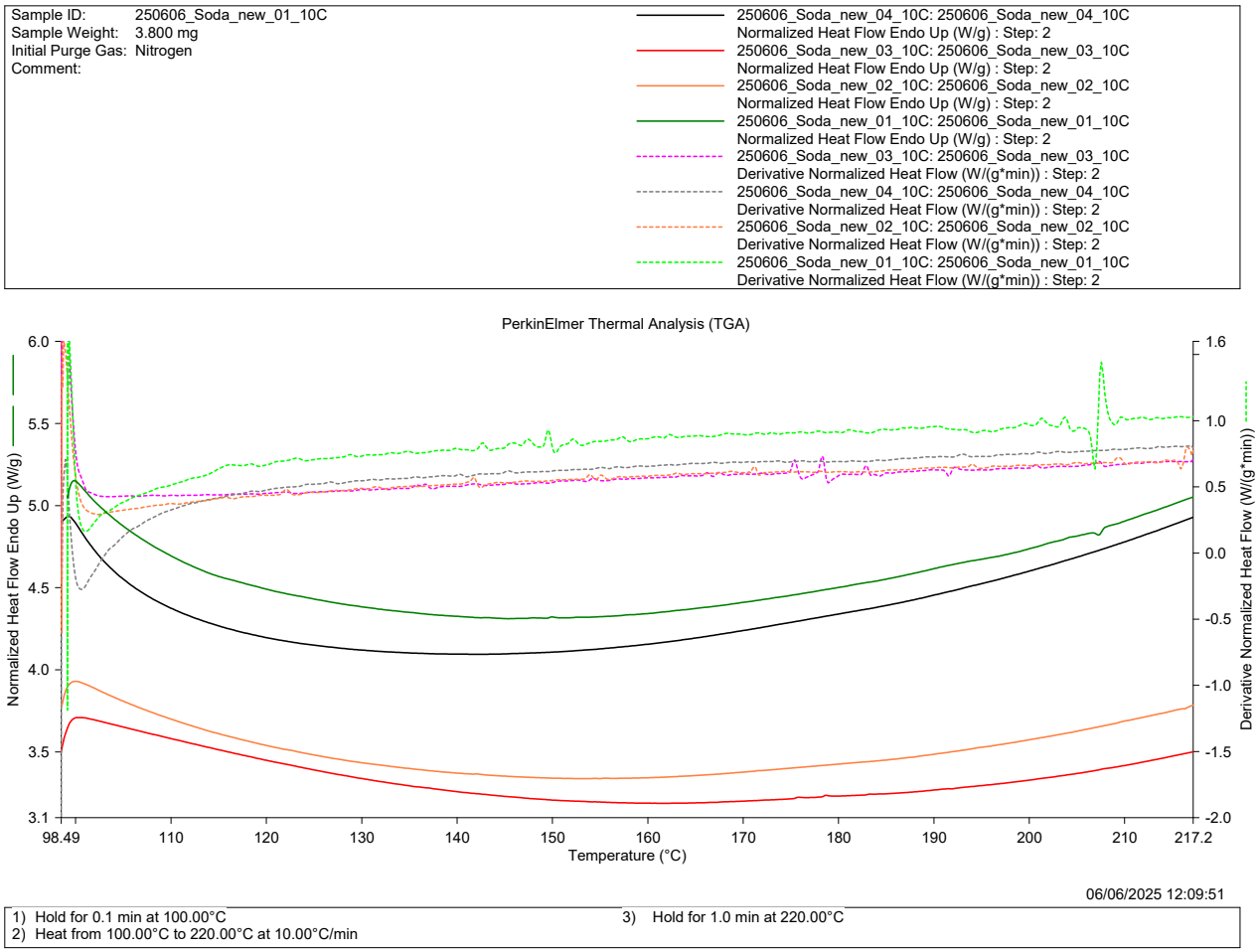

Appendix Figure 9. Repeated heatflow graphs of the same type of lignin (Soda lignin), showing no significant artifact or result indicating the T_g of this lignin type

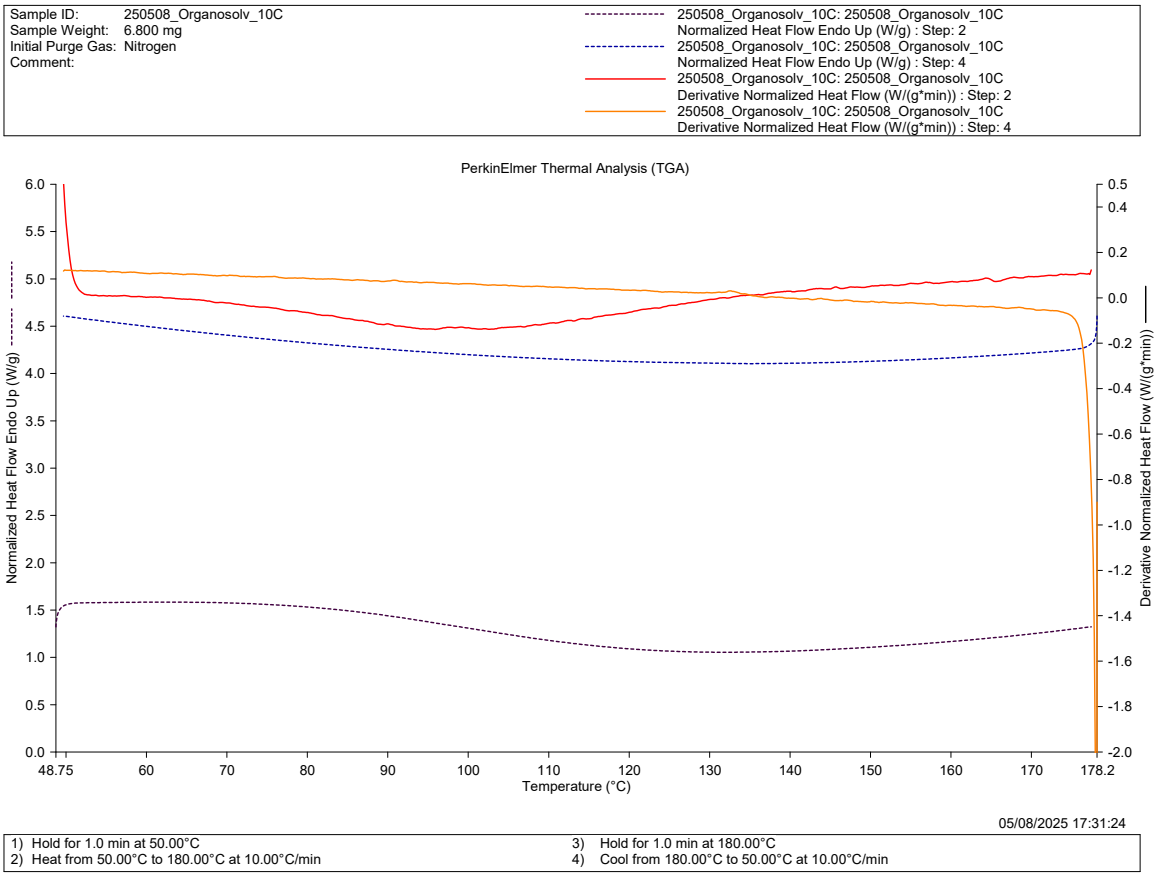

Appendix Figure 10. Heatflow curve of two heating cycles of Organosolv lignin sample, showing no significant artefact or result indicating the T_g of this lignin type

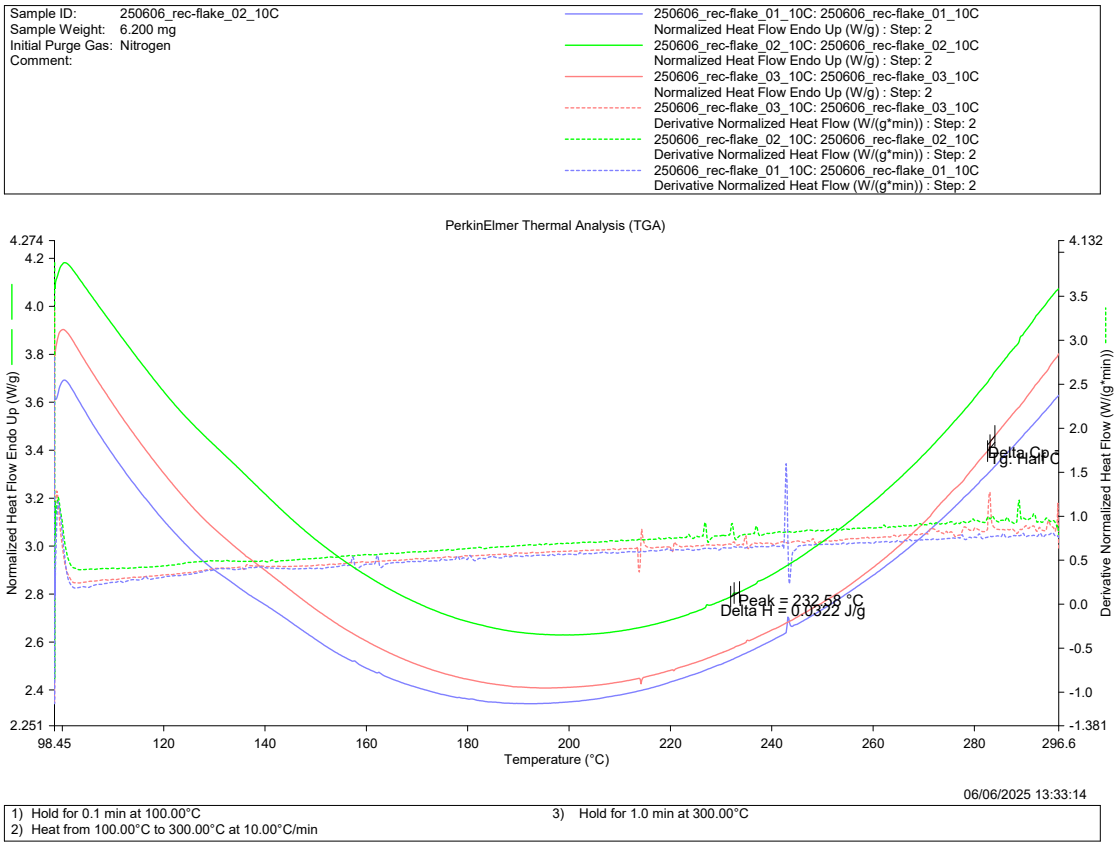

Appendix Figure 11. Repeated heatflow graphs of the same type of recylced sample flake, showing no significant artifact or result indicating the T_g of this lignin type

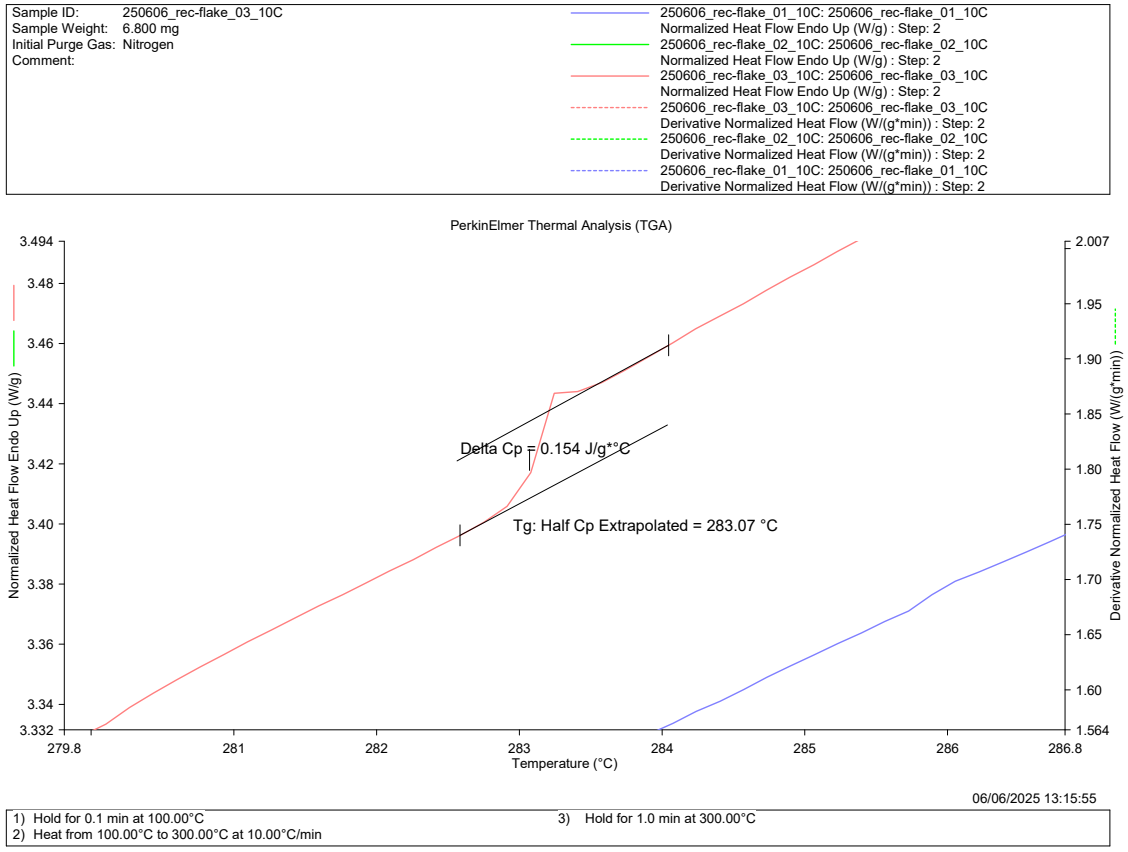

Appendix Figure 13. Zoomed in heatflow curve of the recycled sample flake, showing the determination of the T_g at the step in heatflow. T_g of 283°C can not be attributed to lignin, more fitting to cellulose.

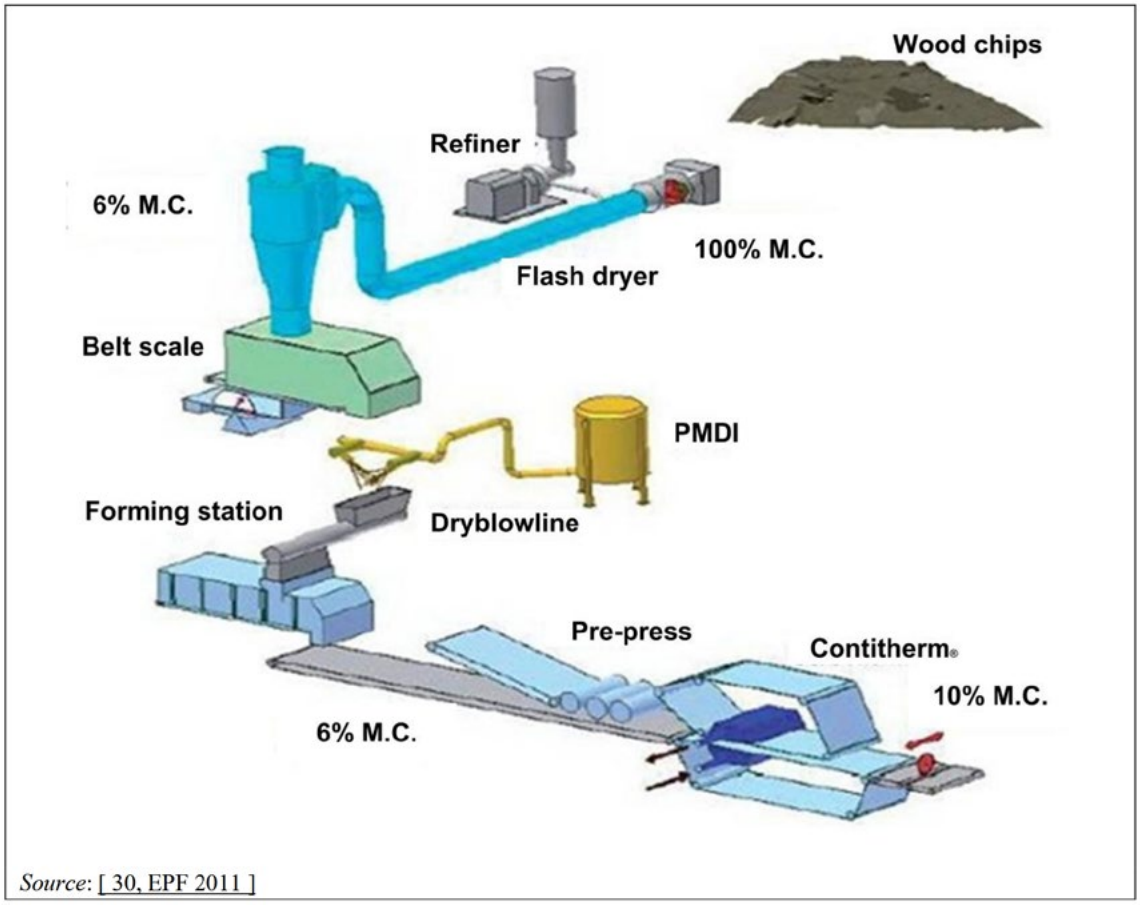

Figure 2.11: Example of main production steps for rigidboards

Appendix Figure 12. Example of main production steps for rigidboards. From Stubdrup et al., 2016

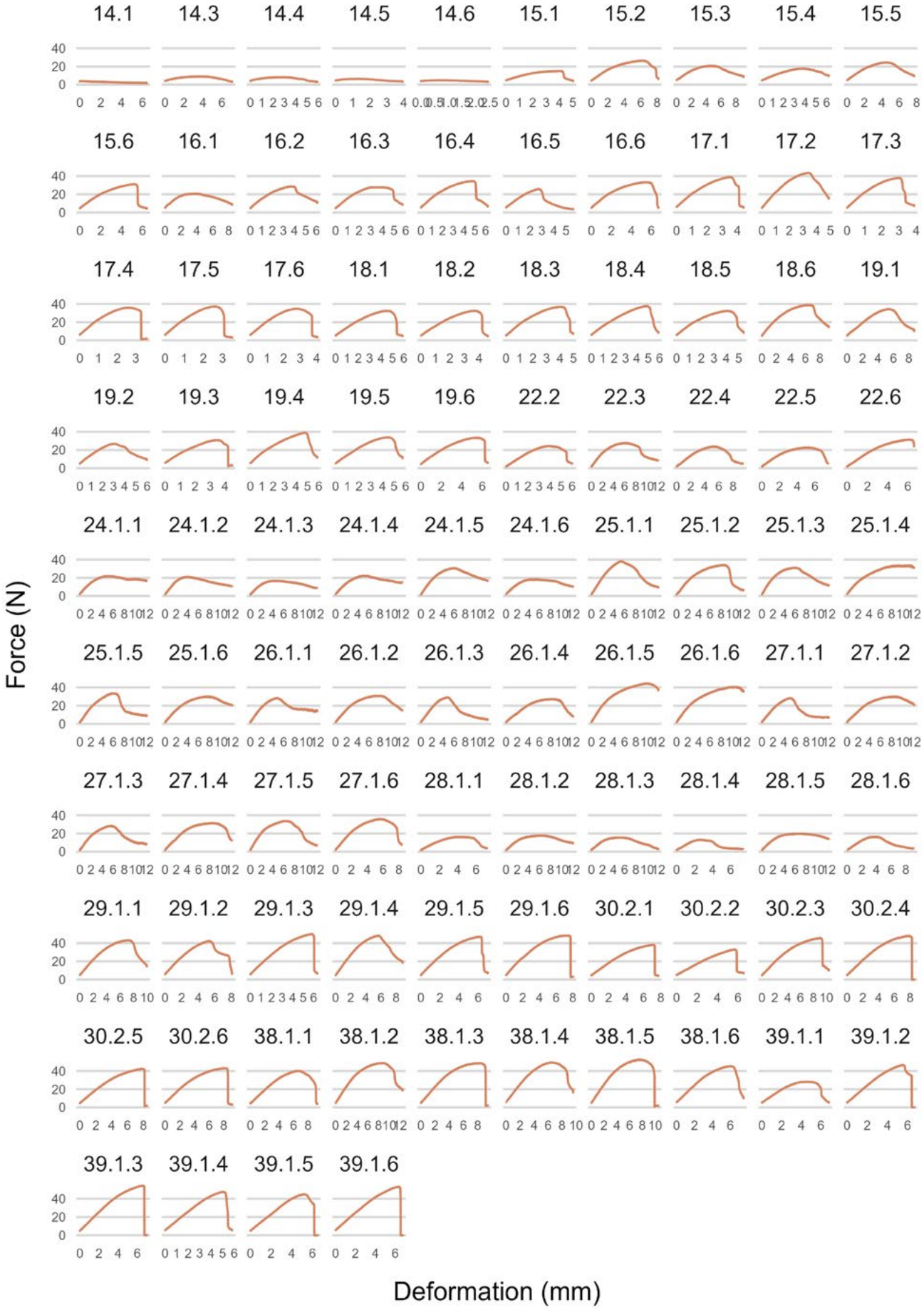

Appendix Figure 14. Bending Test Force-Deformation Curves

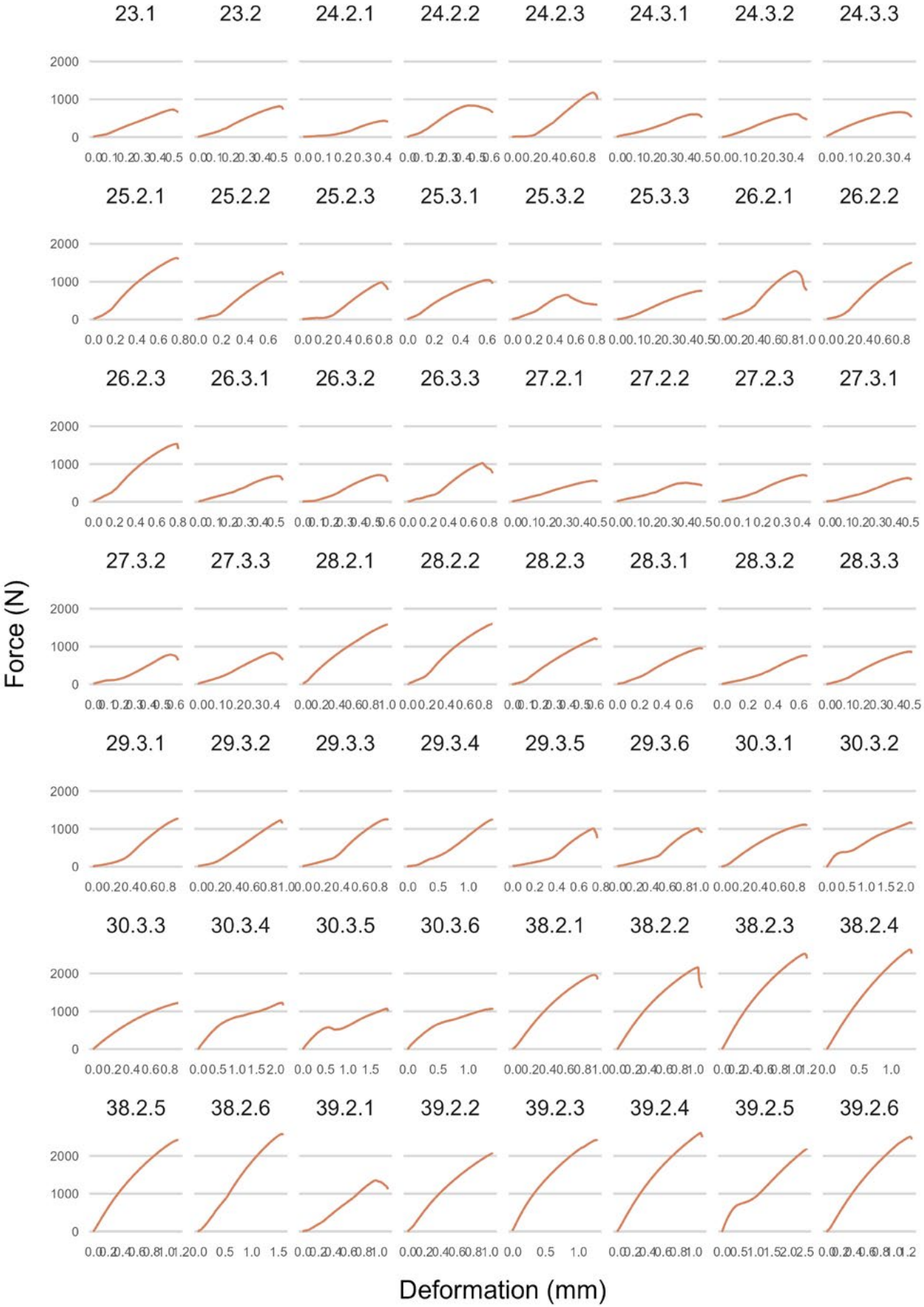

Appendix Figure 15. Compression Test Force-Deformation Curves

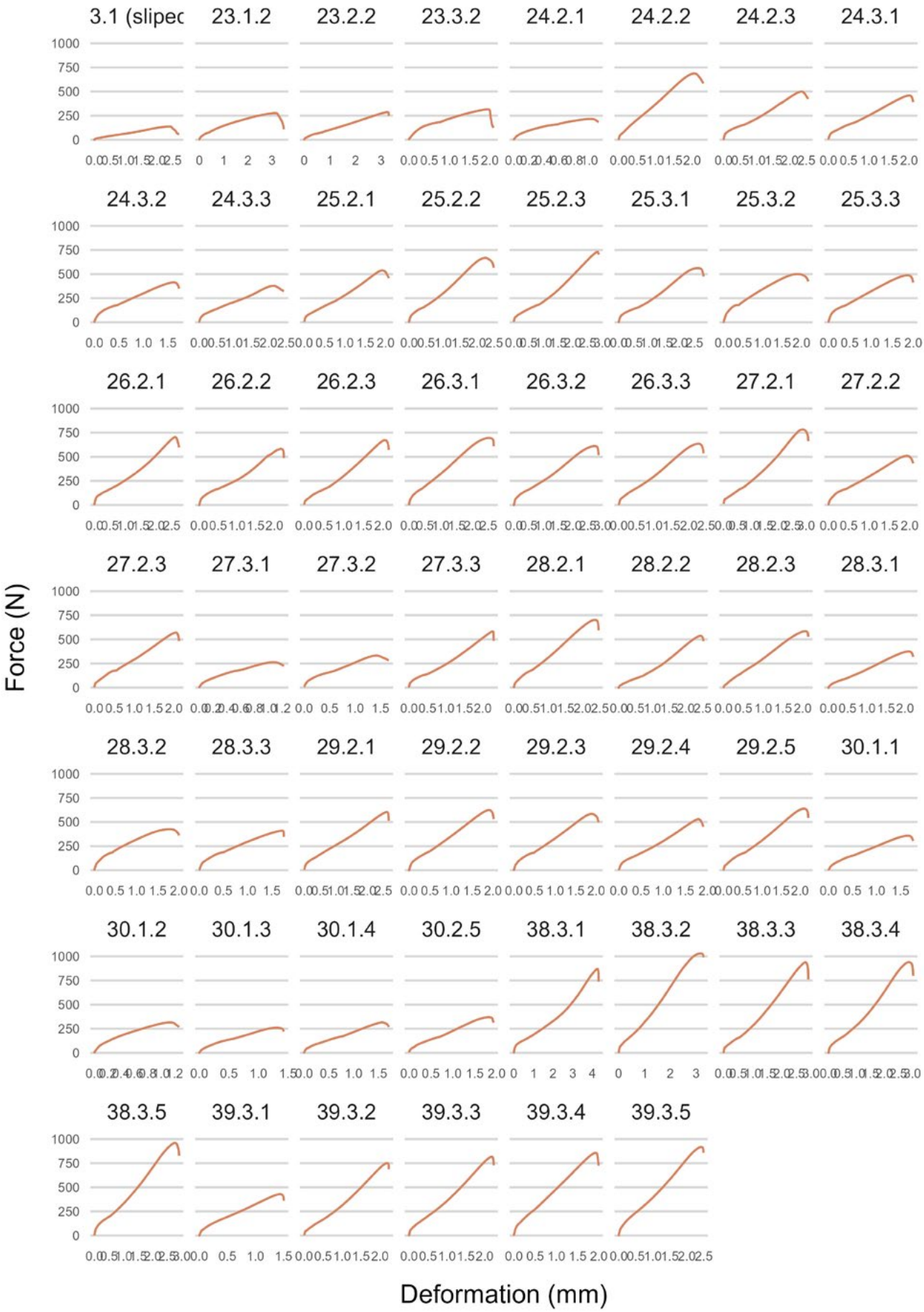

Appendix Figure 16. Tension Test Force-Deformation Curves

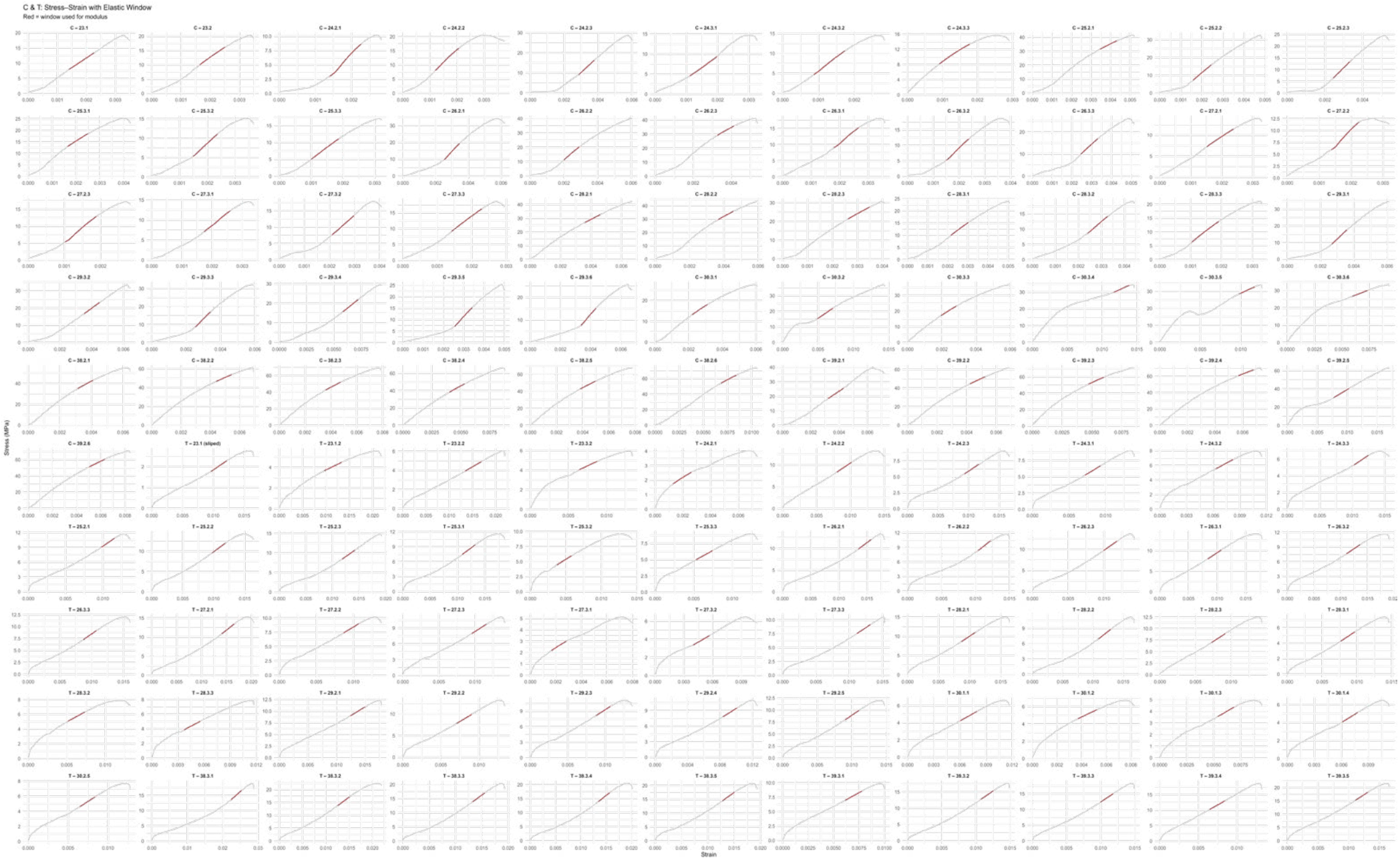

Appendix Figure 17. Determination of Slope for Tension and Compressive Tests from Force and Deformation

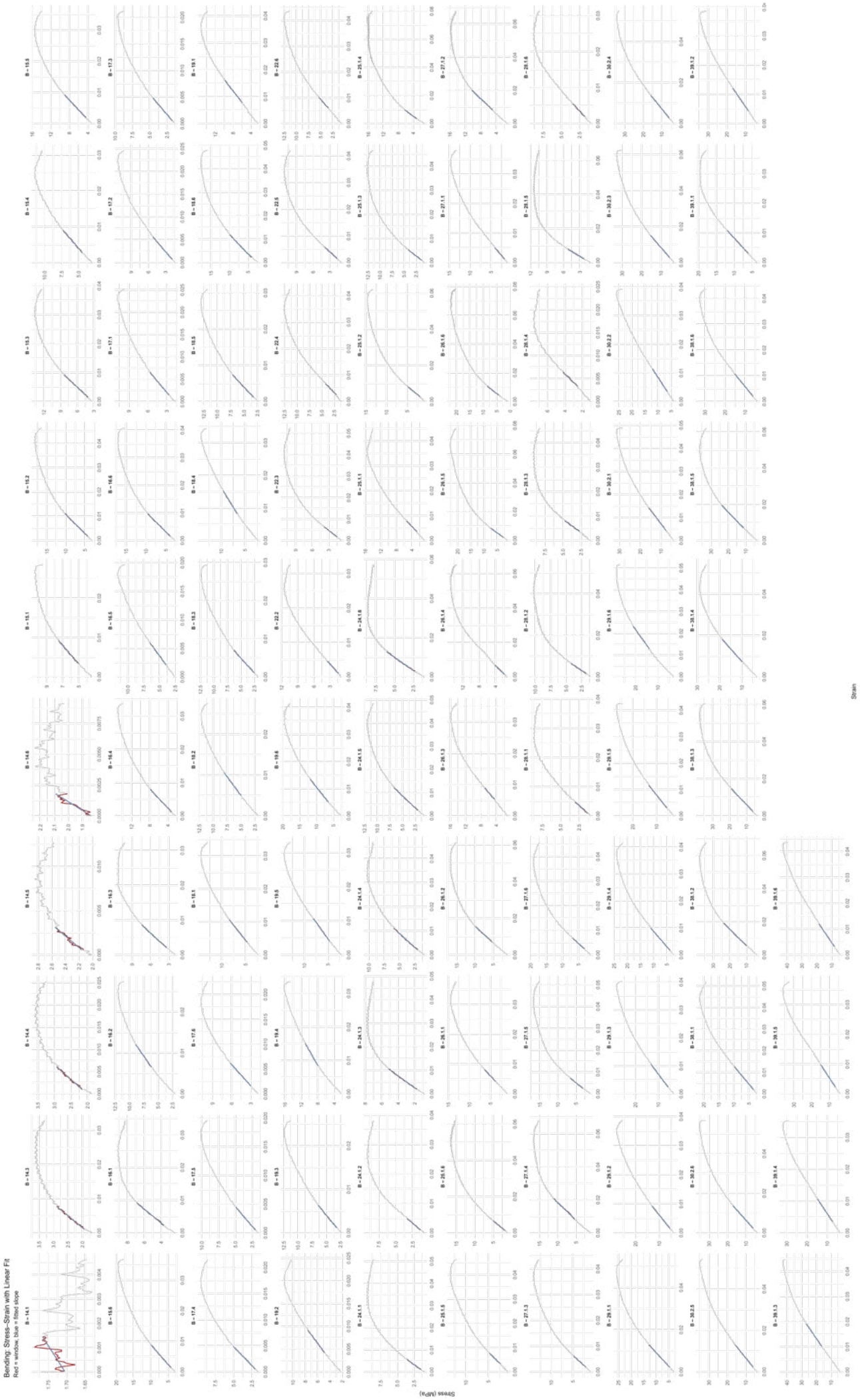

Appendix Figure 18. Determination of Slope for Bending Tests from Stress and Strain

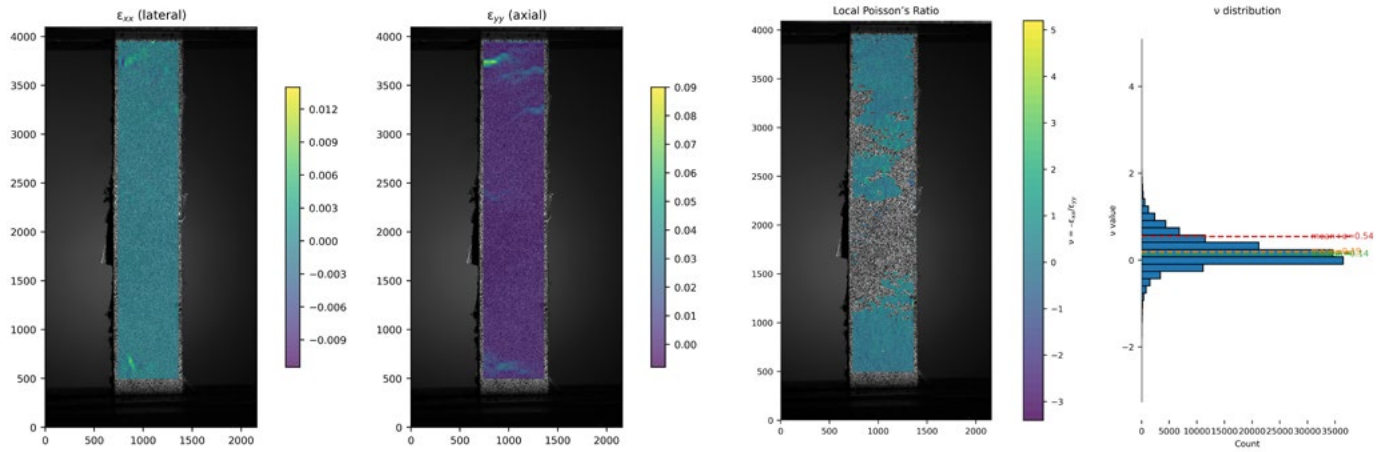

Appendix Figure 19. T.24.2.1 Strain and Poisson's Ratio determination

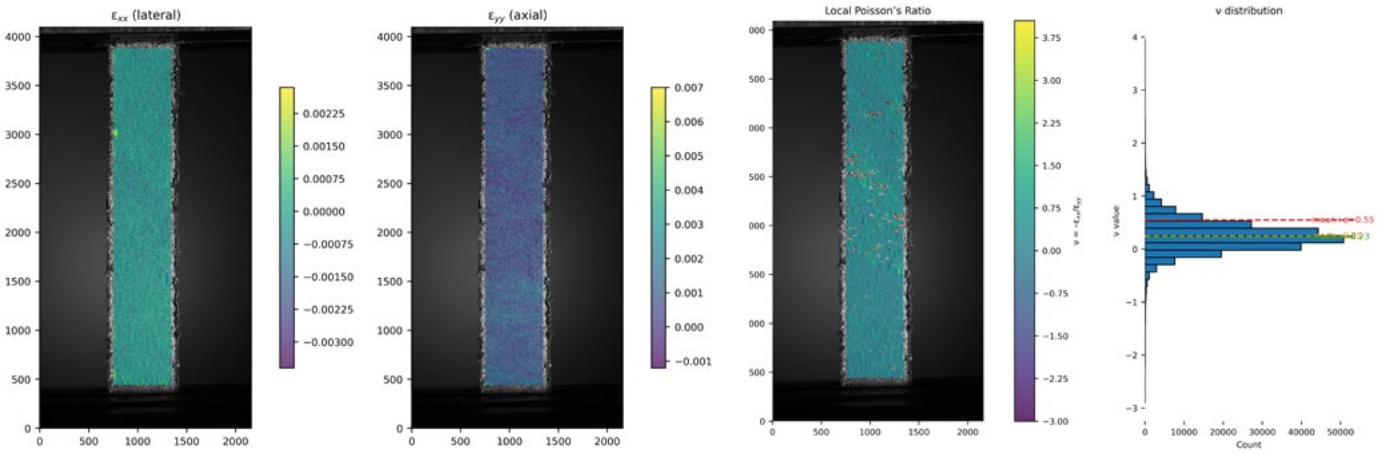

Appendix Figure 20. T.25.3.2 Strain and Poisson's Ratio determination

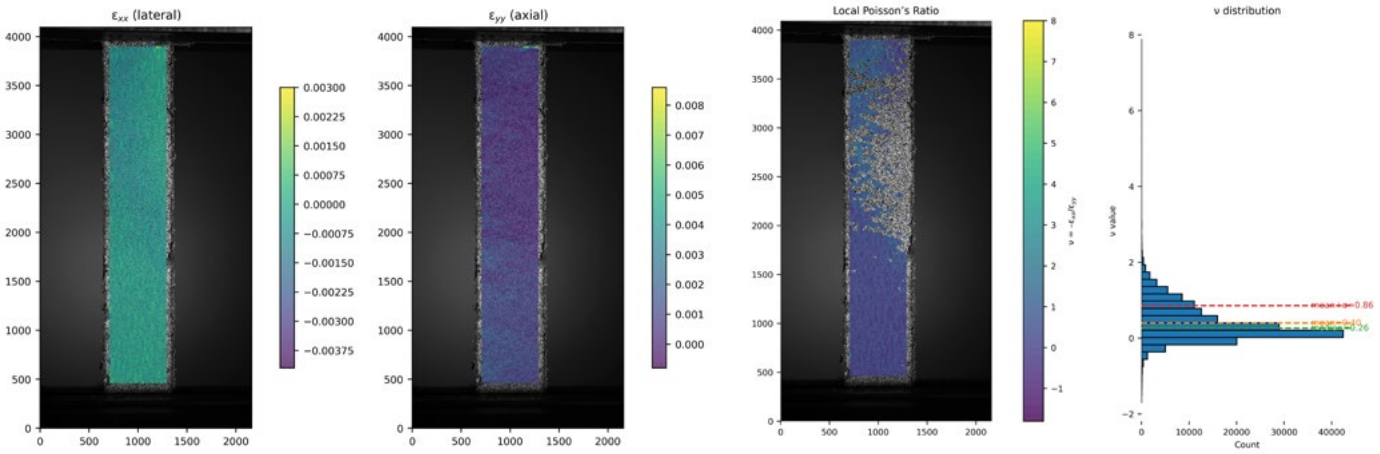

Appendix Figure 21. T.26.3.1 Strain and Poisson's Ratio determination

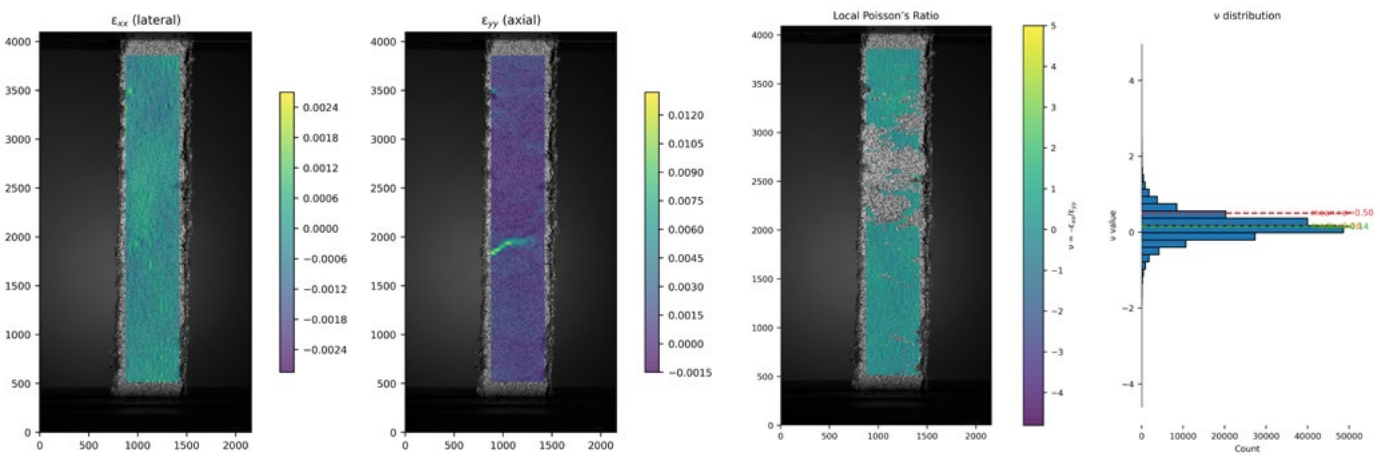

Appendix Figure 22. T.27.3.2 Strain and Poisson's Ratio determination

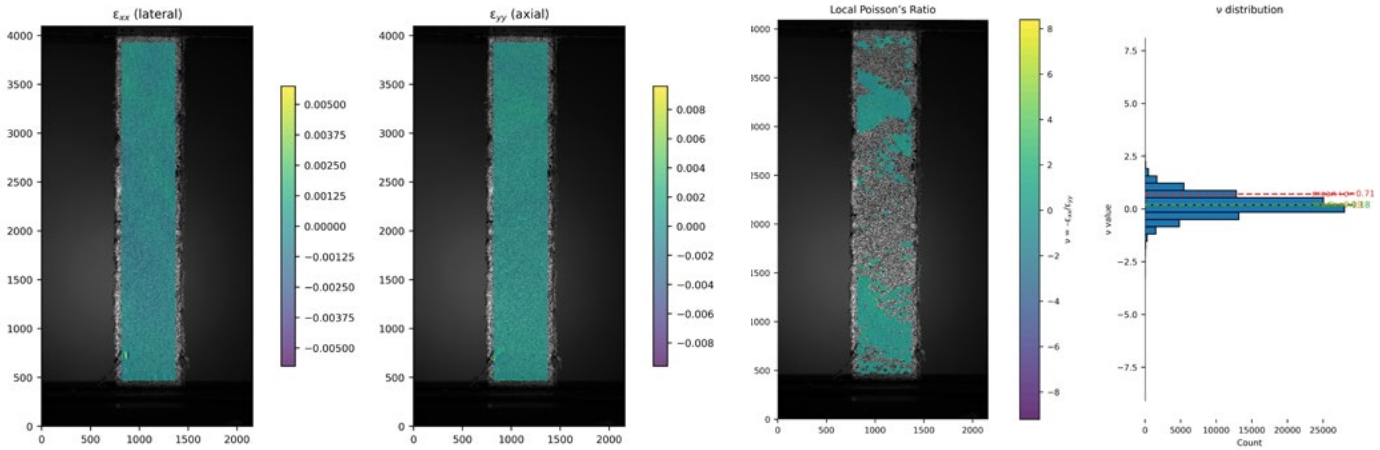

Appendix Figure 23. T.28.3.2 Strain and Poisson's Ratio determination

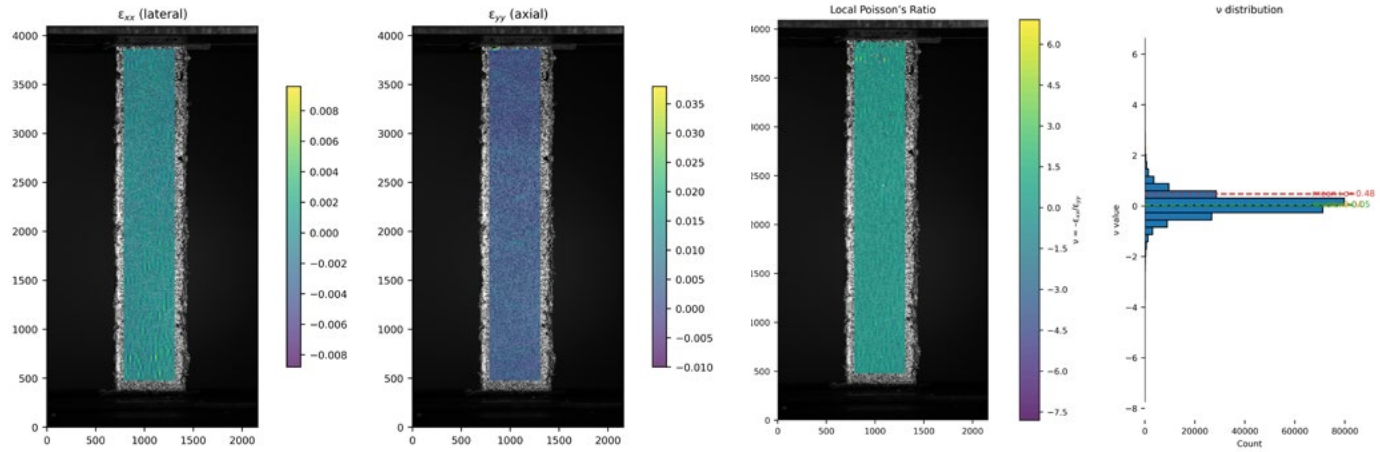

Appendix Figure 24. T.29.2.2 Strain and Poisson's Ratio determination

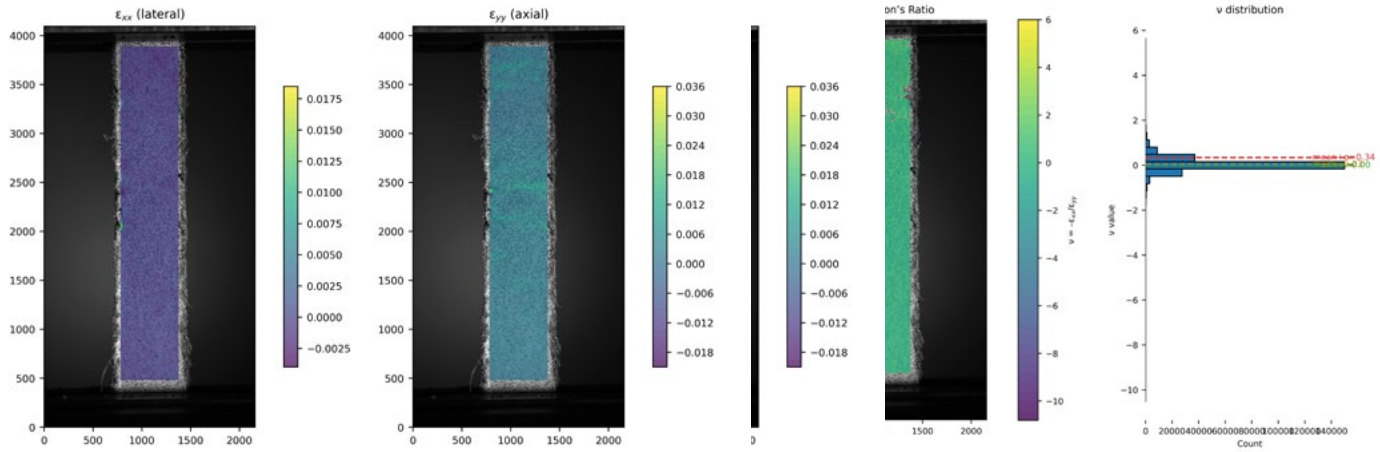

Appendix Figure 25. T.30.1.2 Strain and Poisson's Ratio determination

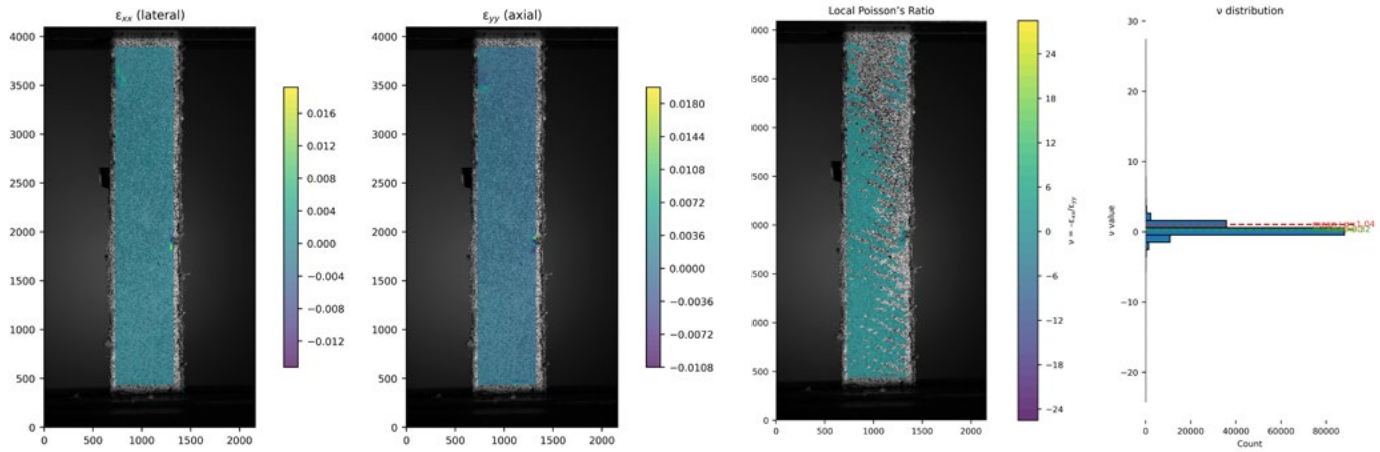

Appendix Figure 26. T.38.3.1 Strain and Poisson's Ratio determination

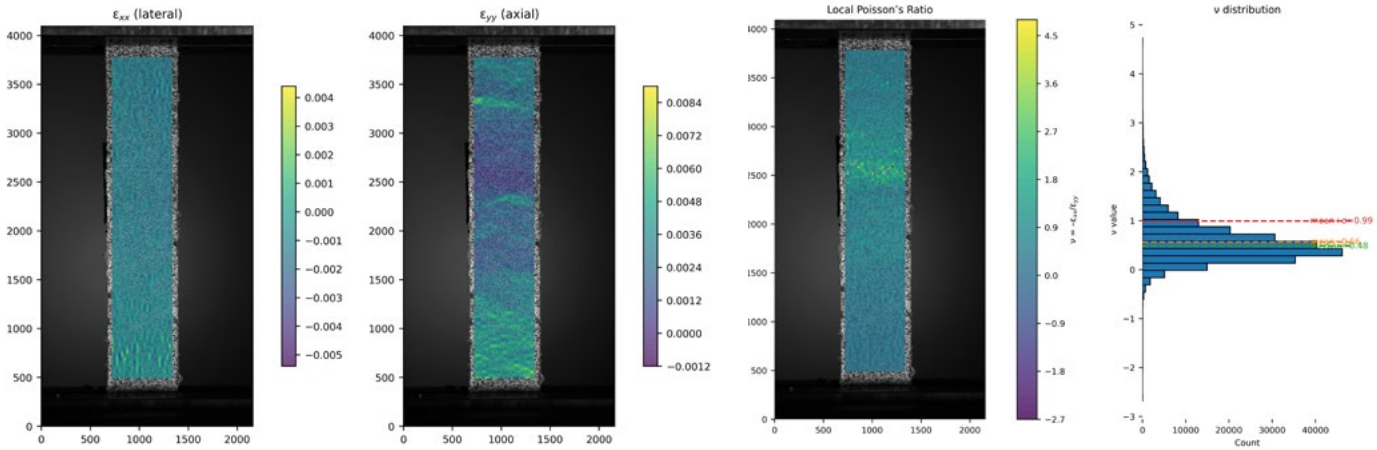

Appendix Figure 27. T.39.3.4 Strain and Poisson's Ratio determination

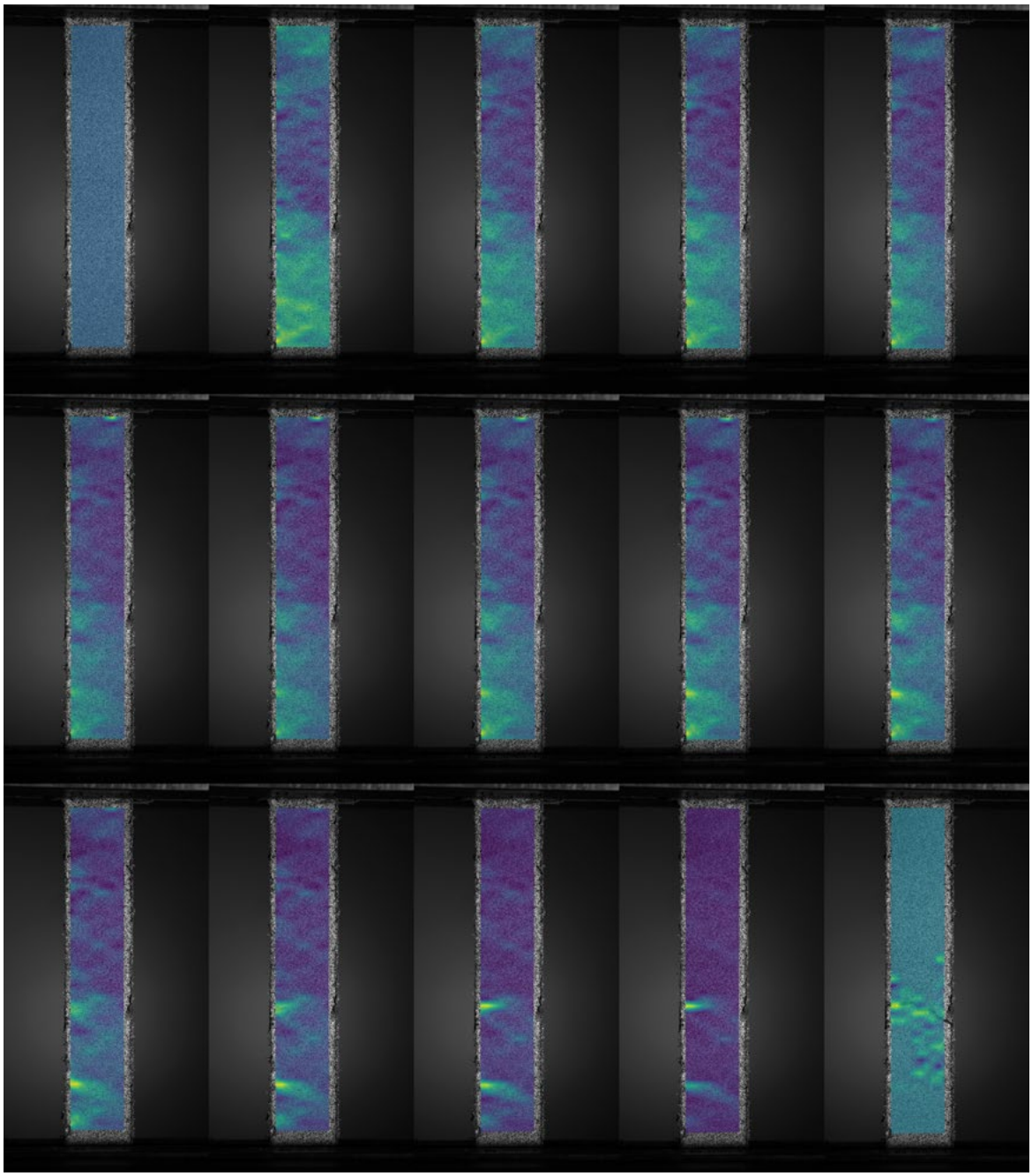

Appendix Figure 28. T.26.3.1 Incremental axial-strain overlays on specimen.